Induced seismicity potential for geothermal projects targeting Dinantian carbonates in the Netherlands

Report by SCAN

April 2020

Ministerie van Economische Zaken en Klimaat
ebn
TNO
Interreg North-West Europe DGE-ROLLOUT

Induced seismicity potential for geothermal projects targeting Dinantian carbonates in the Netherlands

Report written by:
Jan ter Heege, Lonneke van Bijsterveldt, Brecht Wassing, Sander Osinga, Bob Paap, Dirk Kraaijpoel

TNO Applied Geosciences, Utrecht

April 2020

Dit rapport is een product van het SCAN-programma en wordt mogelijk gemaakt door het Ministerie van Economische Zaken en Klimaat

Acknowledgements

We would like to thank Bastiaan Jaarsma, Mara van Eck van der Sluijs and Marc Hettema (EBN) for fruitful discussions in the course of this project. Ben Laenen (VITO) is gratefully acknowledged for organizing a one-day workshop on the Balmatt geothermal project that provided valuable insights for this study. Ulrich Steiner and Alexandros Savvatis (ERDWERK) are also gratefully acknowledged for providing valuable insights on geothermal projects in the Molasse Basin near Munich during a one-day workshop at TNO. Bernard Dost and Elmer Ruigrok (KNMI) were of great help by providing their insights into seismic monitoring strategies for the Netherlands. Discussions with scientists involved in the previous study "*Review of worldwide geothermal projects: mechanisms and occurrence of induced seismicity*" really helped drafting this report. Loes Buijze, Holger Cremer (TNO) and Guido van Yperen (EBN) are thanked for discussions and efforts in that study. Johan ten Veen, Maryke den Dulk, Kees Geel, Renaud Bouroullec and Loes Buijze greatly helped in compiling maps and sections showing fault interpretations. Thibault Candela (TNO) is thanked for reviewing the chapter on modelling approaches.

Table of Contents

Samenvatting en conclusies

Het (mogelijk) optreden van geïnduceerde seismiciteit (aardbevingen) bij geothermie projecten speelt wereldwijd een belangrijke rol bij de ontwikkeling van geothermie projecten. Sommige geothermie projecten met geïnduceerde seismiciteit hebben in het buitenland schade aan infrastructuur veroorzaakt. In Nederland heeft er bij de meeste geothermie projecten geen seismiciteit plaats gevonden[1], maar is er veel aandacht voor het optreden van seismiciteit door gaswinning.

Deze studie spitst zich toe op één type geothermisch reservoir in de Nederlandse ondergrond, te weten reservoirs in de kalksteen formaties uit het Dinantien. Deze reservoirs zijn op verschillende diepte in Nederland te vinden, en bestaan zowel uit ultradiepe Dinantiën kalksteenreservoirs (dieper dan 4 km) die in het kader van de Green Deal UDG[2] bestudeerd worden als uit ondiepere Dinantiën kalksteenreservoirs. Binnen het SCAN programma[3] worden een aantal onderzoeken gedaan om de mogelijkheden én beperkingen van geothermieontwikkeling in het Dinantiën te onderzoeken. Voor alle Dinantiën kalksteenreservoirs geldt dat meer inzicht in de oorzaken van de waargenomen geïnduceerde seismiciteit nodig zijn om ze te ontwikkelen voor geothermie. Dit ligt in dit rapport onder de loep.

Voor de kalksteenreservoirs van Dinantiën ouderdom is in Nederland en in België seismiciteit waargenomen bij geothermie projecten bij Venlo (Californië projecten) en bij Mol in België (Balmatt project). Het optreden van geïnduceerde seismiciteit bij geothermie projecten die warmte winnen uit de Dinantiën kalksteenreservoirs kan de verdere ontwikkeling van aardwarmtewinning uit dit type reservoirs belemmeren. Deze studie heeft tot doel de inzichten over oorzaken voor het optreden van geïnduceerde seismiciteit bij warmtewinning uit de Dinantiën kalksteenreservoirs te vergroten. Op basis van deze inzichten kunnen adequate maatregelen genomen worden die de seismische risico's in toekomstige projecten kunnen beheersen tot een acceptabele niveau, of kan beter gekozen worden om bepaalde potentiële projectlocaties niet of juist wel te ontwikkelen. In Nederland is het streven om seismiciteit bij aardwarmtewinning zo veel als mogelijk te voorkomen. Om te bepalen hoe je seismische risico's kan beheersen, moet je weten hoe seismiciteit veroorzaakt wordt.

Dit rapport draagt bij aan het begrip van mogelijke oorzaken voor het optreden van geïnduceerde seismiciteit in (toekomstige) geothermie projecten die warmte winnen uit kalksteenreservoirs van Dinantiën ouderdom in Nederland. Het onderzoek is gedaan door:

- de belangrijkste factoren die geïnduceerde seismiciteit beïnvloeden te analyseren,
- de mogelijkheid voor het optreden van geïnduceerde seismiciteit voor verschillende regio's te vergelijken,
- het inventariseren van methoden om geïnduceerde seismiciteit te modelleren,
- door methoden voor het bepalen van seismische dreiging en risico te vergelijken,
- door aanbevelingen te doen voor het beter monitoren van geïnduceerde seismiciteit,
- door de gegevens van een aantal relevante geothermieprojecten die warmte winnen uit (Dinantiën) kalksteenreservoirs te analyseren waarvoor in de nabijheid van de projecten geïnduceerde seismiciteit plaatsgevonden heeft.

[1] Zie de eerdere studie van Buijze et al. (2019a), link.
[2] Green Deal UDG (2017), link (in Dutch).
[3] https://scanaardwarmte.nl/

Uit het onderzoek kunnen de volgende conclusies getrokken worden:

1) **Belangrijke factoren die het (mogelijk) optreden van geïnduceerde seismiciteit beïnvloeden zijn:**
   - **De aanwezigheid van natuurlijke seismiciteit**
   - **De afstand tot (kritisch gespannen) breuken**
   - **Het samenspel van de lokale spanningstoestand, populaties van breuken, en stromingsregime in het reservoir**
   - **Reservoirdiepte en temperatuur**
   - **Samenstelling en stijfheid van het reservoirgesteente**
   - **Hydraulische en mechanische (ont-)koppeling met het over- en onderliggend gesteente**
   - **Het samenspel van operationele factoren zoals stromingssnelheid, injectie druk, injectie temperatuur (voor projecten zonder stimulatie van reservoirpermeabiliteit, op basis van vloeistofcirculatie met een balans tussen geïnjecteerd en geproduceerd volume aan vloeistof)**
   - **Interactie met andere activiteiten in de ondergrond zoals gaswinning of zoutwinning.**

   De invloed van deze factoren op het (mogelijk) optreden van geïnduceerde seismiciteit is project- en locatie-specifiek. Op dit moment is het gebrek aan data een belangrijke belemmering voor het kwantificeren van de invloed in verschillende regio's. Er kan daarom alleen een kwalitatieve analyse gedaan worden waarbij voor iedere factor ingeschat wordt of die een kleine, gemiddelde of grote invloed op het optreden van seismiciteit heeft.

2) **De kans op geïnduceerde seismiciteit die door mensen gevoeld kan worden (*potentieel voor voelbare seismiciteit*) is laag tot gemiddeld voor projecten die warmte winnen uit de Dinantiën kalksteenreservoirs. Het betekent voor het huidige type doublet systemen in Nederland dat voelbare seismiciteit zeer waarschijnlijk beperkt zal blijven tot enkele locaties waar de specifieke combinatie van verschillende lokale factoren het optreden van seismiciteit bevordert.**

   In deze studie wordt voor voelbare seismiciteit een grens in (lokale) magnitude van boven 2 ($M > 2$) gebruikt. Er is gekozen om deze grens en de indeling in laag, gemiddeld of hoog potentieel voor voelbare seismiciteit consistent te houden met de eerdere studie[1] die zowel projecten in Nederland als wereldwijd geanalyseerd heeft. Daarin is een hoog potentieel voorbehouden aan projecten in hydrothermale geothermie systemen (meestal reservoirs bestaande uit vulkanische stollings- of uitvloeiïngsgesteenten) en sommige "enhanced geothermal systems (EGS)" waar vloeistof permanent geïnjecteerd wordt om de reservoir permeabiliteit te vergroten. In gebieden met een hoog potentieel voor voelbare seismiciteit kan dit leiden tot het regelmatig voorkomen van voelbare aardbevingen. De gekozen aanpak heeft als voordeel dat de analyse consistent is en projecten beter vergeleken kunnen worden met internationale projecten. Het potentieel voor voelbare seismiciteit is lager als projecten uitgaan van vloeistofcirculatie met gemiddelde stroomsnelheden, injectie drukken en temperatuurverschillen tussen het reservoir en geïnjecteerde vloeistof, *zonder* stimulatie van reservoirpermeabiliteit door vloeistofinjectie en *zonder* gebruik te maken van stroming in breukzones. In Nederland zijn momenteel alleen projecten op basis van vloeistofcirculatie met een balans tussen geïnjecteerd en geproduceerd volume aan vloeistof voorzien, zonder stimulatie van reservoirpermeabiliteit. Dit

betekent dat voor dat soort projecten in Nederland geen gebieden met een hoog potentieel geïdentificeerd zijn. Een *hypothetisch* voorbeeld van een project in Nederland met een hoog potentieel voor voelbare seismiciteit zou zijn als er permanent significante volumes vloeistof geïnjecteerd zou worden in één van de tektonische actieve breuken van de Roerdalslenk. Een dergelijk scenario is voor projecten in Nederland niet aannemelijk. Om het potentieel lokaal of regionaal verder te specificeren is meer data vereist van de lokale geologie, eigenschappen van het reservoir en lokale spanningstoestand. Voor verdere specificatie tussen laag en gemiddeld potentieel is ook meer regio- of locatie-specifiek onderzoek nodig, met name onderzoek dat de effecten van de afkoeling van gesteente rondom de injectieput op korte termijn, en van het hele reservoir op langere termijn, meeneemt. Over het algemeen is het potentieel lager als putten niet binnen een kritische afstand liggen van (i) natuurlijke seismiciteit in de Roerdalslenk, (ii) grote breukzones die grote geologische structuren begrenzen, of (iii) geïnduceerde seismiciteit door gaswinning. Een laag tot gemiddeld potentieel voor voelbare seismiciteit betekent niet dat het optreden van voelbare seismiciteit uitgesloten kan worden. Het aantal en de magnitude van aardbevingen dat kan optreden is afhankelijk zowel geologische als operationele factoren, en van de maatregelen die genomen worden om het voorkomen van voelbare seismiciteit te beperken (bijvoorbeeld het hanteren van een stoplichtsysteem).

3) **De review van methoden om geïnduceerde seismiciteit te modelleren laat zien dat het gekozen type model afhangt van het probleem dat onderzocht wordt, de beschikbaarheid van data en de complexiteit van de lokale situatie. Enerzijds kunnen de verschillende modellen gebruikt worden om het begrip van mechanismen die leiden tot geïnduceerde seismiciteit en de eigenschappen van deze seismiciteit te vergroten. Anderzijds kunnen modellen gebruikt worden voor het genereren van een catalogus van verwachte aardbevingen die als input voor bijvoorbeeld een seismische risico analyse kan dienen.**
   Het volgende grove onderscheid kan gemaakt worden (i) snelle semi-analytische modellen die onzekerheidsanalyses mogelijk maken en gebruikt kunnen worden in probabilistische seismische dreiging en risico bepaling, (ii) langzamere 2D of 3D numerieke modellen die de eigenschappen van een enkele aardbeving of van hele aardbevingscatalogi kunnen voorspellen en die gebruikt kunnen worden om meerdere scenario's met variërende geologische en operationele factoren te onderzoeken. En ander bruikbaar onderscheid is tussen (i) volledig stochastische modellen die robuust en efficiënt zijn waardoor ze gebruikt kunnen worden om voorspellingen over seismische dreiging vrijwel meteen tijdens het optreden te doen en waardoor ze in geavanceerde stoplichtsystemen voor het beperken van aardbevingsrisico's gebruikt kunnen worden, maar vaak wel een beperkte fysische basis hebben, (ii) modellen met een gedegen fysische basis die de onderliggende mechanismen (beter) meenemen, maar die meer parameters hebben die vaak slechter te bepalen zijn, en die meestal veel rekentijd vergen.

4) **Een analyse van seismische dreiging en risico kan met verschillende mate van complexiteit uitgevoerd worden. Huidige methoden variëren van een kwalitatieve bepaling van belangrijke geologische en operationele factoren tot een volledige probabilistische modelketen die seismiciteit van de bron tot aan mogelijke schade doorrekent.**

Een volledige modelketen gebruikt seismische bronmodellen, modellen voor de voortplanting van seismische golven (inclusief opslingeringseffecten van de ondiepe ondergrond), en schademodellen. Een volledige modelketen is vooralsnog niet goed uit te voeren voor de meeste locaties waar Dinantiën kalksteenreservoirs voorkomen, maar onderdelen uit de modelketen zijn zeer bruikbaar voor simpelere analyses (met name seismische bronmodellen). Een seismische dreiging en risico analyse moet altijd project- en locatie-specifiek uitgevoerd worden, dus is niet zomaar tussen verschillende gebieden te extrapoleren of uit te wisselen.

5) **Er zijn vijf algemene strategieën geïdentificeerd die kunnen worden gebruikt om het monitoren van geïnduceerde seismiciteit in diepe geothermiereservoirs zoals de Dinantiën kalksteenreservoirs te verbeteren:**
   - **Op de schaal van projecten kan het type netwerk (nationaal en/of lokaal) en aantal monitoring stations bepaald worden op basis van een seismische dreiging en risico analyse.** Deze strategie wordt nu uitgerold voor geothermie projecten, maar specifieke eigenschappen van de seismische netwerken zijn nog onderwerp van discussie.
   - **Op de schaal van projecten kan eerst een mobiel netwerk van seismometers gebruikt worden om de achtergrondcondities voor ruis en seismiciteit te karakteriseren. Om kosten te beperken kan dit netwerk vervolgens vervangen wordt door een permanent netwerk met iets beperkter resolutie.** In het ontwerp van het permanente netwerk kan beter rekening gehouden worden met de lokale achtergrond voor ruis en seismiciteit
   - **Op de schaal van een regio met meerdere geothermiesystemen kan een dicht netwerk van seismometers geplaatst worden met seismometers zowel aan het aardoppervlak als op diepte in putten.** Hierdoor wordt een hogere resolutie in aardbevingsmagnitude en een betere locatiebepaling verkregen voor meerdere geothermiesystemen tegelijk.
   - **Op de schaal van Nederland, kan een permanente uitbreiding van het nationale netwerk voor het monitoren van seismiciteit plaatsvinden door het plaatsen van extra monitoring stations.** Hierdoor kunnen voor verschillende type (geothermie of andere) projecten aardbevingen met een lagere magnitude gemeten worden dan nu het geval is.
   - **Een betere integratie van de verschillende lokale, regionale en nationale netwerken onderling en met buitenlandse netwerken in België en Duitsland kan bijdragen aan verbeterde monitoring, in het bijzonder in de grensstreek.** Verbeterde seismische monitoring kan zich richten op automatiseren en standaardiseren van het verzamelen, verwerken, analyseren en ontsluiten van seismiciteitsdata.

   Verbeterde monitoringsstrategieën kunnen vooral bijdragen aan een beter begrip van de relatie tussen ondergrondse activiteiten voor warmtewinning en geïnduceerde seismiciteit. Ze leiden tot een betere detectie van seismiciteit zodat eigenschappen zoals locatie en sterkte beter bepaald kunnen worden. Deze gegevens kunnen gebruikt kunnen worden om het mogelijk optreden van voelbare seismiciteit eerder en beter te voorspellen.

6) **De review van aardbevingen bij bestaande geothermieprojecten die warmte winnen uit verbreukte Dinantiën kalksteenreservoirs in het tuinbouwgebied Californië in Noord-Limburg (maximale lokale magnitude van 1.7), in Balmatt in België (maximale lokale magnitude van 2.1), en in het Molasse Bekken in Duitsland (maximale lokale magnitude van 2.4) laten zien dat:**
   - **Voelbare seismiciteit (M > 2) zeldzaam is in de projecten die geanalyseerd zijn. Als geïnduceerde seismiciteit optreedt, vindt het meestal plaats bij de injectieput.**
   - **Het aantonen van relaties tussen ondergrondse activiteiten voor warmtewinning en geïnduceerde seismiciteit is vaak lastig vanwege een gebrek aan nauwkeurigheid in de snelheidsmodellen van de ondergrond.** Deze modellen zijn nodig om de locatie van aardbevingen goed te kunnen bepalen.
   - **De tijd die zit tussen het optreden van geïnduceerde seismiciteit en (veranderingen) van ondergrondse activiteiten kan sterk verschillen.** Met name de tijd tussen het starten of stoppen van activiteiten en het optreden van geïnduceerde seismiciteit kan sterk verschillen. In de Californië en Balmatt projecten zijn maximale magnitudes opgetreden na het stoppen van activiteiten (bewust of onbewust, bijvoorbeeld door een stroomstoring)**,**
   - **Spanningsveranderingen die optreden tijdens het circuleren van vloeistof voor warmtewinning in geothermieprojecten zijn klein, zeker ver van de injectieput. Desalniettemin kunnen deze leiden tot geïnduceerde seismiciteit.**
   - **Er is discussie over de relevantie van het Kaiser effect voor het optreden van geïnduceerde seismiciteit bij warmtewinning in geothermieprojecten.** Bij herhaalde belasting van een gesteente beschrijft het Kaiser effect de afwezigheid van seismiciteit als de spanningstoestand de kritische toestand van de eerste belasting niet overschrijdt. De kritische toestand wordt bepaald door het optreden van seismiciteit bij de eerste belasting. Het Kaiser effect wordt vaak gebruikt als argument dat het optreden van seismiciteit onwaarschijnlijk is als de initiële kritische spanningstoestand niet overschreden wordt. Deze argumentatie wordt bekritiseerd, omdat er veranderingen in een geothermiesysteem optreden tijdens warmtewinning (bijvoorbeeld temperatuurveranderingen en veranderingen aan breukzones doordat ze bewogen hebben).

Aanbevelingen

- **Ontwikkel *seismische bronmodellen met een fysische basis* die de interactie tussen thermische, hydraulische en mechanische processen en breuken kunnen simuleren. Valideer de modellen met data uit geothermieprojecten met warmtewinning uit Dinantiën kalksteenreservoirs.**
  Dit soort modellen geeft inzicht in de verdeling en veranderingen van druk, temperatuur en spanning in ruimte en tijd, en de effecten op de frequentie en magnitude van aardbevingen. De modellen kunnen onder meer gebruikt worden om (i) verschillen in het seismisch potentieel van kalksteenreservoirs met matrix of breuk gedomineerde stroming te identificeren, (ii) de effecten van snelle afkoeling bij de injectieput op korte termijn en langzame (geleidelijke) afkoeling van het hele reservoir (op lange termijn) te kwantificeren, en (iii) het effect van insluiten van productie- en injectieputten op het optreden van seismiciteit te onderzoeken.

- **Integreer experimentele en modelleer studies voor het bepalen van breukgedrag in kalksteengesteente *tijdens beweging langs het breukvlak*. Dit soort studies zijn nodig om inzichten te krijgen in het samenspel tussen spanningscondities en mineralogie van breukzones en hoe die het optreden van seismiciteit beïnvloedt.**
  In het bijzonder, inzichten in (i) eigenschappen van breuken in kalksteengesteenten die leiden tot afname van de breuksterkte met toenemende snelheid van bewegen wat een rol speelt bij seismische slip en geïnduceerde seismiciteit, (ii) karakteristieke relaties tussen variaties van breuksterkte in tijd en met toenemende verplaatsing langs breukvlakken die de frequenties en magnitudes van aardbevingen en de invloed van mineralogie daarop beschrijven, (iii) verschillen tussen kalksteenreservoirs (klein aantal projecten in Nederland) en zandsteenreservoirs (veel meer projecten in Nederland), en (iv) de variatie in frequentie-magnitude relaties.

- **Ontwikkel een demonstratie geothermieproject voor de Dinantiën kalksteenreservoirs dat ook geschikt is om methoden te evalueren voor (1) het modelleren en monitoren van geïnduceerde seismiciteit en (2) voor het bepalen van de daarbij horende seismische dreiging en risico.**
  In het bijzonder, kennis over de relatie tussen seismiciteit en activiteiten voor warmtewinning in ruimte en tijd door (i) veranderen van operationele factoren om de relatie tussen activiteiten en aardbevingen (van lage magnitude) beter te bepalen, (ii) verbeteren van lokale snelheidsmodellen om de locaties van aardbevingen op diepte beter te kunnen bepalen, (iii) acquisitie van aanvullende seismische data om de locatie van breuken beter te bepalen, (iv) het plaatsen van seismometers in putten op de diepte van het reservoir om aardbevingen met zeer lage magnitude te kunnen detecteren, (v) het uitvoeren van interferentie testen tussen putten om de hydraulische en mechanische interactie tussen reservoir en breuken beter te begrijpen.

- **Optimaliseer maatregelen die het seismisch risico voor kalksteenreservoirs in het Dinantiën helpen beperken. Maatregelen kunnen geoptimaliseerd worden door middel van verbeterde stoplichtsystemen en, daarmee samenhangend, het optimaliseren van operationele factoren in projecten.**

In het bijzonder, onderzoek naar (i) gebruik van meerdere meetbare eigenschappen van seismiciteit in stoplichtsystemen (bijvoorbeeld magnitude, frequentie, grondbewegingen, ruimtelijke verdeling van aardbevingen, afwijkingen van natuurlijke achtergrondwaarden), (ii) het effect van de manier van insluiten van boringen als kritische waarden in stoplichtsystemen worden overschreden, (iii) het gebruik van eigenschappen van aardbevingen die mogelijk vooraf gaan aan meer problematische aardbevingen (bijvoorbeeld de frequentie van aardbevingen met lage magnitudes of het oplijnen van aardbevingen), (iv) het continue evalueren van voorspellingen van snelle modellen door middel van waarnemingen tijdens geothermieactiviteiten (adaptieve stoplichtsystemen), en (iv) optimalisatie van circulatiesnelheid en warmteproductie uitgaande van beperkingen opgelegd door het mogelijk optreden van seismiciteit.

- **Ontwikkel een wetenschappelijke kennisbasis om discussies over acceptabele seismische risico's beter te kunnen voeren. In het bijzonder voor de ontwikkeling van ultradiepe geothermieprojecten die warmte winnen uit de Dinantiën kalksteenreservoirs is duidelijke afstemming en communicatie van acceptabele seismische risico's belangrijk.**
  In het bijzonder, (i) evaluatie van seismische risico's tegen andere typen risico's (bijvoorbeeld risico's van natuurlijke seismiciteit of andere natuurlijke dreigingen, of risico's van andere industriële activiteiten), (ii) bepaling van locatie-specifieke verschillen die van invloed zijn op het niveau van seismische risico's dat geaccepteerd kan worden voor geothermie projecten, (iii) evaluatie van procedures die helpen te bepalen of seismische risico's beneden acceptabel niveau blijven (bijvoorbeeld evaluatie van parameters en grenswaarden in stoplicht systemen), en (iv) bepaling van relaties tussen meetbare parameters en (acceptabele) seismische risico's (bijvoorbeeld relatie tussen magnitude, grondbeweging en seismisch risico).

Summary and conclusions

Induced seismicity (earthquakes) is a main concern for geothermal projects worldwide and its occurrence has played an important role in the development of geothermal projects worldwide. In the Netherlands, most geothermal operations have taken place without recorded seismicity, but seismicity occurred in the vicinity of geothermal projects targeting the Dinantian carbonates in the vicinity of the Roer Valley Graben and near Mol in Belgium. Occurrences of induced seismicity in projects targeting the Dinantian carbonates could hamper development of geothermal energy in deeper ('ultradeep') reservoirs if not properly assessed, evaluated, mitigated and managed.

This report contributes to the understanding of the induced seismicity potential of the Dinantian carbonates in the Netherlands (1) by analyzing key factors affecting induced seismicity potential, (2) by assessing the seismogenic potential for different regions, (3) by reviewing induced seismicity modelling approaches, (4) by comparing approaches for seismic hazard and risk assessment, (5) by providing recommendations for seismic monitoring, and (6) by reviewing selected case studies.

The research allows the following conclusions to be made:

1) **Key factors that affect the *induced seismicity* potential are (i) occurrence of *natural seismicity*, (ii) distance to larger (critically stressed) faults, (iii) interacting stress field, fracture populations and flow regime, (iv) reservoir depth and temperature, (v) composition and competency of reservoir rock, (vi) hydraulic and mechanical decoupling with over- and underburden, (vii) interacting operational factors (flow rate, injection pressure, injection temperature), and (viii) interaction with other subsurface activities such as gas depletion or salt mining.**
   The influence of these factors on the induced seismicity potential is project- and location-specific. At this moment, quantification of the influences in different regions in the Netherlands is hampered by a general lack of data for the Dinantian carbonates. Therefore, only a rough qualitative (small, medium or large effect) analysis can be performed.

2) **The potential for *'felt' induced seismicity* (seismogenic potential) is low to medium for geothermal projects targeting the Dinantian carbonates.**
   The division in low, medium and high seismogenic potential is partly based on a previous review of induced seismicity in projects worldwide[4]. It has been chosen to keep the division consistent between this study and the previous study. In the previous study a high seismogenic potential is mainly associated with geothermal projects in hydrothermal areas with reservoirs consisting of volcanic (igneous) rocks, or with Enhanced Geothermal Systems (EGS) where net fluid injection is performed to stimulate reservoir permeability. In areas with a high seismogenic potential, frequent occurrence of felt seismicity may be observed. The chosen approach has the advantage that the analysis is consistent and that the seismogenic potential can be better compared to international case studies. The seismogenic potential is lower if projects are based on fluid circulation with moderate flow rates, injection pressures and temperature differences between the reservoir and re-injected fluid, *without* stimulation of reservoir permeability by fluid injection and *without* hydraulic

[4] Buijze et al. (2019a), link.

connection to fault zones. Currently, geothermal projects in the Netherlands rely on fluid circulation without stimulation of reservoir permeability by fluid injection. The current approach means that for this type of projects there are no areas with a high seismogenic potential. A high seismogenic potential may only occur if fluid is injected at relatively high pressure or with high flow rates in larger fault zones. Such operations may cause significant stress changes in the faults due to pressure changes or cooling, and can potentially lead to seismic events with frequency and magnitude that are considerably higher than local baselines. The key factors would indicate a high seismogenic potential in that case. A *hypothetical* example of a case with high seismogenic potential would be fluid injection in one of the tectonically active faults of the Roer Valley Graben. Such a scenario is not envisaged for geothermal projects in the Netherlands. To further specify the local or regional seismogenic potential of the Dinantian carbonates, more data on local geology, reservoir properties, and local stress state is needed. Further specification between low and medium seismogenic potential also requires more region- or location-specific research, in particular on the effects of short term cooling at injection wells and on long term cooling of the entire reservoir. In general, the seismogenic potential is lower if wells are not within a critical distance not within a critical distance of (i) natural seismicity in the Roer Valley Graben, (ii) gas depletion induced seismicity or (iii) larger fault zones that bound major structural units. A low to medium seismogenic potential does not mean that felt seismicity cannot be excluded but most likely is limited to some projects where the combination of site-specific factors promote the occurrence of seismicity. The number and magnitude of earthquakes is dependent on these factors, and on implemented measures that mitigate the occurrence of felt seismicity (for example the implementation of traffic light systems).

3) **The review of modelling approaches indicates that problem-specific modelling can increase the understanding of mechanisms underpinning induced seismicity and provide forecasts of characteristics of single seismic events or seismicity catalogues that can be used as input for a seismic hazard and risk assessment (e.g., adaptive traffic light systems).**
   The following broad distinction can be made (i) fast semi-analytical models that allow assessment of uncertainties and can be used in probabilistic seismic hazard and risk assessment, (ii) slower 2D or 3D numerical models that can simulate single seismic events or seismicity catalogues and can be used to explore scenarios of varying geological or operational factors. Another useful distinction is between (i) fully stochastic modelling approaches that are robust and efficient and be used in near real-time to forecast seismic hazard and in adaptive traffic light systems, but lack a mechanistic basis, and (ii) physics-based models that better account for physical processes underpinning induced seismicity, but require more, often poorly constrained, input parameters and are generally computationally intensive.

4) **Seismic hazard and risk analysis can exhibit different complexity. Current approaches range from a qualitative screening of key geological and operational factors to a complete probabilistic model chain that simulates seismicity from subsurface sources to potential damage at surface.**
   A full model chain links seismic source models, wave propagation models, ground motion models and damage models. Currently, it is not really feasible to apply a full model chain to geothermal projects targeting the Dinantian carbonates, but

components from the model chain are very useful to perform simpler analysis of seismic hazards (in particular seismic source models can be applied). Seismic hazard and risk assessment always needs to be site- and project-specific. It cannot be easily extrapolated or exchanged between different regions.

5) **Five general strategies for improved monitoring of induced seismicity in deep geothermal reservoirs such as the Dinantian carbonates can be identified, each with specific scale and cost:**
   - **Project-based design of seismic monitoring (i.e. type of monitoring network, number of monitoring stations) can be based on a project-specific seismic hazard and risk analysis.** This strategy is currently considered best practice, but specific characteristics of suitable seismic monitoring networks are subject of discussion.
   - **Project-based deployment of a high resolution mobile array to characterize noise conditions and monitor background seismicity, followed by local permanent arrays with less resolution to limit costs involved.** Noise conditions and background seismicity determined by the high resolution network can be used to better design the permanent network.
   - **Area-based placement of dense array of both surface and borehole stations can be deployed in areas where multiple doublets are foreseen.** A higher resolution of earthquake magnitude and better assessment of hypocentre locations can be achieved for multiple geothermal systems that are operational in an area.
   - **Nationally, permanent expansion of the national seismic monitoring network to permanently reach lower magnitude completeness level in all parts of the Netherlands.** Higher network resolution can be obtained for different (geothermal and other) projects.
   - **Better integration of different local, regional and national seismic monitoring networks, both within the Netherlands and with networks in Belgium and Germany.** Improved seismic monitoring can focus on automating and standardizing the collection, processing, analysis and publish seismicity data.

   Improved monitoring strategies can contribute to a better understanding of relations between geothermal operations and induced seismicity, and to better detection of seismic events and properties of a seismic cloud (for example, hypocentre and magnitude distribution). This information can be used to better predict the possible occurrence of felt seismicity by identifying precursors such as alignment of events or changes in frequency-magnitude relations.

6) **The review of case studies targeting fractured carbonates in Californië in the Netherlands (max. M_L 1.7), Balmatt in Belgium (max. M_L 2.1) and the Molasses Basin near Munich in Germany (max. M_L 2.4) indicate that:**
   - **Felt seismicity (M > 2) is rare in the case studies reviewed. If induced seismicity occurs, it is generally observed in the vicinity of injection wells.**
   - **Demonstration of spatial relations is critically hampered by lack of resolution of hypocentre locations caused by uncertainties in local seismic velocity models.**
   - **Temporal relations between seismicity and operations may be complex.** In particular, the time between the onset or cessation of operations and the occurrence of induced seismicity may vary. In the Californië and Balmatt projects maximum seismic magnitudes are recorded after (accidental) shut-in, but the time between shut-in and seismic events may vary.

- **Small stress changes caused by fluid circulation may lead to induced seismicity, in particular away from the injection and production wells.**
- **There is debate about the applicability of the Kaiser effect to geothermal operations.** The Kaiser effect describes the absence of seismic events below the stress initially required to induce seismicity, suggesting that seismicity may only occur if this initial stress is exceeded. Its applicability to geothermal operations is questionable because of changes in the physical state of the geothermal system (i.e. temperature changes occur, different fault segments may become reactivated, the physical state of fault zones may change).

Recommendations

- **Development of physics-based seismic source models that can simulate the interaction between coupled thermo-hydro-mechanical processes and faults, in combination with model validation using data from projects targeting the Dinantian carbonates.**
  Such models provide insights into the spatial distribution of pressure, temperature and stress changes and seismicity as well as effects on seismicity rates and magnitudes. In particular, addressing (i) differences in the seismic response of carbonates with fracture- or matrix dominated flow, (ii) short term (fast) cooling at the injector and long term (gradual) cooling of the entire reservoir, and (iii) shut-in of wells and delayed seismicity with relatively large magnitude and seismicity rate.

- **Integration of experimental and modelling studies for post failure rupture behaviour of faults in carbonate rocks to provide insights into the interaction of stress conditions and fault zone mineralogy.**
  In particular, addressing (i) the brittle, velocity-weakening behaviour of fault zones in carbonate rocks which makes them prone to seismic slip and induced seismicity, (ii) characteristic relations between fault strength variations in time and with fault displacement that can describe the frequency and magnitude of seismic events as well as the influence of mineralogy on these relations, (iii) the difference between carbonate (few case studies in the Netherlands) and sandstone (more case studies in the Netherlands) reservoirs.

- **Developing a demonstration field case for the Dinantian carbonates where induced seismicity monitoring and modelling approaches as well as seismic hazard and risk assessment can be evaluated.**
  In particular, addressing spatial and temporal relations between seismicity and operations by (i) applying operational changes to better monitor the temporal correlations of operations and (low magnitude) seismic events, (ii) improving local velocity models to better asses hypocentre locations, (iii) acquiring additional seismic data to improve interpretation of fault locations, (iv) deploying downhole seismometers at reservoir level to detect lower magnitude seismic data, (v) performing well interference tests to better understand the hydraulic and mechanical interactions between reservoir and faults.

- **Optimizing mitigation measures regarding the design of traffic light systems and optimization of operations for the Dinantian carbonates.**
  In particular, addressing (i) multiple characteristics of seismicity in traffic light systems (e.g., magnitude, frequency, ground motions, spatial distribution of events, deviations from natural baselines), (ii) the effect of the way wells are shut-in if traffic light thresholds are exceeded, (iii) precursors to problematic seismicity (e.g., frequency of low magnitude events, or alignment of seismic events), (iv) continuous evaluation of fast (hybrid) model forecasts against observations during operations (adaptive traffic light systems), (iv) dual objective optimization to obtain maximum flow rates given induced seismicity constraints.

- **Analysis of location-specific technical, economic and social factors that help to assess the level of acceptable risk for geothermal projects targeting the Dinantian carbonates.**
  In particular, (i) evaluation of seismic risks against other types of risks (e.g., natural seismicity or other natural hazards, other industries), (ii) assessment of location-specific differences that affect the acceptable level of induced seismicity, (iii) evaluation of procedures that help assessing if seismicity will remain below acceptable levels (for example, evaluation of thresholds in traffic light systems), (iv) relation between measurable parameters and (acceptable) risks (for example, relation between seismic magnitude, ground motion and seismic risk).

1. Introduction

1.1 Project scope

The study reported in this document is a result of SCAN, a large government funded, program to scope out the potential of geothermal energy, including the potential of ('ultradeep') Dinantian carbonate reservoirs. The program is carried out by EBN and TNO, in collaboration with consultants and other stakeholder organizations with interest in 'ultradeep' geothermal energy in the Netherlands. It includes a range of subsurface studies of Dinantian carbonates in the Netherlands. The results of the SCAN studies are released in the public domain and are available via the NLOG data repository[5]. The Green Deal 'UltraDiepe Geothermie' (UDG)[6] agreement has been signed by the industry, knowledge institutes and the government. The purpose of the agreement is to assess the feasibility of Dinantian carbonate rocks at depths over 4 km for hot geothermal projects. The results of SCAN studies are input to activities within this Green Deal UDG agreement as well.

This report is the result of an analysis of factors, models and case studies that are relevant for potential induced seismicity associated with (ultradeep) geothermal projects targeting the Dinantian carbonates in the Netherlands. It is a follow-up of an earlier TNO study "*Review of worldwide geothermal projects: mechanisms and occurrence of induced seismicity*", carried out in the period September 2018 to January 2019 in collaboration with EBN[7]. This earlier review did not focus on any particular reservoir or depth, but rather provided a general overview of seismicity in geothermal projects that is useful for comparison with more detailed analysis of specific geothermal reservoirs or plays.

The present study aims to collect and analyse available data and insights on the relation between geothermal operations and induced seismicity that are relevant for current and future development of (ultradeep) geothermal projects in the Dinantian carbonates.

In particular, the study focusses on the following broad topics:

(1) Key geological and operational factors affecting induced seismicity;

(2) Assessment of seismogenic potential;

(3) Modelling approaches for induced seismicity;

(4) Seismic hazard and risk analysis;

(5) Recommendations for seismic monitoring;

(6) Review of relevant case studies.

For these topics, general concepts are reviewed and implications for development of geothermal projects in the Dinantian carbonates are discussed.

[5] https://www.nlog.nl/scan
[6] Green Deal UDG (2017), link (in Dutch).
[7] Buijze et al. (2019a), link.

1.2 Background

Induced seismicity is a main concern for geothermal projects worldwide and its occurrence has caused public concern and damage at surface infrastructure in some cases outside the Netherlands (Buijze et al., 2019a). Significant delays in development or even cessation of geothermal operations have occurred in certain regions. Relevant examples of induced seismicity that has been associated with geothermal projects in carbonate reservoirs in Europe include projects targeting Malm carbonates in the Molasse Basin near Munich in Germany where seismic events with a maximum magnitude of M_L 2.4 occurred[8]. Although under attention by public, government and researchers, this occurrence of seismicity has not caused significant delays in development of geothermal projects in that area. Another relevant project near Mol in Belgium targets similar Dinantian carbonates as can be found in the Netherlands. Seismic events with a maximum magnitude of M_L 2.1 occurred during operations in that project.

In the Netherlands, most geothermal operations have taken place without recorded seismicity. However, seismicity occurred in the vicinity of geothermal projects targeting the Dinantian carbonates around the Roer Valley Graben in the southeastern part of the Netherlands. This area is known for the occurrence of natural seismicity, and relations between seismicity and geothermal operations are currently under investigation. Induced seismicity has particular focus of attention in the Netherlands due to the frequent occurrence of seismicity associated with depletion of gas, in particular for the Groningen gas field in the North of the Netherlands (Figure 1-1). The occurrence of induced seismicity is determined by a combination of site-specific geological and operational factors (Candela et al., 2018; Buijze et al., 2019a). Most examples of 'felt' ($M > 2$) seismicity associated with geothermal projects occurred in geological settings that are very different from settings in the Netherlands, in particular concerning geothermal systems, reservoir rock types and tectonic regimes. Some operational factors can be varied (within limits) to minimize seismicity. Many site-specific factors can only be taken into account in the design of geothermal projects (e.g., avoiding pore pressure changes in large critically-stressed faults). It is therefore the subject of discussion to what extent findings can be extrapolated outside the regions where geothermal projects induced seismicity. Even within geothermal plays, site-specific variations in factors affecting induced seismicity may hamper the use of general statements. In any case, seismic hazard and risk analysis should be performed for individual projects rather than for regions or entire plays. We therefore focus in this study on analysis of factors affecting induced seismicity for Dinantian carbonates in the Netherlands, their variation within the geothermal play, and their influence on the likelihood of felt seismicity ('seismogenic potential') for specific regions rather than seismic hazards and risks for individual locations.

Concerns related to induced seismicity could hamper development of geothermal energy in the Dinantian carbonates if not properly addressed and understood by the various stakeholder groups. It is therefore of the utmost important for geothermal operators to understand seismic risks associated with projects in the Dinantian carbonates, and to ensure safe and efficient geothermal operations. A robust management plan for dealing with seismic risks is a prerequisite to maintain a social license to operate in the Netherlands.

This report contributes to the knowledge base on induced seismicity that is potentially associated with geothermal operations in the Dinantian carbonates by (1) providing analysis

[8] See Buijze et al. (2019a) for definition of different concepts used in the analysis of induced seismicity, including seismic magnitude scales, natural/triggered/induced seismicity, and ground motions (PGA or PGV), p. 14-16 (section 1.3).

of important factors, (2) outlining modelling options that help understanding seismic risk and forecasting induced seismicity, (3) providing recommendations for seismic monitoring, and (4) presenting detailed analysis of selected case studies relevant for the Dinantian carbonates. Literature, data and field cases from publicly available sources that were published before December 2019 were included in the research.

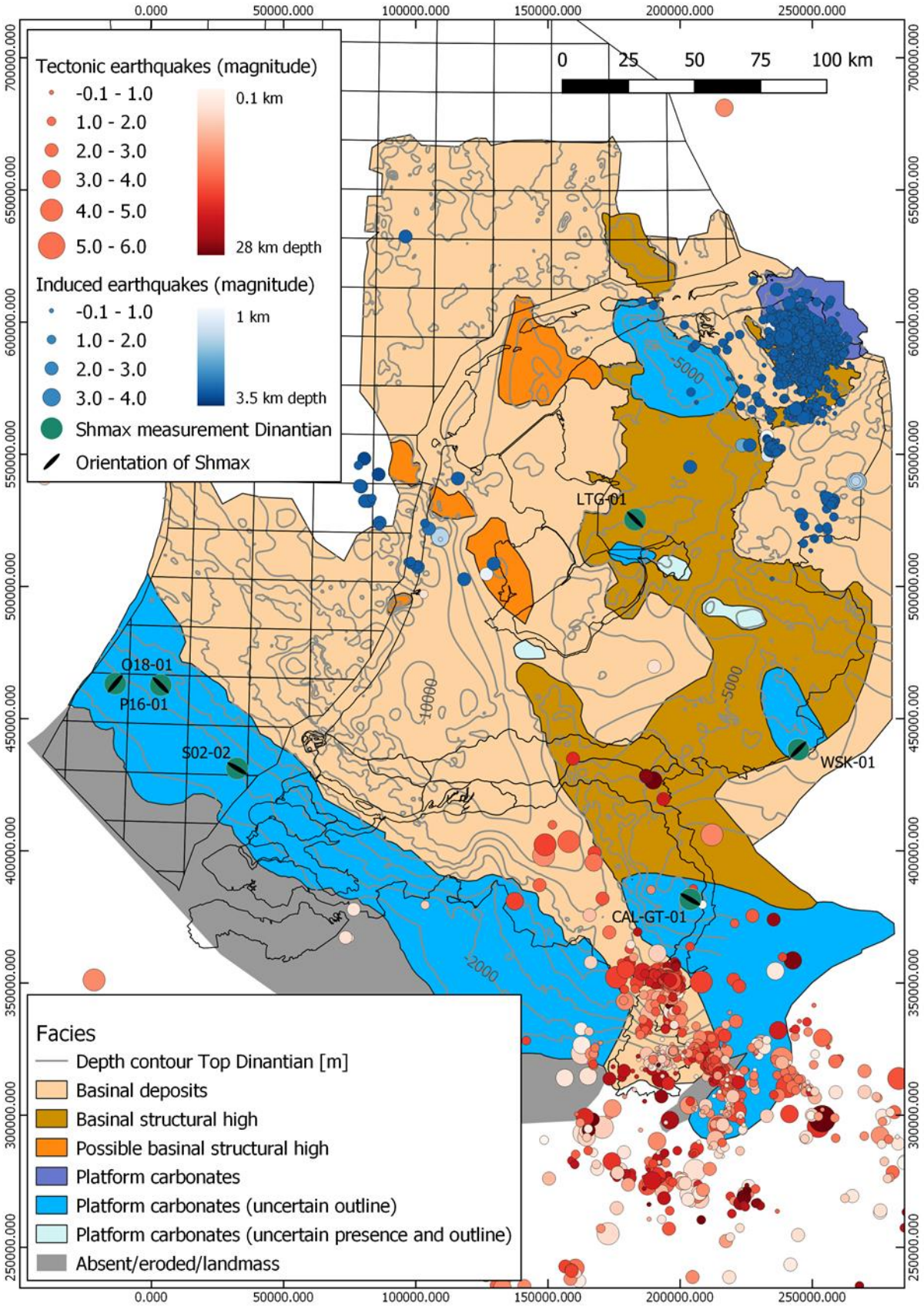

Figure 1-1 Possible spatial distribution of the Dinantian carbonates in the Netherlands (compiled by Mozafari et al., 2019 and Ten Veen et al., 2019) with occurrences of natural and induced seismicity (indicated with red and blue dots, compiled in this study), orientation of intermediate principal stress S_{Hmax} (indicated with light green dots with black line, compiled by Osinga and Buik, 2019).

2. Key factors affecting induced seismicity potential in Dinantian carbonate geothermal reservoirs

One of the main findings of the review study by Buijze et al. (2019a)[9] was the identification of several geological and operational factors that influence the occurrence of induced seismicity. In this section we focus on the factors that are most relevant for Dinantian carbonate reservoirs.

As some factors are better addressed in an integrated manner and others are better differentiated for different areas in the Netherlands, we distinguish the following main geological factors in this study:

- Occurrence of natural seismicity and regional natural seismic hazard;
- Distance to large (critically stressed) faults;
- Stress field, fracture populations and flow regimes (i.e. matrix- or fractured-dominated flow, or a combination of both);
- Reservoir depth and temperature;
- Hydraulic and mechanical coupling with over- and underburden;
- Composition and competency of reservoir rock;

The main operational factors that have been identified by Buijze et al. (2019a) are:

- Difference between initial reservoir pressure and pressure during fluid injection;
- Difference between initial reservoir temperature and temperature of the injected fluid;
- Net injected volume during geothermal operations;
- Interaction between different subsurface activities (such as operations for geothermal energy, gas production, salt mining, storage of gasses or fluids that are performed relatively close to each other at the same time or that are performed sequentially at the approximately the same location so that subsurface effects interfere).

It should be noted that some of these factors are interrelated and therefore interaction of different factors should be considered when applying them in site-specific analysis of induced seismicity. For example, higher reservoir temperatures may be present at larger depth, but deeper reservoirs may also be tighter (lower matrix porosity and permeability), more competent, and more prone to fracture-dominated flow. Flow patterns in fractured reservoirs are often more anisotropic and hydraulic connection to larger critically stressed faults will be governed by fracture properties rather than by matrix permeability. Also, higher fluid pressures are needed in tight reservoirs to obtain similar flow rates as in more permeable (shallower) reservoirs.

Current geothermal projects in the Netherlands are based on circulation of fluids from (relatively) hot sedimentary aquifers using, in most cases, doublet systems, or, in some cases, systems with multiple injection and production wells. Some projects perform chemical stimulation to clean the wells or enhance near well reservoir permeability. Hydraulic stimulation to enhance reservoir permeability is not performed in geothermal projects in the Netherlands. Geothermal systems targeting Dinantian carbonate reservoirs in the Netherlands also rely on fluid circulation (i.e. the Californië projects, cf. section 7.1). Given large uncertainties in reservoir characteristics, stakeholder perceptions and economics of geothermal projects, it is uncertain whether hydraulic stimulation will be considered in future

[9] See Buijze et al. (2019a), p. 49-58 (section 3.2, Table 3-2).

development of the Dinantian carbonate geothermal play. These points are important as felt seismicity in geothermal projects is mostly associated with Enhanced Geothermal Systems (EGS) or Hydrothermal Systems (HS) rather than with Hot Sedimentary Aquifers that are typical for geothermal reservoirs in the Netherlands (Figure 2-1, see also Buijze et al. 2019a).

In the following sections we analyse the different factors for the Dinantian carbonate geothermal plays. A qualitative classification of the factor is outlined, distinguishing between small, medium and large effect of factors on the *potential* occurrence of induced seismicity. It should be noted that a general consideration is the lack of data for the Dinantian carbonates in most regions in the Netherlands. A description of data availability and associated limitation of the analysis is therefore included for each factor. In general, analysis of each factor is subject to large uncertainties and should be treated as a first order screening rather than a detailed assessment. Factors that affect the occurrence of induced seismicity are site-specific, and the current analysis of effects is regional. The analysis is not suitable to assess seismic risks of individual projects. In any case, seismic hazard and risks analysis for projects requires site-specific analysis of factors (cf. sections 3 and 0).

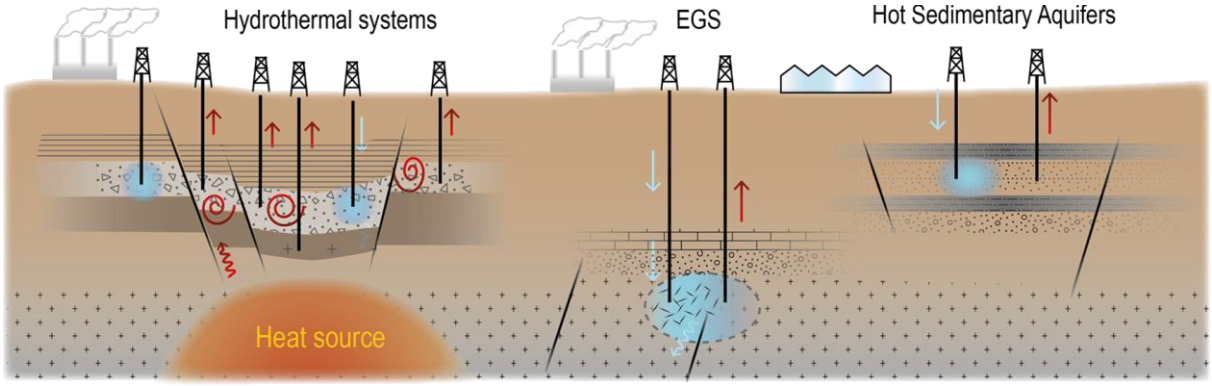

Hydrothermal systems/Geothermal Fields (HS/GF)	Enhanced Geothermal Systems (EGS)	Hot sedimentary aquifers (HSA)
Active tectonic areas, convection-dominated	Active or inactive areas	Tectonically quiet. Conduction-dominated
Electricity, direct-use T > 400 °C	Electricity, direct-use. T > 220 °C	Direct-use, electricity (T 30 - 170 °C)
No stimulation	Stimulation required, dP 10 - 90 Mpa	No stimulation. Porous/permeable sediments
Production wells (+ reinjection wells)	Doublet	Doublet
Volcanics, metamorphic, sediments	Crystalline, tight sediments	Porous sandstones, permeable carbonates

Figure 2-1 Main types of geothermal systems with some characteristics. Note that all geothermal systems in the Netherlands are Hot Sedimentary Aquifers that rely on fluid circulation without hydraulic stimulation of reservoir permeability. From: Buijze et al. (2019a).

2.1 Occurrence of natural seismicity and regional natural seismic hazard

Effects of natural seismicity and natural seismic hazard on induced seismicity

The occurrence of natural seismicity is a clear indication of the presence of critically stressed faults with properties that lead to seismic slip. If geothermal operations influence the stress state at these faults, the timing, frequency and magnitude (or typical Gutenberg-Richter relations between magnitude and frequency of seismic events)[8] may change (McGarr et al., 2002). Seismic events with $M_L > 2$ are more frequent in areas with elevated natural hazard (typically above 0.8 m/s^2 for igneous rocks, Evans et al., 2012). However, cases exist where $M_L > 2$ events occurred in areas with low seismic hazard (e.g., M_L 2.4 for carbonate reservoirs in the Molasse Basin[10] with PGA of ~0.7 m/s^2, cf. section 7.3).

Data availability and limitations relevant to natural seismicity and seismic hazard

Data on the occurrence of natural seismicity is routinely acquired, processed and stored on a publicly accessible repository by the Royal Netherlands Meteorological Institute (KNMI)[11]. Natural seismicity is mainly confined to large faults in the Roer Valley Graben (RVG), which is the north-western extension of the Rhine rift system (**status 1st October, 2019**; Figure 2-2 to Figure 2-4; see also Figure 7-3; Dost and Haak, 2007). The temporal evolution of natural seismic events indicate the recurrence interval of larger magnitude events (Figure 2-5). Dost and Haak (2007) suggest that hazard analysis based on historical seismicity indicate a maximum expected magnitude of M_L 6.3, and an average recurrence interval of 2000-3000 year for events of one magnitude higher. The strongest event (M_L 5.8) over the last 100 years occurred on April 13, 1992, just south of Roermond, and was associated with the Peel Boundary Fault. Dost and Haak (2007) indicate that the average error in epicentre location is ~1 km, and the depth resolution is several kilometres. The lack of depth resolution is mainly caused by uncertainties in velocity model (mainly lack of shear wave data)[12]. Limits in hypocentre resolution for natural seismic events are important as disentangling natural and induced seismicity in areas with active tectonics can usually only be performed by detailed analysis of spatial and temporal correlations between subsurface operations and seismic events (preferably in combination with detailed modelling of likely stress changes associated with the operations)[13]. Some studies also consider triggered seismicity to interact with induced seismicity in areas with active tectonics (McGarr et al., 2002)[8]. Areas with natural seismicity often have elevated natural seismic hazard (expressed as the peak ground acceleration, PGA, with 10% chance of exceedance in 50 years, Giardini, 1999). Natural seismic hazard is generally low in the Netherlands (PGA < 0.4 m/s^2) with elevated levels (up to PGA ~1.2 m/s^2) in the south-eastern part of the Netherlands where natural seismic events are common[14]. These values are from global seismic hazard maps and therefore have limited resolution for the Netherlands.

Natural seismicity and natural seismic hazard for Dinantian formations

Except for some isolated events, the occurrence of natural seismicity in the Netherlands is constrained to the area in the vicinity of the Roer Valley Graben (RVG, Figure 2-2). The spatial extent is roughly south of the river Waal between Nijmegen and Tiel, and east of the line between Tiel and Tilburg. Seismicity is mainly concentrated in a NW-SE trending area

[10] See also Buijze et al. (2019a), p. 54-55 (Figure 3-12).
[11] https://www.knmi.nl/nederland-nu/seismologie/aardbevingen
[12] See also Buijze et al. (2019a), p. 72-74 (section 5.2.2).
[13] See also Buijze et al. (2019a), p. 86-88 (section 6.4).
[14] See also Buijze et al. (2019a), p. 12 (Figure 1-2).

south of Roermond bounded by the Peel Boundary and Feldbiss Fault zones (Figure 2-3). This area is characterized by an elevated natural seismic hazard (PGA ~0.8-1.2 m/s^2). Accordingly, a large effect of natural seismicity and natural seismic hazard may be expected for the area where natural seismic events are concentrated. The Dinantian formations are expected to be mainly characterised by deep basinal deposits in this area. A medium effect may be expected for other parts of the RVG where some natural seismic events occur, but natural seismicity is less prominent. The Dinantian is characterised by basinal structural highs or platform carbonates in these parts. A small effect may be expected for parts of the Netherlands with isolated natural seismic events. For other parts of the Netherlands, the effect is absent.

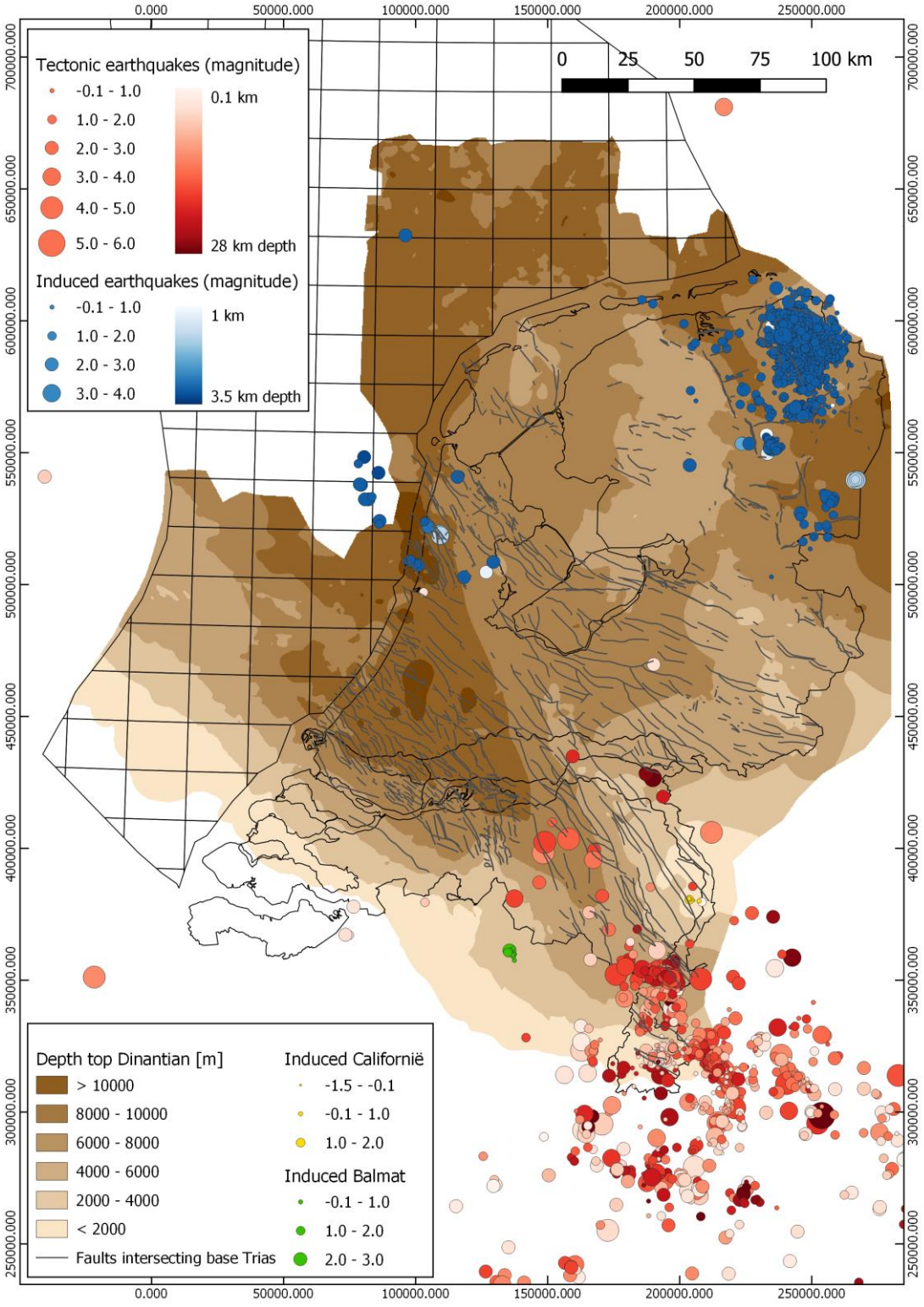

Figure 2-2 Natural (tectonic earthquakes) in the Netherlands and surrounding regions in Belgium and Germany. Induced seismicity related to gas production in the Netherlands (blue dots) and for the Californië (yellow dots; Burghout et al. 2019) and Balmatt (green dots, seismicity between 01-01-2019 and 01-10-2019; KSB[15]) geothermal projects (status 1st October 2019). Seismicity is plotted on top of a depth map for the Top Dinantian. Main faults intersecting the base Trias are also indicated. Note that mapping of these faults has been subject to limited quality control and should be used as an overview rather than a detailed fault map (cf. section 2.2).

[15] Royal Observatory of Belgium (Koninklijke Sterrenwacht van België), link

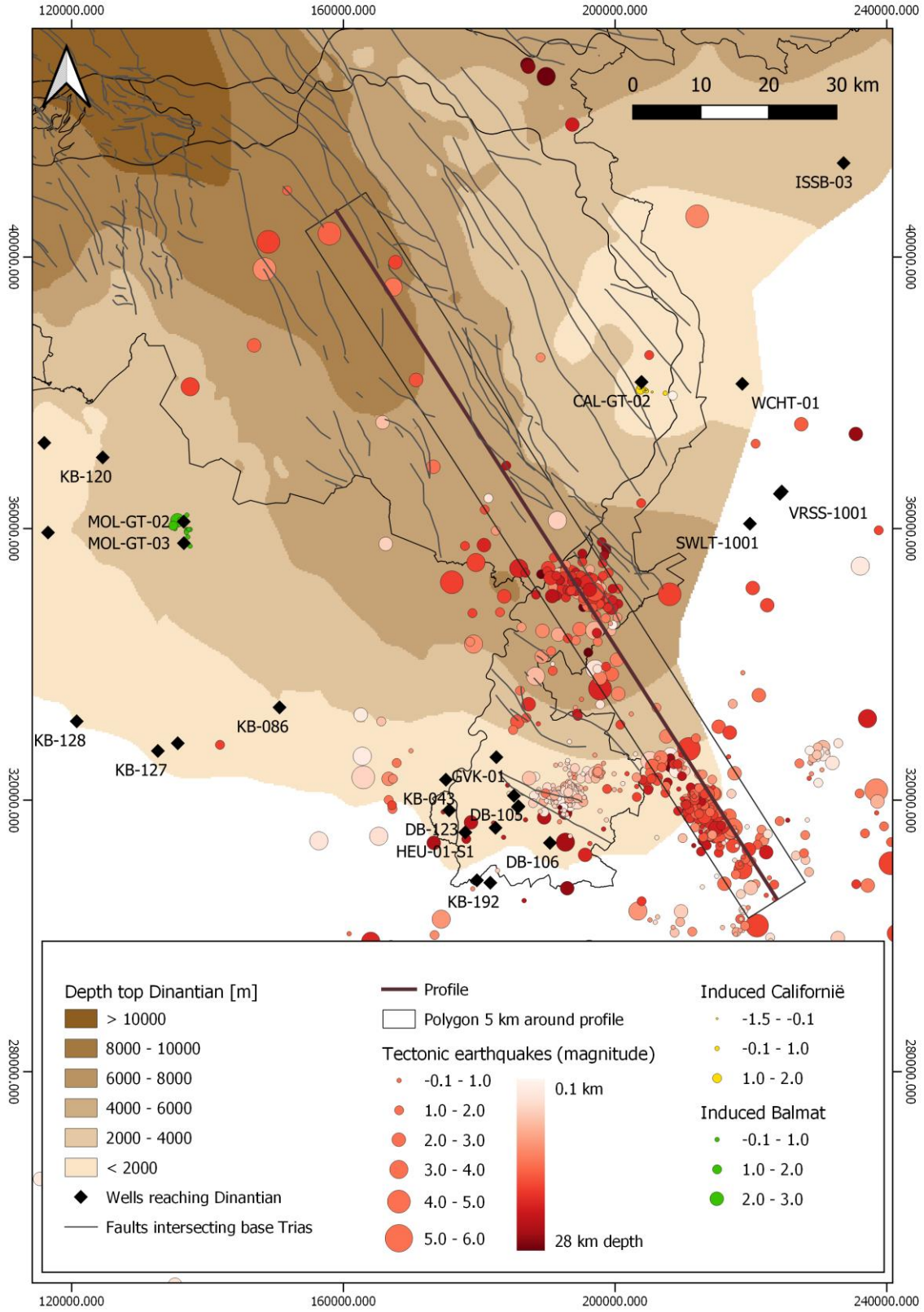

Figure 2-3 Natural (tectonic) seismicity in and around the Roer Valley Graben (red circles), induced seismicity at the Balmatt (green circles) and Californië (yellow circles) projects, and wells reaching Dinantian formations (diamonds with labels). The profile line is indicated in purple with a 5 km wide polygon around it to indicate the earthquakes which are projected on the profile shown in Figure 2-4. The profile is approximately parallel to the strike of the main faults within the Roer Valley Graben, covering part of the area bounded by the Peel Boundary and Feldbiss Fault zones.

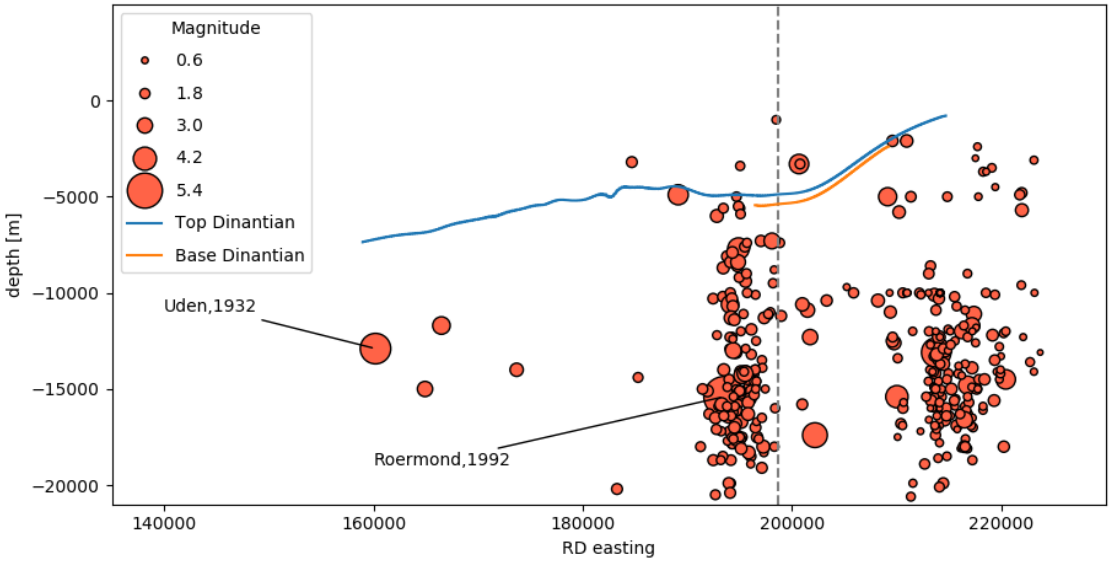

Figure 2-4 *Natural* seismicity along a profile that is approximately parallel to the strike of main faults around the Roer Valley Graben, and that is partly covering an area bounded by the Peel Boundary and Feldbiss Fault zones with interpreted top and base of Dinantian and natural seismicity within a 5 km radius of the profile (cf. Figure 2-3). Vertical grey dotted line indicates the border between The Netherlands and Germany. Note that the depth uncertainty of the hypocenters is in the order of several kilometres (Dost and Haak, 2007). Uncertainty in the depth of the Dinantian horizon is indicated by mis-ties of wells and horizons from seismic data. The mis-tie in wells CAL-GT-01 and CAL-GT-02 closest to the profile line is 159-272 meter (Ten Veen et al., 2019). The uncertainty in the depth of both the top and base of the Dinantian horizons in this profile is also considerable.

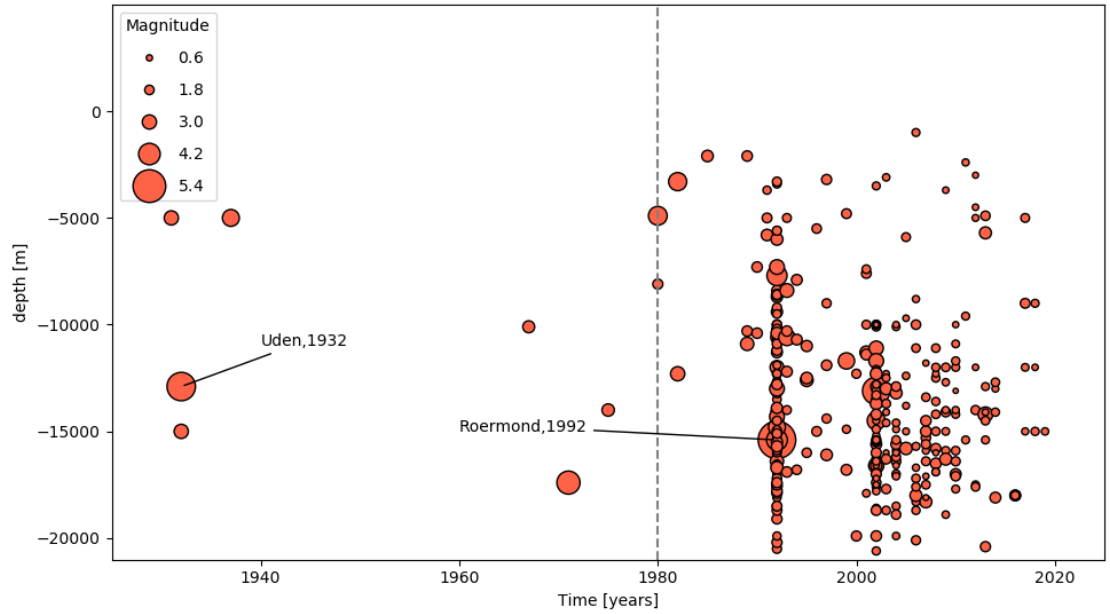

Figure 2-5 Temporal evolution of natural seismic events in the Roer Valley Graben covered by the polygon indicated in Figure 2-3. Grey dotted line indicates the timing of improved seismic network with an increased number of seismological instruments, resulting in a lower detection threshold and a larger number of detected earthquakes (Dost and Haak, 2007).

2.2 Distance to large (critically stressed) faults

Effects of distance to large (critically stressed) faults on induced seismicity

This factor combines three fault properties that are required for a fault to be reactivated and cause felt seismicity: (1) the fault needs to be large enough to accommodate a seismic event that can be felt at the surface and (2) the stress state has to be such ('critically stressed') that the fault can be reactivated by small stress changes resulting from geothermal operations, and (3) the composition of the fault rock must be such that fault slip can be seismogenic (i.e. brittle, velocity weakening behaviour that leads to unstable slip as faults become weaker with increasing slip rate, Scholz, 1998).

It is useful to adopt the concept of ***critical distance of geothermal operations to faults*** at which induced seismicity may occur. Operations within this critical distance may lead to fault reactivation and induced seismicity if conditions favourable for seismic slip are met, while the effect of operations (i.e. stress changes) at larger distance is negligible. This critical distance depends on many factors, both related to the type of operations as well as to fault properties. Interacting direct pore pressure, poroelastic and thermoelastic effects determine the stress changes ***in and around*** the reservoir, and are controlled by operational factors such as ***injection pressure, rate, volume and temperature***[16] for specific reservoir properties. The critical distance is generally larger for higher injection pressure, rate, volume and temperature differences between injection and reservoir fluids.

For geothermal (doublet) systems based on circulation of fluids, changes in reservoir pore pressure are generally limited. Changes in reservoir temperature will be more significant for deeper targets (cf. section 2.4). The ***initial state of stress along pre-existing faults*** is of key importance in determining the critical pore pressure and stress changes for fault reactivation and induced seismicity (cf. section 2.3). Only minor perturbations in pore pressure may already lead to seismicity in the case of critically stressed faults, while in case of non-critically stressed faults induced seismicity may only be observed after significant pressure changes have occurred (Candela et al., 2018). As pore pressure and stress changes generally decrease away from wells, the critical distance is larger for critically stressed faults than for non-critically stressed faults. ***Hydraulic connections to fault zones*** promote fault reactivation due to a large contribution of direct pore pressure effects. Besides pore pressure and stress changes, ***reservoir rock type, fracture populations and fault zone architecture*** (i.e. the structure of a fault zone, including fault core and damage zone) control hydraulic connection with faults and thereby the critical distance. ***Fault size, displacement and damage zone width*** are interrelated as demonstrated by compilations of fault scaling laws (Bonnet et al., 2001; Torabi and Berg, 2011; Ter Heege, 2016), and need to be taken into account in assessment of hydraulic connections to fault zones and critical distance of operations to faults.

The rupture area required to induce an *M* 2 earthquake can be as low as ~70 meter (Zoback and Gorelick, 2012)[17], so faults that can accommodate *M* 2 seismicity may not be visible on data from seismic surveys. The ***spatial distribution of induced seismicity*** (i.e. lateral extent of the seismic cloud) can be used as an approximate indication of the extent of stress changes due to geothermal operations for individual projects. Without more detailed site-specific data, models that assess the relation between operations and spatial distribution of stress changes

[16] See also Buijze et al. (2019a), p. 24-33 (sections 2.4-2.5).
[17] See Buijze et al. (2019a), Fig. 6-2, p. 84.

for specific geological and operational parameters may be used to provide an approximate indication of a typical critical distance between operations and faults (Ter Heege et al., 2018a, see section 4). The spatial distribution of induced seismicity around injection wells is typically below 1 km (mainly EGS[18], but also Balmatt in Belgium, cf. section 7.2). For karstified or fractured carbonate reservoirs, analysis of the critical distance is complicated by the ***heterogeneous reservoir properties and occurrence of karsts and fracture populations***. These features may lead to highly anisotropic reservoir permeability and associated preferred fluid flow directions, i.e. flow patterns may show large deviations from radial patterns in reservoirs with isotropic permeability. Pore pressure, temperature and stress changes in preferred directions of flow may be extended beyond the radial patterns observed in (sandstone) reservoirs with more isotropic permeability. Accordingly, more complex flow patterns may be expected and the critical distance is more difficult to assess.

Data availability and limitations relevant to distance to faults

A clear limitation is that to date no complete fault data set exists for faults intersecting the Dinantian carbonates in the Netherlands (see also the SCAN seismic interpretation and depth conversion study; Ten Veen et al., 2019). Some faults have been (re-)interpreted and approximate timing of fault movement has been determined, mainly on the basis of 2D seismic surveys (Figure 2-6; Appendix 11; see also SCAN burial and reconstruction study, Bouroullec et al., 2019). In addition, some faults intersecting the Dinantian have been interpreted on 3D seismic data in the North of the Netherlands around the Uithuizermeeden and Friesland platforms (Figure 2-7). There are indications for the presence of major carbonate platform bounding faults at the Uithuizermeeden, Friesland and Luttelgeest platforms as well as intra-platform faults. A map was constructed with faults intersecting the base Trias to identify larger faults that are likely to reach down to the Dinantian (Figure 2-6). This map is a compilation of different studies, carried out on different scales, resulting in a varying degree of detail and fault densities throughout the map. It has been subjected to limited quality control. It should only be used as a rough indication of larger fault structures and orientations in the Netherlands, and not as a map with accurate fault locations.

Accordingly, some important general limitations for analysis of the distance to large (critically stressed) faults for the Dinantian carbonates are:

- Detailed fault analysis at Dinantian level is prohibited by a lack of sufficient seismic data;
- All interpretations of faults intersecting the Dinantian are subject to considerable uncertainty, and fault maps have been subject to limited quality control and cannot be regarded as a complete fault map of the Netherlands;
- Due to poor seismic resolution at greater depths, it is unclear to what depth the major faults extend that bound major structural elements in the Netherlands;
- Data on timing of fault movement and magnitude of fault throw from structural restoration techniques are also subject to assumptions in applied techniques and uncertainties related to the data used, and therefore should be considered as rough estimates only.

Distance to large (critically stressed) faults for Dinantian carbonates

A large effect of distance to faults on induced seismicity potential may be expected for large faults that are critically stressed and within the critical distance to operations. The occurrence of *natural* seismicity in the Roer Valley Graben (section 2.1) is a good indicator of the

[18] See Buijze et al. (2019a), p. 121-232 (appendix A).

presence of critically stressed faults. A medium effect may be expected for the large faults with unknown stress state that intersect the Dinantian, for example faults separating major structural units (e.g., carbonate platforms) in the Netherlands, in particular the ones for which relatively recent stages of fault movement have been constructed (Figure 11-1; Figure 11-2; Figure 11-3). A small effect may be expected for smaller faults that are within the critical distance for operations, which can be determined by modelling (cf. section 4).

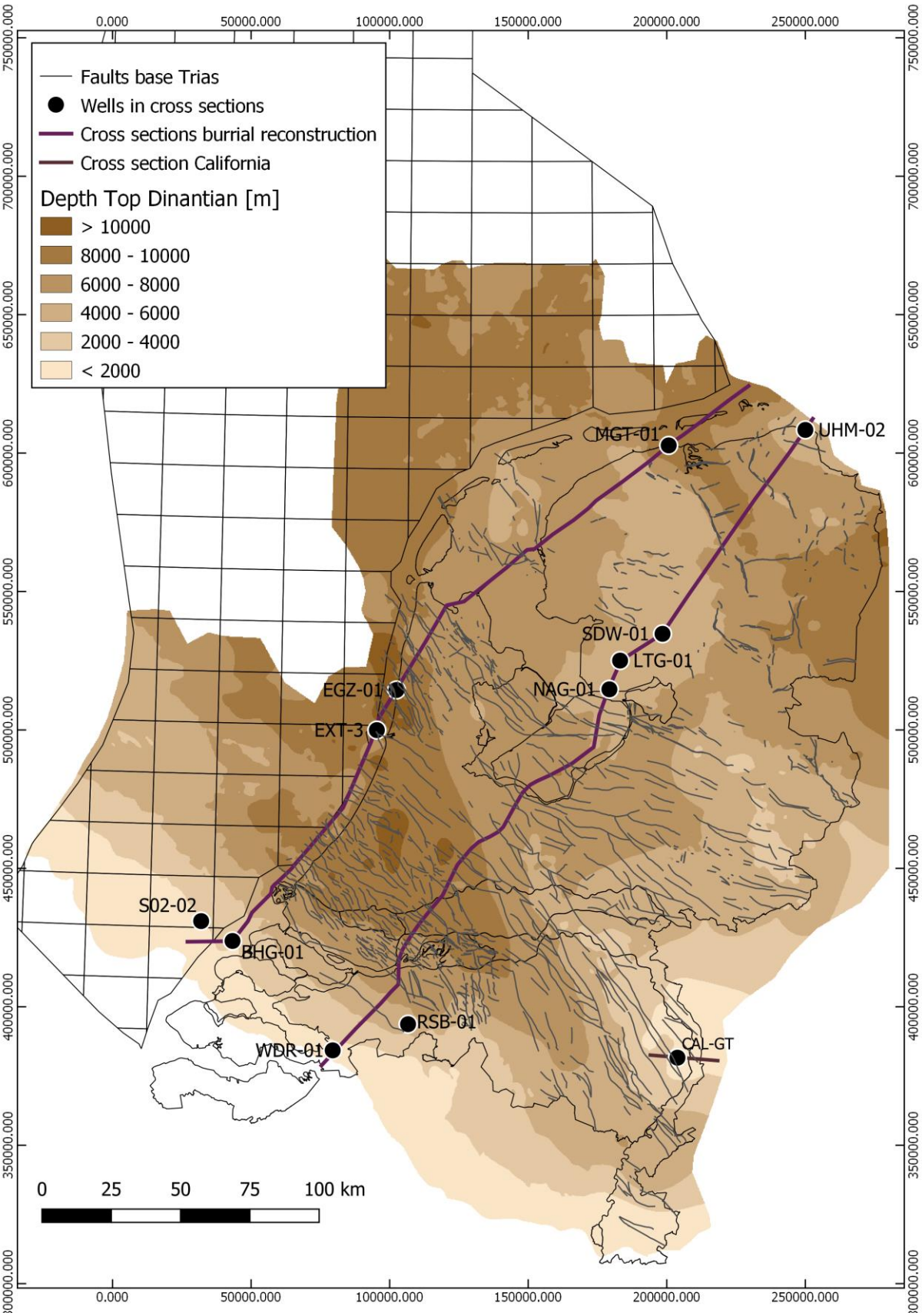

Figure 2-6 Depth map of ***top Dinantian*** overlain by faults intersecting the ***base Trias***. The two purple lines indicate the two cross-sections (Western: Figure 11-1 and Central: Figure 11-2) that were constructed in the SCAN Burial and Reconstruction study Bouroullec et al. (2019). The brown line indicates the cross section reconstructed around the CAL-GT well (cf. Figure 7-1). Faults intersecting the base Trias are uncertain and subject to limited quality control (see text for details).

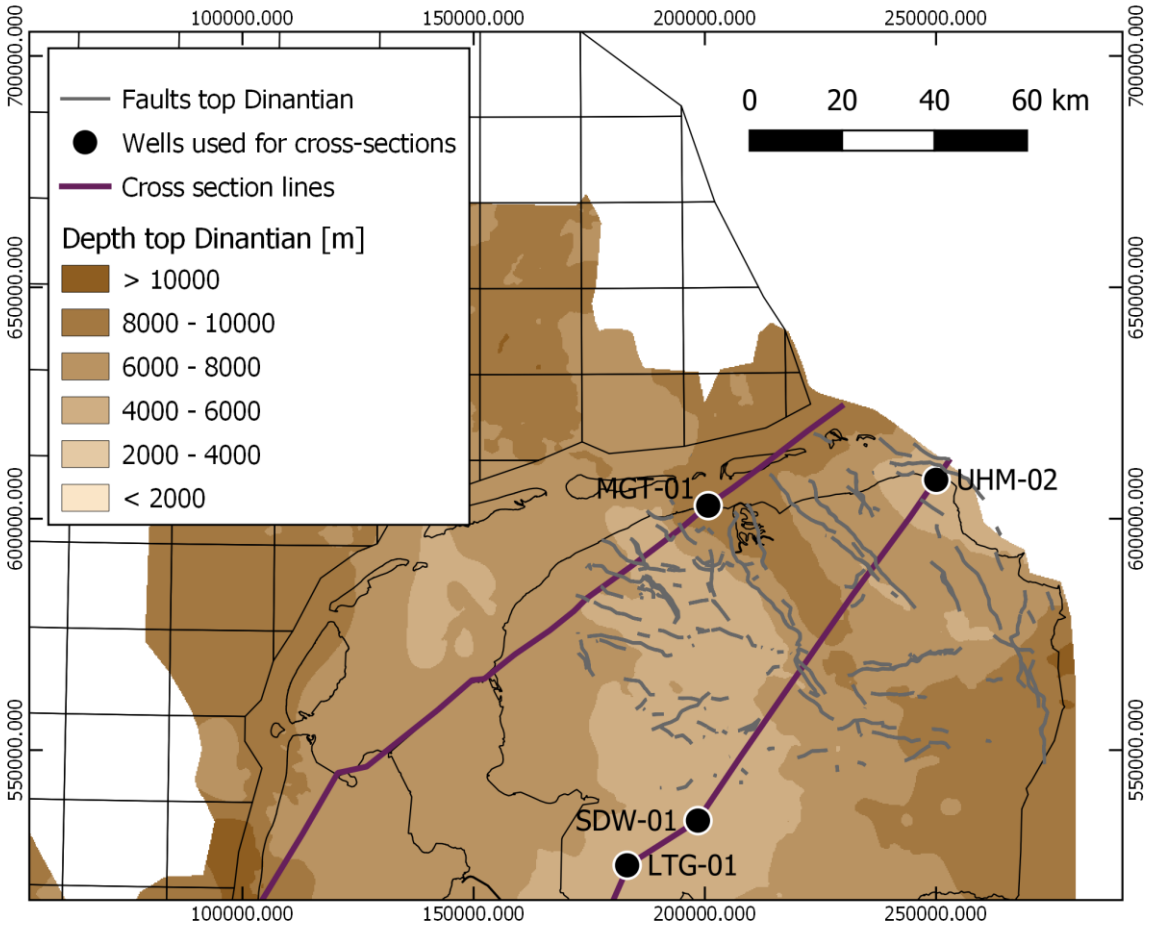

Figure 2-7 Intersection of interpreted fault planes with top Dinantian, projected on the depth map of the top Dinantian. The purple lines show the cross-sections interpreted in the SCAN burial and reconstruction study (cf. Figure 2-6)

2.3 Stress field, fracture populations and flow regimes

Effects of stress field, fracture populations and flow regimes on induced seismicity

The stress field, fractures and fluid flow interact in determining the effects on induced seismicity. Together with stress changes due to subsurface operations, the local stress field determines the stress state and stability of faults. Lower ***differential stresses*** (S_1-S_3, i.e. S_v-S_{hmin} for normal faulting regimes) promote fault stability, and thereby lower the likelihood of fault reactivation and induced seismicity. The prevailing stress field also determines properties of fracture populations, such as ***fracture orientation, density and flow properties***. Anisotropic stress fields may result in ***preferred fracture orientations***. Large differential (compressional) stresses promote ***shear fracture initiation, reactivation and slip*** along new or existing fractures. Slip along fractures generally result in dilatation and larger ***hydraulic aperture*** which enhances fluid flow rates. Tensile stresses also promote ***open tensile (hydraulic) fractures*** and enhance fluid flow, but these may only occur *naturally* in cases of high reservoir overpressures (e.g., in case of tectonic inversion). ***Reservoir rock type*** and ***fault zone architecture*** also control properties of fracture populations and fluid flow. Fractures are closely related to faults. Fracture density increases in ***damage zones*** of large fault zones (Faulkner et al., 2010), and ***fracture orientations*** generally have specific angular relations with fault planes (i.e. Riedel orientations, Tchalenko, 1970). ***Fault size, displacement and damage zone width*** are interrelated (cf. section 2.2), so fracture populations can show a larger spatial extent around larger fault zones with large displacement compared to smaller fault zones. Accordingly, fluid flow in fractured reservoirs and around fault zones is governed by a complex interplay between stress field and fracture properties which lead to more complex (anisotropic) flow patterns and spatial extent of stress changes compared to reservoirs that are not fractured. Hydraulic interference between wells and between wells and fault zones are therefore more difficult to predict in fractured and faulted reservoirs.

Data availability and limitations relevant to stress field, fracture populations and flow regimes

Recent reports by Osinga and Buik (2019), and Van Leverink and Geel (2019), which were conducted in the framework of the SCAN project, describe the characterization of the stress field and fractures of the Dinantian carbonates in the Netherlands. Data on both the stress field and fractures is very limited (Figure 2-8). Analysis of the stress field is based on well data alone. An important limitation is that currently available stress data only reports directions of S_{Hmax}. Data from (extended leakoff) well tests that can be used to determine magnitude of S_{hmin} are not available (Osinga and Buik, 2019). Fracture data is based on analysis of core samples and (formation micro-imager, FMI) well data (Van Leverink and Geel, 2019). Combined stress, fracture and flow (well test) data for the Dinantian are rare (Figure 2-9). Good examples where stress field, fracture and flow resulted in a working geothermal system are the Californië and Balmatt geothermal projects (cf. section 7), but induced and/or natural seismicity are critical factors in these projects. The presence of karsts in Dinantian carbonates has also been shown to play an important role in promoting flow, and can dominate or interfere with flow through networks of open fractures (Amantini et all., 2009; Reith et al., 2010).

Stress field, fracture populations and flow regimes for Dinantian carbonates

The direction of S_{Hmax} in the Dinantian carbonates (NW-SE, mean direction 317°-137°) aligns with the generally dominant direction of S_{Hmax} in the Dutch subsurface (NW-SE to NNW-SSE, mean direction for the Limburg Group, 325°-145°). For some areas in the eastern (WSK-01) and southern offshore (O18-01), S_{Hmax} in the Dinantian is ~90° rotated (NE-SW direction). In general, the stress state in the upper 3-4 km of the crust in the Netherlands

indicates a normal faulting regime ($S_v > S_{Hmax} > S_{hmin}$), with a relatively small anisotropy in horizontal stresses of ~5-20%. The state of stress may become fully isotropic ($S_v = S_{Hmax} = S_{hmin}$) in formations that exhibit plastic creep deformation, such as salt and clayey shales (cf. section 2.5), which lead to more stable faults. Source mechanisms derived from deeper (10-25 km) natural earthquakes in the south of the Netherlands (cf. Figure 2-3 and Figure 7-3) also show a largely normal faulting character, and a NW-SE direction of S_{Hmax}. A small strike slip ($S_{Hmax} > S_v > S_{hmin}$) component is present that becomes more important towards the south of the Roer Valley Graben (South Limburg Block, Dost and Haak, 2007). For deeper parts of the crust in other parts of the Netherlands, the stress state is largely unknown. The general alignment of the stress field between the Limburg Group and Dinantian formations suggests that the stress state in the crust down to the Dinantian is coupled so that the overburden stress state is also indicative for the stress state in the Dinantian. The main strike direction of both faults and fractures aligns with the dominant direction of the main structural units and faults in the Netherlands (i.e. NW-SE to NNW-SSE, cf. Figure 2-6 for faults at base Triassic level and Figure 2-9 for fractures in Dinantian carbonates). If slip tendency is considered (cf. ***BOX 4.1***), faults in the Dutch subsurface are most likely to be reactivated when they are dipping at ~60° and have a NW-SE strike (~135-215°). The reactivation is most likely to occur in normal faulting mode with dip parallel fault slip. Since the anisotropy in horizontal stress tends to be small, deviations in strike are less important than deviations in dip. Given that heterogeneous reservoir properties and occurrence of karsts and fracture populations are expected in the Dinantian carbonates (Mozafari et al., 2019; Van Leverink and Geel, 2019), fluid flow and hydraulic interactions between wells and faults in the Dinantian carbonates will be complex and anisotropic.

As the influence of critically stressed faults is already addressed (cf. section 2.2), the interaction between stress field, fracture populations and karstification and the influence on the flow regime in the reservoir is considered here. It is assumed that the induced seismicity potential is smaller for reservoirs with relatively large permeability (e.g. due to karstification) and for reservoirs with isotropic flow patterns, while the induced seismicity potential is larger for relatively low permeabilities (likely higher injection pressures required) and anisotropic flow patterns. These effects are potentially amplified by the fact that injection pressures need to be higher in low permeability reservoirs with fracture-dominated flow to obtain similar flow rates as in more permeable reservoirs with matrix-dominated flow. Accordingly, a small effect may be expected for Dinantian carbonates where flow is dominated by relatively high matrix porosity or karstification (i.e. relatively high permeability) with little influence of fracture populations. A medium effect may be expected for fractured Dinantian carbonates with flow dominated by conductive fractures that are approximately randomly orientated (for example due to limited anisotropy in horizontal stress), which would lead to isotropic (radial) flow patterns and smaller spatial extent of stress changes for similar flow rates. A large effect may be expected for fractured Dinantian carbonates with strong preferred orientation of fractures and large anisotropy in stresses (i.e. large slip tendency of the fractures), which would lead to anisotropic flow patterns and potentially large spatial extent of stress changes in preferred flow directions (and larger probability that these stress changes reach fault zones).

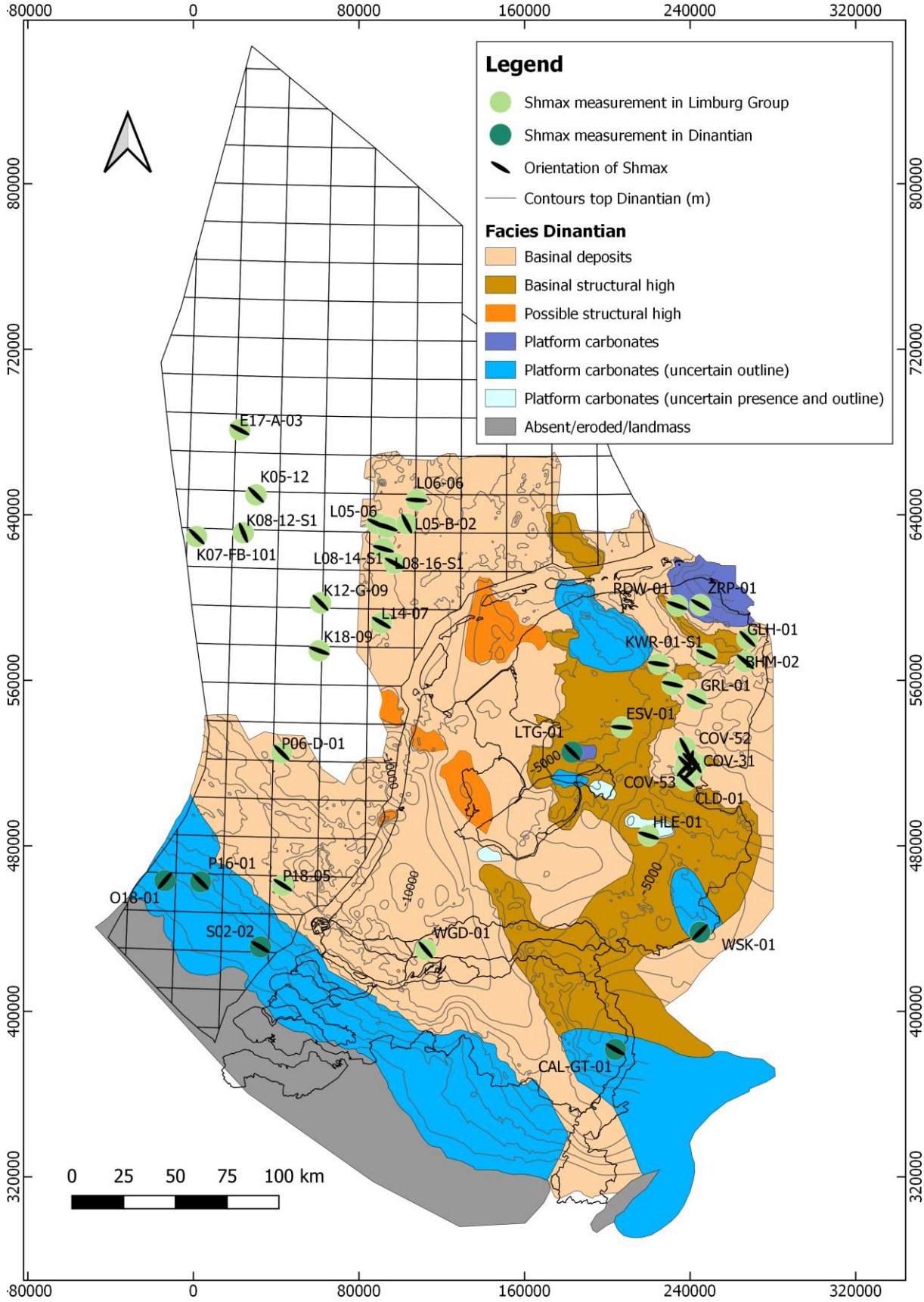

Figure 2-8 Map with available stress field data for the Dinantian and overlaying Limburg Group. Stress data from Osinga and Buik (2019).

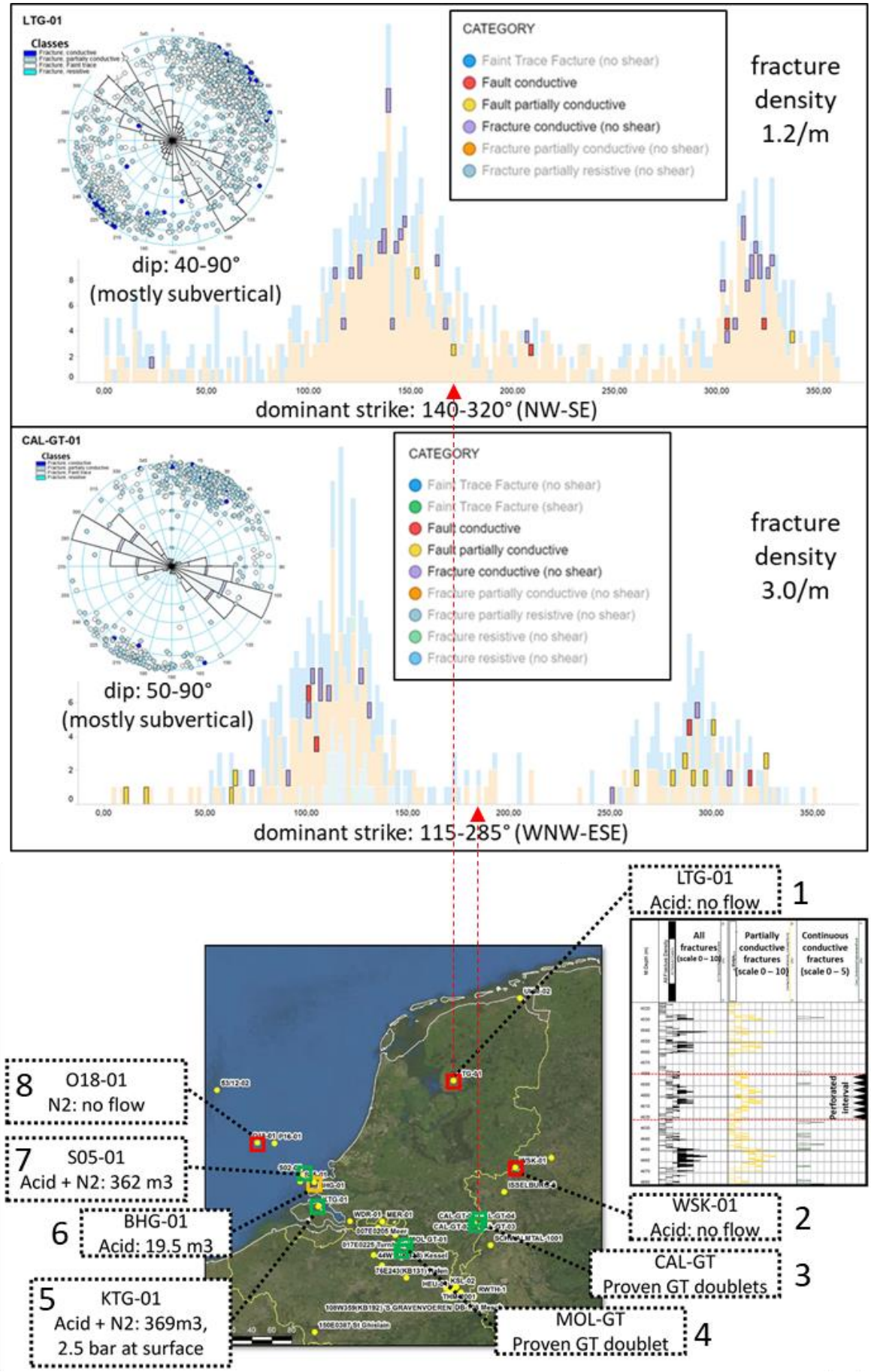
LTG-01
Classes
CATEGORY
Faint Trace Facture (no shear)
Fault conductive
Fault partially conductive
Fracture conductive (no shear)
Fracture partially conductive (no shear)
Fracture partially resistive (no shear)
fracture density 1.2/m
dip: 40-90° (mostly subvertical)
dominant strike: 140-320° (NW-SE)
CAL-GT-01
Classes
CATEGORY
Faint Trace Facture (no shear)
Faint Trace Facture (shear)
Fault conductive
Fault partially conductive
Fracture conductive (no shear)
Fracture partially conductive (no shear)
Fracture partially resistive (no shear)
Fracture resistive (no shear)
Fracture resistive (no shear)
fracture density 3.0/m
dip: 50-90° (mostly subvertical)
dominant strike: 115-285° (WNW-ESE)
LTG-01
Acid: no flow
1
All fractures (scale 0 – 10)
Partially conductive fractures (scale 0 – 10)
Continuous conductive fractures (scale 0 – 5)
Perforated interval
WSK-01
Acid: no flow
2
CAL-GT
Proven GT doublets
3
MOL-GT
Proven GT doublet
4
KTG-01
Acid + N2: 369m3, 2.5 bar at surface
5
BHG-01
Acid: 19.5 m3
6
S05-01
Acid + N2: 362 m3
7
O18-01
N2: no flow
8

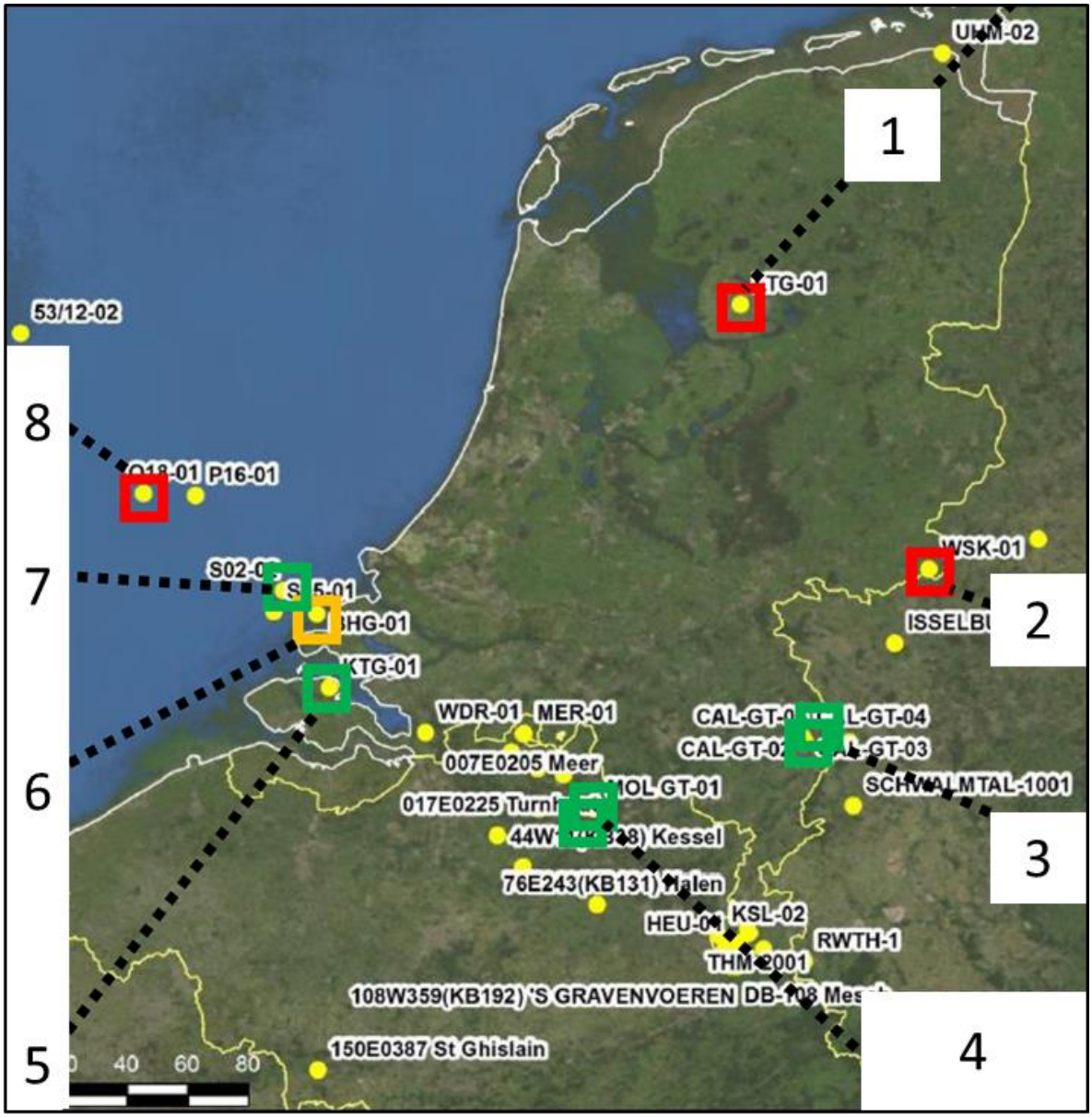

Figure 2-9 Previous page: Compilation of stress, fracture and well test data for the Dinantian. This page: Location of wells with data for Dinantian formations. Numbers link to flow data (bottom figure on previous page). Stress data from Osinga and Buik (2019), fracture and flow data and figure from Van Leverink and Geel (2019).

2.4 Reservoir depth and temperature

Effects of depth and temperature on induced seismicity

The depth of the reservoir affects many reservoir properties, such as reservoir temperature and pressure, but also the mechanical and flow properties of the rock (Buijze et al., 2019a). Effective stresses increase with depth with ratios between effective vertical and minimum horizontal stresses typically between 0.32 and 0.67, depending on the friction coefficient of critically oriented faults and assuming that these faults control local stress magnitudes (Figure 2-11; cf. ***BOX 4.1*** ; Jaeger et al., 2007; Van Wees et al., 2014). The assumption of critical stress state of faults may not always apply, and stress changes leading to fault reactivation may vary. The lack of distinct breakouts in many wells, combined with some 90 degree

rotations in the directions of breakouts suggests a stress state with a smaller anisotropy in horizontal stresses (S_{Hmax} ~5-20% higher than S_{hmin}, cf. section 2.3, Osinga and Buik, 2019). The interaction of direct pore pressure, poroelastic and thermoelastic effects with local stresses during geothermal operations will determine stress changes at faults and the potential for fault reactivation (slip tendency) and associated induced seismicity.

Another effect of increasing reservoir depth is that reservoirs may become closer to more competent (basement type) formations, which has been identified as an important factor in determining the occurrence of felt seismicity (Buijze et al., 2019a)[19]. However, the depth of basement type formations and mechanical properties of rocks at large depth is unknown in the Netherlands (cf. section 2.6). Temperature also increases with depth (Figure 2-10), and thermoelastic effects may be expected to increase with depth. Local cooling of the reservoir leads to thermal contraction and a decrease in horizontal stresses, and therefore has a destabilizing effect on these faults. This effect will be most pronounced at the injection well, and will increase over the lifetime of geothermal projects as larger parts of the reservoir progressively cool down. A review of case studies shows that maximum magnitudes of seismic events increase for reservoir temperatures above ~125°C, but this threshold temperature depends on many other factors including rock type and fluid injection pressures and volumes (Buijze et al., 2019a)[19].

Data availability and limitations relevant to depth and temperature

The spatial distribution and depth of the Dinantian carbonates were re-interpreted and updated within the framework of the SCAN project (Figure 1-1; Ten Veen et al., 2019). An update of the temperature model has also been performed (Figure 2-10; Veldkamp, 2020). In large parts of the Netherlands, seismic surveys that cover Dinantian formations are lacking. In general, uncertainties in the data increase with depth due to poorer coverage by seismic surveys and lack of quality of seismic data. There are no few wells penetrating Dinantian formations in the areas where the Dinantian is interpreted to be at depths below ~5.5 km, and few wells (UHM-02, LTG-01, WSK-01, cf. Figure 2-10) that drilled Dinantian formaions between 4 and 5 km). This means that the presence and depth are highly uncertain for large parts of the subsurface in the Netherlands. The reader is referred to the above-mentioned reports for additional discussion on methodologies and uncertainties associated with depth and temperature predictions.

Reservoir depth and temperature for Dinantian carbonates

For the Dinantian carbonates in the Netherlands, reservoir depth and temperature roughly follow the spatial distribution of interpreted structural highs and platform carbonates (Figure 1-1; Figure 2-10). The depth of the Dinantian carbonates varies from a couple of meters in the far south to more than 10 kilometers in the central west of the Netherlands (Figure 2-10). There is also a variation in depth for the Dinantian platforms, i.e. the platforms are generally deeper and hotter in the north than in the south. Depth of the platforms may reach ~5000 meter depth and temperatures ~200°C at the edges of the structural highs and platforms. If Dinantian carbonates in these deeper parts were to be explored for geothermal energy, thermoelastic stressing is an even more critical point of attention in assessing the potential for induced seismicity compared to shallower targets. Reservoir temperatures of 125°C have been found in the Balmatt project where induced seismic events reached M_L 2.1 (cf. section 7.2). Critical threshold reservoir temperatures and their relation to induced seismicity potential are highly uncertain for the Dinantian carbonates and depending on many other site-specific

[19] See also Buijze et al. (2019a), p. 53 (Figure 3-11), p. 55 (Figure 3-12).

factors. We therefore roughly distinguish small (< 1.5 km, T < 75°C), medium (1.5-3.5 km, T = 75-125°C) and large (T > 125°C) effects of reservoir depth and associated temperature on induced seismicity potential. It is important to note that this distinction is only a first indication as thermoelastic stress changes depend on rock properties (e.g., stiffness and thermal expansion coefficients) as well as temperature changes. The distinction should be substantiated by modelling of thermoelastic stress changes around geothermal doublets to assess relations between reservoir temperature and induced seismicity potential in more detail.

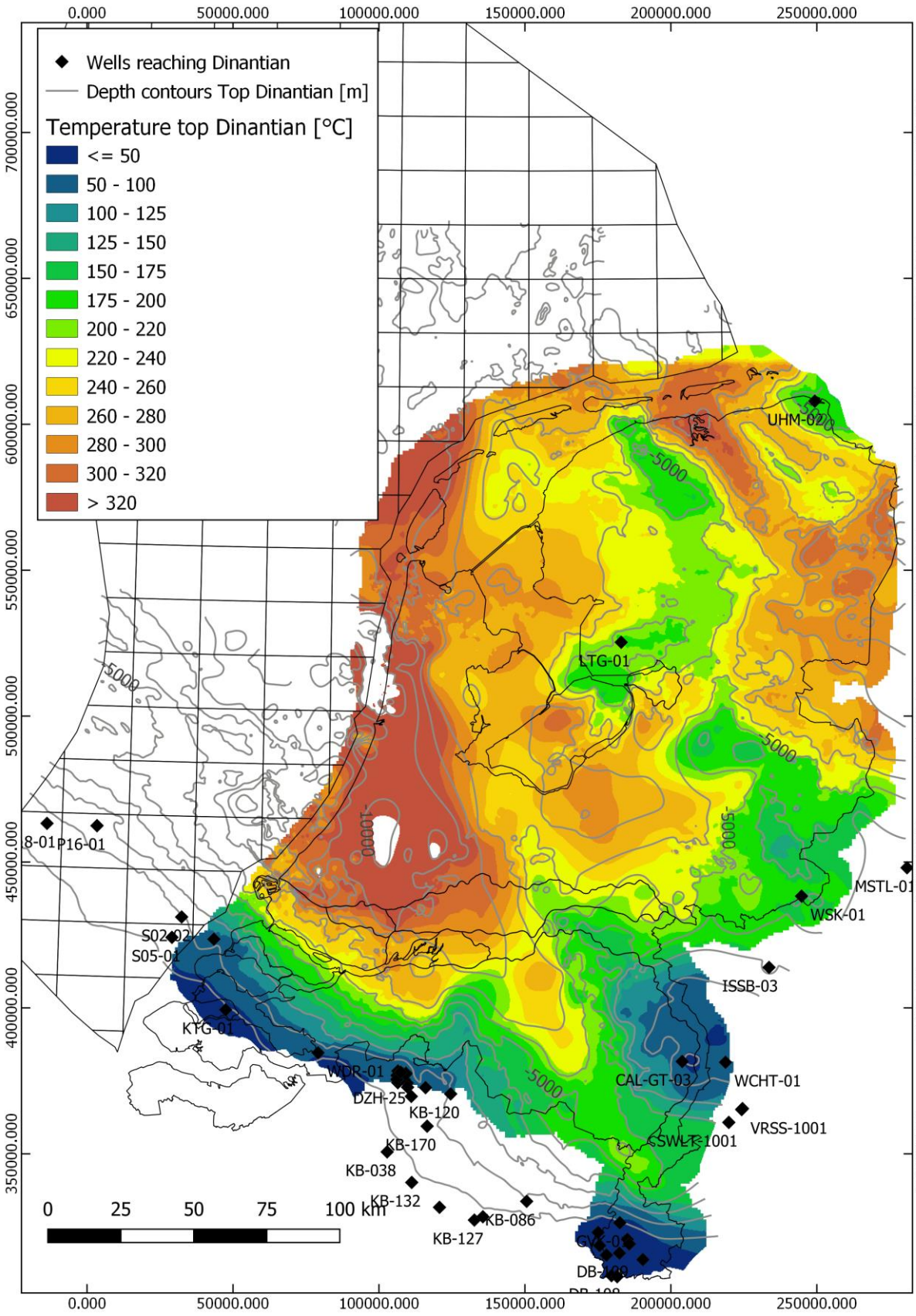

Figure 2-10 Temperatures at top Dinantian overlain by depth contour lines of the top Dinantian. Locations of wells with temperature data for the Dinantian are also indicated (black diamonds with well name). The white spots in the temperature map are caused by the cut-off of the temperature model at 10 km depth. From: Veldkamp (2020), status December 2019.

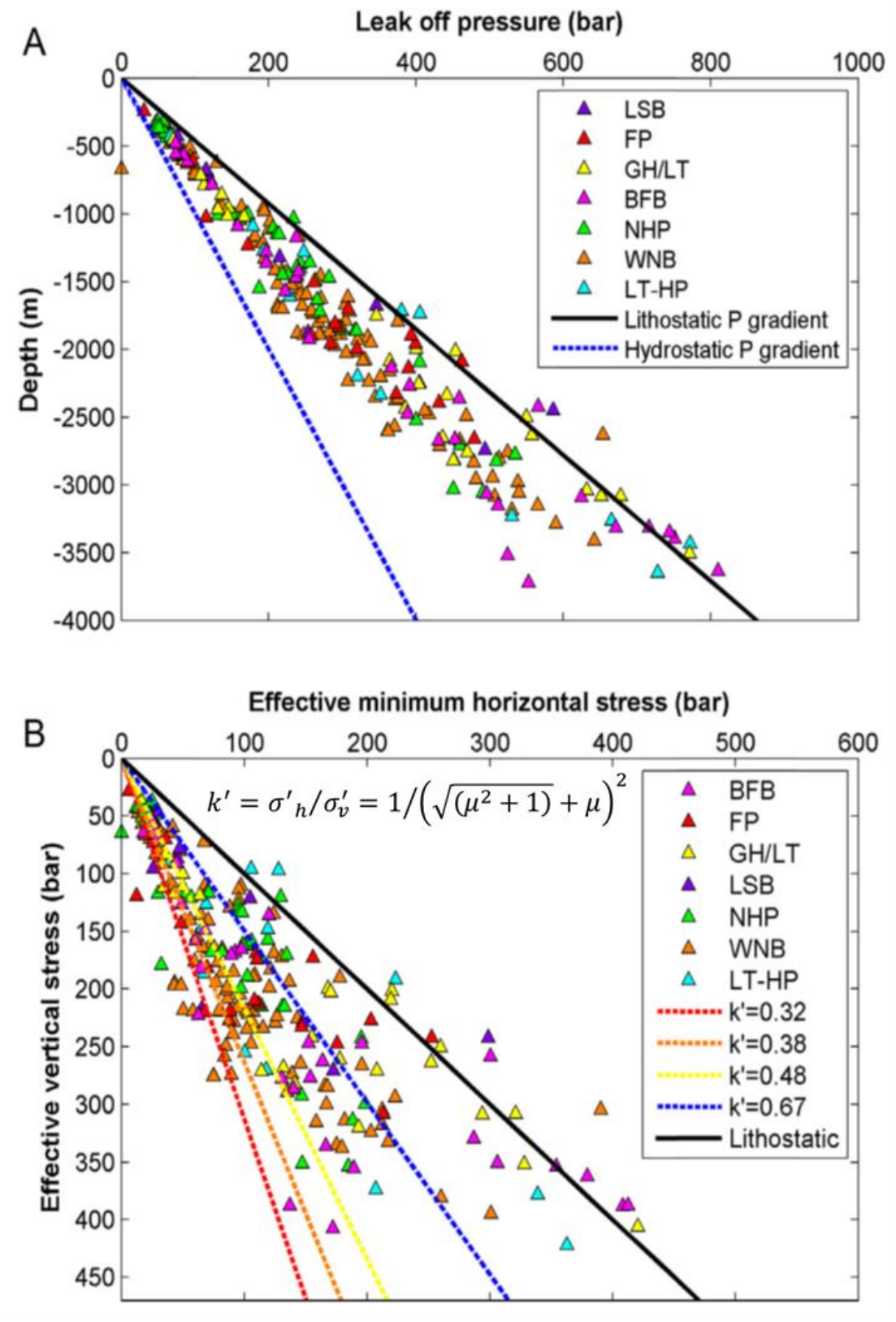

Figure 2-11 Leak off pressure test (LOT) data from the onshore Netherlands and calculated effective stresses. (A) Measured leak off pressures and hydrostatic gradient (1 bar/10 m) and lithostatic (2.2 bar/10 m) gradients. (B) Effective minimum horizontal and vertical stress, interpreting leak off pressures as S_{hmin}, and taking lithostatic pressure as S_v (in accordance with dominant normal faulting regime, cf. section 2.3) with a correction for pressure as explained by Van Wees et al. (2014). BFB: Broad Fourteen Basin; FP: Friesland Platform; GH/LT: Groningen High/Lauwerszee Trough; LSB: Lower Saxony Basin; NHP: Noord Holland Platform; WNB: West Netherlands Basin; LT-HP: Lauwerszee Trough-Hantum Platform. From: Van Wees et al. (2014).

2.5 Composition and competency of reservoir rock

Effects of reservoir composition and competency on induced seismicity

Besides flow properties, ***reservoir rock composition*** also affects the mechanical properties and behaviour of the reservoir during geothermal operations. ***Rock competency*** can be used to qualitatively indicate the resistance of rocks to deformation. More competent (***stiffer***) rocks can build up more stress and are therefore more likely to fail in a brittle manner (potentially accompanied by release of seismic energy), while less competent (***compliant***) rock can accomodate more deformation elastically. Rock competency can be considered in terms of the elastic modulii ***Young's modulus and Poisson ratio***, with more competent rocks exhibiting high Young's modulus and low Poisson ratio and less competent rocks exhibiting low Young's modulus and high Poisson ratio[20]. Besides ***elastic and inelastic*** brittle deformation, some rocks show ***time-dependent deformation (i.e. creep)*** under differential stress. Creep is particularly important for rocks such as claystones, shales and rocksalt (Urai et al., 1986; Herrmann et al., 2019), and can locally relieve differential stress by ***aseismic deformation***, resulting in a (more) isotropic stress state. Creep of rock formations is of importance for induced seismicity as it affects the transfer of stress between formations. Geothermal operations in competent rocks may lead to larger stress changes than similar operations in less competent rocks. Accordingly, ***critical conditions for fault reactivation*** are affected by the composition and competency of reservoir rock. Besides the mechanical behaviour of the reservoir and local stress state at faults, rock composition also affects fault rock composition and texture and thereby the ***strength of faults*** (as determined by cohesion and friction coefficient, cf. ***BOX 4.1***). Accordingly, rock composition also plays a role in fault stability, slip tendency and post-failure (seismic or aseismic) slip[21].

Data availability and limitations relevant to reservoir composition and competency

Regional variations of the composition and competency of Dinantian carbonate reservoirs can only directly be determined using cores of wells. The number of cores of Dinantian carbonate rocks in the Dutch subsurface is limited (Figure 2-12). Indirectly, some insights may be obtained by considering spatial variations in depositional environment and diagenesis (Mozafari et al., 2019), but these are mostly very general and have large uncertainties due to lack of seismic and well data.

Reservoir composition and competency for Dinantian carbonates

Reservoir composition and competency of the Dinantian carbonates is strongly linked to depositional environment and diagenesis. Matrix porosity, degree of karstification, dolomitization and fracture development are important factors determining reservoir competency and can be determined using core data (Figure 2-12). In many locations, the Dinantian reservoirs are interpreted to consist of fractured carbonates. Analogue plays of this type are characterized by medium to high rock competency with a medium to high effect on induced seismicity (Buijze et al., 2019a)[9]. Mozafari et al. (2019) indicate low porosity and permeability in non-dolomitized limestones, potentially locations with extensive karstification in the SE and SW of the Netherlands, and dolomitization in some wells (e.g., O18-01, KTG-01, BHG-02, LTG-01) with potentially higher fracture density in dolomite bodies and in fault zones. Reliable assessment of reservoir competency can only be derived from tests on available core and is currently hampered by a lack of cores and data. Matrix porosity tends to

[20] See also Buijze et al. (2019a), p. 23-24 (section 2.3).
[21] See also Buijze et al. (2019a), p. 33 (Figure 2-8).

lower the competency of rocks, but dolomitization and textural changes during diagenesis also affects rock competency.

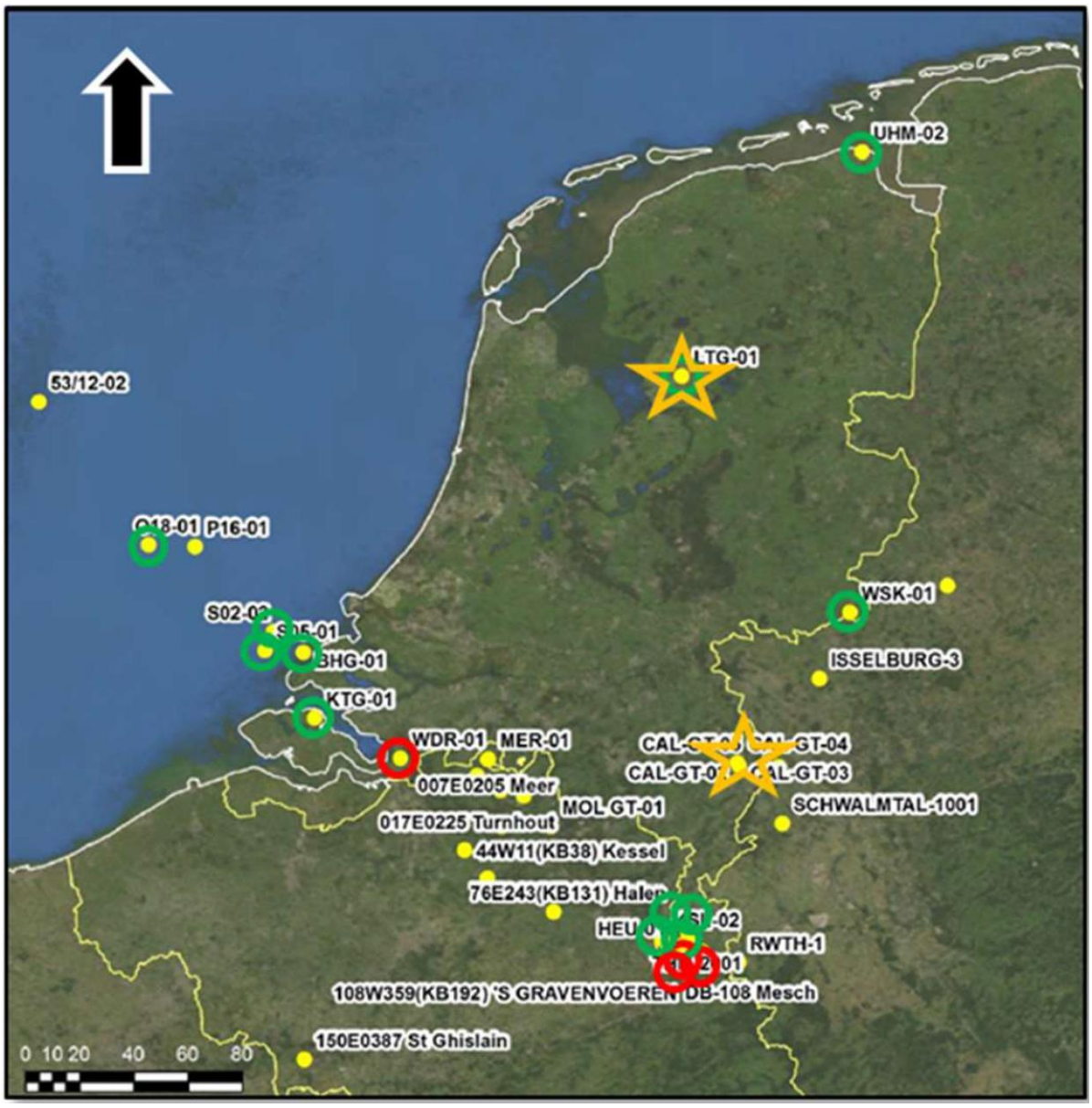

Figure 2-12 Map of the Netherlands indicating wells with cores from the Dinantian carbonate rocks (green). Wells with (also) FMI are indicated by the stars. From: Van Leverink and Geel (2019).

2.6 Hydraulic and mechanical decoupling with over- and underburden

Effects of hydraulic and mechanical decoupling on induced seismicity

Hydraulic and mechanical coupling with other formations are of interest as pressure communication or transfer of stresses between formations may lead to stress changes beyond the reservoir. Formations in the vicinity of geothermal reservoirs may exhibit a different stress state that may be affected by stress changes due to geothermal operations and thereby may become prone to induced seismicity. In particular, it has been observed in case studies that interaction with underlying critically stressed and seismogenic (crystalline) basement can be an important factor for induced seismicity (cf. section 2.6; Buijze et al. 2019a)[9]. Buijze et al. (2019a) indicated an important effect of hydraulic and mechanical connection to depth in cases worldwide, in particular with competent basement rocks, on induced seismicity[9]. Their review of case studies showed that maximum magnitudes of seismic events increase if separation between operations and basement is less than ~1 km (Buijze et al., 2019a)[22]. The definition of basement is not straightforward, i.e. usually it is used to indicate (crystalline) metamorphosed or igneous rocks that have mechanical properties that are distinct from overlying sediments. These formations may be affected by large scale tectonic processes, while the overlying reservoir may be at a different stress state if decoupled. Within the context of induced seismicity potential the different mechanical properties and stress state are most relevant as these may lead to different seismic response than sedimentary reservoirs if affected by geothermal operations (cf. section 2.3). In EGS, basement rocks may be the geothermal target so stress changes directly affect the stress state of potentially seismogenic basement. The factor describing the interaction between geothermal operations and potentially seismogenic basement can be extended to include hydraulic and mechanically (de)coupling with the over- and underburden. Mechanically decoupling between a geothermal reservoir and the underburden due to the presence of creeping formations can be beneficial as the stress state of the basement rocks is not transferred to the geothermal reservoir. Hydraulic or mechanical coupling with overlying formations is likely if sealing or creeping formations are absent above the reservoir. Depth and, if known, depth to basement (cf. section 2.4), flow regimes (cf. section 2.3) and rock composition of over- and underburden are important factors.

Data availability and limitations relevant to hydraulic and mechanical coupling

Little is known of the (variations in) hydraulic and mechanical properties of the formations under- and overlying the Dinantian carbonates. It is important to note that there is no evidence of a critically stressed, seismogenic basement in the Netherlands. Hypocentres of natural seismicity in the Roer Valley Graben show a large spread in depth and occur up to shallow depths (Figure 2-2 to Figure 2-5), but uncertainties in depth are several kilometres and seismicity is associated with tectonic movement along major faults. A change in hypocentre distribution of natural seismic events that potentially indicates a transition to seismogenic basement is not observed. Although the resolution of seismic surveys is poor at depth, a lack of visible reflectors suggest a more gradual transition to more tight and competent formations. These insights may become relevant in case projects targeting the deeper parts of the Dinantian carbonates are considered.

Hydraulic and mechanical decoupling of Dinantian carbonates

Some insights into hydraulic and mechanical decoupling or coupling of the Dinantian carbonates can be derived from information of the over- and underlying formations. The

[22] See Buijze et al. (2019a), p. 55 (Figure 3-13).

Dinantian carbonates are overlain by shaly claystones of the Geverik Member (Namurian) interfingering with fine sand and siltstone, throughout the Netherlands. Except for the south and south-east (Venlo and Maastricht area) of the Netherlands, where a Cretaceous unconformity is present at top of the Dinantian carbonates, overlain by sandstones and limestones from the Ommelanden formation (Mozafari et al., 2019). Consistent S_{Hmax} directions throughout the upper crust in the Netherlands and alignment of S_{Hmax} between the Dinantian carbonates and formations of the Limburg Group suggest a coupling of the stress state in the crust down to the Dinantian (cf. section 2.3). Leak off pressures also do not show evidence of hydraulic or mechanical decoupling, at least down to ~3800 meter (Figure 2-11).

Limited information is available on the lithologies underlaying the Dinantian Carbonates. Data available comes from the few wells that have been drilled below the Dinantian. From this data a rough spatial distribution of the direct Dinantian underburden can be made. In East and Southeast Netherlands (based on wells WSK-01, CAL-GT and KSL-02), the reservoir is underlain by claystone or shale lithologies from the Pont d'Arcole formation. In the Southwest of the Netherlands the Dinantian carbonates overlay the Upper Devonian silty to sandy deposits of the Bosscheveld formation (based on wells BHG-01 SO2-01, KTG-01 and O18-01) and in the central and North clay/shale deposits alternating with sandstones are found below the Dinantian platforms (LTG-01 and UHM-02). It is not clear if these formations lead to hydraulic or mechanical decoupling.

Given the uncertainties associated with analysis of hydraulic and mechanical decoupling based on regional mapping of over- and underlying formations, a classification into small, medium and large effects for the Dinantian carbonates is highly speculative. It seems unlikely that separation between operations and basement will be less than ~1 km for Dinantian carbonates accessible by geothermal operations, which suggest an overall low effect.

2.7 Summary of the effects of geological factors on induced seismicity

The qualitative classification of small, medium and large effects of geological factors on the *potential* occurrence of induced seismicity is summarized in Table 2-1. As mentioned before, important considerations are (1) the lack of data for the Dinantian carbonates in most regions in the Netherlands, and (2) the analysis is regional and not site-specific as required for seismic hazard and risks analysis of projects.

Factor	**Small effect**	**Medium effect**	**Large effect**
Natural seismicity	No or isolated natural seismic events	Some natural seismic events	Concentration of natural seismic events
Distance to large (critically stressed) faults	Smaller faults within critical distance to operations	Large faults intersecting the reservoir	Large critically stressed faults within critical distance to operations
Stress field, fracture populations & flow regime	Matrix or karst dominated flow	Fractured dominated flow, small anisotropy in stress & fractures & flow	Fractured dominated flow, anisotropy in stress, fractures & flow
Reservoir depth & temperature	Shallow depth (< 1.5 km)	Intermediate to large depths (1.5-3.5 km)	Large depths, (> 3.5 km)
Reservoir composition & competency	- (higher porosity)	-	- (lower porosity)
Hydraulic & mechanical decoupling	Vertical separation with basement > 1km	-	-

Table 2-1 Summary of the effect of geological factors on the *potential* occurrence of induced seismicity focussed on Dinantian carbonates in the Netherlands. Note that the analysis of the effects is highly uncertain for some factors and is based on generic considerations in some cases. See text for motivation of classification into small, medium and large effect.

2.8 Operational factors

Two geothermal projects in the Netherlands (i.e. the Californië projects, cf. section 7.1) and one project in Belgium (i.e. the Balmatt project, cf. section 7.2) target the Dinantian carbonates. Some insights into the effect of operational factors on induced seismicity is also provided by analogue cases in the Molasse Basin (cf. section 7.3). The relation between operational factors and induced seismicity is described in these sections and in Buijze et al. (2019a)[9]. As described in the beginning of this section, current geothermal projects in the Netherlands are based on circulation of fluids from (relatively) hot sedimentary aquifers without net fluid injection. Operational factors (i.e. flow rate, injection pressure, injection temperature) for such geothermal systems generally lead to more limited pressure and temperature changes compared to Enhanced Geothermal Systems (EGS) or Hydrothermal Systems (HS) (cf. Figure 2-1, see also Buijze et al. 2019a)[9]. Therefore, they are expected to lead to relatively small stress changes as direct pressure, poroelastic and thermoelastic effects are relatively small. An exception may be thermoelastic effects of progressive cooling of the entire reservoir over the lifetime of a geothermal project. Despite the expected small changes in stress, felt seismicity has occurred in some of these projects. It shows the importance of interaction between the geological factors described above and operational factors. It also makes clear that operational factors should be optimized for individual projects, taking mitigation of felt seismicity into account (for example dual objective optimization to obtain maximum flow rates given induced seismicity constraints, cf. TerHeege et al., 2018).

An important factor in the Netherlands is the interaction of geothermal activities with other subsurface activities such as gas production or salt mining. In particular in the north of the Netherlands the Dinantian carbonates are at depths that may be reachable for geothermal operations but are also affected by frequent occurrence of induced seismicity caused by gas production (Figure 2-13). In these areas, direct pressure, poroelastic and thermoelastic effects associated with geothermal operations may interact with stress changes due to gas depletion. Despite relatively large vertical separation between the Dinantian carbonates and Rotliegend sandstone gas reservoirs, interaction may occur, even during drilling of wells[23]. The effects on induced seismicity will be complex, and it is questionable if geothermal projects can be considered in such areas[24].

[23] See also Buijze et al. (2019a), p. 35 (section 2.8).
[24] See also Buijze et al. (2019a), footnote on p.13.

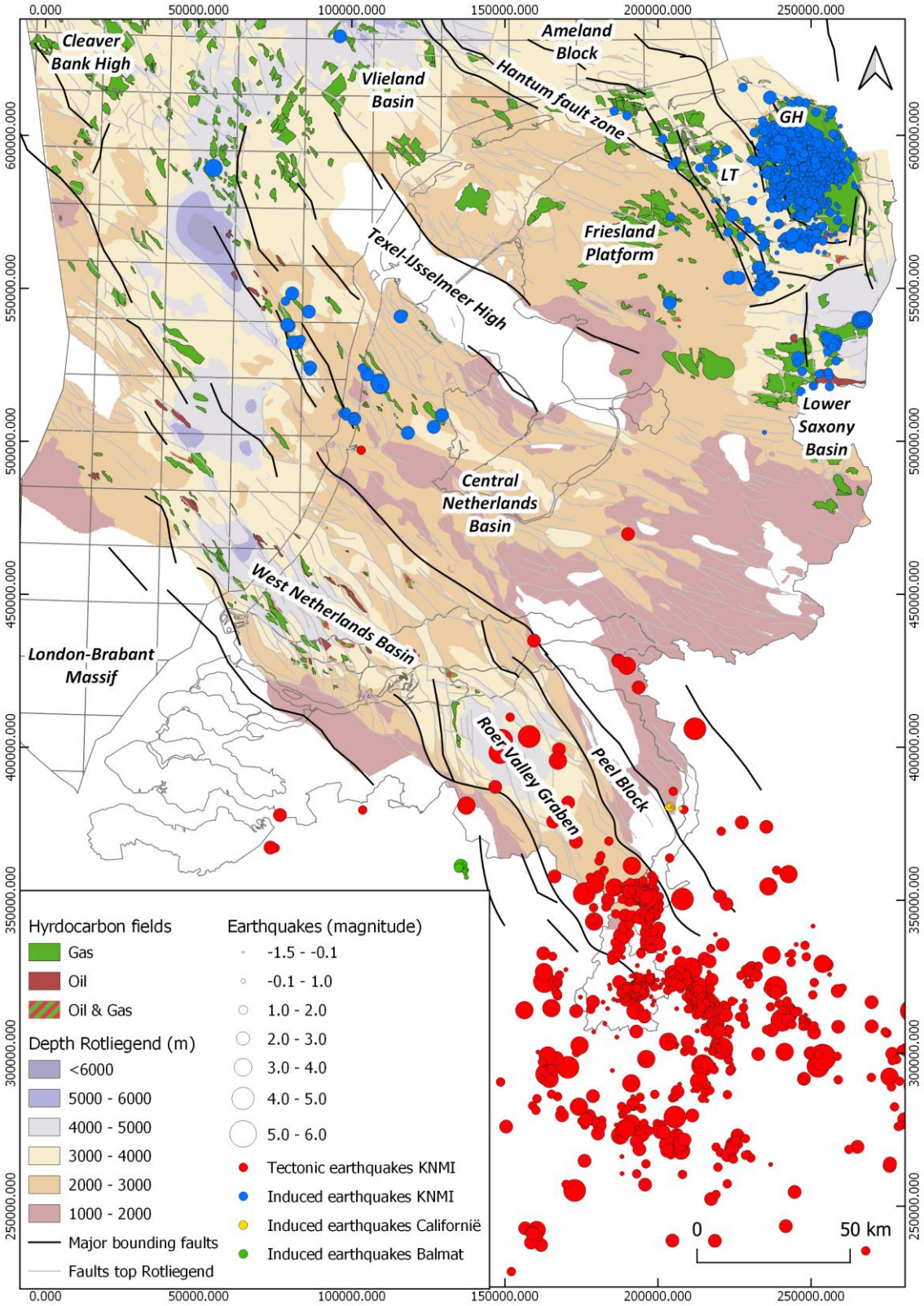

Figure 2-13 Overview of natural and induced seismicity in the Netherlands and parts of Belgium and Germany. Epicentres of tectonic (natural) earthquakes (red circles), induced earthquakes related to gas production (blue circles), and induced earthquakes related to geothermal projects near Californië (yellow circles) and Balmatt (green circles) are plotted on a map with major structural units and depth of the top Rotliegend that is one of the major hydrocarbon plays in the Netherlands. Gas fields (green polygons) and oil fields (red polygons) are also indicated. The area around the Groningen Platform (GP) and Lauwerszee Trough (LT) are of particular importance for considering interaction between geothermal operations and gas depletion. Modified from: Van Wees et al. (2014).

3. Seismogenic potential of Dinantian carbonate geothermal reservoirs

A qualitative method to assess the likelihood of inducing 'felt' seismicity (*seismogenic potential*) for geothermal projects has been outlined by Buijze et al. (2019a)[25], based on mechanisms, key factors and case studies. In the current study, we extend that analysis to differentiate between different regions in the Netherlands where development of Dinantian carbonate geothermal reservoirs may be considered. It should be emphasized that both seismogenic potential and seismic risks critically depend on local conditions. Therefore, *the current analysis is not meant to discard or promote specific regions for development of potential geothermal projects targeting the Dinantian carbonates on the basis of likelihood of inducing seismicity*. It merely serves as information that can be used in planning of projects and in focusing efforts for potential mitigation of seismic risks so that data acquisition and analysis for geothermal projects can be more efficiently planned. *Assessment of seismogenic potential, seismic risks and mitigation measures for individual projects should always be based on site-specific analysis, and tailored to the specific geothermal system and operations.*

3.1 Method to determine seismogenic potential

In Buijze et al. (2019a), an analysis of the seismogenic potential for geothermal plays is outlined with seismogenic potential indicating the likelihood of inducing 'felt' seismicity. A threshold magnitude (M) of 2 was taken in this study to distinguish felt seismicity from seismicity that is only detectable by seismic networks but not felt by humans (see also Evans et al., 2012). Note that while a threshold of M 2 may be considered low for many regions worldwide, frequent events with $M > 2$ have been problematic for gas depletion-induced seismicity in the Netherlands (van Thienen-Visser & Breunese, 2015).

Buijze et al. (2019a) base the seismogenic potential of geothermal plays or regions on the following criteria[25]:

1) the current presence or absence of seismicity in the plays
2) the presence or absence of felt seismicity as reported for case studies in basins with analogue geological settings in Europe, and
3) the effect of key geological and operational factors on the (local) seismogenic potential.

The analysis for individual geothermal plays can be extended by assessing the same criteria for different regions (Table 3-1). Regardless if the analysis is performed on the scale of a geothermal play or on the scale of a region, a qualitative ranking (low, medium or high) of seismogenic potential can be determined on the basis of the criteria. The scale is important in the overall assessment of seismogenic potential, i.e. the overall seismogenic potential of a play may be low or medium, while it may be higher for a specific region or location within that play. This approach is chosen to maintain consistency between this study and the study by Buijze et al. (2019a) that assesses seismogenic potential for geothermal systems and plays worldwide, including hydrothermal and EGS systems that do not occur in the Netherlands. Consistency is important as it allows comparison between regions and plays, both within and outside of the Netherlands. Given that only one project in the Netherlands has shown seismicity (cf. section 7.1), such comparison is crucial to establish a benchmark and framework for assessing, evaluating and comparing seismogenic potential and the potential impacts of induced seismicity.

[25] See Buijze et al. (2019a), p. 16-18 (section 1.4) and p. 88-92 (section 6.5).

The current study focusses on assessing the seismogenic potential for Dinantian carbonates in different regions in the Netherlands. Analogous to the approach in Buijze et al. (2019a), a low, medium or high seismogenic potential is assigned to a region based on the criteria described above and in Table 3-1:

- A low seismogenic potential is assigned to a region if (1) no felt seismicity is reported in the Netherlands, (2) no felt seismicity is reported in analogue cases worldwide, and (3) key factors for the region also indicate a low seismogenic potential (Table 3-1). A low seismogenic potential is meant to indicate that induced felt seismicity is unlikely to occur, although isolated events cannot be excluded;
- A medium seismogenic potential is assigned to a play or region if felt ($M > 2$) seismicity has been reported to have occurred in the Netherlands or in analogue cases, and key factors for the region indicate a low-medium seismogenic potential. For geothermal plays in the Netherlands, a medium seismogenic potential is meant to indicate that induced seismicity may be expected in some cases with the number and magnitude of seismic events depending on the site-specific geology, type of operations, operational parameters and mitigation measures. A quantitative threshold for the number and magnitude of seismic events is rather arbitrary at this point as it, for example, depends on the level of acceptable risk which is currently not very well established (cf. section 9). The distinction between medium and high seismogenic potential is therefore mainly based on key factors affecting the induced seismicity potential.
- A high seismogenic potential is assigned to a play if felt induced seismicity has occurred in the Netherlands and is frequent in analogue cases, and key factors for the play or region indicate a high seismogenic potential. For geothermal plays in the Netherlands, a high seismogenic potential is meant to indicate that induced seismicity may be expected in many cases and mitigation measures are needed to control the number and magnitude of seismic events.

Seismogenic potential of play or region	Felt induced seismicity in play or region	Felt induced seismicity in analogue cases	Effect of key geological and operational factors
Low	Absent	Absent	Low
Medium	Present	Absent/Present	Medium
High	Present	Present	High

Table 3-1 Criteria for ranking (low, medium, high) of seismogenic potential based on felt induced seismicity.

3.2 Seismogenic potential of Dinantian carbonates compared to other geothermal plays in the Netherlands

In Buijze et al. (2019a), the seismogenic potential of plays in the Netherlands is compared, and discussed within the framework of case studies of geothermal projects worldwide[25]. For the Netherlands, 5 current and potential future geothermal plays are distinguished: (1) Jurassic/Cretaceous permeable porous sandstone reservoirs, (2) Triassic and Permian tight or permeable porous sandstone reservoirs, (3) Dinantian fractured or karstified carbonate reservoirs affected by active tectonics in the Roer Valley Graben (RVG Dinantian carbonates), (4) Dinantian fractured or karstified carbonate reservoirs in western, central or northern parts of the Netherlands, away from the Roer Valley Graben (CNNNLD Dinantian carbonates), (5) deeper (Devonian) sedimentary reservoirs.

The *play-based* analysis of seismogenic potential yielded a low-medium seismogenic potential for the CNNNLD Dinantian carbonates and a medium seismogenic potential for the RVG Dinantian carbonates (Table 3-2). A high seismogenic potential was not found for geothermal plays in the Netherlands. The review of case studies worldwide only indicate a high seismogenic potential for igneous/volcanics geothermal plays, and potentially (depending on operational factors) for regions prone to seismicity such as regions close to large critically stressed faults or close to competent critically stressed basement (e.g., the Basel and Sankt Gallen projects)[26].

Geothermal play	# systems producing/ total (NL)	Seismicity occurred in play?	Analogues (similarity, cause)	Seismicity analogue case	Effect of key factors	Seismogenic potential
Jurassic/Cretaceous sandstones	11	No	North German & Danish Norwegian basins (good)	0/8	Low	Low
Permian/Triassic sandstones	6	No	North German & Danish Norwegian basins (good)	0/8	Low-medium	Low-medium
RVG Dinantian carbonates	2	Yes (Californië[1], Balmatt)	Molasse Basin (reasonable, basement)	3/27	Medium	Medium
CNNNLD Dinantian carbonates	-	-	-	-	Low-medium	Low-medium
Deeper (Devonian) sedimentary targets	-	-	-	-	Medium	Medium (uncertain)

Table 3-2 Seismogenic potential for the 5 geothermal plays distinguished in the Netherlands. [1]No felt seismicity for current definition (max. M_L 1.7), causal relation between operations and seismicity under investigation (cf. section 7.1).

[26] See Buijze et al. (2019a), p. 57 (Table 3-2), p. 123-125 (section A.1), p. 146-148 (section A2.4).

3.3 Seismogenic potential of Dinantian carbonates for different regions in the Netherlands

As described in in detail in section 3.1, the current study extends the analysis to different regions of the Dinantian carbonate play in the Netherlands, specifying the key factors for different regions (cf. section 2) and the occurrence of induced seismicity in analogue cases (cf. section 7) in more detail. Based on the re-interpreted and updated spatial distribution and depth of the Dinantian carbonates (Figure 1-1, Ten Veen et al., 2019) and the analysis of key factors affecting the induced seismicity potential (section 2), we distinguish 5 regions where the Dinantian is (potentially) located at depths shallower than 6 km (Figure 3-1). Each of these regions has different characteristics relevant for induced seismicity and seismogenic potential:

(1) Platform carbonates with uncertain outline in the vicinity of the Roer Valley Graben, south of the river Waal between Nijmegen and Tiel and east of the Tilburg-Tiel boundary for the occurrence of natural seismicity in the Netherlands (Southeast, Roer Valley Graben- SERVG)
(2) Platform carbonates with uncertain outline in the southwestern part of the West Netherlands Basin, west of the Tilburg-Tiel boundary for the occurrence of natural seismicity in the Netherlands (Southwest, West Netherlands Basin- SWWNB);
(3) The S-N trending basinal structural high between SERVG in the South and Ameland in the North, containing platforms near Winterswijk (WSK-01), Luttelgeest (LTG-01), Haarle (HLE-01, uncertain), and the northern part of the Friesland Platform (South-North Basin Structural High- SNBSH)
(4) The area north of SWWNB, northwest of SERVG and west of SNBSH, containing basinal structural high and possibly a platform north of Utrecht (Central, North Basin Structural High- CNBSH)
(5) The Groningen Platform in the northeastern part of the Netherlands (Northeast, Groningen Platform- NEGPF)

Following the analysis of key factors in section 2 (cf. Table 2-1), Table 3-3 gives a *rough (qualitative) indication* of the effects of the main geological and operational factors for these regions. As described in the method section 3.1, the *overall seismogenic potential for the Dinantian carbonates in the Netherlands remains low-medium* (which is importance for reference to case studies worldwide, Buijze et al., 2019a). The analysis is *qualitative, based on current data and insights, and indicates relatively small, medium and large effects of key factors*. Thereby it points to factors that are most important in distinguishing low to medium seismogenic potential for the Dinantian carbonates in different regions. It also helps in identifying the needs for further data acquisition and research that contribute to mitigating seismic risks.

Factor	SERVG	SWWNB	SNBSH/CNBSH	NEGPF
Natural seismicity	medium	small	small	small
Distance to large (critically stressed) faults	large (RVG)	small-medium (stress state faults?)	small-medium (stress state faults?)	small-large (Groningen faults)
Stress field, fracture populations & flow regime	small-medium (karstified, hydraulic connection fault)	?	?	?
Reservoir depth & temperature	small-large (varying depth)	small-large (depth < 5 km)	medium-large (depth > 1.5 km)	large (depth > 5 km)
Reservoir composition & competency	? (karstified)	?	?	?
Hydraulic & mechanical decoupling	Small	small	small	small
Presence of induced seismicity	X (CLG/CLW/ Balmatt*)	X (Balmatt*)	X (some smaller gas fields)	X (Groningen gas field)
Possible interference other subsurface activities	small (mining?)	small (gas fields?)	medium-large (gas fields/salt)	large (Groningen gas field)

Table 3-3 Summary of the effect of geological factors that affect the seismogenic potential of the Dinantian carbonates for different regions in the Netherlands. Some important considerations are indicated between brackets. Note that the analysis of the effects is highly uncertain for some factors and is based on generic considerations in some cases. See section 2 for motivation of classification into small, medium and large effect. SERG- Southeast, Roer Valley Graben; SWWNB, Southwest, West Netherlands Basin; SNBSH- South-North Basin Structural High; NEGPF- Northeast, Groningen Platform. *The Balmatt site is located at the SW side of the Roer Valley Graben with almost equal SW-NE distance from the central NW-SE axis of the graben as the NE-SW distance of the Californië projects, but also close to the southern boundary of the SWWNB region. The influence of tectonic movements along faults in the Roer Valley Graben at Balmatt is unclear as nearest epicentres of natural seismic events are located more than 30 km from the project location (cf. section 7.2).

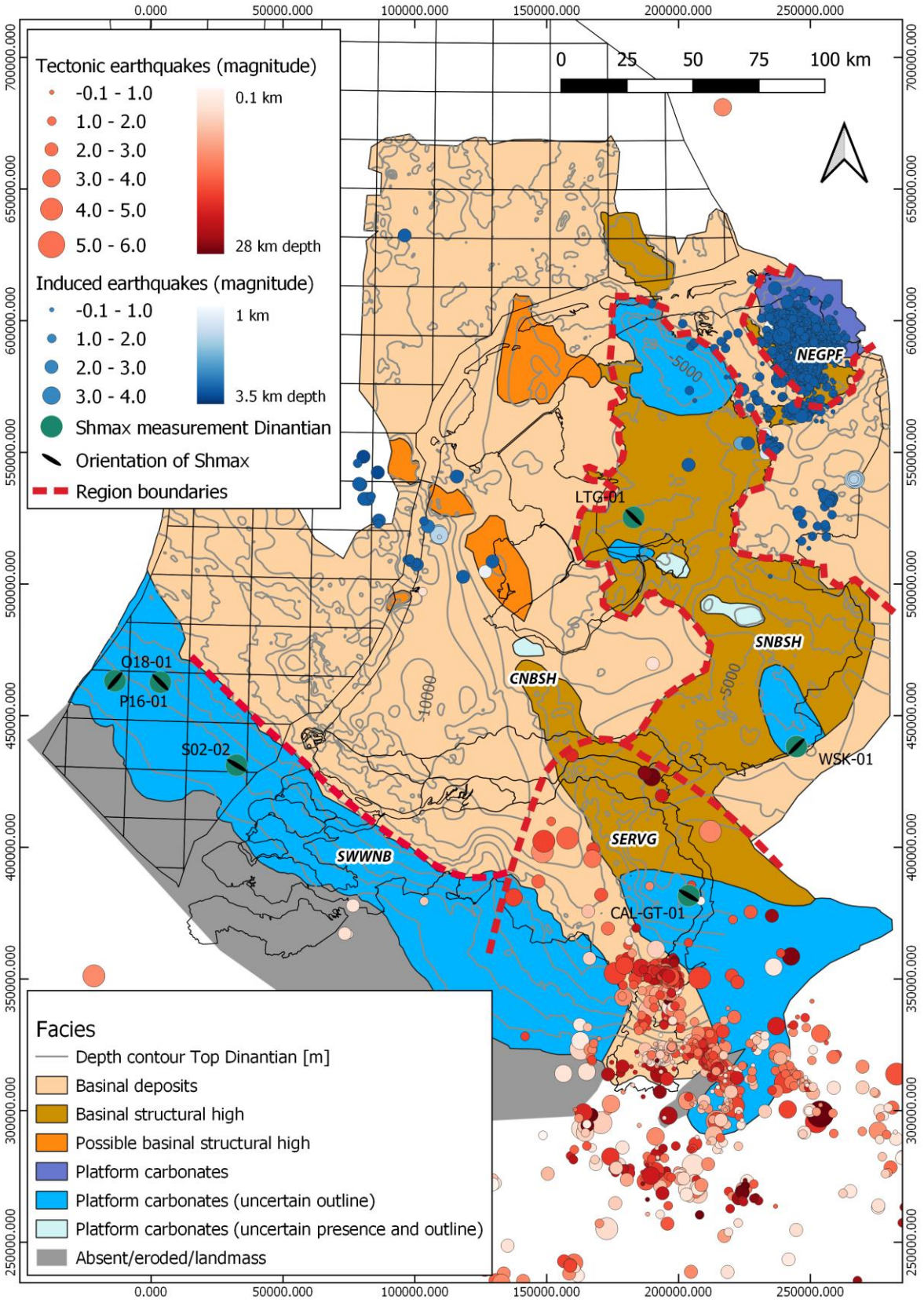

Figure 3-1 Possible spatial distribution of the Dinantian carbonates in the Netherlands (compiled by Mozafari et al., 2019 and Ten Veen et al., 2019) with occurrences of natural and induced seismicity (indicated with red and blue dots, compiled in this study), orientation of intermediate principal stress S_{Hmax} (indicated with light green dots with black line, compiled by Osinga and Buik, 2019). Regions with different characteristics that are distinguished for assessment of seismogenic potential are indicated by red dashed contours. See section 3.3 for description of regions and abbreviations.

4. Induced seismicity modelling approaches relevant for Dinantian carbonate geothermal reservoirs

A wide range of approaches for modelling induced seismicity in geothermal operations have been reported in literature[27]. Reviewing all possible approaches is beyond the scope of this study. In this section, we specifically focus on seismic source models for induced seismicity associated to ultradeep geothermal operations in the Dinantian carbonate reservoirs. Some commonly used geomechanical parameters and relations for the description of stress state, fault stability, fault rupture and seismicity that are used throughout this report are given in ***BOX 4.1***.

Carbonate reservoirs are generally heterogeneous. Differences in sedimentary facies and (post-depositional) diagenesis, and specifically the presence of natural fracture networks and karstification may add to the heterogeneity in the rock mass. Buijze et al. (2019a) identified the mechanisms of pore pressure diffusion, poroelasticity, thermoelasticity and dynamic stress transfer due to seismic events as important drivers for induced seismicity associated to geothermal operations. Recently, the role of stress transfer by aseismic creep as a driver for induced seismicity has also been highlighted in literature (Eyre et al., 2019). These mechanisms have to be considered for induced seismicity associated to UDG operations in the Dinantian carbonate reservoirs. In addition to these processes, Kang et al. (2019) suggest that (long-term) chemical processes can lead to a reduction of fault strengths, thus increasing fault reactivation potential. Simultaneously, Seithel et al. (2019) hypothesize that this decrease of frictional fault strength leads to a decrease of elastic energy released in earthquakes, and suggest the chemical processes of carbonate dissolution might partially explain features like the time-delay in seismicity at the geothermal site of Poing[27] and the decline of seismicity that has been observed several years after injection at the geothermal site of Unterhaching[27]. It is currently unclear in what way chemical processes during geothermal operations in the Dinantian carbonates can affect flow, heat transfer and related fault stress changes, and the frictional properties of the faults (in terms of static fault strength and post-reactivation friction behaviour).

Flow and temperature fields, their contribution to the above processes and fault stress changes depend on whether or not fracture networks and/or karstification are present, the characteristics of these natural fractures and the scale of karstification of the rocks.

Some modelling approaches account for the presence of fracture networks, however mostly in relation to stimulation of Enhanced Geothermal Systems in low-permeability basement rocks. Operational conditions for EGS are different from the geothermal doublets in carbonate rocks as developed or planned in the Dinantian carbonate reservoirs in the Netherlands[27]. Rock properties, such as relative contributions of storage and flow in fractures and matrix, and the mechanical response of matrix and fracture system in these low permeability systems may also be different from fractured carbonates. Modelling can give further insights in the way the different operational conditions and geology will affect the processes of pore pressure

[27] See also Buijze et al. (2019a), for review of mechanisms (section 2), case studies (section 3 & appendices), and many references to model studies (section 9 of that study). Poing & Unterhaching are described in section A2.2 & A2.5.

diffusion, poroelasticity, thermoelasticity, stress transfer and chemical changes, and ultimately the seismic response of the rocks.

In the next section, we will give an overview of different modelling approaches for fault reactivation and induced seismicity. We will address the pro's and con's and the applicability, specific requirements and limitations of modelling approaches for the Dinantian fractured carbonates reservoirs in the Netherlands.

BOX 4.1 BRIEF OVERVIEW OF SOME GEOMECHANICAL PARAMETERS AND RELATIONS FOR THE DESCRIPTION OF STRESS STATE, FAULT STABILITY, FAULT SLIP AND SEISMICITY

The stress state in the subsurface and at faults can be described by three **principal total stresses** (S_1, S_2, S_3). In the Netherlands, in most situations the **vertical stress** is the maximum principal stress (S_1=S_v), the intermediate principal stress is the **largest horizontal stress** (S_2=S_{Hmax}) and the minimum principal stress is the **smallest horizontal stress** (S_3=S_{hmin}). This stress state promotes **normal faulting (S_v>S_{hmax}>S_{hmin})**. Note that orientations and magnitudes of principal stresses may deviate, for example near salt domes or fault zones (i.e. S_1 may not be vertical in those settings, and hence S_v, S_{Hmax} or S_{hmin} may not be aligned with the principal stresses).

Fault stability is controlled by **effective stresses ($\sigma'_x = S_x - \alpha P_f$)** with the maximum, intermediate or minimum principal stress indicated by subscript x= 1, 2 or 3, **pore fluid pressure (P_f)** and **effective stress coefficient (α)**. For linear poroelasticity of porous rock, the effective stress coefficient is also known as **Biot's coefficient** and determines the elastic response of rocks to changes in fluid pressure (i.e. it determines the relative contribution of σ' that is carried by the fluid compared to that carried by the solid framework). For rock failure or fault reactivation, the effective stress coefficient is generally observed to be unity (α = 1).

Local effective stresses result in an **effective normal stress (σ_n')** and a **shear stress (τ)** at faults. The Mohr–Coulomb failure criterion **($\tau_f = C + \sigma'_n tan\varphi = C + \sigma'_n \mu$)** is most commonly used to describe brittle failure of rocks under compressive stresses, and is dependent on the **cohesion (C), friction angle (φ) or friction coefficient (μ)** of faults.

Adopting the Mohr-Coulomb failure criterion for rocks, fault stability and fault reactivation potential can be expressed in terms of **slip tendency ($ST = \tau/\sigma'_n$)**, i.e. cohesionless faults tend to reactivate and slip if **ST>μ**. Another way of expressing fault stability under changing pore pressure conditions is by the **shear capacity utilization ($SCU = \tau/\tau_{max} = \tau/(C + \mu\sigma'_n)$)**, i.e. faults are stable for **SCU<1** and fault reactivation occurs if **SCU=1**.

Coulomb stress changes ($\Delta C = \Delta\tau - \Delta\sigma_n\mu$) are a useful way of describing stress changes due to subsurface operations as they (or the Coulomb stressing rate) can be linked to the seismicity (rate).

More background on these parameters and relations can be found in Buijze et al. (2019a), section 2, and in geomechanical textbooks such as Jaeger et al. (2007); Zoback (2010); Fjaer et al. (2008).

4.1 Stochastic, hybrid and physic-based modelling approaches

The added value of modelling for fault reactivation and induced seismicity strongly depends on the type of model used, the timing in relation to the geothermal operations (before, during or after geothermal operations), and the specific question addressed. The overview of seismic hazard and risk analysis (SHRA) for the Groningen gas field (section 5.3) addresses the seismic source model as a main component of a SHRA. Different approaches to model seismic sources exist and they can be used in different ways.

In general, seismicity models can be used to:

- **Assess fault reactivation and seismogenic potential** associated with geothermal operations. For example, synthetic seismicity catalogues can be generated with these models and used as input to (probabilistic) seismic hazard and risk assessment of the geothermal operations (as for the Groningen model chain, section 5.3);
- Support in the **interpretation of field observations of induced seismicity** occurring at or in close vicinity of a geothermal site, and thereby further our understanding of the relation between geothermal operations and induced seismicity at a specific site (potentially also including other subsurface operations that may take place prior to or in the vicinity of geothermal operations);
- **Identify the dominant mechanism(s)** driving induced seismicity during and following geothermal operations. Models can be used to explain typical features of injection-induced seismicity, such as the 'Kaiser effect'[28], the dominance of post shut-in seismicity, and the occurrence of large seismic ruptures outside the area of stress perturbance;
- Gain **insights in the value of additional data, measurements and monitoring programs** that further constrain predictions and uncertainties in seismic hazard assessment;
- **Forecast in near-real time seismic hazard (and risk)** during geothermal operations, e.g., as a component of adaptive traffic light systems (Kiraly et al., 2016; Buijze et al., 2019a);
- **Design strategies to mitigate seismicity** related to geothermal activities, e.g., optimization of well production and injection strategies for minimizing induced seismicity.

The choice of model type and complexity should be based on the problem at hand (Figure 4-1). As such, there is no 'best-practice' or preferred approach for modelling fault reactivation and induced seismicity, neither in general nor for carbonate reservoirs in particular.

Various approaches have been described in literature for modelling the occurrence of induced seismicity associated with subsurface operations in general, and, more specifically, associated with geothermal operations. These approaches range from fully stochastic models, hybrid approaches in which physics-based and stochastic models are combined, to fully (deterministic) physics-based models. As stochastic models do generally not account for the physical processes underpinning seismicity, they cannot discriminate between different types

[28] In rocks subject to repeated cycles of stress, for example due to injection and depletion cycles, the Kaiser effect describes the absence of seismic events below the stress initially required to induce seismicity, i.e. seismicity only occurs if this initial stress is exceeded (Kaiser, 1950; Kurita and Fuji, 1979, Tang et al., 1997).

of reservoir rocks. In the next section, we shortly discuss the stochastic models. However, as we are interested in modelling approaches for (fractured) Dinantian carbonates, further focus is on hybrid- and physics-based models.

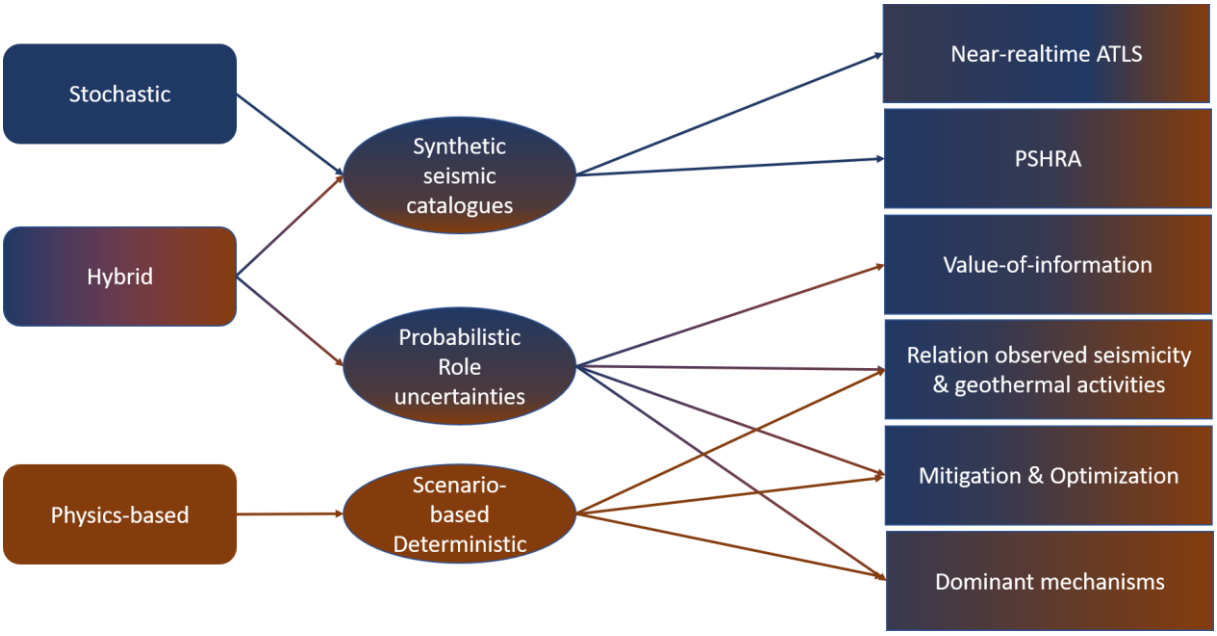

Figure 4-1 Possible applications of stochastic, hybrid and physics-based models to address questions related to induced seismicity caused by geothermal activities.

Stochastic models

Purely *stochastic models* do not, or only to a limited extent, incorporate the underlying physical processes of induced seismicity, but are based on the description of a random process. Frequently, stochastic models use data on observed seismicity combined with a scaling relationship like the Gutenberg-Richter relation, to assess probabilities of larger earthquakes based on recurrence rates of small earthquakes. Stochastic approaches are thus used to reproduce catalogues of observed induced seismicity in order to forecast seismic events in near real-time (Gaucher et al., 2015). One well-known example of such a stochastic model is the statistical Epidemic Type After Shock model (ETAS) for earthquake clustering (Ogata, 1998, see ***BOX 4.2***).

BOX 4.2 : EXAMPLE OF EPIDEMIC AFTERSHOCK MODEL (ETAS) FOR STIMULATION IN AN EGS IN BASEL, SWITZERLAND

The ETAS model is a so-called 'self-exciting' stochastic point process model. The model is based on the assumption that earthquake magnitudes are distributed according to Gutenberg-Richter scaling, and each seismic event generates its own 'child'–events, with an aftershock rate described by the empirical Omori-Utsu law. The ETAS model has been applied in retrospect to model induced seismicity during the stimulation of the EGS reservoir in Basel (Bachmann et al., 2011). Forecasts based on the ETAS model fit the seismic data quite well, in particular when the underlying injection rates are accounted for (Figure 4-2). This indicates that a stochastic model like ETAS can be applied as a valuable tool for real-time hazard estimation, under the condition that sufficient observations on seismic events are available.

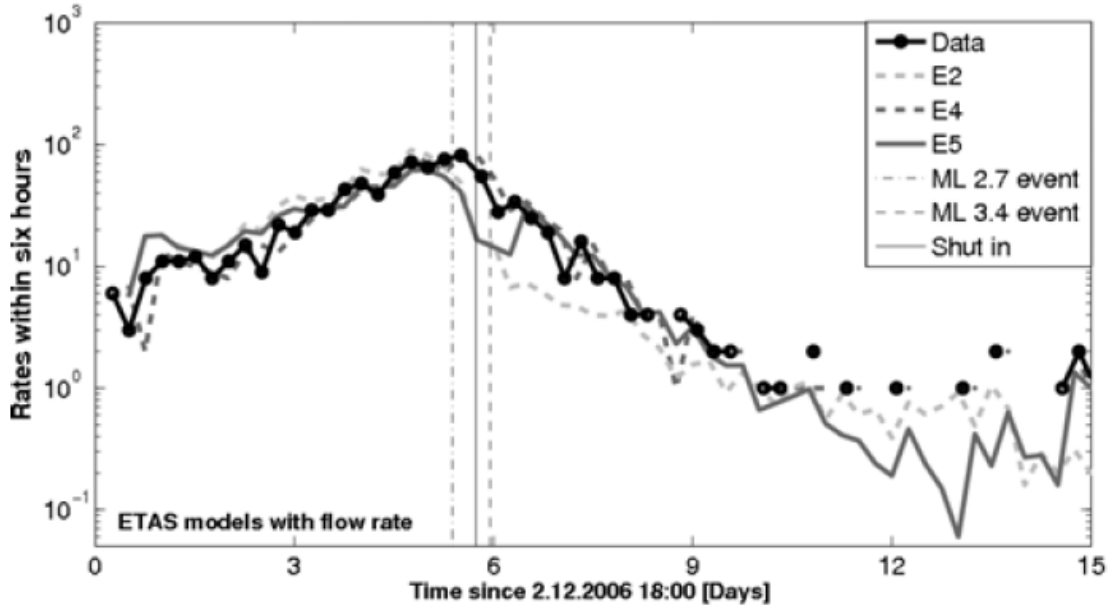

Figure 4-2 Results of stochastic model forecasts (in retrospect) for The Basel EGS site. Forecasts based on ETAS models (E2,E4,E5 in grey) for the next six hours as a function of time are compared to actual observations on seismicity rates at the Basel EGS site (bold black line with dots). ETAS models E2,E4 and E5 include information on injection rates. Timing of shut-in, and the timing of a Ml 2.7 and Ml 3.4 that led to actions within the traffic light are also shown. Source: Bachmann et al., 2011.

Hybrid and physics-based models

In contrast to fully stochastic models, *physics-based and hybrid models* do consider key physical processes which cause induced seismicity. Hybrid models combine physical-based models with statistical approaches. They are often designed to ensure computational efficiency. Hybrid approaches generally capture the key physical processes of induced seismicity in a simplified manner, which makes them fast enough to allow for a random sampling of model parameters. This way they can be used to give probability distributions of modelling results and incorporate uncertainties in model outcome. The seismic source model used in the seismic hazard and risk assessment for the Groningen gas field is an example of a hybrid model (cf. section 5.3). In this section we will give an overview of a range of hybrid and physics-based modelling approaches, which may be applicable to modelling induced seismicity in the Dinantian carbonate reservoirs.

Four key mechanisms affecting the evolution of seismicity during geothermal operations have been identified, i.e. pore pressure diffusion, poroelastic and thermo-elastic effects, and stress transfer (Buijze et al., 2019a, section 2). In addition chemical processes affecting fault strength (e.g., dissolution and precipitation processes) can be relevant for carbonates. Physics-based models can account for one or more of these key mechanisms.

A physics-based approach to model induced seismicity associated to geothermal operations generally consists of the following components:

1) Spatial and temporal evolution of **pressure and temperatures** (and, in some cases, chemical processes)
2) Spatial and temporal evolution of **stress**, including fault stress changes and fault stressing rates, fault reactivation potential
3) Optionally: (Seismic) **fault slip and fault rupture** (for a single event)
4) Optionally: **Seismicity rates and frequency magnitude relations** (multiple events)

Physics-based models can range from simplified 2D to 3D full field models and from (semi-) analytical to fully coupled thermo-hydro-mechanical-chemical models, capturing the complex interaction between flow, thermal, chemical and mechanical processes (Fokker and Wassing, 2019; Gaucher et al., 2015; Lu and Ghassemi, 2019). This interaction is particular important in karstified and/or fractured carbonate reservoirs, and it is extremely challenging to develop coupled models that capture the full complexity of the interaction between flow, thermal, chemical and mechanical processes.

4.2 Modelling pressure and temperature fields

Pore pressure and temperature changes caused by geothermal operations may lead to fault reactivation and induced seismicity. In order to assess the potential of induced seismicity related to geothermal operations in the Dinantian carbonate reservoirs and enable mitigation, it is crucial to understand the interplay between faults and pressure-, temperature- and associated stress changes near these faults. The spatio-temporal evolution of pore pressure and temperature fields can be modelled either **(semi-)analytically or numerically**.

Semi-analytical models

(Semi-)analytical solutions can only be applied for simplified geometries, such as axisymmetrical or horizontally layered reservoir configurations. Candela et al. (2018b) model flow throughout a single fault and focus on the combined poro-thermo-elastic stressing at the fault and its surroundings. They assume injection in the reservoir is dominated by a single fracture, and show thermally induced stresses control the rate of seismicity. Fokker et al. (2019) use a coupled semi-analytical model for the assessment of pore pressure, temperature and stress changes around a single injection well. They assume a plane-strain, axisymmetrical model geometry and homogeneous rock properties. The latter model can be used to obtain a first order assessment of pore pressure, temperature and stress changes around an injection well, when little is known on fault locations, offset, sealing properties and fracture distributions. Though (semi-) analytical models are fast and therefore suited for uncertainty analysis and probabilistic assessments, they cannot fully capture the key processes relevant for geothermal operations in the Dinantian carbonate reservoirs. Pore pressure and temperature fields around geothermal doublets will deviate from radial symmetry (e.g., Ter Heege et al., 2018b). Moreover, heterogeneities and flow anisotropy caused by different lithologies, layering, fault offset and sealing faults cannot easily be incorporated in these simplified models. In carbonate rocks, karstification may potentially affect the permeability of the rocks. Moreover, if fracture networks are present in the Dinantian reservoir rocks, the geometry, density and orientation of natural fracture networks will affect reservoir permeability.

Numerical models

The above effects can be captured in different types of numerical reservoir models. Here we distinguish three main classes (an extensive overview of flow modelling approaches in heterogeneous fractured rocks is given in e.g. National Research Council, 1996):

Equivalent continuum approach: In this approach, fluid flow in fractured media is modelled similar to fluid flow in porous rocks. The fractured rock mass is modelled as an equivalent porous medium, with upscaled hydraulic properties. Hence, it is not possible to distinguish flow in the fractures from flow in the matrix. Equivalent continuum presentations of complex fracture reservoirs have for example been used for rocks with very low matrix porosity and permeability and fracture-dominated flow. In this case carbonate rocks are modelled as a single medium, characterized by an (upscaled) fracture porosity-permeability. Computation times of equivalent continuum models for flow are much shorter than for dual-porosity-dual permeability models and discrete fracture network models. The equivalent continuum approach has e.g. been applied to simulate flow and thermal processes in the Malm carbonates of the Molasse Basin (Savvatis et al., 2019 – see ***BOX 4.3***).

BOX 4.3: EXAMPLE OF EQUIVALENT CONTINUUM APPROACH TO MODELLING PRESSURE AND TEMPERATURE CHANGES FOR A GEOTHERMAL DOUBLET IN THE MOLASSE BASIN, SOUTHERN GERMANY

In their publication, Savvatis et al. show the effects of pore pressure and temperature changes on stress changes in a geothermal doublet in the Malm Carbonates of the Southern Bavarian Molasse Basin (Figure 4-3). They model a number of production scenarios, from which a thermal and hydraulic worst case scenario is selected. Pressure and temperature fields are modelled in Eclipse™, using an equivalent porous medium approach, with upscaled permeability. Flow and temperature fields are then used as input to a 3D geomechanical model in VISAGE™, using one-way coupling. Based on their modelling results, the authors conclude that after 50 years of operation, the impact of cooling and thermal stressing by far exceeds the impact of the pressure changes.

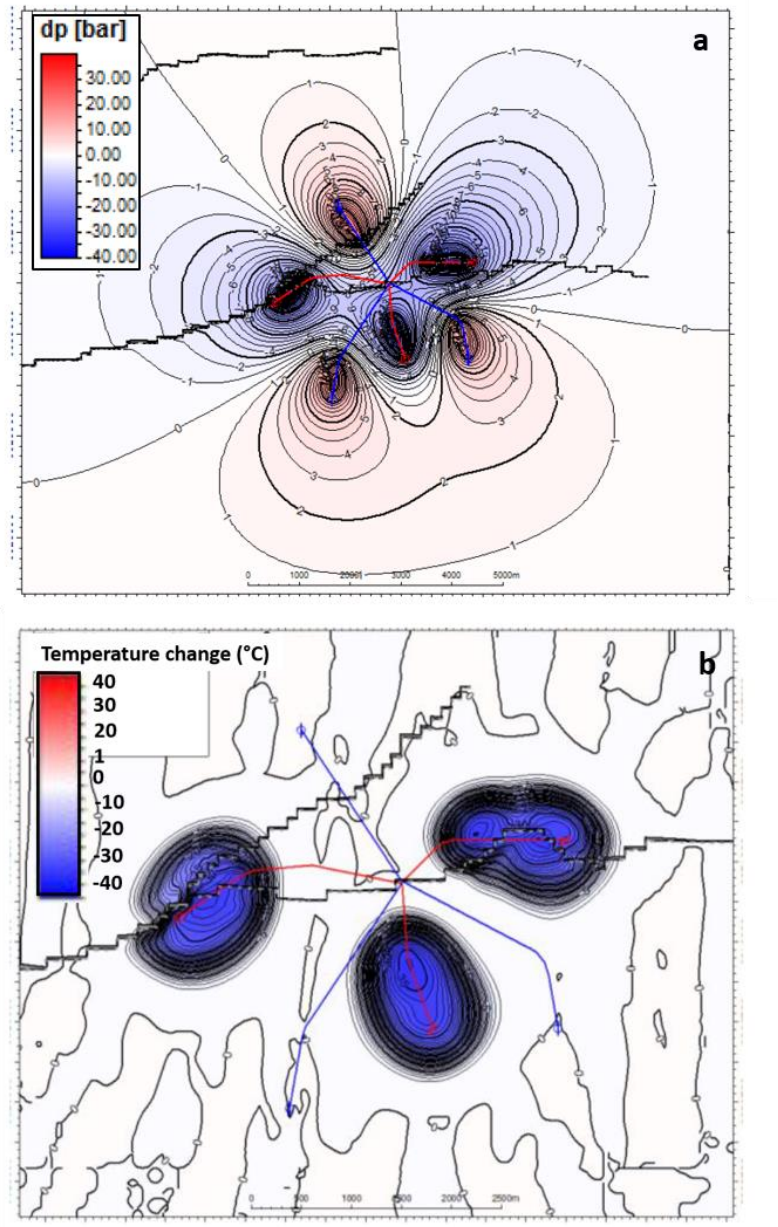

Figure 4-3 a) Pressure and b) temperature change after 50 years of geothermal production in Malm carbonates of the Bavarian Molasse Basin, for a 'worst case' hydraulic scenario. Black continuous (stair-stepped) lines indicate position of faults. Production wells in red, injection wells in blue). From: Savvalis et al. (2019).

Dual-porosity-dual permeability models: In naturally fractured carbonate reservoirs the highly permeable fractures and the relatively low permeable rock matrix will generally form two interconnected systems. The permeability and porosity of the matrix and fractures will determine the interaction between the two systems, and will thereby determine the flow behavior and temperature in the rocks. Depending on the interaction between fractures and matrix, the reservoir can thus be modelled as a 'dual porosity – single permeability' or a 'dual porosity – dual permeability' medium (Figure 4-4). Bruijnen (2019) expect dual-permeability models to be most representative for the Dinantian carbonates. Dual-porosity models have been applied for geothermal applications in fractured rock. As an example, in Gan and Elsworth (2014) a dual porosity – single permeability model in the flow simulator Tough2 is used to investigate the likelihood fault reactivation and induced seismicity by thermally driven stress changes (see ***BOX 4.4***).

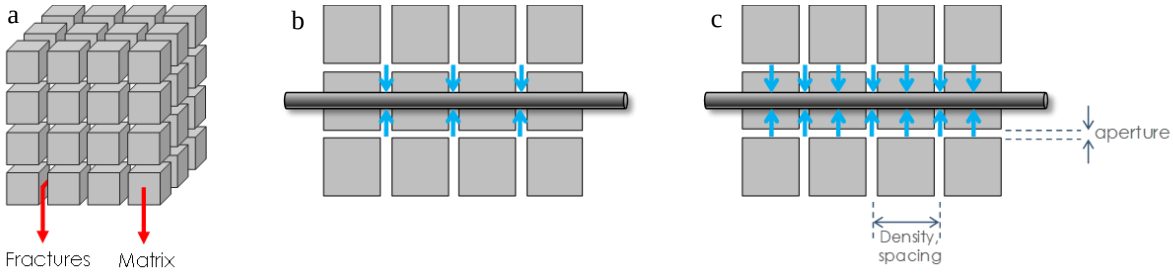

Figure 4-4 a) Schematic representation of a dual porosity model ; b) dual porosity – single permeability, with fracture dominated flow, c) dual porosity – dual permeability, with fracture/matrix dominated flow. Horizontal cylinder represents the wellbore. Source: Bruijnen (2019).

Discrete fracture networks: Alternative to the approaches described above, individual fractures can be modelled as a set of discrete fractures with known position and orientation or as stochastic realizations of fracture networks, known as discrete fracture networks (DFN, e.g. Kohl et al., 2007; Lu et al., 2019).). These discrete fracture networks can be generated based on specified distributions for fracture size, density, shape, orientations, location, aperture and fracture permeability (see Figure 4-5). Unlike the approaches described above, discrete fracture modelling explicitly takes into account fracture geometry and connectivity. It is noted here that results from DFN models such as equivalent fracture network permeability and porosity can be used as input to dual porosity/dual permeability and equivalent continuum models. An example of a model based approach using DFN is given in ***BOX 4.8***.

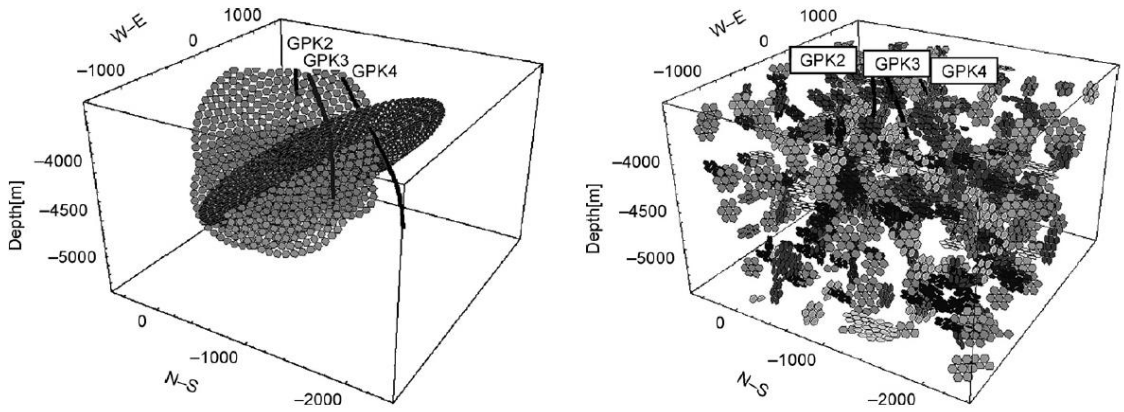

Figure 4-5. Examples of a 3D flow model with deterministic fracture zones (left) and a realization of stochastically generated fracture zones, representing the geothermal reservoir at 5km depth in Soultz-sous-Forêts (Kohl et al., 2007).

BOX 4.4: EXAMPLE OF DUAL POROSITY, SINGLE PERMEABILIT MODELLING OF FLOW, FAULT REACTIVATION AND SEISMIC SLIP IN GEOTHERMAL RESERVOIRS

Gan and Elsworth (2014) use an equivalent dual porosity – single permeability model in the flow simulator Tough2, coupled to the mechanical simulator of FLAC3D (Taron and Elsworth, 2009) to investigate the likelihood of late-stage fault reactivation and induced seismicity by thermally driven stress changes. The dual porosity – single permeability is used to model the heat transfer between the fractures and low porosity rock matrix. The dual porosity medium is represented by orthogonal fracture sets spaced equally in 3 directions, with uniform aperture and an impermeable matrix. In general, the heat exchanged between fracture fluid and rock matrix is controlled by the area of heat transfer, the temperature gradient between the circulating fluid and rock and the fluid velocity. For a geothermal doublet, they show fracture spacing and injection rates control the form of the cooling front which propagates through the reservoir. At high flowrates, the heat transfer from the rocks to the fluids is small and thermal drawdown in the reservoir is uniform, without a distinct thermal front. In contrast, when flow rates are low, a distinct cooling front propagates slowly through the reservoir. They find the pattern of fault reactivation and induced seismicity is strongly affected by the form of the cooling front (Figure 4-6). ***Continued on next page.***

BOX 4.4 (CONTINUED)

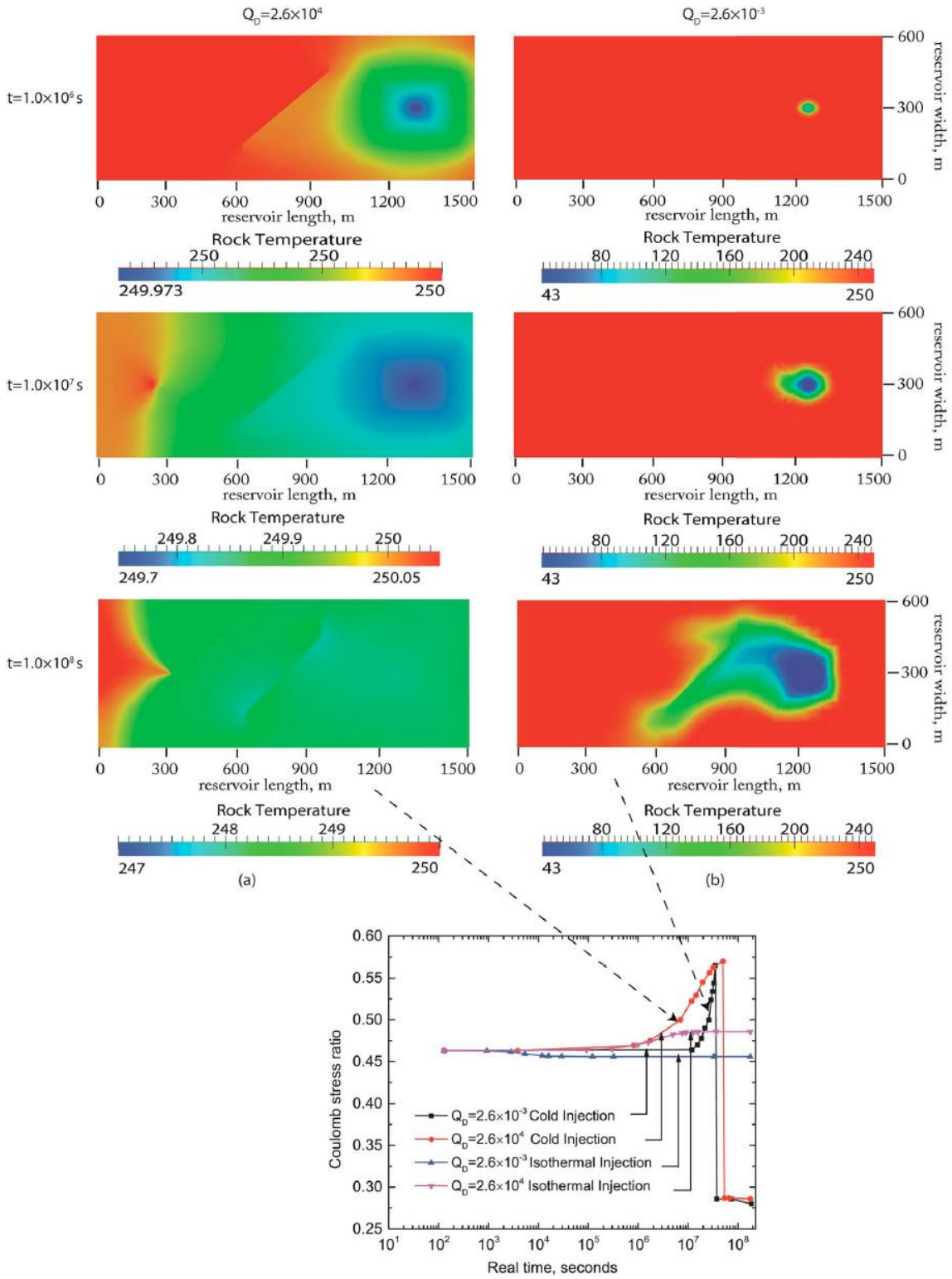

Figure 4-6. Evolution of rock temperature distributions between a producer and injector well of a geothermal doublet, at t = 1.0e6 s, t=1.0e7s and 1.0e8 s, for high (left column) and low flow (right column) rates. Flow rates are dimensionless. Figure represents a vertical cross section of the reservoir between injector and produced well. Location of injection well at right side. Lower figure represent the evolution of Coulomb stress ratio for the two flow rates, under isothermal and non-isothermal conditions. From: Gan and Elsworth (2014).

Coupling of flow, temperature and mechanics and chemical processes: The effect of coupling between flow, temperature and mechanics can be of significant importance for fractured carbonate rocks. Homuth et al. (2015) observed a significant increase in permeability for the carbonate reservoir rocks of the Molasse Basin, caused by cooling and thermal contraction of the rock matrix, under typical reservoir conditions. They conclude that for tight reservoir carbonates the permeability is temperature-controlled. Fracture permeability can also change due to fracture slip and dilation, or chemical processes. Iteratively coupled or fully coupled thermo-hydro-mechanical-chemical (THMC) models can be used to assess the impact of the coupled processes on permeability evolution, flow, temperature and stress evolution near faults. Fully coupled THMC modelling and an example of THMC model for geothermal applications is presented below (section 4.4 and ***BOX 4.8***).

4.3 Modelling stress and fault reactivation potential

The potential for fault reactivation may be evaluated by **static geomechanical models**, which analyze the stresses in the reservoir and at fault planes, based on pore pressure and temperature changes obtained from reservoir models. Again, the choice of model complexity will vary and depend on the specific question to be addressed, the trade-off between computation times and complexity of geology, flow behavior and data availability to constrain this complexity (Ter Heege et al., 2018a).

1D analytical models for fault stability

The simplest one dimensional (1D) analytical models for fault stability can be used as a screening tool to assess fault stability. They require a minimum of input, are efficient in terms of computational costs, and can provide a first-order estimate of fault stability under changing pore pressure and temperature conditions. As the models are computationally efficient, they can be used to account for uncertainties in input parameters and sensitivity analysis. They require input on initial stress conditions, elastic reservoir properties, fault orientation and fault strength to calculate fault stability and reactivation potential.

1D analytical solutions for poro- and thermoelastic stress changes (Buijze et al., 2019a) can be used to derive reservoir stress changes caused by pressure and temperature changes. Fault stability and fault reactivation potential can then be expressed in terms of slip tendency, shear capacity utilization, Coulomb stress changes on the fault, or in terms of critical pore pressures to reactivate the fault (see ***BOX 4.1*** and Buijze et al., 2019a for definitions). One of the basic assumptions of the 1D fault stability models is that stress changes take place in a laterally extended and uniform reservoir layer, where pore pressure, temperature and stress changes are uniform (uniaxial deformation). The models do not account for the effects of (strong) spatial gradients in pressure and temperature, reservoir heterogeneity, and stress arching caused by sharp changes in reservoir geometry (fault offset, reservoirs of limited extent, sealing faults).

BOX 4.5 COMPARISON BETWEEN 1D ANALYTICAL MODEL AND 2D NUMERICAL MODEL OF COULOMB STRESS CHANGE FOR 2D PRESSURE AND TEMPERATURE CHANGES AROUND A GEOTHERMAL DOUBLET

Figure 4-7 a shows an example of pore pressure and temperature field obtained from DoubletCalc2D for a geothermal doublet in a typical Dutch sandstone reservoir. The spatio-temporal pore pressure and temperature field is used as input to a 1D geomechanical analytical approach (one-way coupling). Based on local pore pressure and temperature changes, local (uniaxial) poroelastic and thermoelastic stress changes are computed. Effects of stress arching are ignored. Stress arching is caused by differential expansion and compaction of the reservoir rocks, due to abrupt changes in pressure and temperature gradients, Faults are not explicitly modelled, but assumed to be ubiquitous over the reservoir. Local reservoir stress changes are translated to fault Coulomb stress changes. Results are shown for a fault set with orientation E-W dip direction and dip of 60°. Results of the 1D analytical approach are compared to results of a numerical FLAC3D model, which can take into account the effects of stress arching. Figure 4-7b. shows that in this specific case the 1D approach can be used as a first order estimate of fault reactivation potential. ***Continued on next page.***

BOX 4.5 (CONTINUED)

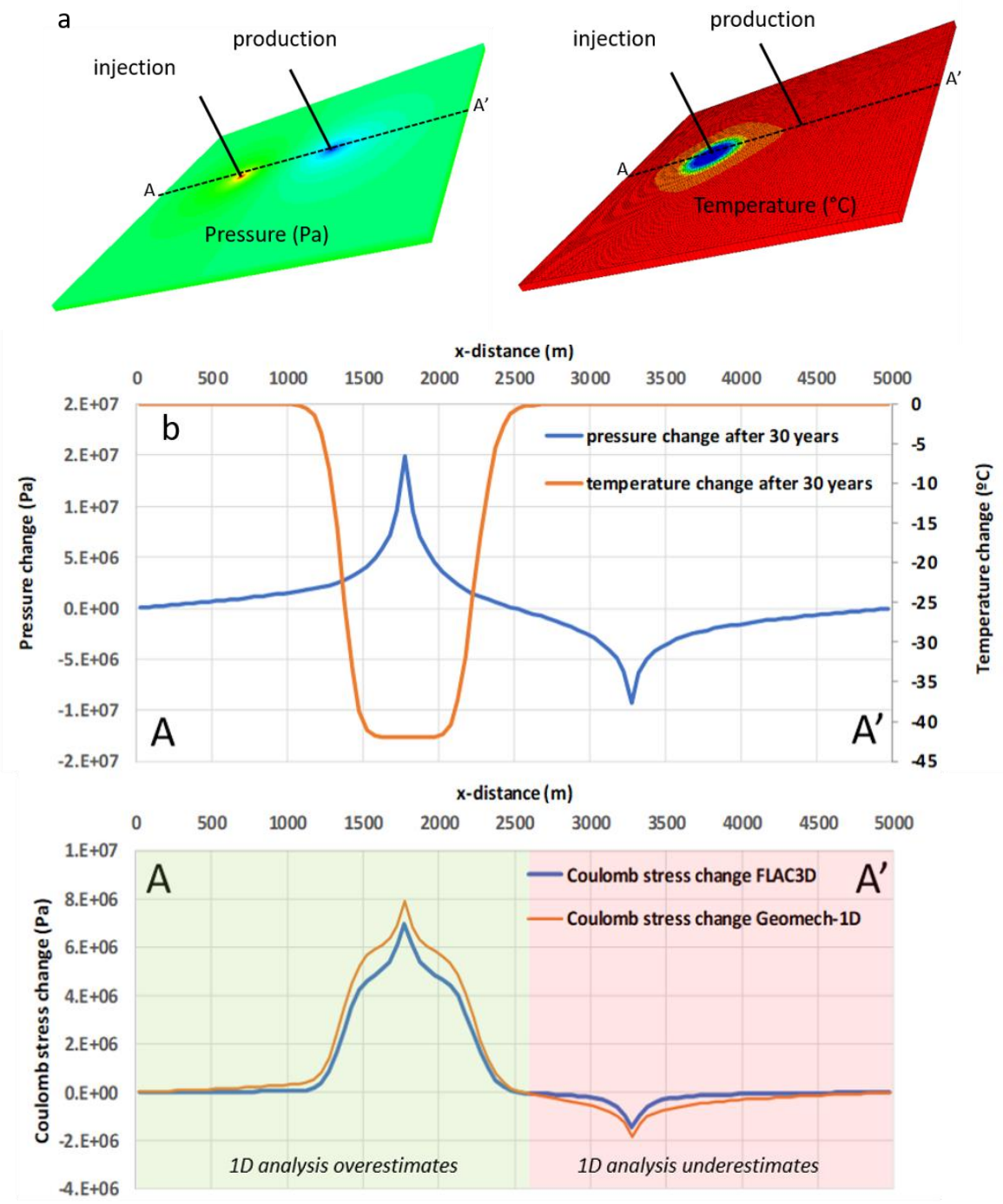

Figure 4-7 a) shows the results of pore pressure and temperature fields from DoubletCalc2D, b) upper: pressure and temperature change along cross section A-A', after 30 years of geothermal operations; lower: comparison of Coulomb stress changes computed based on a 1D fault stability approach and computed in the 3D numerical model in FLAC3D. Differences in Coulomb stress changes can, for example be explained by effects of stress arching caused by differential compaction and expansion of the rocks. For this specific case, 1D geomechanical analysis overestimates Coulomb stress change around the injection well and underestimate Coulomb stress changes around production well. Source: TNO.

1D analytical fault stability models require input on pressure and temperature changes. They can be combined with simple reservoir flow models, or more complex dynamic reservoir models. ***BOX 4.5*** presents an example of a 2D numerical flow and temperature calculation in DoubletCalc2D (TNO, 2014), combined with a 1D analytical fault stability model. ***BOX 4.5*** shows that in this specific case the 1D approach can be used as a first order estimate of fault reactivation potential.

Walsch and Zoback (2016) use the 1D fault stability approach to perform a probabilistic assessment of potential fault slip related to waste water injection in Oklahoma. They incorporate uncertainties in the stress tensor, pore pressure, coefficient of friction and fault orientation to obtain a cumulative distribution function of the pore pressure changes required to cause fault slip on each fault mapped in the area. This way, they can assess the probability of fault reactivation for each known fault in the area affected by the injection-induced pressure changes. A similar approach has been applied by Seithel et al. (2019) for the carbonate reservoirs in the Molasse Basin (for example see ***BOX 4.6***).

2D analytical and numerical fault stability models

Two dimensional (2D) models can be used to simulate the effect of spatial gradients in pore pressure and temperature, and geometrical complexity on stress arching (albeit limited to 2D, i.e. 'plane strain' conditions). The numerical fault stability models can be coupled with reservoir numerical or analytical flow models, to incorporate (in 2D) the spatial distribution of pore pressures and temperatures.

BOX 4.6 EXAMPLE OF PROBABILISTIC 1D FAULT STABILITY MODELLING TO ANALYZE FAULT REACTIVATION FOR A GEOTHERMAL DOUBLET IN THE MALM CARBONATES OF THE MOLASSE BASIN, S. GERMANY

Seithel et al. (2019) use a probabilistic 1D fault stability model to analyze the fault reactivation potential in the Malm carbonates of the Bavarian Molasse Basin (Figure 4-8). By means of a Monte Carlo simulation, they investigate the effect of variations of in-situ stress magnitudes and S_{hmax} orientation, fault friction (μ) and cohesion (C) on shear stress (τ), normal stress (σ_n) and fault reactivation potential. In their approach, fault reactivation potential is expressed in terms of a 'critical pore pressure for failure', which equals the pressure change needed to reach the Mohr Coulomb envelope (P^c_{eff}):

$$P^c_{eff} = (\sigma_n - P_p) - (\frac{\tau - C}{\mu})$$

For every known fault in the area of interest they compute the probability of fault reactivation (RP), assuming an expected maximum pressure change of 20 bar. ***Continued on next page.***

BOX 4.6 (CONTINUED)

Workflow for the assessment of fault reactivation potential RP in the Molasse Basin:

a) Normal distributions of input parameters used as input to the probabilistic analysis
b) Derivation of critical pore pressure (P^c_{eff}) for each iteration of the Monte Carlo analysis
c) Cumulative probability distribution for three faults in the fault set –and selection of the reactivation potential RP for each fault section, based on a reference maximum pressure increase of 20 bar.

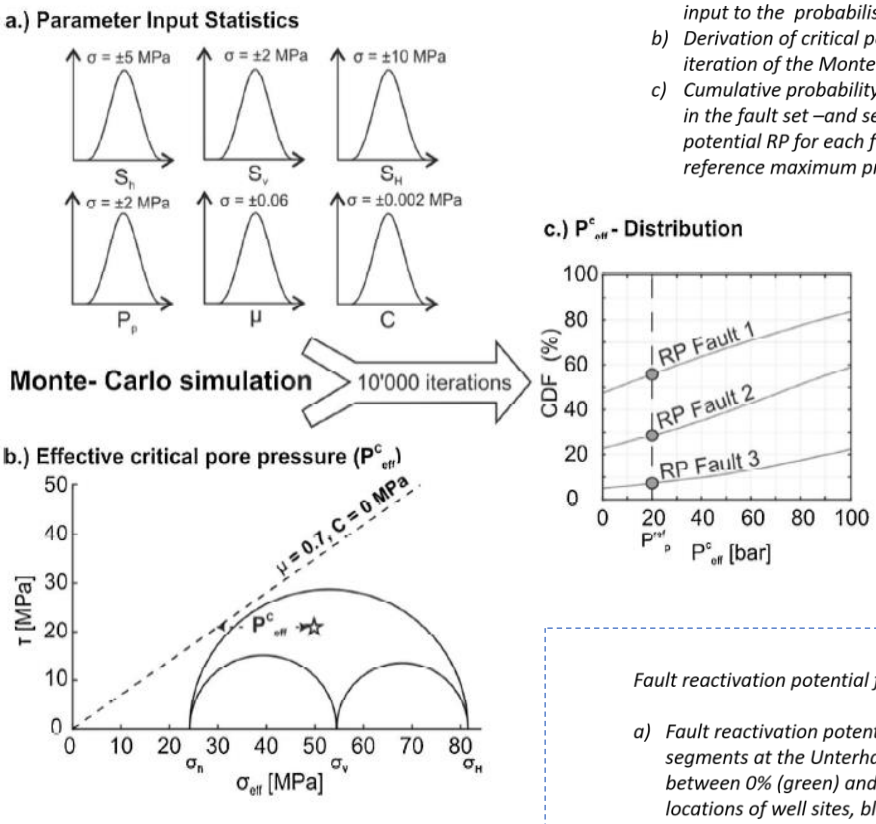

Fault reactivation potential for the Unterhaching site:

a) Fault reactivation potential for known fault segments at the Unterhaching site; RP is scaled between 0% (green) and 80% (red); block dots are locations of well sites, black and blue lines represent open hole section for production, resp. injection; red symbols are seismic events with Ml>=1.
b) Reactivation potential distribution for stress rotation, and histogram presenting the local strike of the faults.

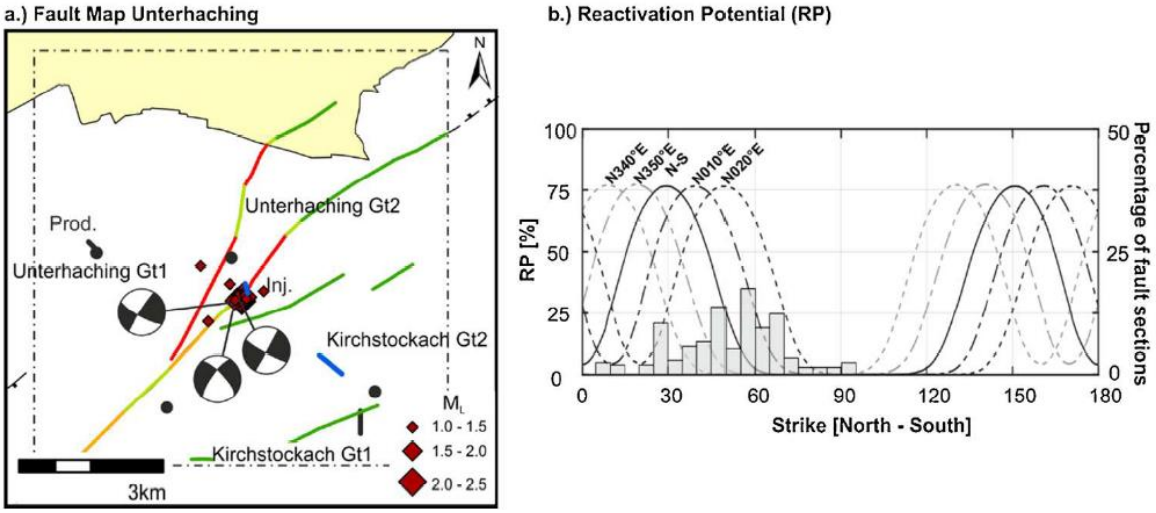

Figure 4-8. Fault reactivation potential and the spatial-temporal evolution of seismicity at the geothermal sites in part of the Bavarian Molasse Basin are compared. Based on the comparison, the authors suggest that for critically stressed faults, like occurring in Unterhaching, small changes in hydro-mechanical conditions may dominate seismicity, whereas in case of low reactivation potential (like in Poing) slower processes like thermo-mechanical changes and alteration of fault strength by carbonate dissolution may dominate. From: Seithel et al. (2019).

3D numerical fault stability models

Three dimensional (3D) models have to be used when plane-strain, or axisymmetrical assumptions cannot be made. This applies to geothermal doublets in a reservoir which is offset by a fault, doublets in heterogeneous reservoirs, or in case sealing faults are present. ***BOX 4.7*** shows a 3D numerical flow calculation in OPM (Open Porous Media simulator) which is well suited for single phase coupled flow and temperature calculations in geothermal reservoirs. Results have been combined with a 3D computation of fault stability in the semi-analytical software of MACRIS (Van Wees et al., 2019b). As shown in Figure 4-9, fault offset and particularly fault transmissivity have a significant effect on the evolution of fault stresses due to pressure and temperature changes around a geothermal doublet. Since 2D and 3D numerical models are computationally expensive, they cannot be used to fully address the uncertainty of model input parameters (unlike 1D models). Sensitivity of model parameters can however be addressed by simulation of several realistic model scenarios. 3D models can be developed in conjunction with 1D or 2D models to address uncertainty of input parameters.

BOX 4.7 EXAMPLE OF 3D ANALYSIS OF FAULT OFFSET AND TRANSMISSIBILITY ON SPATIAL PRESSURE, TEMPERATURE AND STRESS DISTRIBUTION FOR A GEOTHERMAL DOUBLET IN A SANDSTONE RESERVOIR

Van Wees et al. (2020) analyze the impact of geothermal doublet configuration, fault offset and fault transmissivity on development of pore pressure and temperature fields and associated fault stress changes during geothermal production in a typical Dutch geothermal aquifer. They use OPM (Open Porous Media simulator) to model the temperature and pressure field around the producing geothermal doublet. Pressure and temperature fields are used as input to the semi-analytical MACRIS (Van Wees et al., 2019) Mechanical Analysis of Reservoir Induced Seismicity) tool for analysis of fault stresses, taking into account the role of fault offset and fault transmissivity in fault stressing.

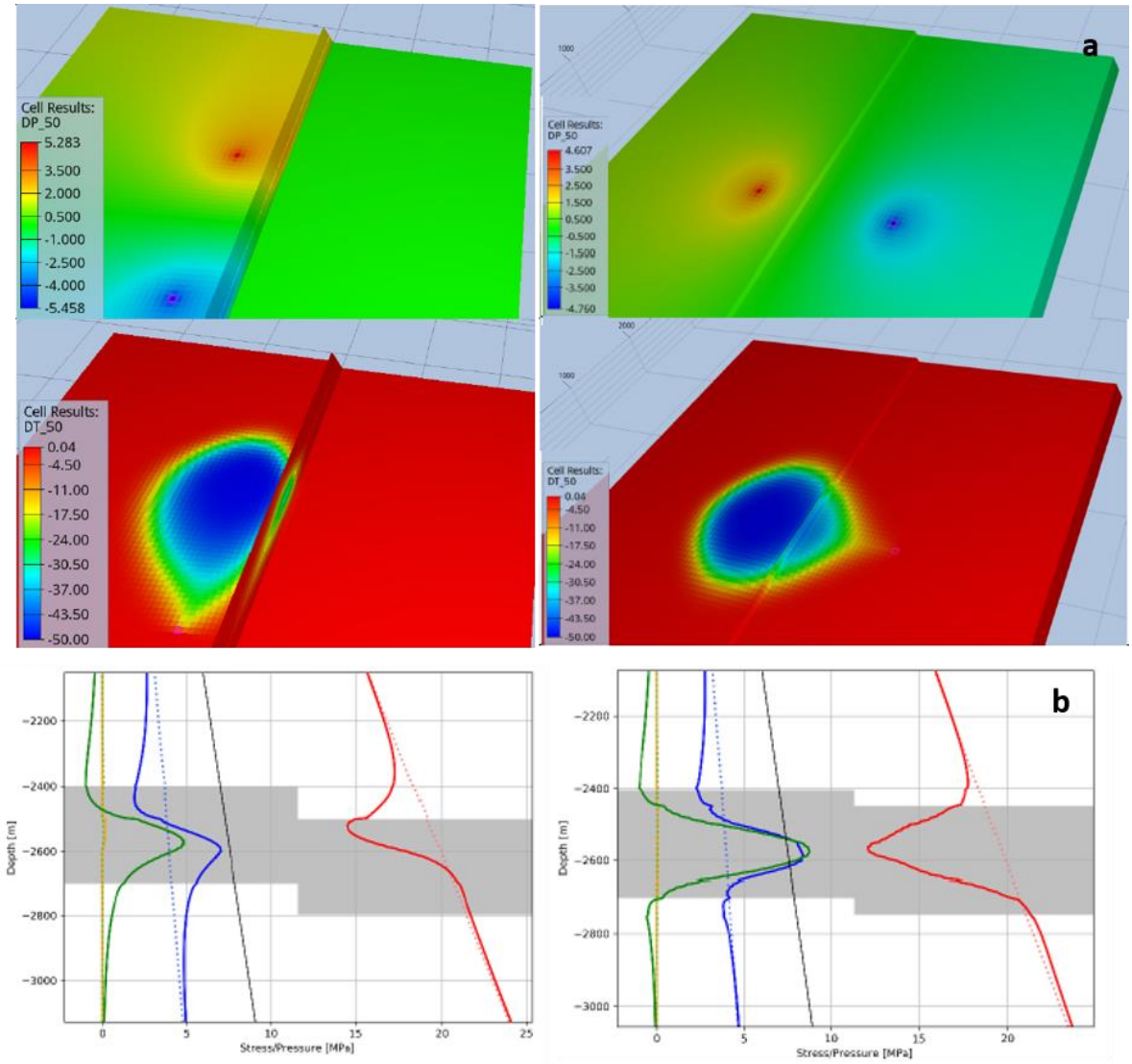

Figure 4-9 a) shows an example of pore pressure and temperature field obtained from the OPM flow simulator, for two typical geothermal doublet configurations in a typical Dutch sandstone reservoir. Left: sealing fault, right open fault. Fields are shown after 30 years of direct heat production from a 100 m thick homogeneous porous geothermal aquifer. Injection temperature is 30ºC, ambient reservoir temperatures of 80 ºC. b) Associated (Coulomb) stresses and pressures at the fault for the two cases, computed in MACRIS. Dashed lines indicate initial stress and pressure gradients, continuous lines stress and pressure after 30 years. Blue: shear stress, red: effective normal stress, green: Coulomb stress, orange pore pressure change. Black line: Coulomb failure criterium. From: Van Wees et al., 2020.

4.4 Fully coupled thermo-hydro-mechanical-chemical models

The majority of the modelling approaches for the assessment of fault stability discussed above use a 'one-way' coupling between flow, temperature and geomechanics. Pore pressure and temperature fields are used as input to geomechanical analysis to assess Coulomb stress changes and fault reactivation potential. The effects of mechanical processes (such as stress changes and deformation) on flow and temperature are not taken into account. As mentioned before, full thermo-hydro-mechanical-chemical (THMC) coupling may be required if the mechanical and/or chemical response of the reservoir results in significant changes in transport properties, which in turn affect the pore pressure and temperature distribution, or if chemical processes effect flow and mechanical strength of faults (Figure 4-10). Specifically for fractured carbonates like the Dinantian, coupling between mechanics, flow and temperature and potentially chemical processes may be important. An example of a fully coupled thermo-hydro-mechanical-chemical model has been described by Izadi and Elsworth (2014) (see ***BOX 4.8***).

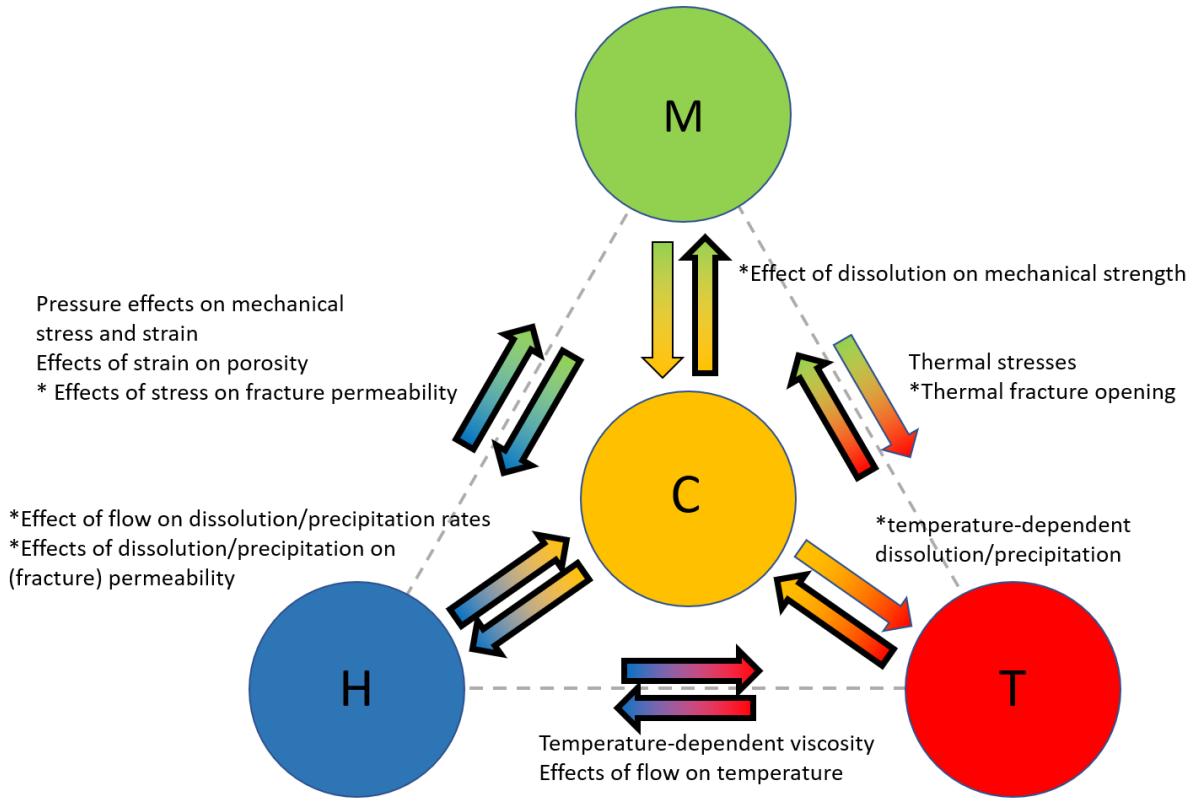

Figure 4-10 Schematic presentation of the coupled processes that play a role in Dinantian carbonates. M: mechanics, T: thermal, H: hydraulic, C: chemical processes. Coupling processes relevant for the Dinantian carbonates are show as bold arrows. Coupling in (fractured & karstified) carbonates is generally more complex than in homogeneous porous sandstone reservoirs. Additional processes that can play a role in carbonates, which have no to little importance in sandstones are marked with a *.

BOX 4.8 EXAMPLE OF FULLY COUPLED THERMO-HYDRO-MECHANICAL-CHEMICAL MODELLING OF THE SPATIAL DISTRIBUTION OF PERMEABILITY, STRESS DROP AND MOMENT MAGNITUDE FOR THE NEWBURY EGS SITE IN OREGON, U.S.A.

Izadi and Elsworth (2014) apply a fully coupled THMC continuum model to assess permeability enhancement and evolution of seismic rupture in space and time during short term stimulation of the fractured reservoir at the Newbury EGS site (Figure 4-11). They use the fully coupled FLAC3D-TOUGHREACT code, in which FLAC3D is used for the mechanical, and TOUGHREACT for the interaction of thermal, flow and chemical processes. They include a discrete fracture network of variable density and connectivity and allow for computation of permeability changes from the coupled THCM processes, such as from mechanical deformation, and the precipitation and dissolution of calcites and amorphous silicas. Fracture failure is calculated from the evolution of normal and shear stresses in FLAC3D. A static-dynamic frictional strength-drop is used to determine the seismic energy release for small (scale ~10m) to large fractures (~1200m) which are embedded in an elastic matrix.

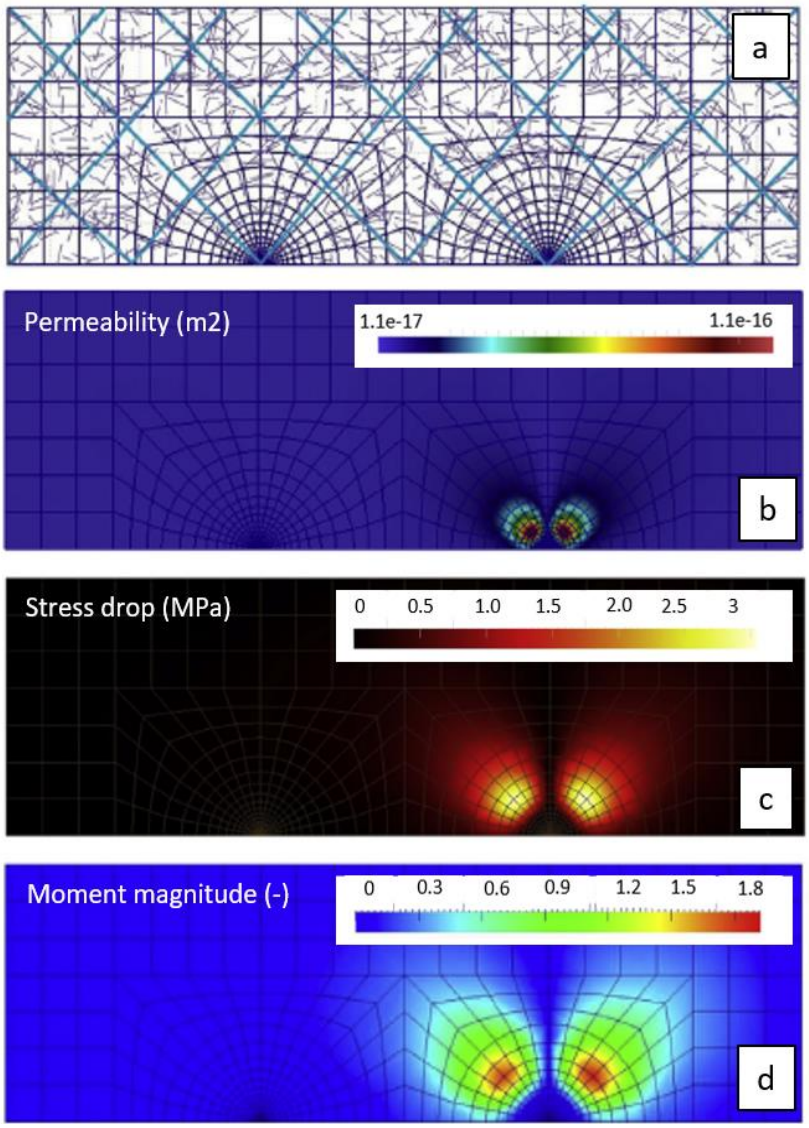

Figure 4-11 Results of the THMC-coupled model of hydraulic stimulation at the Newsbury EGS site in TOUGHREACT-FLAC3D. a) (Part of) model layout, including discrete fracture network, b) permeability enhancement around injection well, c) stress drops of reactivated fractures, d) magnitudes of associated seismic events. Adapted from Izadi and Elsworth (2014).

4.5 Modelling fault slip and seismic fault rupture (for a single event)

The fault stability models described above focus on the development of stresses and their effect on fault reactivation potential. Accordingly, the fault stability models can provide valuable information on the timing and location of potential fault reactivation, caused by the pressure and temperature changes at a geothermal site. Fault stability criteria as slip tendency, shear capacity utilization and critical pore pressures are based upon the Mohr Coulomb criterion, which defines the strength of a (often assumed to be cohesionless) fault. As the ideal plastic Mohr-Coulomb failure criterion cannot be used to describe the post-failure behaviour of faults, it is less well suited to determine the magnitude and areal extent of fault slip, nor to address the question whether seismic or aseismic slip will occur. Also, the 2D and 3D numerical fault stability models described above are usually based on quasi-static physics. This means the effects of inertia forces, related to the (de)acceleration of the rock mass during fault rupture, is not taken into account.

Dynamic rupture models include the effects of inertia on fault slip, and are used to investigate the time-dependent evolution of the seismic fault rupture process (Jin and Zoback, 2018, Buijze et al., 2019b). They are commonly based on advanced constitutive laws for fault frictional behaviour, such as the slip-weakening law, or the rate and state friction law (Dieterich, 1994), which are more suitable to describe the post-failure behaviour of the fault after the onset of fault slip. Dynamic rupture models give insight into the dynamic behaviour of the fault after the onset of fault reactivation. These models can be used when one is interested in the controlling factors of seismic versus aseismic slip behaviour and the propagation and arrest of seismic rupture. Accordingly, they are used to analyse what controls the size of the rupture area, the total slip displacements, stress drops and (seismic or aseismic) rupture velocities. The outcome of the models can be used to assess e.g. the potential for fault rupture to extend outside the area of pressure and temperature disturbance and what controls the likelihood of relatively large-magnitude seismic events.

Dynamic rupture models are computationally expensive, and mainly used in 2D models, to model the characteristics of a single seismic event. As such, they do not provide information on the frequency of seismic events, and cannot be used to create synthetic catalogues of seismic events. Additionally, they require input parameters for the advanced fault friction laws, which are usually poorly constrained. Using scenario and sensitivity analysis, they can however give valuable insight into the main factors controlling the physics of nucleation, propagation and arrest of seismic events. An example of dynamic rupture modelling used for analysis of the dynamics of fault rupture in depleting gas fields is presented in ***BOX 4.9***.

BOX 4.9 EXAMPLE OF DYNAMIC RUPTURE MODELLING TO CONSTRAIN THE NUCLEATION AND SIZE OF A SINGLE SEISMIC EVENT INDUCED BY GAS DEPLETION IN SANDSTONE RESERVOIRS

In Buijze et al. (2019b), dynamic rupture models are used to investigate the factors that control the nucleation and size of earthquakes which are induced by reservoir production (Figure 1-13). They use a linear slip weakening law to characterize the post-failure frictional behavior of a fault. A quasi-static 2D numerical model of a fault intersecting a reservoir is used to simulate the stress evolution and onset of fault slip during reservoir depletion.

The quasi-static analysis is followed by a dynamic rupture analysis to simulate the seismic rupture process on the fault. The sensitivity of earthquake nucleation and fault rupture size to geological factors like criticality of the initial stress conditions, fault frictional properties and fault offset are investigated. It was found that a critical fault length (or nucleation length) is required to slip before a seismic rupture can occur. Rupture propagation outside the reservoir and large seismic magnitudes are found to be promoted by critical initial stress, large stress drops and small fracture energy (both related to the post-failure fault frictional properties) and not too little fault offset.

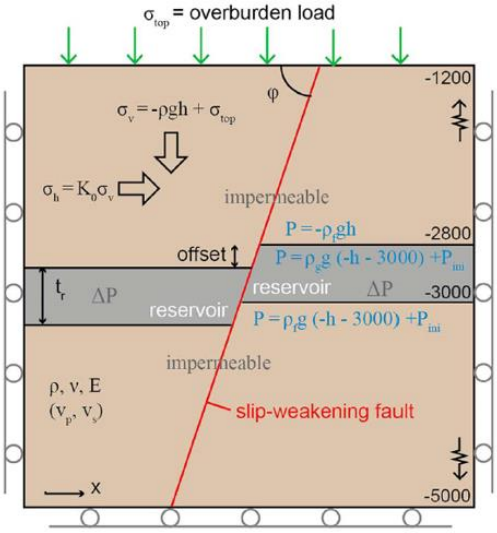

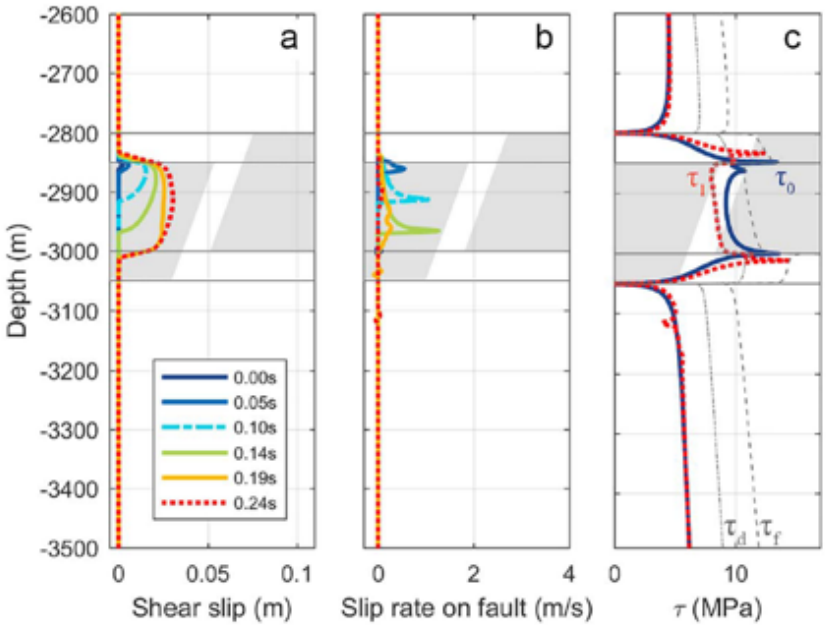

Figure 4-12 Upper right: Model geometry of a fault with 50m offset intersecting a producing gas reservoir. Fault is presented in red and characterized by a slip-weakening post-failure law; reservoir is shaded- grey. Bottom: Results of the dynamic rupture model, with location of reservoir in shaded-grey: a) evolution of on-fault shear as a function of depth for different points in time, b) on-fault slip rates as a function of depth and time and c) on-fault shear stress as a function of depth for different points in time. Grey dashed and continuous line represent failure stress τ_f, respectively dynamic shear stress τ_d at the start of rupture. From: Buijze et al. (2019b).

4.6 Modelling seismicity rates and frequency magnitude relations (multiple events)

Currently, fully dynamic rupture models are used to model the rupture process of a single seismic event. Probabilistic Seismic Hazard Assessment and Adaptive Traffic Light Systems generally rely on the availability of synthetic catalogues of multiple seismic events. Hybrid approaches, combining key physical processes in a simplified manner with statistics, have been used to model frequencies and magnitudes of multiple seismic events events to obtain synthetic catalogues of induced seismicity. Gischig et al. (2013) describe a hybrid model for induced seismicity around an injection well, based on a simplified 2D axisymmetrical pore pressure diffusion model in the multiphysics modelling package COMSOL, combined with a geomechanical seed model. The geomechanical seed model enables fast computation of catalogues of seismic events (see ***BOX 4.10***).

Besides being coupled to the axisymmetrical flow model, the geomechanical seed model has been coupled to more advanced numerical flow models. Rinaldi and Nespoli (2017) combine the numerical TOUGH2 flow simulator with the geomechanical seed model. They extent the geomechanical seed model to account for static stress transfer, following the approach of Baisch et al. (2010) and Catalli et al. (2016). Karvournis and Wiemer (2019) describe a hybrid model that combines a 3D discrete fracture network with the geomechanical seed model for earthquake generation. The model is used to forecast induced seismicity and study different injection scenario's for optimizing reservoir performance.

Many other approaches for modelling frequency-magnitude distributions, synthetic catalogues of seismic events and/or total seismic moment released during subsurface activities exist. Van Wees et al. (2019b) model the total seismic moment released during geothermal operations based on fault Coulomb stress changes in their semi-analytical geomechanical fast model (MACRIS, see also ***BOX 4.7***). They translate on-fault positive ***Coulomb stress changes*** (cf. ***BOX 4.1***) in terms of average excess Coulomb stress over a slip length l, relative to a Mohr Coulomb failure law. Using fracture mechanics, seismic moment can be related to fracture size and stress drop (Madiaraga, 1979). The total seismic moment released per unit strike length of the fault can be calculated for every modelled timestep and associated pore pressure change. Other approaches for modelling multiple seismic events have been described by Baisch et al. (2010) and Candela et al. (2019a).

In the approaches above, elastic ***Coulomb Stress Changes*** are used to derive seismicity and seismic moment release. An alternative approach for modelling seismicity is based on the relation between ***Coulomb Stressing Rates*** and ***seismicity rates*** (rate-and-state seismicity, Dieterich, 1994). Segall et al. (2015) use a simplified version of rate-and-state seismicity, to relate the relative seismicity rate (defined as the ratio of the rate of seismicity to the tectonic background seismicity rate) to the Coulomb Stressing Rate. A similar approach was used by Zhai et al.(2019) to model induced seismicity by waste water injection in Oklahoma. They combine a coupled poroelastic model to a rate-and-state seismicity model, and find that stress perturbance on prestressed faults, enhanced by poroelastic effects, is the main driver for induced seismicity in Oklahoma. Candela et al. 2019b use a combination of a mechanical fast model to compute rates of Coulomb stress changes and seismicity rates on faults in the Groningen field.

BOX 4.10 EXAMPLE OF HYBRID PHYSICAL-STATISTICAL MODELLING OF MULTIPLE SEISMIC EVENTS TO SIMULATE THE DEVELOPMENT OF SEISMICITY CATALOGUES DURING HIGH PRESSURE FLUID INJECTION

Gischig et al. (2013) generate earthquake sequences by coupling a simplified 2D radial symmetrical pressure diffusion model of an injection well in the multiphysics modelling package COMSOL to a geomechanical stochastic seed model (Figure 4-13). A pressure-dependent permeability is used in COMSOL, which mimics the irreversible permeability increase related to fracture opening by shear dilation. In the stochastic seed model potential earthquake locations are represented as points ('seed-points' or 'seed-faults') which are uniformly and randomly distributed over the entire model. Each seed point is characterized by a local in-situ (differential) stress condition and a fracture orientation, drawn from a probabilistic distribution. Alternatively seed points can be characterized by an optimally oriented fracture orientation. In the model the combination of initial differential stress, fracture orientation and fault strength (defined by a Mohr Coulomb failure criterium) determines the fault criticality at each seed point. Depending on the pressure-induced stress-change a fault at a certain seed-point can be reactivate and trigger a seismic event. Once an event is triggered, a magnitude is randomly drawn from a set of 10^5 magnitudes forming a frequency magnitude distribution, with a b-value depending on the differential stress at the seed-point. The empirical relation used for defining b-values, is based on the observation that large magnitudes are more likely in areas of high differential stresses.

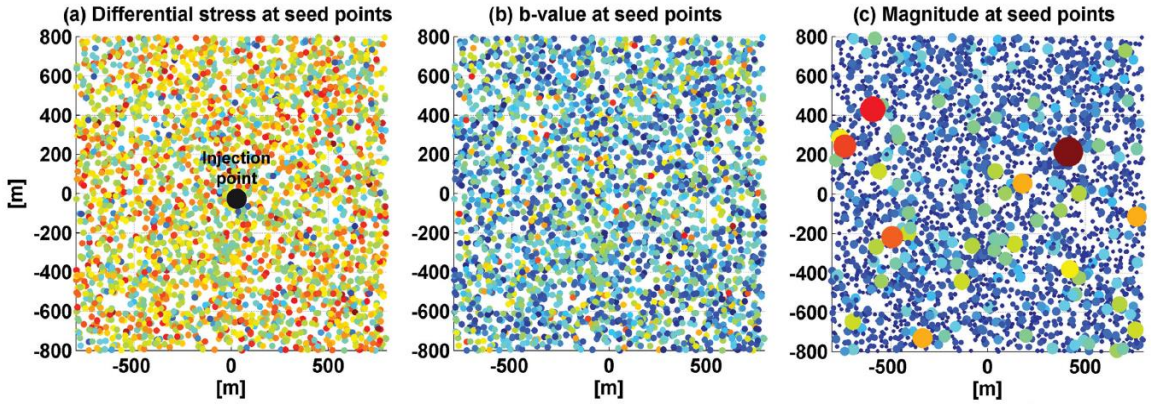

Figure 4-13 Geomechanical stochastic seed model of induced seismicity as used for the Based EGS site. a) Initial differential stresses are drawn from a normal distribution of minimum and maximum stress, with average stress defined by initial stress at the Basel site and a standard deviation of 10%, b) a linear negative relation between differential stress and b-values is used to define the frequency-magnitude relation of earthquakes at each seed point, c) if an event is triggered by the pore pressure increase at a specific seed-point, a magnitude is drawn from the a set of 10^5 earthquakes, which honors the frequency magnitude distribution at the specific seed point. Source: Gischig et al. (2013).

4.7 Relevance to modelling induced seismicity for Dinantian carbonates

From the current overview it is clear that a wide spectrum of approaches for induced seismicity modelling exists. The added value of a model is largely determined by the specific problem at hand, i.e. whether the interest is in fast semi-analytical models that allow assessment of uncertainties or the efficient production of synthetic seismic catalogues, or in slower 2D or 3D numerical models that can simulate single seismic events and can be used to further our understanding of underlying mechanisms by running scenario-based analyses.

The fully stochastic modelling approaches, as one end-member of the entire spectrum of modelling approaches, are generally robust and efficient. This means they can be run in near real-time and be used to forecast seismic hazard in near future in Adaptive Traffic Light Systems (ATLS). Compared to physics-based models, the amount of physical parameters that is needed as model input is limited. On the downside, stochastic models do not, or only to a very limited degree, take into account the underlying physical processes. This generally means that they rely heavily on calibration against observed induced seismicity. Hence, they have limited added value to furthering our understanding of the mechanical processes driving induced seismicity associated with geothermal operations in reservoirs like the Dinantian carbonates (or for geothermal reservoirs in general).

On the other end of the spectrum, physics-based models do take into account the underlying physical processes; in that sense their performance in upfront seismic hazard forecasts is expected to be better. They can be used to test the sensitivity of fault reactivation and induced seismicity to site specific geological and operational conditions. However, physics-based models, in particular the full field 3D ones and those taking into account the full coupling between flow, mechanics and temperature, need a lot of input parameters which are often badly constrained (see Figure 4-14). Fully coupled physics-based models are generally computationally intensive, and cannot be run in near real-time. This means they have limited value in Adaptive Traffic Light Systems and cannot be directly used for probabilistic seismic hazard and risk assessment. They can however give valuable insights into the mechanisms that play a role during geothermal operations, in particular when they are validated against observations. This way they can give valuable information on prioritizing and increasing effectiveness of mitigation measures for induced seismicity. In between the two end-members many combinations of modelling options are possible.

Figure 4-14. Summary of input parameters for physics-based coupled THMC models (left) and related observations/measurements of data for input and model validation.

It may not always be necessary to use fully coupled physics-based models. If simplifying model assumptions apply or simplified models yield results that are close enough to fully coupled models, less computationally intensive models may be used. Most processes affecting induced seismicity interact to some extent (cf. Figure 4-10), but some interactions may have limited effect on rock properties, fault reactivation or induced seismicity or may have limited effect at operational conditions relevant to fluid circulation in doublet systems. Also, some interactions may take place on timescales that are not relevant for geothermal operations.

Besides not explicitly modelling coupled processes, computation times may be decreased by reducing model size, for example by constructing models with radial or half symmetry. The best way of determining whether simpler and faster models can be used is by benchmarking the fast models against coupled physics-based models, i.e. comparing results from both types of models and assessing differences. Uncertainties in model parameters and (probabilistic) model forecasts can be used as a criterium to assess what type of model is most suitable. If uncertainties in forecasts of coupled models due to uncertainty of model input parameters are larger than the variation in forecasts of the different models (i.e. with and without coupling of processes), faster models without explicit coupling processes may be preferred. That is, if the interest is in model forecasts of fault reactivation or induced seismicity. If the interest is in increasing the understanding of mechanisms leading to induced seismicity during geothermal operations, coupled models may be preferred. For example, fast semi-analytical models such as a 1D slip tendency (Mohr circle) analysis could be based on direct pressure, poroelastic and thermoelastic effects without coupling effects of temperature on pore pressure and fluid properties. In general such analysis is only suitable if (1) the interest is in fault reactivation only without explicitly forecasting characteristic of seismicity such as frequency or magnitude of events, (2) flow and associated pressure changes are isotropic so that pressure changes at faults can be easily assessed based on pressure changes at wells, and (3) local geological settings allow the mechanical response of the geothermal system to be approximated by models with simplifying assumptions (for example assumptions regarding plane strain, fully elastic deformation and regarding reservoirs that are radially symmetric or infinite in extent, cf. Ter Heege et al., 2018). Another approach may be to use fast semi-analytical models to determine critical operational conditions or critical geological parameters such as reservoir permeability for which coupling of processes is not required. For example, semi-analytical modelling of the effects of steam pressures on thermal spalling during heating of rock suggest that the effect of temperature on pore pressure is negligible if permeability exceeds a certain threshold (i.e. coupling of temperature and flow is not required, Hettema et al. 1998).

In theory, the approaches presented can be applied to seismicity modelling for the Dinantian carbonates. A first assessment of the reactivation and seismicity potential of a new geothermal site can consist of a (probabilistic) assessment of a (simplified) geological / reservoir model combined with a 1D or ‘fast’ 3D fault stability model such as described in ***BOX 4.5*** to ***BOX 4.7***. Currently only two geothermal doublets have produced from the Dinantian carbonates in the Netherlands (and one doublet have produced from the Dinantian carbonates in Belgium). Both geological and seismicity data availability is limited. Therefore, physics-based models need to be developed first to give insight into the main drivers for induced seismicity associated with geothermal operations in Dinantian carbonate reservoirs. Based on these insights, and taking into account the poor constraint on many of the model input parameters, it can be decided which key processes and parameters should be captured in the fast models.

The current review highlights some key questions that need additional modelling and data acquisition efforts to further the understanding and prioritize mitigation measures for seismic risks associated with geothermal operations in fractured reservoirs. Key questions which are of particular interest to (ultradeep) geothermal in Dinantian carbonates can be addressed with the help of dedicated models, such as fully coupled THMC models, advanced hybrid models or dynamic rupture models:

Q1: What are the dominant mechanisms driving fault reactivation in the Dinantian carbonates? What is the relative contribution of pressure diffusion, poro- and thermoelasticity and stress transfer to fault reactivation in matrix- and fractured dominated Dinantian carbonates? What is the role of fractures and karstification? Do we expect differences in the fault reactivation potential of carbonates with fracture- or matrix dominated flow? What is the role of chemical processes?

Q2: What post-failure behaviour of faults can be expected in the Dinantian carbonate rocks? Carbonate rocks generally show brittle, velocity-weakening behaviour, which makes them prone to seismicity (Carpenter et al., 2014); how does this effect the post-failure behaviour and seismicity potential of the Dinantian carbonates? How does the interaction of pore pressure changes and cooling, both leading to low mean reservoir and normal fault stresses, effect the post-failure behaviour and seismicity potential of the faults? Thermal stress changes are generally large, but thermal stressing rates are expected to be low (and lower than loading rates due to pore pressure changes). How does this affect the post-failure and seismic response of the faults?

Q3: What is the relation between the operational activities, geological setting and occurrence of seismicity at both sites that have targeted the Dinantian carbonates? Currently, only two geothermal sites (the Balmatt project in Belgium and the two Californië projects in the Netherlands) have been developed in the Dinantian carbonates. Interestingly, both sites have experienced largest seismic events after a (relatively abrupt) shut-in of the wells. What controls the spatio-temporal evolution of seismicity after shut-in? (Simplified) physics-based models, combined with the observational data at the sites, can give important further insight into the relation between the operations and the driving mechanisms of the seismicity.

Q4: Which key processes for the Dinantian carbonates need to be included in fast (hybrid) models to be reliably used in probabilistic seismic hazard and risk analysis and Adaptive Traffic Light Systems?

Q5: What is the likelihood of reactivation of deeper seismogenic basement faults below the carbonate reservoirs? Distance to basement was found to be an important factor for inducing felt seismicity in geothermal projects worldwide (Buijze et al. 2019a). What is the depth of the seismogenic "basement-type" formations in the Netherlands, and what are their properties relevant to seismogenic potential? What is the magnitude of expected stress changes versus depth, associated to pore pressure diffusion, poro-elastic effect, thermo-elastic effect and dynamic stress transfer due to earthquakes in the reservoir?

Q6: What are the optimum doublet emplacement strategies with respect to pre-existing fault systems (parallel of perpendicular to fault systems)?

5. Seismic hazard and risk analysis

5.1 Hazard and risk recap

Although often used interchangeably in informal language, hazard and risk are distinctly different (e.g., Okrent 1980; Smith 2013). A ***hazard*** is something that has the *potential* to cause harm, while a ***risk*** is the *likelihood* of a hazard actually causing harm (see ***BOX 5.1***). Accordingly, the level of risk is dependent on (i) the combination of the likelihood of the hazard and (ii) the (severity of) *impacts* of the hazard if it occurs. For hazard and risk analysis it is useful to consider the causes and effects of hazards and risks.

BOX 5.1 ILLUSTRATION OF THE DIFFERENCE BETWEEN HAZARD AND RISKS

The commonly used example to explain the difference between hazard and risks considers a shark near a beach. A shark in coastal water is a hazard, since it has the potential to cause harm. The risk of being harmed by the shark depends on whether you are on the beach (low risk), or swimming near the shark (higher risk). It also depends on the type of shark, i.e. the risk of swimming with an adult Great White shark will be higher that swimming with a baby shark or Whale shark. In order to assess the risk posed by our metaphorical shark, it is helpful to first define which risk(s) are of interest. This forces us to think about which hazards exist, and helps determine which models will be needed. It is important to realize that a general 'risk of sharks' is meaningless, and a more specific description is required. For example, the risk of a person suffering from fatal injuries as a direct consequence of a shark being present. One can imagine that to assess this risk, a model is needed that describes the likelihood of a shark attacking, the likelihood of the attack being harmful (and to what extent), the likelihood of making it out of the water, the likelihood of succumbing to the injuries, etc.

In order to assess the risk posed by (induced) seismicity, it is helpful to first define what risk(s) are considered. Possible risks that may be valuable to assess are:

1. The risk of a person being injured dying as a direct consequence of an induced earthquake (personal injury/personal risk)
2. The risk of buildings/residences being damaged (economic harm/economic risk)
3. The risk of critical infrastructure being damaged (both economic and personal risk)

Seismic hazard and risks critically depend on local surface conditions as well as characteristics of seismic events, such as seismic magnitude and ground motions. It is important to note that seismic hazard is generally defined as the probability that specific ground motion (usually expressed as Peak Ground Acceleration, PGA, or Peak Ground Velocity, PGV) occurs in an area over a certain timespan (Giardini et al., 2013).

5.2 Comparison of factors affecting seismic hazard and risk analysis (SHRA)

The current study identifies a number of geological and operational factors that may affect potential occurrences of induced seismicity in Dinantian carbonates (cf. section 2). Buijze et al. (2019a) also analysed critical values for geological and operational factors that accompany felt seismic events with $M > 2.0$. Baisch et al. (2016) define first order screening framework for seismic hazard assessment in geothermal projects that distinguishes three hazard levels based on screening of key parameters. An important difference between our studies and Baisch et al. (2016) is that their analysis is *project-based* while ours are *play- or region-based*. We use the factors for regional assessment of induced seismicity (seismogenic) potential rather than for SRHA for individual project.

The framework of Baisch et al. (2016) adopts a decision tree to assess the appropriate level of seismic hazard (SHA) or seismic risk assessment (SRA) for individual projects. The decision tree includes the following decision criteria and SHA levels:

- Three initial criteria determine if projects can use a level 1 SHA:
    - Projects with major fault zones within 100 meter of operations, or that are based on circulation of fluids through existing faults
    - Projects in the tectonically active area of the Roer Valley Rift System
    - Projects that are influenced by the Groningen gas field

  If these criteria do not apply, a level 1 SHA needs to be performed to determine the seismicity potential. If one of these criteria applies, a level 2 SHA needs to be performed, regardless of the screening of key parameters.
- Level 1: A quick scan of factors (basement connection, inter-well pressure connection, re-injection pressure, circulation rate, epicentral distance to natural earthquakes, epicentral distance to induced seismicity, distance to fault, orientation of fault in current stress field, net injected volume) needs to be performed and combined into one normalized factor (0-1) to indicate low, medium or high seismicity potential. Projects with a medium or high potential require a level 2 SHA.
- Level 2: A location-specific SHA including mitigation measures and design of a traffic light system needs to be performed that describes the following key aspects for the project location: (1) relevant physical processes that may cause seismicity, (2) geological and seismo-tectonic situation, (3) previous natural and induced seismicity, (4) planned subsurface operations, (5) justification of the SHA methodology, (6) SHA for all planned operations (including drilling, stimulation and fluid circulation), (7) mitigation measures, (8) definition of a traffic light system including response time for applying mitigation measures, and (9) estimation of number of buildings exposed to certain critical ground motions (PGV) presented in a risk matrix (probability versus consequences).
- Level 3: A location-specific SRA that quantitatively assesses the economic and fatality risk associated with the geothermal projects. The considerable effort and challenge of this effort considering uncertainties and limited data availability is acknowledged. It is suggested to include a probabilistic seismic risk analysis (PSRA, cf. section 4.1 and 5.3).

The factors identified in these studies and key parameters from Baisch et al. (2016) are compared in
Table 5-1. Most factors are similar or aim to quantify comparable indicators for the likelihood of induced seismicity, i.e. the occurrence of natural seismicity, distance and stress state of nearby faults, reservoir flow behaviour, hydraulic connections with other formations,

injection pressure, flow rate, injection volume and interaction with other subsurface activities are identified as important factors in all studies. This study and Buijze et al. (2019a) identified reservoir temperature, composition and competency as additional factors, while Baisch et al. (2016) put more emphasis on inter-well pressure communication. The factor distance to faults includes assessment of the stress state in this study, while Baisch et al. (2016) treats distance to faults and orientation of faults in stress field (linking to slip tendency, cf. section 4) as separate factors. Baisch et al. (2016) propose a scoring scheme with a score 0, 3, 7 or 10 for each factor that can be used to calculate a normalized factor. Overall low, medium or high seismicity potential is based on this normalized factor. Some factors (e.g., distance) use threshold values to distinguish between different scores, while scores for other factors (i.e. basement connection, inter-well pressure communication, orientation of fault in current stress field) are based on a qualitative assessment (e.g., likely or unlikely). The current study uses a *qualitative classification* distinguishing between small, medium and large effect of geological and operational factors on induced seismicity and seismogenic potential throughout.

Factor (this study) **Buijze et al. (2019a)***	**Effects: - small** **- medium** **- large** **- Lowest value with *M* > 2.0** **- Threshold value increasing *M***	**Key parameter (Baisch et al., 2016)**	**0. Level 1 score 0** **3. Level 1 score 3** **7. Level 1 score 7** **10. Level 1 score 10** **> Level 2 criteria**
Natural seismicity	- No or isolated natural seismic events - Some natural seismic events - Concentration of natural seismic events	Epicentral distance to natural earthquakes	0. D > 10 km 3. D = 5-10 km 7. D = 1-5 km 10. D < 1 km
Peak Ground Acceleration*	- PGA 0.1 m^2/s - PGA > 0.8 m^2/s		> project in tectonically active Roer Valley Graben
Distance to large (critically stressed) faults	- Smaller faults within critical distance to operations - Large faults intersecting the reservoir - Large critically stressed faults within critical distance to operations	Distance to natural faults	0. D > 1.5 km 3. D = 0.5-1.5 km 7. D = 0.1-0.5 km 10. D < 0.1 km > major fault zone < 100 m or circulation through fault
		Orientation of natural faults in current stress field	0. locked 3. shearing unlikely 7. shearing possible 10. favorable
Stress field, fracture populations & flow regime	- Matrix or karst dominated flow - Fractured dominated flow, small anisotropy in stress & fractures & flow - Fractured dominated flow, anisotropy in stress, fractures & flow	Inter-well pressure communication	0. yes 3. likely 7. unlikely 10. no
Reservoir depth & temperature	- Small to intermediate depth, T < 125°C - Intermediate to large depths, T = 125-150°C - Large depths, T > 150°C		
Reservoir composition & competency	- High matrix porosity or karstification - Both matrix and fracture porosity - Fracture dominated porosity		
Hydraulic & mechanical decoupling	- Vertical separation with basement > 1km	Hydraulic connection to basement	0. no 3. unlikely 7. possible 10. yes
Max. wellhead pressure*	- P = 0.5 MPa - P > 10 MPa	Re-injection pressure	0. P < 1 MPa 3. P = 1-4 MPa 7. P = 4-7 MPa 10. P > 7 MPa
Max. flow rate*	No relation	Circulation rate	0. R < 50 m^3/h 3. R = 50-180 m^3/h 7. R = 180-360 m^3/h 10. R > 360 m^3/h
Net injected volume*	- V = 100 m^3 - V > 100 m^3	Net injected volume	0. V < 100 m^3 3. V = 100-500 m^3 7. V = 5000-20000 m^3 10. V > 20000 m^3
Interaction other subsurface activities	Interaction with gas depletion-induced seismicity (Groningen or smaller gas fields), mining activities (historic coal or salt solution), gas storage	Epicentral distance to induced seismicity	0. D > 10 km 3. D = 5-10 km 7. D = 1-5 km 10. D < 1 km > influenced by Groningen gas field

Table 5-1 (previous page). Comparison of geological and operational factors affecting the *potential* occurrence of induced seismicity. The first column indicates factors as defined in this study or in Buijze et al. (2019a, indicated with asterisk*). The second column indicates the criteria to distinguish between small, medium, and large effects of the factors on seismicity potential as defined in this study (cf. section 2). The second column also indicates threshold values for parameters (e.g., PGA or wellhead pressure) indicating first occurrence of M > 2 seismic events or onset of increasing seismic magnitude as compiled by Buijze et al. (2019a). The third column indicates screening parameters as defined in Baisch et al. (2016). The fourth column indicates threshold values for different scores and criteria used to distinguish between level 1 and level 2 SHA as used in Baisch et al. (2016).

5.3 Seismic hazard and risk assessment for the Groningen gas field

In this section the methodology for the seismic hazard and risk assessment used in the Groningen gas field, or the so-called 'Groningen Model Chain' (GMC) is described. This chain of models describes both the hazard (ground motions) and risk (of a person suffering from fatal injuries due to building damage as a result of ground motions) caused by induced seismicity from gas production from the Groningen gas field.

It should be emphasized that seismic hazards and risks for gas depletion are not directly applicable to Ultra Deep Geothermal (UDG) energy extraction from Dinantian carbonate reservoirs. Different subsurface effects and different earthquake mechanisms are associated with these very different types of subsurface operations[29].

The section is included as the overall methodology adopted in the GMC has many aspects that are of interest or can be translated to SHRA to the (ultradeep) geothermal Dinantian carbonate plays.

Model chain for seismic hazard and risk assessment in Groningen

In the most basic, zoomed out view, the model chain for SHRA in Groningen consists of three parts:

1) A (set of) model(s) describing the earthquakes (the so-called Seismic Source Model, or SSM).
2) A (set of) model(s) describing how the earthquakes at depth translate to ground motions (the so-called Ground Motion Model, or GMM).
3) A (set of) model(s) describing how the ground motions translate to damage or loss of value of infrastructure the resulting risks to people inside those buildings (the so-called Damage Model, or DM).

[29] See Buijze et al. (2019a), section 2.4.3 (p. 28-30), section 2.11 (p. 36-37), section B3 (p. 246-249).

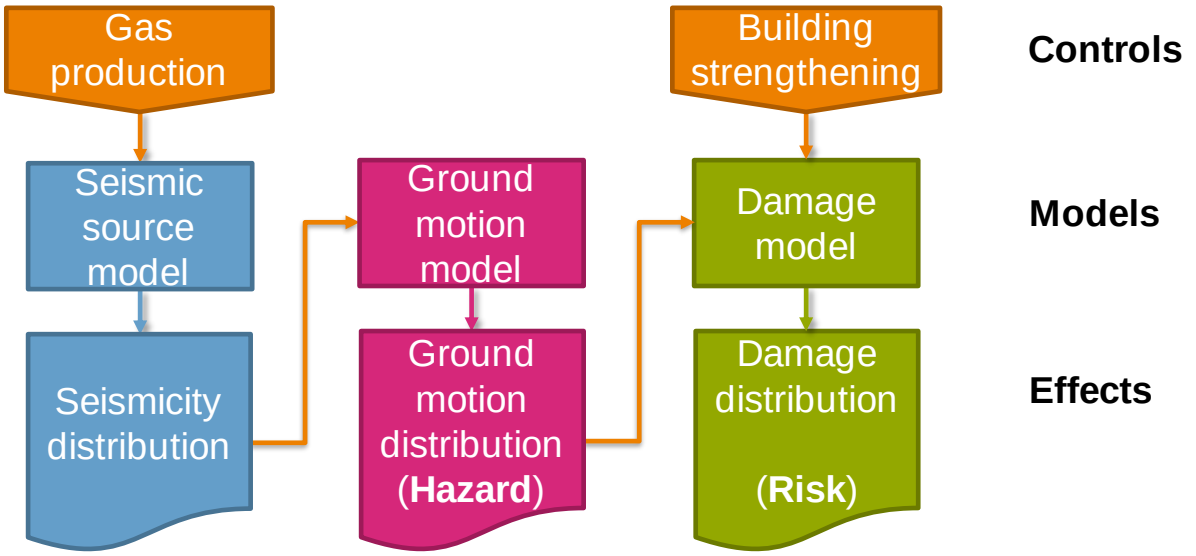

Figure 5-1 Schematic overview of the controls, models and effects in the Groningen Model Chain.

These models could be (and often are) subdivided into smaller sub-models. The representation in Figure 5-1 clusters the models in three distinct outputs (seismicity, hazard, and risk). However, there are many intermediate results which could well be of interest in some cases as well.

Some important features of the model chain are:

- Events are described ***probabilistically*** (Probabilistic Seismic Hazard and Risk Analysis - PSHRA). The seismicity distribution (in time, space, and magnitudes) does not describe a deterministic scenario, but rather a representation of the expected *seismicity rate* for each location, moment in time and earthquake magnitude. The ground motions are described as the probability of exceeding a certain acceleration in a given time window. The damage to buildings is described as a probability of a number of damage states in a given time window. This is important, because in the end we are interested in the probability of a hazardous event taking place (i.e. the risk).
- ***Causality***. In the model chain, every (intermediate) modelling result is passed on to a next (sub)model. This has the advantage that you can calculate the probability of exceeding a certain damage state, or exceeding a certain probability of fatality, *as a direct consequence of gas production.*
- Ability to perform ***disaggregation***. Because of the causality in the model, you can perform what is called disaggregation. This effectively means breaking up the total risk into its composing factors. For example, you can determine to what extend small and frequent earthquakes contribute to risk compared to larger, less frequent earthquakes. Or how much the type of building matters for the risk at a given location.
- ***Modularity***. Every model component is free to convert its input to output in whatever way the modeller decided. For example, the ground motion model requires a distribution of earthquakes in space, time and magnitudes. It does not matter how the seismic source model produced these. Similarly, the damage model requires a probability of ground motions occurring, without the need to 'know' how the ground motion model produced these. This means different configuration of the chain are possible, and elements can be re-used for other (related) hazard or risk assessments.

- ***Trainability***. Each model predicts (the probability of) some physical effect (e.g., peak ground velocity at surface) occurring as a result of some other physical effect (e.g., characteristics of soil controlling seismic wave propagation). Many of these physical effects can be measured in the real world, allowing us to reduce the difference between the model predictions and the real world observations.

Seismic Source Model (SSM)

The seismic source model that is being used for the Groningen SHRA is published in Bourne and Oates (2017) and Bourne et al. (2018). It uses a dynamic reservoir flow model to forecast pore pressure changes in the Groningen gas field. Using a compaction model, these pore pressure changes are converted into vertical strains. The compaction model is calibrated using surface levelling data collected over several decades (Bierman et al., 2015). The vertical strains are convolved with the locations and properties of mapped faults in the reservoir. This procedure results in a 2D (map view) representation of Coulomb Stress changes[30] in the field, through time. These Coulomb Stress changes are assumed to be the main driver for inducing seismicity. In the SSM, the relation between Coulomb Stress change (ΔC) and main seismicity rate (λ_m) is given by:

$$\lambda_m(\boldsymbol{x}, t) = \theta_1 h(\boldsymbol{x}) \dot{\Delta C}(\boldsymbol{x}, t) \exp(\theta_0 + \theta_1 \Delta C(\boldsymbol{x}, t)) \quad (1)$$

where $\boldsymbol{x}$ is the 2D position vector, t is the time, h is the thickness of the reservoir, ΔC is the Coulomb Stress change, and $\dot{\Delta C}$ is the time-derivative of the Coulomb stress change, $\{\theta_0, \theta_1\}$ are scalar parameters describing the absolute functional relation between the model variables and the seismicity rate. The SSM includes a standard Epidemic Type Aftershock Sequence (ETAS) model that introduces a main seismicity rate dependent spatio-temporal aftershock rate, using additional model parameters (see ***BOX 4.2*** and Ogata, 1998).

Independent from the total (main + aftershock) seismicity rate, the model determines the slope of the frequency-magnitude distributions (the Gutenberg-Richter *b*-value) from

$$b = b_0 + \left(\frac{\Delta C(\boldsymbol{x}, t)}{C_0}\right)^{-n} \quad (2)$$

where b_0, C_0, n are model parameters.

The frequency-magnitude distribution is bounded by a maximum magnitude value (M_{max}). The value of M_{max} is not known and is described by a probability mass function constructed by an expert panel (NAM, 2016).

For a given spatio-temporal Coulomb Stress change distribution and a single set of model parameters, a unique expectation value exist for each point in x-y-time-magnitude space. Using historic seismicity records, the model can be 'trained' on how well each set of model parameters can retroactively predict the past seismicity. The trained model can then be used to forecast expected seismicity for a given gas production scenario.

In such a forecast, the earthquake expectation values in x-y-time-magnitude space describes the hypocentre locations. In order to describe the earthquakes as finite line sources, rather than infinitely small point sources, a statistical rupture model is applied to the hypocentre distribution to obtain a distribution of rupture planes with associated magnitudes. This rupture

[30] See Buijze et al. (2019a), p.34 & Eq. 2-5, for definition of Coulomb Stress Change.

model is based on the general fault characteristics of the Groningen gas field and typically scaling relationships for rupture planes and earthquake magnitudes (Leonard 2010, 2012).

Ground Motion Model (GMM)

The ground motion model gives a probabilistic forecast of expected ground motions for an earthquake at a given distance and with a given magnitude. This forecast is given for 23 spectral acceleration periods (ranging from 0.01s to 5.0s, see Bommer et al., 2018; Paz and Kim, 2019) and for Peak Ground Velocity (PGV). For any point at the surface, the ground motions are first modelled for a hypothetical surface at the base of the North Sea Group (NS_B). The ground motions are dependent on a source term and a path term, the former of which is only magnitude-dependent, while the latter depends on both the magnitude and the distance between the point at the surface and the rupture plane of the earthquake.

These ground motions at NS_B level are not only described by a median expectation value, but also an expected distribution around the median. The model includes between-earthquake variability and within-earthquake variability. Correlations between ground motions at different spectral acceleration periods are also included.

The shallow subsurface is included in the model through the use of site-amplification zones which translate the motions at NS_B level to ground motions at surface, depending on the properties of the shallow subsurface. Again, variability in the model is included through a site-to-site variability component.

This GMM model parameters are calibrated using data from surface accelerometer stations and well as borehole geophones. By using the output of the SMM as input for the GMM, a probabilistic ground motion forecast can be generated for a given gas production scenario.

Damage model (DM)

The damage model has two main components:

- A Fragility Model;
- A Consequence Model

The fragility model describes the behaviour of 54 ’standard’ buildings or *typologies* when subjected to certain ground motions. These typologies are intended to capture all the buildings in the Groningen earthquake area. The model defines a number of damage/collapse states. The probability of exceeding a damage or collapse state depends on the intensity of the ground motion. By using the output of the GMM as input for the fragility model, a probabilistic forecast of damage and collapse states of all building typologies can be generated for a given gas production scenario.

The consequence model describes the probability of fatal injuries as the result of structural collapse of a building. The current national norm in the Netherlands is based on the so-called *local personal risk*, which is the risk for a single ’hypothetical’ person who is assumed to be permanently present within the building (Crowley and Pinho, 2017). The location of the hypothetical person is spread uniformly across the floor area of the building, and is assumed to be inside the building for 99% of the time and outside of building (but within 5m of the perimeter) for 1% of the time.
The consequence model describes the probability of fatal injuries for this hypothetical person, based on the probability of exceeding different building collapse states, each having a certain contribution to the total risk. Damage states which do not lead to (partial) collapse are not

considered to be dangerous and do therefore not contribute to the risk, since the risk metric is based on building collapse alone and does not include building damage.

5.4 Relevance to a seismic hazard and risk analysis for Dinantian carbonates

Projects targeting the Dinantian carbonates may require a seismic hazard and risk analysis (SHRA) that includes some of the components from the Groningen Model Chain. If a first order evaluation indicates a potentially elevated seismogenic potential, different model components can underpin the SHRA. The level of modelling can range from models forecasting stress changes caused by geothermal operations that support the design of traffic light systems to a full SHRA with many of the same (but maybe not all, and adjusted to fit the new purpose) components as in the Groningen Model Chain, depending on the local seismogenic potential of the Dinantian carbonates. It is important to note the Groningen Model Chain is developed to assess the hazard and risks resulting from gas depletion induced seismicity in the Groningen area, supporting attempts to manage both the cause and the effects. It can be used to forecast the effects of gas production on induced seismicity in a situation of frequent occurrence of felt ($M > 2$) seismic events over years of gas production. That scenario does not really apply to geothermal projects as they probably will have been put on hold or shut-in at a much earlier stage (given current thresholds in traffic light systems). However, it is important to understand hazard and risk for geothermal projects regardless of these differences in situations. If induced seismicity may be associated with geothermal operations, a SHRA needs to be implemented that helps mitigating and managing the effects. Mechanisms of induced seismicity are different for gas production (differential compaction due to cumulative gas extraction[31]) compared to geothermal operations (combination of direct pressure, poroelastic and thermoelastic effects during circulation of fluids[27]). Despite these differences, many of the modelling steps (source of seismicity, ground motions and effects on buildings/infrastructure and people) and properties (probabilistic, based on measurements and physical understanding, modularity) of the Groningen Model Chain can be modified and applied to projects targeting geothermal energy in Dinantian carbonates and geothermal projects in general. Many of these models require a large degree of site-specificity, but the Groningen Model Chain provides a framework on which these models can be based. The seismogenic potential associated with geothermal operations is linked to operational factors such as injected/produced volumes, geothermal reservoir pressures, temperature changes as well as geological factors such as presence of faults, tectonic stresses, elastic parameter of the reservoir. Ideally, the effects of these factors would be represented by a model that relates physical properties and processes to a probabilistic forecast of earthquake activity. However, in absence of such a Seismological Source Model, part of the model chain can still be used to perform scenario studies (e.g. are there any buildings in the region that are exposed to a risk above the legal norm when the geothermal project leads to an earthquake of magnitude M at a certain depth).

[31] See Buijze et al. (2019a), p. 37, p. 246-249 (section B.3).

6. Recommendations for seismic monitoring

In the current chapter we propose some options for improved seismic monitoring strategies for ultradeep (> 4 km) geothermal (UDG)[6] plays in the Netherlands, including the Dinantian geothermal plays (Section 6.3). First, we summarize some general considerations relevant for monitoring seismicity and traffic light systems (TLS) for geothermal production sites (Section 6.1), and we discuss the characteristics of the existing national monitoring network in Section 6.2.

6.1 General considerations for seismicity monitoring and traffic light systems

Several considerations should be taken into account that apply to seismic monitoring of induced seismicity in general, and that are relevant for monitoring at UDG sites in particular. Part of the following considerations are adopted from the report of Buijze et al. (2019a).

The seismic monitoring can be differentiated into three operational phases with complimentary purposes:

1) During the *preparational phase* of geothermal production, preferably before any on-site activity, monitoring is aimed at establishing the seismicity baseline of the site. Knowledge of the (ambient) noise level and variability can be used to enhance the design of the seismic network to be installed in later phases. Also, the baseline results may help to identify local seismic noise sources (e.g. traffic, industrial activity) that are unrelated to future geothermal operations. A few surface stations measuring at the anticipated geothermal site for a typical period of 6-12 months prior to drilling and production is sufficient to quantify background noise levels.
2) During the *operational phase* (mainly drilling, completion and fluid circulation), the main purpose of seismic monitoring is to detect and characterize seismicity. To mitigate seismic risks, a traffic light system (TLS) based on monitoring data can be used to guide operational decisions. In addition, seismic monitoring may provide insight into the performance and conformance of the reservoir and production activities, for example by monitoring changing reservoir properties which may be indicative for changes in temperature distribution. Depending on the background noise levels measured during phase 1, and the required sensitivity and resolution, sensors may need to be placed in boreholes, which is often the case for reservoir monitoring (Bohnhoff et al., 2018).
3) During the *post-operational* phase, continued monitoring may be required until equilibrium stress state is approached after shut-in. The required intensity of monitoring may in general depend on the experiences in phase 2.

A differentiation in low, medium and high seismic hazard areas can be made as proposed by Baisch et al. (2016), or low, medium and high seismogenic potential for projects as proposed in this study (cf. section 3). The needs for seismic monitoring and the availability of a TLS vary per hazard level (cf. section 0). The sensitivity and coverage of a seismic monitoring network should also meet the requirements imposed by the regulator. Often, existing national/regional monitoring networks are too sparse, and densification with additional stations at the geothermal site needs to be realized, depending on the outcomes of the initial seismic hazard assessment.

A TLS can be used to manage operational decisions and to minimize the risk of seismicity rather than to prevent seismicity (Buijze et al., 2019, Baisch et al., 2019).

A justification for the choice of threshold values implemented within a TLS is crucial to explain to stakeholders why certain operational decisions are made during geothermal production. Within a TLS, threshold values for various parameters can be defined, such as magnitude, peak ground velocity, seismicity rate, spatial extent of the seismicity cloud, and number of complaints from citizens due to felt seismicity (Bommer et al., 2006; Ellsworth, 2013; Hirschberg et al., 2015; Majer et al., 2012; NAM, 2017). Also, the site-specific geology (e.g. physical properties of overburden), operational factors and public perception should be taken into account when defining threshold values in a TLS (cf. section 9). To a certain extent the definition of a TLS will be guided by legal requirements defined in the mining law. However, the precise settings within a TLS may vary between different regions even within the Netherlands, depending on the site-specific aspects mentioned above and the related hazard level. In practice, the monitoring costs at a particular site will depend on the hazard-based monitoring needs.

The efficacy of the monitoring does not only depend on the network design and the local noise conditions, but also on the existing knowledge of the local subsurface. The accuracy of estimated earthquake locations depends to a large extent on the accuracy of the seismic velocity model used. In earthquake seismology, a distinction is made between primary- and secondary seismic velocities, respectively corresponding to the velocity of the primary (P) and secondary (S) seismic phase. Typically, only P-wave velocity information is acquired during 2D/3D seismic field campaigns and with well logs. P-wave velocity information is contained in VELMOD, which is the seismic velocity model of the Netherlands (Pluymakers et al., 2017). Additional S-wave velocity information helps in constraining source locations and reducing the uncertainties. Therefore, in many regions, new seismic and log data need to be acquired to improve velocity models.

In practice, the monitoring costs at a particular site will depend on the required monitoring needs. Within a local network design study, the goal should be to limit seismic risks as much as realistically possible. Costs of monitoring will inevitably play a role in the network design, i.e. required sensitivity and accuracies need to match costs that are acceptable given the economically feasibility and business case of a project. Collaboration between operators and other stakeholders such as KNMI, knowledge institutes and governmental organizations in data sharing and interpretation can help increasing the efficiency of monitoring efforts.

6.2 Potential of existing national monitoring network

Purpose and characteristics of KNMI network

The national seismic network of the Netherlands, governed by the Royal Netherlands Meteorological Institute (KNMI), has been set up to monitor seismic and acoustic events. Over the past decades the network gradually extended, and nowadays it is used to detect induced and tectonic earthquakes originating both within and outside of the Netherlands. Figure 6-1 shows a map of the current network lay-out (status 2019), consisting of broadband seismometers, geophones, accelerometers as well as infrasound sensors (Colette et al., 2011). All sensor data is publicly accessible through standardized webservices[32]. Additionally, seismic stations in Belgium and Germany in the vicinity of the Netherlands are plotted in this map, respectively collected from the Royal Observatory of Belgium[33], the German regional seismic network (GRSN)[34], and Erdbebenstation Bensberg (University of Cologne)[35].

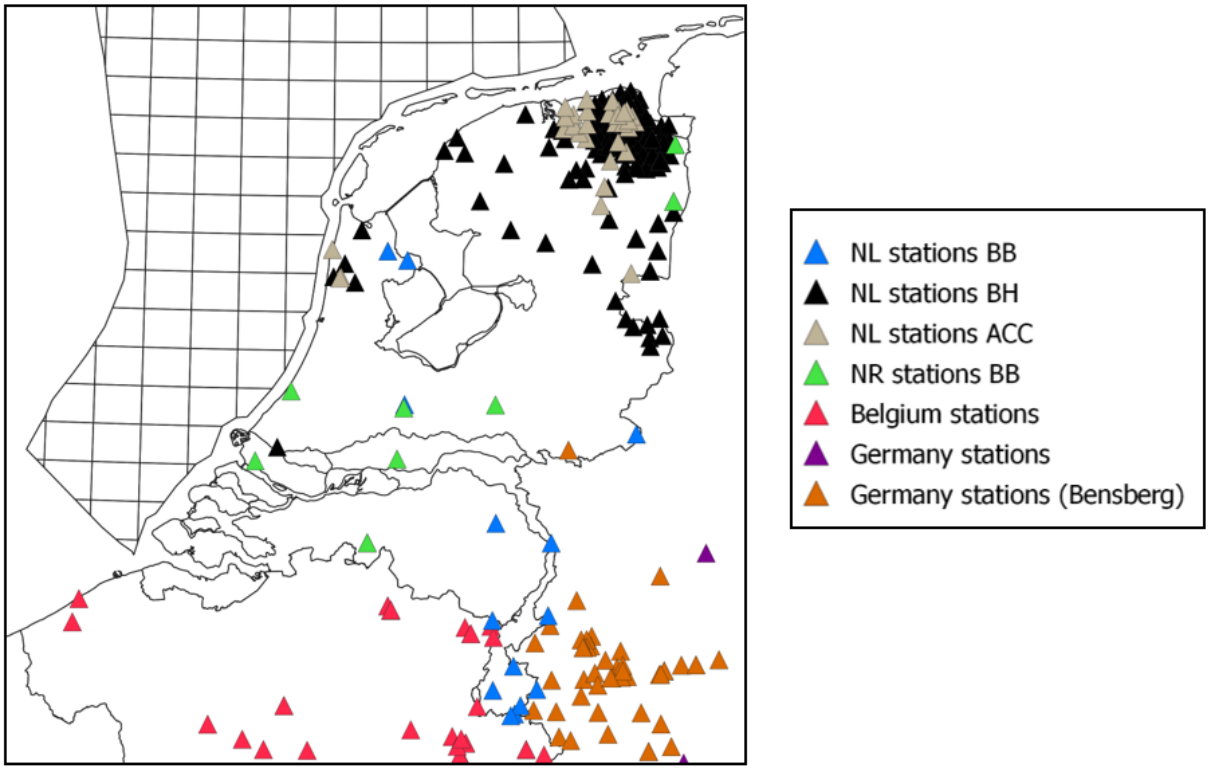

Figure 6-1 Overview of lay-out of national seismic monitoring network consisting of stations of the KNMI (NL) and NARS (NR) networks in the Netherlands [2]. Accelerometers (ACC), borehole sensors (BH) and broadband sensors (BB) of KNMI are respectively marked with grey, black and blue triangles. Positions of stations of the NARS network are indicated in green. Positions of Belgian stations indicated in red were taken obtained from the Royal observatory of Belgium[3]. Positions of German stations indicated in purple and orange were collected respectively from the German regional seismic network[3] and Erdbebenstation Bensberg[5].

As Figure 6-1 shows, there is a strong variation in station coverage throughout the Netherlands with highest station density in the Groningen area, where the monitoring network is designed to accurately monitor induced seismicity related to gas production of the Groningen gas field. Also, increased station coverage is present near other subsurface operations such as the gas fields in Drenthe, the Bergermeer gas storage site in Noord-

[32] http://rdsa.knmi.nl/dataportal/
[33] http://seismologie.be/en/the-service/seismic-network
[34] https://www.seismologie.bgr.de/doi/grsn/
[35] http://www.seismo.uni-koeln.de/station/netz.htm

Holland, salt mining in Friesland waste water injection in Twente, as well as in southern Limburg with some natural seismicity. However, the major part of the Netherlands has a much sparser station coverage (Figure 6-1).

The differences in station density throughout the Netherlands introduces strong variations in the sensitivity and resolution of the network, affecting the ability to pick up seismic events of certain magnitude and the accuracy of estimations of earthquake source locations, respectively. For the greater part of the Netherlands the national network is not designed for detailed characterization of local shallow (induced) earthquakes. The nearest station may be typically tens of kilometres away from the actual earthquake's hypocentre resulting in poor sensitivity and resolution.

This is illustrated in Figure 6-2 showing contour maps of the network sensitivity, expressed as the location threshold magnitude (also known as magnitude of completeness, i.e. lowest earthquake magnitude that can be detected and located with a seismic network) throughout the Netherlands. The left panel in Figure 6-2 was taken from Dost et al. (2017) and represents the situation around 2012. The right panel was provided by the KNMI on request and is based on the station configuration as currently in place (November 2019). The figure shows that, for instance, in the central part of the Groningen area, the station densification resulted in a decrease in location threshold magnitude from 1 to 0.5, although the majority of the Netherlands currently has threshold levels of 1.5-2.0. Current efforts focus on improving threshold magnitudes in the southwestern part of the Netherlands by placing 3 additional seismic stations. Threshold magnitudes are expected to decrease below 2.0 in that area, once the station become operational in 2020.

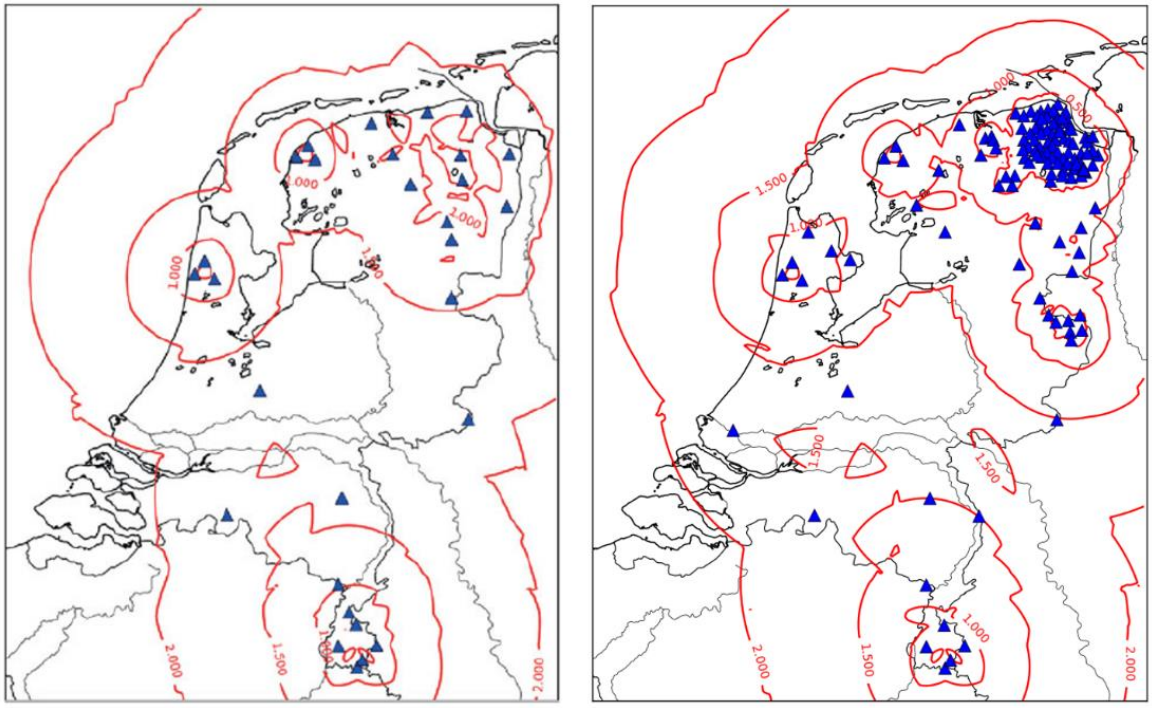

Figure 6-2 Contour map of the location threshold of the KNMI network before (left) and after (right) densification of the network. Left figure adopted from Dost et al. (2017) and right figure provided by KNMI in December 2019.

Restrictions of existing KNMI network with respect to Dinantian geothermal production

The necessity of intensifying the monitoring effort in a specific area depends on the likelihood that geothermal projects will commence in such an area. This will in turn depend on the geothermal potential, which relies on factors such as depth, temperature, porosity and permeability of the reservoir, as well as on the outcomes of a seismic hazard and risk assessment (cf. section 0). Figure 6-3 and Figure 6-4 show maps of the depth and temperature distribution of the top of the Dinantian, respectively (Veldkamp, 2020. It should be mentioned that depth and temperature are only two of the afore mentioned factors that partially determine the geothermal potential, and that the maps are subject to large uncertainties (see Ten Veen et al. 2019; Veldkamp, 2020 for more details). However, Figure 6-3 and Figure 6-4 can be used to assess to which extent existing seismic stations are covering regions that are of interest for geothermal energy development in (ultradeep) Dinantian carbonate reservoirs. It is important to note that for some projects, local seismic networks have been installed that monitor seismicity in specific regions at higher resolution than the KNMI network (for example, the Californië projects, cf. section 7.1). Although the monitoring data from local networks is usually analysed by the KNMI, it is not incorporated in the national seismicity database.

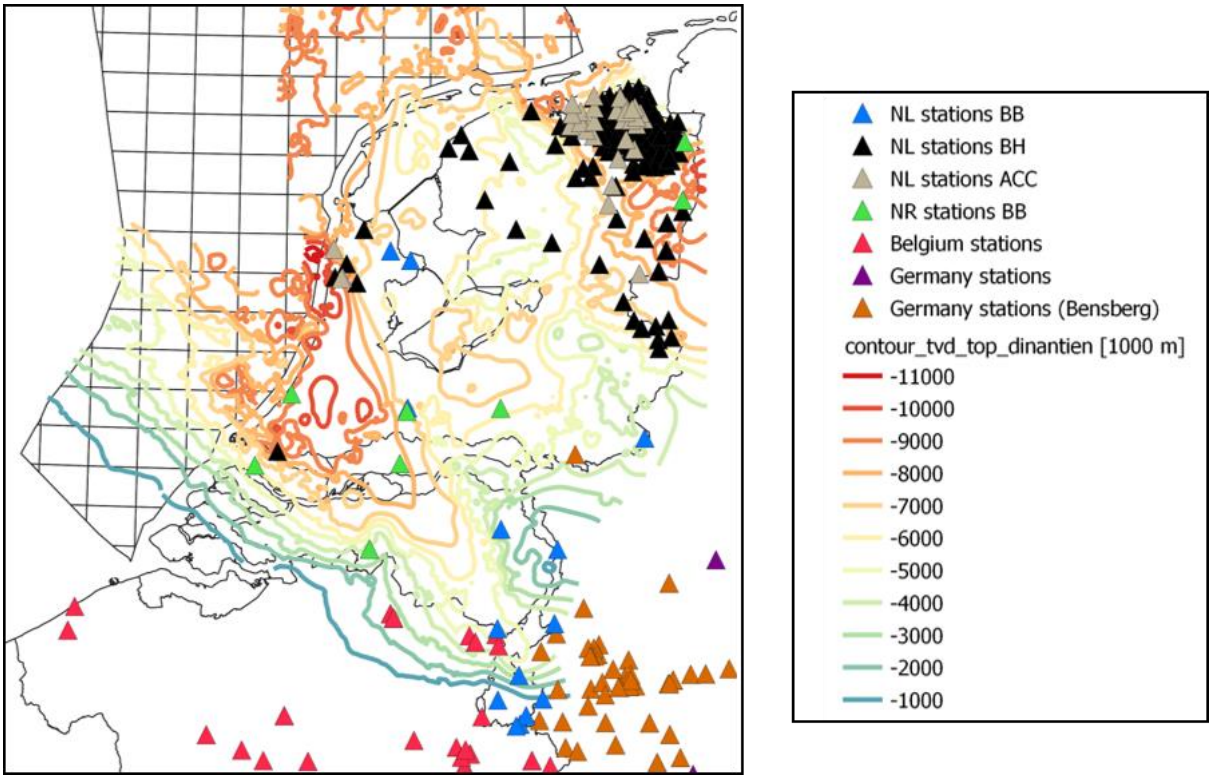

Figure 6-3 Map of depth of the top of the Dinantian (Ten Veen et al., 2019) with position of seismic stations in the Netherlands. See caption of Figure 6-1 for detailed explanation of symbol legend.

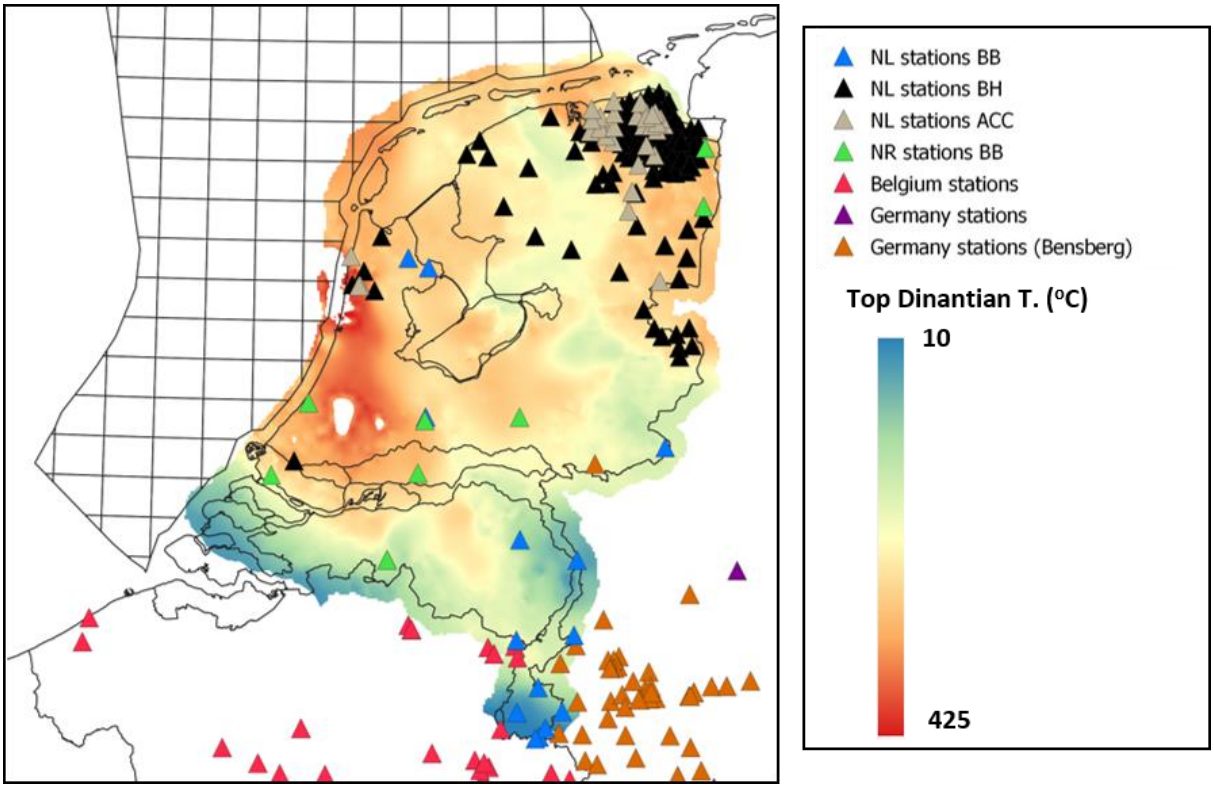

Figure 6-4 Map of the temperature distribution of the top of the Dinantian (Veldkamp, 2020), together with the position of seismic stations. See caption of Figure 6-1 for detailed explanation of symbol legend.

To conclude, given the significant depth variation of the Dinantian carbonates, in practice, the location accuracy and completeness-of-detection magnitude level will vary throughout the Netherlands even when a denser station network would be deployed. These variations should be translated in to accuracies and included in earthquake catalogues.

6.3 Seismic monitoring strategies for Dinantian carbonates

We identify five options for improved monitoring strategies for projects targeting the Dinantian carbonates in the Netherlands, including both ultradeep geothermal (UDG)[6] as well as shallower Dinantian carbonates. Other (hybrid) strategies can also be considered, depending on site-specific requirements as well as economic considerations.

Option A: Using existing national monitoring network and local monitoring networks
This option follows the approach proposed by Baisch et al. (2016). For most geothermal systems classified as having a low potential for induced seismicity the national monitoring network of KNMI is sufficient. A low potential for induced seismicity corresponds to the hazard level 1 scenario according to Baisch et al. (2016). A single additional monitoring station may need to be placed close to the geothermal site if seismicity has occurred previously or if the national network is not sensitive enough.

For geothermal systems with medium or high seismic hazard (i.e. hazard level 2 and 3 according to Baisch et al. 2016) the sensitivity and resolution of the KNMI network is often not sufficient and a dedicated local seismic network is required, as worked out in options B-D.

Option B: Mobile high resolution seismic array followed by local permanent arrays at UDG sites
This option starts with the use of a mobile seismic array that is installed temporarily for 6-12 months at planned locations for geothermal projects prior to geothermal operations and prior to drilling. This mobile array will be used to characterize noise conditions and monitor background seismicity. Subsequently, the design of a permanent network for the operational phase will benefit from the measured baseline results to meet the required monitoring sensitivity and resolution. Deployment of the permanent network can thus be more cost effective as the number of station (and sensitivity and resolution) can be optimized based on the data from the (higher resolution) mobile array.

Option C: Initial placement of dense array (high sensitivity) during start of activities in certain UDG area where multiple doublets are planned.
Alternatively, a dense seismic monitoring network can be installed in a larger area with high geothermal potential where installation of multiple doublets are foreseen in the future. The difference between this option and option B is that it integrates monitoring efforts for multiple projects rather than focussing on individual projects. It is therefore only suitable if multiple projects are planned in an area. Progressive expansion of seismic networks that accompany progressive development of UDG projects can be considered. The seismic network should have a relatively high sensitivity, consisting of both surface and borehole stations. This results in a high signal-to-noise ratios allowing detection of weak events (e.g. down to M=0) and inversion of observed data to source parameters (e.g. moment tensor inversion, stress drop). This is important for verifying that the actual geomechanical response of the geothermal system lies within the predictions obtained from geomechanical modelling.

Option D: Expanding network on a national level to permanently reach lower completeness level for the whole of the Netherlands
A more elaborate option would be to intensify the existing KNMI network by adding stations to reach a lower completeness level for the entire Netherlands. This option can be attractive if network development is aligned with both development of deep, intermediate and shallow

geothermal projects, as well as with monitoring at potential gas storage sites and production (of small gas) fields. Here, the roll-out of new stations would be organized centrally by the government or a designated organization such as the KNMI. The entire network should be governed by the KNMI ensuring a standardized analysis and quality of seismicity data. On the long run this option has the advantage that a uniform monitoring standard is reached for seismicity monitoring in the Netherlands, removing barriers for operators to commence geothermal projects or perform other subsurface related activities. It can also be better tailored to regulatory requirements imposed by the State Supervision of Mines, in terms of required resolution of seismic monitoring at specific locations for planned UDG projects.

Option E: Integration of networks, hardware and data handling
Better integration of data from the national KNMI networks with local or regional networks can improve the resolution of seismic monitoring data, in particular at project locations with local monitoring networks. In addition, extension of the spatial coverage of high monitoring data can be obtained by integrating data from national seismic monitoring networks in the Netherlands, Belgium and Germany. Network design, data processing, data handling, and unlocking data to the public is governed by the KNMI. It is common for geothermal operators in the Netherlands to hire a subcontractor that performs the data analysis and reports observed seismicity. The governance of instrumentation, data handling and analysis is generally arranged by the operator. Data from local networks is usually made available to the KNMI, but integration, processing and quality control of data could be improved if procedures are standardized and automated.

Regarding governance of seismic monitoring instrumentation, data handling and data analysis, a similar approach as used for oil and gas fields may be followed for all projects. For oil and gas projects the operator is typically responsible for the installation of a monitoring network following the advice of a network design study. Once, the local network is acquiring data, other parties (usually the KNMI in the Netherlands) can take over responsibility of data handling, data storage and data analysis, while the operator facilitates hardware maintenance. Combining the local seismic data with data acquired by the national monitoring network, has the advantage of detecting lower magnitude seismic events that may act as precursors to larger magnitude events. Such data can greatly help the understanding of processes driving induced seismicity at project locations. Hence, more context can be given to observed local seismic events. In addition, quality of the data can be ensured by following a standardized processing workflow that rely on more broadly shared domain knowledge of monitoring and analysing seismic data.

7. Case studies relevant to Dinantian carbonate geothermal projects in the Netherlands

Prior to the current study, an extensive review was conducted of case studies with (lack of) felt seismicity, including geothermal and other types of projects involving subsurface operations (Buijze et al., 2019a). This review includes cases relevant to Dinantian geothermal projects in the Netherlands, including the Californië projects near Venlo[36], the Balmatt project near Mol in Belgium[37] and projects in the Molasse Basin near Munich in Germany[38]. Other geothermal plays in carbonate rocks (e.g., the Paris Basin) are reviewed in Buijze et al. (2019a)[39] as well. The Paris Basin is of interest as induced seismicity has not been reported in many years of operation. Given that high matrix porosity (typically 15%) and permeability generally controls flow in Paris Basin reservoirs, the projects are only relevant for areas in the Netherlands where flow in the Dinantian carbonates is matrix controlled (i.e. mostly shallower reservoirs as, for example, comparable to the limestone reservoirs targeted for gas storage in Loenhout (Belgium, Amantini et al., 2009). For deeper Dinantian carbonates that target fault zones, flow is probably mainly fracture controlled (Mozafari et al., 2019). However, some cases show an influence of fracture controlled porosity due to fracturing and dissolution. Also, it cannot be excluded that Dinantian carbonates with locally high matrix porosity or intense karstification exist where flow is not fracture controlled.

Within the framework of the current study, one day workshops were organized with VITO[40], the operator of the Balmatt project, and with the geothermal consultancy company Erdwerk[41]. Erdwerk has extensive expertise with the development of geothermal projects in the Molasse Basin near Munich, Germany. A short description of these cases is given in this section. Most of the information in this section is based on literature that is publicly available (**status December, 2019**), with additional valuable insights in the projects derived from the workshops. The purpose of the case study descriptions is to provide an overview of ***known existing data and insights*** for cases most relevant to Dinantian geothermal projects in the Netherlands. Additional analysis of the mechanisms underpinning the occurrence of seismicity or adequacy of seismic monitoring and mitigation measures ***have not been performed*** as part of this study.

7.1 Californië geothermal projects in the Netherlands

Two geothermal projects targeted the Dinantian carbonate reservoirs near Venlo in the Netherlands, i.e. Californië Wijnen Geothermie (CWG, 2012) and Californië Leipzig Gielen (CLG, 2015). Following a decision by State Supervision of Mines (SodM) on 10 May, 2018, the CWG project has been suspended, and the CAL-GT-01, CAL-GT-02 and CAL-GT-03 wells have been closed in[42]. Following a M_L 0.0 seismic event on 25 August, 2018 and decisions by SodM on 28 August 2018 and 10 July, 2019, operations at the CLG project are currently on hold[43]. Potential relation between recent seismicity and operations at CLG are currently under investigation and review (**status December, 2019**). The description given

[36] See Buijze et al. (2019a), p. 212-215 (section A.11.4).
[37] See Buijze et al. (2019a), p. 215-217 (Figure A-65).
[38] See Buijze et al. (2019a), p. 137-151 (Section A.2).
[39] See Buijze et al. (2019a), p. 168-170 (Section A.4).
[40] https://vito.be/nl/diepe-geothermie/balmatt-site
[41] https://www.erdwerk.com/en
[42] https://www.sodm.nl/actueel/nieuws/2018/05/29/cwg-staakt-productie-aardwarmte-na-tussenkomst-sodm (visited 10/01/2020).
[43] https://www.sodm.nl/actueel/nieuws/2019/07/11/aardwarmteproject-nabij-venlo-nu-niet-hervat (visited 10/01/2020).

here is based on publicly available documents (Spetzler et al., 2018; Burghout et al., 2019; Reith et al., 2019; SodM, 2019).

Geological setting of the Californië projects

The CWG and CLG projects target fractured and karstified limestones of the Zeeland Formation (also referred to as 'Kolenkalk' Group), and are also hydraulically connected to the underlying Pont d'Arcole Formation, Bosscheveld Formation and Condroz Group (Burghout et al., 2019; Table 7-1; Figure 7-1). The Zeeland Formation is of Early Carboniferous (Dinantian) age. The limestones of the Zeeland Formation were deposited in varying environments: marginal marine to shallow marine carbonates and mudflats, open marine shelf carbonate shoals with restricted lagoonal platform carbonates, and open marine carbonate slopes (Kombrink, 2008; Reijmer et al., 2017; Mozafari et al., 2019).

For the Zeeland Formation in this area, two sources of secondary porosity are known: karst- and fault-related porosity. Due to (repeated) subarial exposure events, karstification may have led to high secondary porosity below geological unconformities. An example of karstified reservoirs are the limestones targeted for gas storage in Loenhout (Belgium, Amantini et al., 2009). The base of the Dinantian is not properly defined and often is assigned to the base of the Zeeland Formation, while the Bosscheveld and Pont d'Arcole Formations may have the same age (Mozafari et al., 2019; Van der Voet et al., 2020). The Pont d'Arcole Formation consists of dark greenish, very fissile to black shales, which become progressively more calcareous towards the top with rare sandstone intercalations. The Pont d'Arcole Formation are at the base of the limestones of the Zeeland Formation, and show a gradual transition with an upward increase in carbonate content. The Bosscheveld Formation forms the transition from Devonian siliciclastic deposits to the Dinantian limestones, and consists of interbedded dark-grey, partly calcareous mudstones, fine-grained sandstones and limestones, often nodular in character. The Condroz Group consists of sandstones at the location of the Californië projects (Van Adrichem Boogaert and Kouwe, 1993-1997; Mozafari et al., 2019; Van der Voet et al., 2020).

The area is located in the tectonically most active area of the country, directly adjacent to the Roer Valley Graben between the Tegelen and Viersen Fault zones (Figure 7-1, Houtgast and Van Balen, 2000). The Tegelen Fault separates the Peel Horst and Venlo Fault blocks, and had its main period of activity in the Early Quaternary (Bisschops et al., 1985). Locations of major faults have been interpreted on the basis of two seismic profiles (2D). The faults control groundwater flow in the Roer Valley Graben (Lapperre et al., 2019), which indicates they extend to shallow groundwater systems. The Roer Valley Graben is known for frequent occurrence of natural seismicity (cf. section 2.1), but few hypocentres are located in close vicinity of the Californië projects (Figure 2-3).

Relation between operations and seismicity for the two Californië projects

The CWG geothermal system was originally designed with two production wells (CAL-GT-01 and CAL-GT-03) in close vicinity of the Tegelen Fault Zone, and a single injector (CAL-GT-02) drilled away to the northeast from the Tegelen Fault Zone (Burghout et al., 2019; Figure 7-1; Table 7-2). It was intended to inject into karst zones away from the fault zone. After clogging of CAL-GT-02, it was decided to use CAL-GT-03 as an injection well. CAL-GT-03 had partly collapsed in the fault zone reservoir section, and injection therefore takes place in the younger strata of the Zeeland Formation.

The CLG doublet has one production (CAL-GT-04) and one injection (CAL-GT-05) well (Burghout et al., 2019). The project is situated ~1.5 km from the CWG system and targets the same Dinantian limestones of the Zeeland Formation, but production is at a slightly deeper level. Both the CAL-GT-01 and CAL-GT-04 production wells are interpreted to produce from permeable zones close to the Tegelen Fault Zone (Burghout et al., 2019). Whereas CAL-GT-03 injects in the vicinity of the Tegelen Fault Zone, injection well CAL-GT-05 is drilled away from the fault zone, in north-eastern direction (Figure 7-1). Both the CWG and CLG geothermal systems are based on circulation of fluid, i.e. an approximate fluid balance is maintained by re-injecting all produced water.

Over the operational lifespan of the CWG project, a total of ~9.1×10^6 m^3 fluid has been produced and re-injected (www.nlog.nl; Burghout et al., 2019; Table 7-1). After an initial constant CWG monthly production of ~1.1×10^3 m^3/month between January and October 2014, four stages of increasing production can be distinguished with increasing peak productions of ~1.8×10^5 m^3/month in March 2015, ~2.4×10^5 m^3/month in February 2016, ~2.8×10^5 m^3/month in January 2017, and ~2.9×10^5 m^3/month in January 2018. Production increase roughly follows expected higher demand in the winter months with increasing peak production each year after start of the project. Average and maximum production rates over the operational lifespan of the project (after January 2014) are ~1.7×10^5 m^3/month and ~420 m^3/h (117 l/s, March 2018).

CLG has produced and injected ~1.3×10^6 m^3 fluids so far. CLG monthly production rates are much less than for CWG (peak of ~1.6 m^3/month in November 2017 with a maximum production rate of ~260 m^3/h or ~72 l/s in March 2018) and cover a shorter operational lifespan between July 2017 and August 2018. Temporal and spatial relations between seismicity and operations are subject of investigation (Burghout et al., 2019; SodM, 2019).

The first of 17 seismic events recorded since the seismic monitoring network became operational was detected on 18 August 2014. Except for the maximum M_L 1.7 event on 3 September 2018, all events are of low magnitude (M_L<0.3). The first 6 events occurred when only CWG was operational. Both CWG and CLG were operational during the M_L -0.2 event on 8 April 2018, and only CLG was in operation during the M_L 0.0 event on 25 August 2018. Burghout et al. (2018) suggest a temporal relation with decrease in CWG production rates for 6 seismic events occurring between August 2015 and February 2017. There also seems to be a temporal relation between CLG production shut-in and the 9 events occurring in the first two weeks of September 2018 as the remaining 9 events occurred after both systems were shut down. The M_L 1.7 event occurred 6 days after CLG production shut-in on 28 August 2019. Definite conclusions on spatial correlations between operations and recorded seismicity are hampered by poor accuracy of the seismic wave velocity model in the region. Different models yield an earthquake hypocentre for the M_L 1.7 event between 3.2 and 9.2 km depth (Spetzler et al., 2018). Burghout et al. (2018) depict hypocentre locations between 5.7 and 6.3 km with an error (2σ) of maximum 1.4 km based on different assumptions for the velocity model. Deeper estimates for hypocentre locations would indicate a large (km's) separation between the wells and seismic events. Except for the M_L -0.5 event on 2 April 2016 and the M_L 0.0 on 25 August 2018, event hypocentres cluster together. Mechanisms that may explain the observed spatial and temporal relations between seismicity and operations, including direct pressure, thermoelastic and poroelastic effects, are subject of ongoing investigations (**status December, 2019**; see Burghout et al., 2019; SodM, 2019).

Seismic monitoring and mitigation measures for the Californië projects

A seismometer was placed near the CLG site during drilling of wells (Burghout et al., 2019). A seismic monitoring network with 3 seismometers (K01-K03) was operational from September 2014 onwards, and was extended to 5 seismometers (K01-K05) in November 2015 (Table 7-1). Minimum magnitude of seismic events detected was M_L -1.2, but network resolution may be higher. Measures to mitigate seismic risks are mainly the implementation of a traffic light system based on peak ground velocity (PGV) measurements with green (PGV < 0.1 mm/s), orange (PGV ≥ 0.1 mm/s), and red (PGV ≥ 0.3 mm/s) stages and associated actions (Table 7-1). SodM (2019) states that ”*CLG was allowed to produce geothermal heat under the condition that production would be stopped if an earthquake occurred in the area*”[43]. Production was stopped after the M_L 0.0 event on 25 August 2018 with PGV of ~0.03 mm/s (Table 7-1). The PGV of ~1.1 mm/s associated with the M_L 1.7 event that occurred after CLG shut down exceeded the traffic light threshold for stop of operations.

Country & place (lat, lon):	The Netherlands, Californië Californië Wijnen Geothermie – CWG (51.42218805, 6.09139302) Californië Lipzig Gielen – CLG (51.43318034, 6.08359037)			
Activity:	Geothermal production			
Start date – End date:	20 – 01- 2013 to 10 – 05 – 2018 (CWG) 01 – 07- 2017 to present (CLG)		Closed-in Temporary suspended	
Fluid + Fluid balance:	Water		Balanced, circulation	
Maximum activity depth:	2.1 km (CWG) 2.7 km (CLG)			
Activity formations & rock types:	Zeeland Formation (Dinantian carbonates), Bosscheveld Formation, Pont d'Arcole Formation, Condroz Group (sandstone)			
In-situ temperature	75 °C (CWG); 87 °C (CLG)			
ΔT in-situ – fluid:	~40 °C (CWG); expected max. ~47 °C (CLG)			
Cumulative V pumped:	9145505 m^3 (CAL-GT-01); 1342600 m^3 (CAL-GT-04)			
Bottomhole pressure:	134 bar (CAL-GT-01-S1); 184 bar (CAL-GT-04); 160 bar (CAL-GT-05)			
Maximum flow rate:	117 l/s (CWG); 72 l/s (CLG)			
Monitoring system:	3 seismometers (K01-K03) from September 2014; 5 seismometers (K01-K05) from November, 2015			
Monitoring resolution:	Minimum magnitude detected: M_L -1.2 (5 seismometer network)			
Mitigation measures:	Traffic light system (PGV based): 1. Green- PGV < 0.1 mm/s: No actions 2. Orange- PGV ≥ 0.1 mm/s: (1) Investigate likely cause and potential mitigation measures, (2) report to regulator 3. Red- PGV ≥ 0.3 mm/s: (1) Stop operations, (2) Report immediately to regulator (next business day)			
Seismicity (M_{max} in bold):	Date	Time	Magnitude (M_L)	Peak Ground Velocity (PGV)
	18.08.2015	02:47:05	-0.1	
	05.12.2015	08:07:28	0.3	
	26.01.2016	02:47:00	-0.3	
	02.04.2016	14:17:16	-0.5	
	25.01.2017	16:27:12	-0.3	
	31.01.2017	04:01:56	-0.5	
	08.04.2018	10:29:27	-0.2	
	25.08.2018	16:43:27	0.0	0.03 mm/s
	03.09.2018	18:11:23	-0.8	
	03.09.2018	18:12:35	-0.4	
	03.09.2018	**18:20:31**	**1.7**	**1.1 mm/s**
	03.09.2018	18:26:37	-0.3	
	03.09.2018	20:44:12	-1	
	04.09.2018	00:13:15	-1.2	
	06.09.2018	15:27:20	-0.4	
	06.09.2018	15:58:22	-0.5	
	09.09.2018	20:50:22	0.0	

Table 7-1 Characteristics of the Californië (CWG & CLG) geothermal projects near Venlo in the Netherlands (Burghout et al., 2019; SodM, 2019; www.nlog.nl). Status December, 2019.

Wells [name]	MD [m]	TVD [m]	Drilling start-end date	Type	Status	Project
CAL-GT-01-S1	2697	2477	20/06/2012 - 07/08/2012	production	Closed-in	CWG
CAL-GT-02	1662	1450	20/08/2012 - 21/09/2012	injection*	Closed-in	CWG
CAL-GT-03	2944	2223	11/11/2012 - 20/01/2013	injection*	Closed-in	CWG
CAL-GT-04		~2700	02/12/2015 - 04/02/2016	production	On hold	CLG
CAL-GT-05		~2000	07/02/2016 - 05/04/2016	injection	On hold	CLG

Table 7-2 Characteristics of the wells drilled for the Californië (CWG & CLG) geothermal projects near Venlo in the Netherlands (www.nlog.nl; Burghout et al., 2019). Status December, 2019.

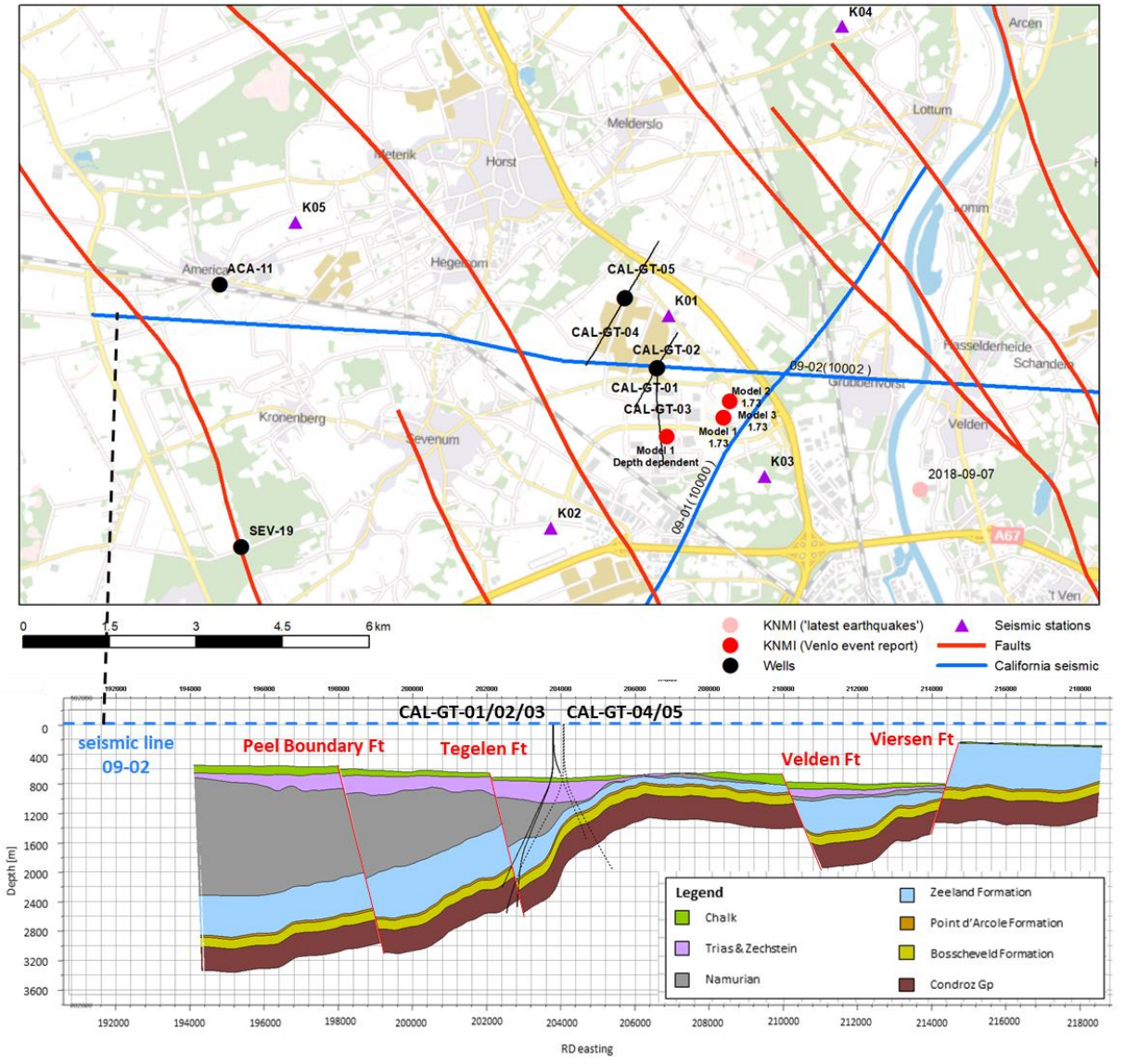

Figure 7-1 Map view (top) and cross section of 2D seismic interpretation (bottom) around the CAL-GT wells. The map view is a topographic map of the area overlain with location of wells (black dots and lines), major faults (red lines), 2D seismic lines 09-01 and 09-02 (blue lines), seismometers of the seismic monitoring network (K01-K05, purple triangles), epicentre locations of the M_L 1.7 seismic event on 03/09/2018 for different seismic wave velocity models (red dots). From: TNO[36].

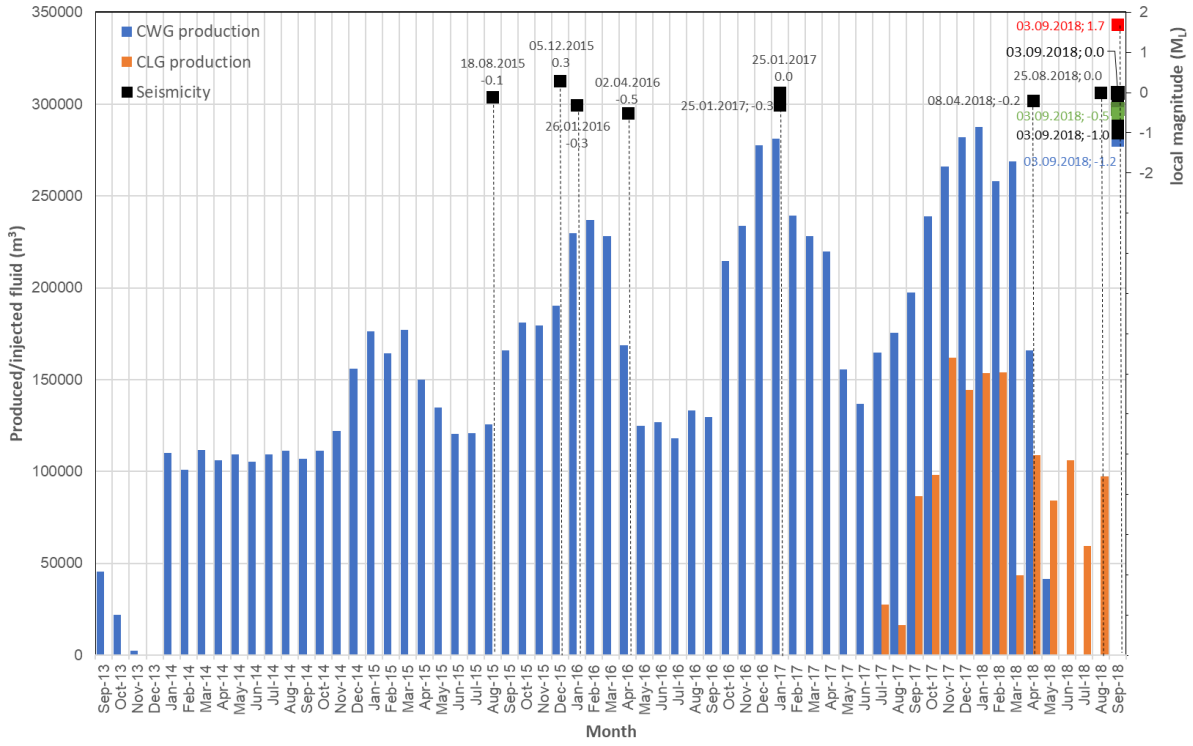

Figure 7-2 Produced/injected fluid for CLG & CLW projects with occurrence of seismic events in the area. Source: TNO (www.nlog.nl; Burghout et al., 2019).

7.2 The Balmatt geothermal project in Belgium

VITO operates the Balmatt geothermal project near Mol in Belgium[40]. Following a M_L 2.1 seismic event on 23 June 2019, operations are currently on hold (**status December, 2019**)[44]. The description given here is based on publicly available information[40] and literature (Table 7-3, Bos and Laenen, 2017; Broothaers et al., 2019; Van der Voet et al., 2020).

Geological setting of the Balmatt project

The geological setting at the Balmatt site is in some aspects comparable to that at the Californië sites. The Balmatt site is located at the SW site of the Roer Valley Graben with almost equal SW-NE distance from the central NW-SE axis of the graben as the NE-SW distance of the Californië projects (Figure 7-3). However, the location of Balmatt within the Campine-Brabant Basin (a NW-SE trending Variscan foreland basin) is closer to the London-Brabant Massif which will yield differences in structural setting (i.e. local tectonics, stress field and depth of basement). The Lower Carboniferous (Dinantian) Limestone Group, time equivalent to the Zeeland Formation in the Netherlands, is located at varying depths in the Campine-Brabant Basin (Langenaeker, 2000; Bos and Laenen, 2017; Reijmer et al., 2017; Mozafari et al., 2019; Van der Voet et al., 2020). The MOL-GT-01 production well targets the Goeree and Loenhout formations at the top of the Lower Carboniferous Limestone Group, consisting of fossiliferous mudstones, bio- and lithoclastic wacke- to grainstones and boundstones, locally intercalated with clayrich layers (Van der Voet et al., 2020). Predominantly clastic Devonian sediments unconformably overlie the Caledonian Basement.

The area is transected by a predominant set of (N)NW - (S)SE striking normal faults, which locally display a shear component (Bos and Laenen, 2017). Some of these faults have been active over large period of time, in some cases up to today (Figure 7-1). Locally, NW-SE striking, elongated fault blocks that are generally tilted towards the north/northeast are formed by intersection of the (N)NW - (S)SE striking faults with subordinate N-S to NE-SW striking thrust faults that are relicts of the compressional regime related to the Variscan uplift of the basin (Langenaeker, 2000; Deckers et al., 2019).

Epicentres of natural seismic events associated with tectonic movement along faults in the Roer Valley Graben are at 30-39 km from the Balmatt project, i.e. at Lage Mierde (M=3.5, 1932-11-02, 30 km), Bocholt (M=2.7, 1990-08-12, 31 km) and Wuustwezel (M=1.8, 2001-08-01, 39 km; cf. Figure 7-3).

Relation between operations and seismicity for the Balmatt project

The Balmatt geothermal system was designed with a production well (MOL-GT-01-S1) and two injection wells (MOL-GT-02 and MOL-GT-03). The MOL-GT-01-S1 well targeted a normal fault zone in the Loenhout Formation dipping ~60° in NE direction accompanied by a zone with persistent NNW-SSE striking fractures (Bos and Laenen, 2017). The MOL-GT-02 well deviated from the MOL-GT-01-S1 well with an inclination of ~40° to the NE, parallel to the seismic line MH10-04 (Figure 7-6). MOL-GT-02 targeted reservoir sections that are not influenced by faults and reached a distance with MOL-GT-01-S1 of at least 1500 meter in the targeted Carboniferous Limestone Group. The MOL-GT-03 well targeted the same faulted and fractured zone as MOL-GT-01-S1 (Broothaers et al., 2019), and was drilled further into the underlying Devonian formation for exploration purposes.

[44] https://vito.be/nl/nieuws/diepe-geothermie-vito-toelichting-over-de-technische-haalbaarheid-de-resultaten-en-de

Operational and earthquake hypocentre data of the Balmatt project are publicly available for research purposes from VITO[40] upon request. Earthquake epicentres are published on together with well trajectories and locations of seismic stations by VITO (2020) (Figure 7-4; Figure 7-5). Currently, operations are on hold following an accidental power cut on the local electricity grid on 21 June 2019 (**status December, 2019**; see VITO[44]). At the Balmatt site, 267 seismic events were recorded with M_L -1.0 to 2.1 since the start of operations in December 2019. The events cluster near the injection well MOL-GT-02 (see VITO[44]). The first events were recorded during injection tests in September 2016, and during start-up of the geothermal plant in December 2018 (see VITO[45]). The events are interpreted to be associated with injection of cold fluids[45]. There seems some evidence for a relation between induced seismicity and variation in injection temperature. Since 5 December 2018, development of earthquake epicentres can be followed through a website maintained by VITO (Figure 7-4; Figure 7-5). Four interesting observations are that (1) the seismic cloud progressively extends in SSE direction over the last year (mainly up to end of June 2019, just after cessation of production), (2) there is a swarm of events in the week prior to the stop of operations, (3) the maximum M_L 2.1 seismic event on 23 June 2019 occurred ~2 days after production had stopped, (4) the event rate quickly dropped after 23 June 2019 (only 4 events have been recorded with maximum M_L 0.3).

Seismic monitoring and mitigation measures for the Balmatt project

Seismicity was recorded since injection tests in September 2016 (see VITO[44]). The current monitoring network consists of 7 seismic stations surrounding the well site with seismometers placed between 30 and 600 meter depth (Figure 7-4). The minimum magnitude of seismic events reported was M_L -1.0, but network resolution may be higher. Measures to mitigate seismic risks are mainly the implementation of a traffic light system based on four criteria (Table 7-3; Figure 7-4): (1) maximum corrected magnitude (M_C), (2) maximum event rate (#/hr), (3) maximum E-W distance of the seismic cloud, and (4) maximum peak ground velocity (PGV). Threshold levels and associated action for green, orange and red stages of the traffic light system are given in Table 7-3. Maximum reported values are M_C 2.2 (corresponding to M_L 2.1 as determined by the national network Royal Observatory of Belgium, KSB[46]), maximum event rate of 2 events per hour, maximum E-W distance of 359 meter, and a maximum PGV of 1.0 mm/s.

[45] https://vito.be/nl/vito-seismometernetwerk-onderzoekt-aardbevingen
[46] http://seismologie.be/en

Country & place (lat, lon):	Belgium, Balmatt (51.223401, 5.096735)				
Activity:	Geothermal production				
Start date – End date:	14 – 09 – 2015 (well MOL-GT-01 spudded)			Operations temporary on hold	
Fluid + Fluid balance:	Water			Balanced, circulation	
Wells	MOL-GT-01 MOL-GT-01-S1 MOL-GT-02 MOL-GT-03	Exploration Production Injection Injection	 3610 MD 4341 MD 4905 MD	 3583 TVD 3830 TVD 4236 TVD	14/09/2015 - 19/01/2016 04/2016 - 10/2016 10/2017 - 07/2018
Maximum activity depth:	~3.4 km (production); ~3.8 km (injection)				
Activity formations & rock types:	Goeree, Loenhout and Steentje-Turnhout formations of the Lower Carboniferous (Dinantian) 'Kolenkalk' Group				
In-situ temperature	138-142°C (reservoir), 120-128°C (wellhead temperature, depending on flow)				
ΔT in-situ – fluid:	65-70°C (injection temperature). ΔT varied with heat demand. Currently, variation in injection temperature is kept as constant as possible to limit induced seismicity.				
Flow rate:	Production rates ~150 m3/h (~42 l/s); lower injection rates Productivity index MOL-GT-01-S1 of 4-5 m^3/h/bar				
Monitoring system:	7 seismometers (3 directions, placed at 30-600 meter depth)				
Monitoring resolution:	Minimum magnitude detected: M_L -1.0				
Mitigation measures:	Traffic light system (based on local magnitude, event rate in #/hr, E-W distance seismic cloud, PGV and PGA): 1. Green (no actions): M_L < 1.5; *rate* < 1/hr; *E-W* < 300 m; *PGV* < 0.4 mm/s; PGA ≤ 0.02 m/s^2 2. Orange (decrease flow rate & pressure): M_L 1.5-2.5; *rate* 1-3 hr^{-1}; *E-W* 300-500 m; *PGV* 0.4-1.0 mm/s; PGA 0.02-0.04 m/s^2 3. Red (shut-in operations): M_L 1.5-2.5; *rate* > 3 hr^{-1}; *E-W* > 500 m; *PGV* > 1.0 mm/s; PGA ≥ 0.04 m/s^2 Note that PGA is not shown on the online dashboard[45].				
Seismicity:	267 events (max. M_L 2.1), max. depth ~4.0 km, see also Figure 7-5				

Table 7-3 Characteristics of the Balmatt geothermal project near Mol in Belgium. Source:VITO[40].

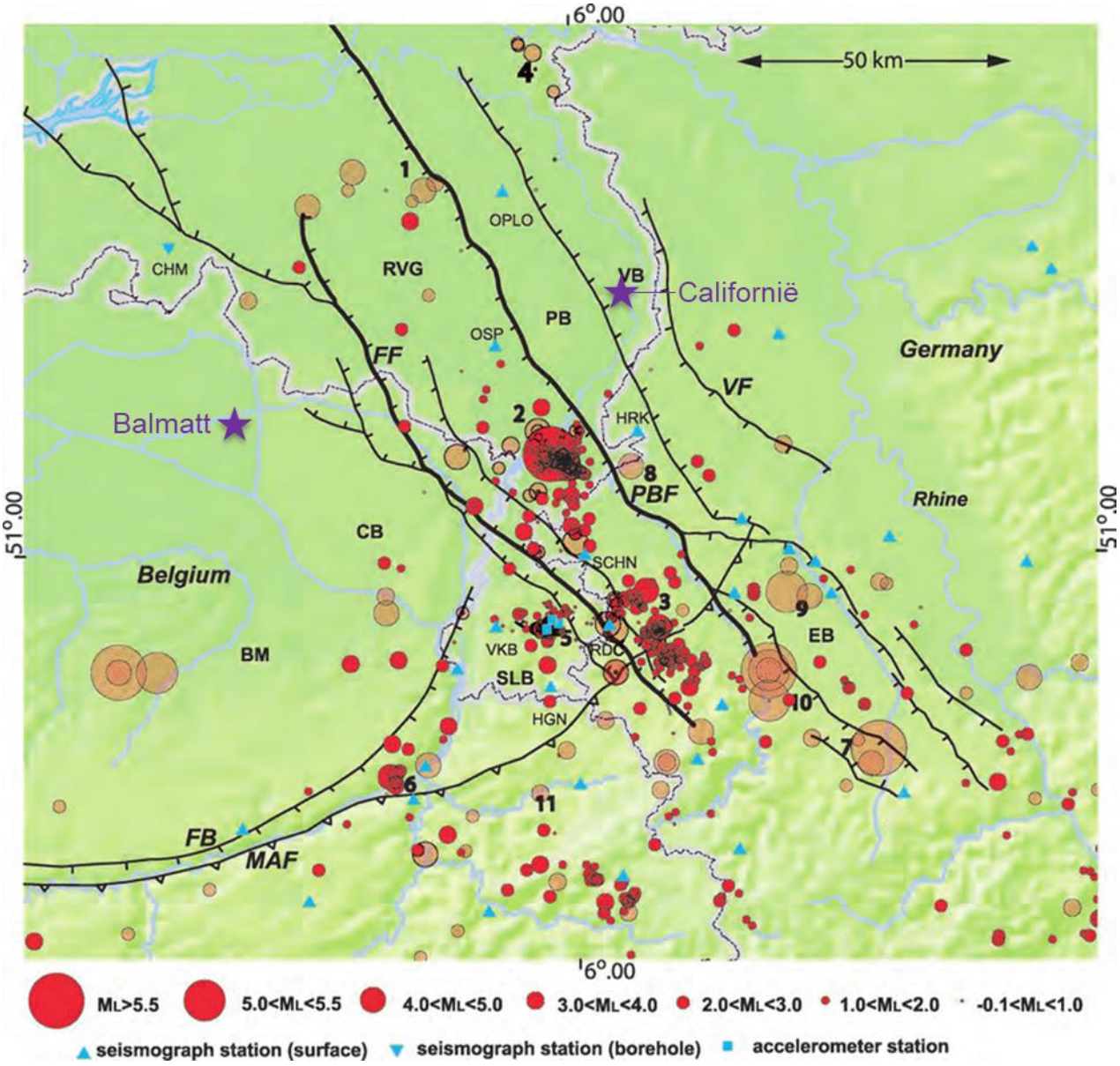

Figure 7-3 Location of Californië and Balmatt geothermal projects relative to the Roer Valley Graben plotted on a map with epicentres of natural earthquakes (red circles, scaled according to magnitude) as detected by the seismic stations (blue triangles) of the national seismic monitoring network in the Netherlands (operated by the KNMI[11]). Natural seismicity is for the period 1700-2003, with a distinction in events before 1980 (light red circles) and after 1980 (dark red circles). Localities are: 1: Uden; 2: Roermond; 3: Alsdorf region; 4: Nijmegen; 5: Voerendaal; 6: Liège; 7: Euskirchen; 8: Heinsberg; 9: Tollhausen; 10: Dueren; 11: Verviers. Tectonic structures are: BM: Brabant Massif; RVG: Roer Valley Graben; PB: Peel Block; VB: Venlo Block; CB: Campine Block; EB: Erft Block; SLB: South Limburg Block; PBF: Peel Boundary Fault; FF: Feldbiss Fault; VF: Viersen Fault; FB: Faille Bordière; MAF: Midi-Aachen Thrust Fault. OPLO, CHM etc. are seismic station codes. From: Dost and Haak (2007).

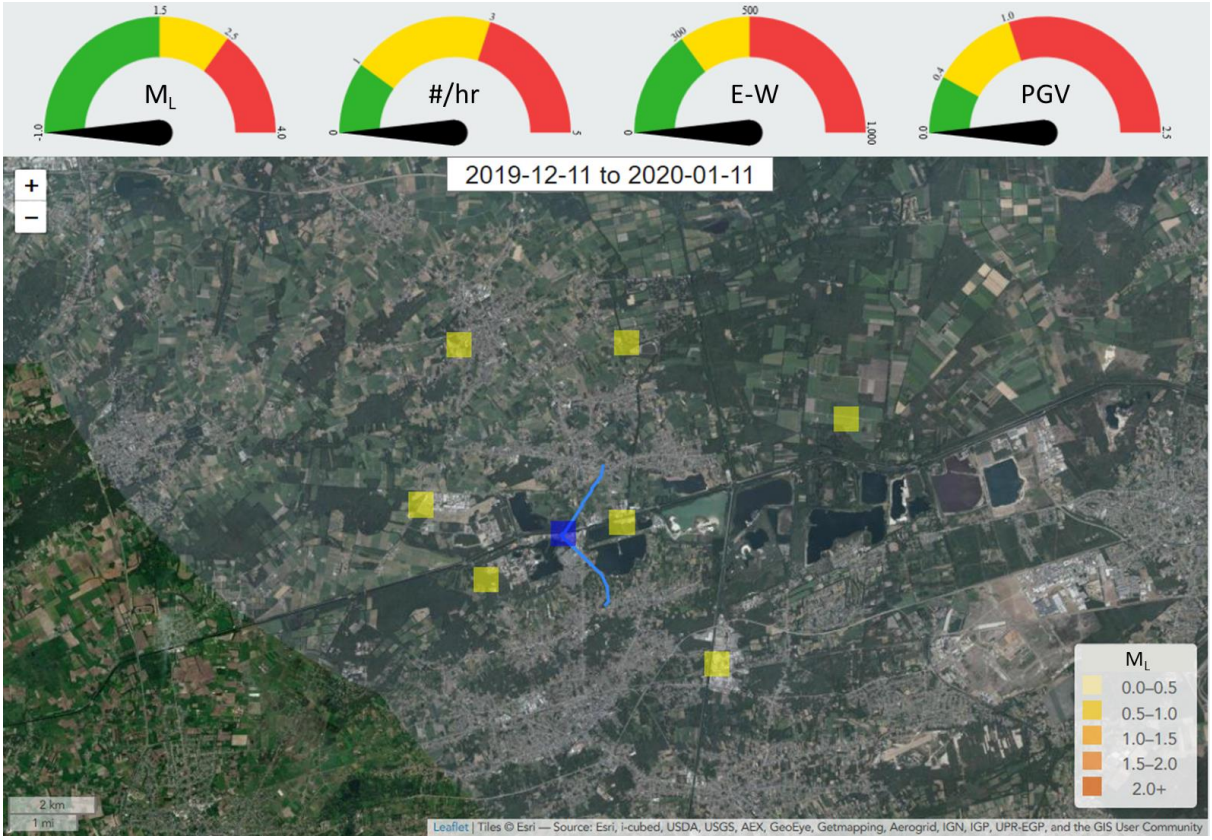

Figure 7-4 Top figure: Traffic light system implemented in the Balmatt project. Meters indicate maximum local magnitude recorded, number of recorded events per hour, E-W distance of the seismic cloud and maximum peak ground velocity, respectively (left to right). Bottom figure: Balmatt site (dark blue square), production wells MOL-GT-02 (blue line in NE direction) and MOL-GT-03 (blue line in SW direction), seismic stations (yellow squares) plot on a satellite image of the area. Source: VITO (2020)[45].

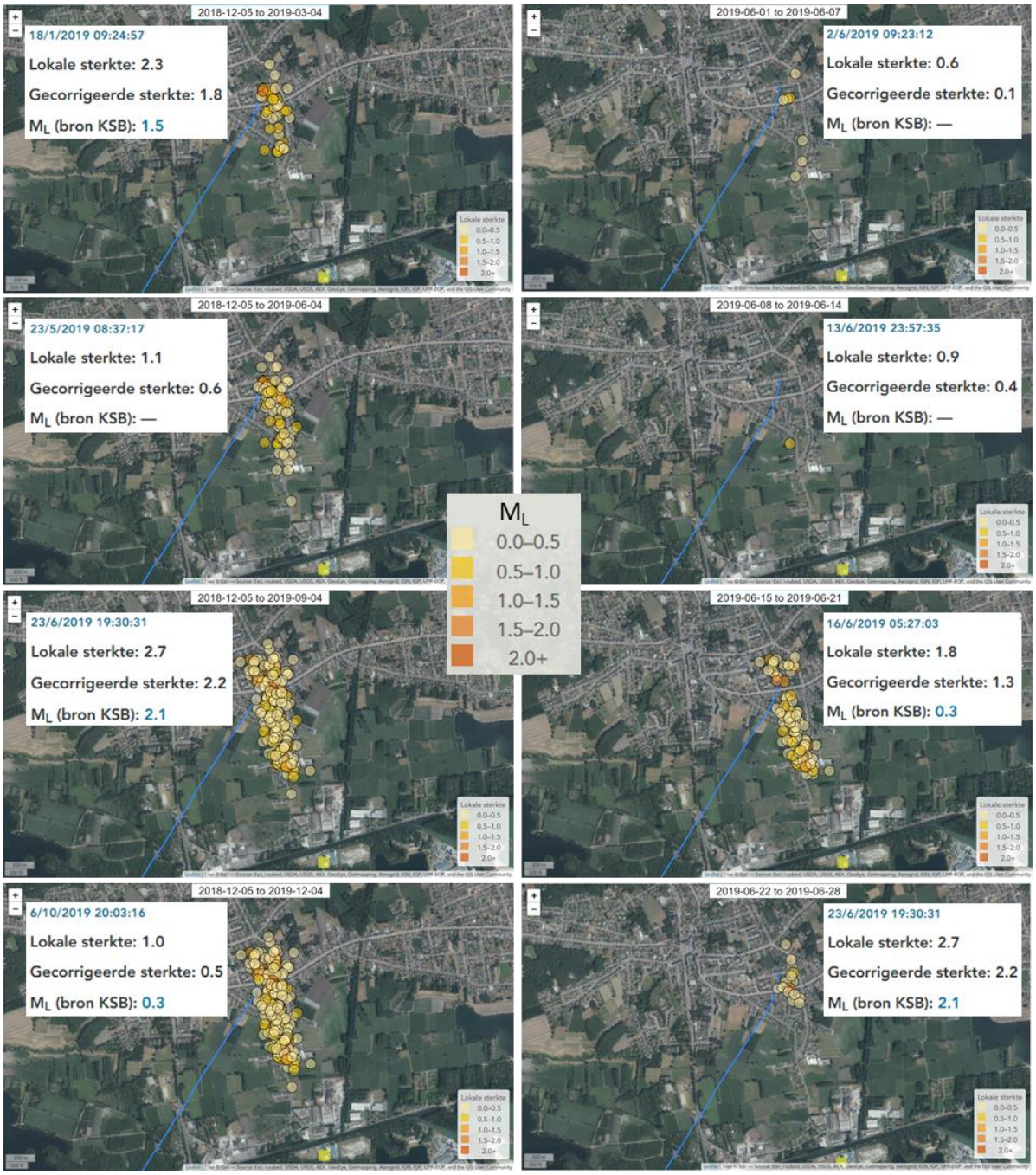

Figure 7-5 Development of seismicity (yellow-orange circles coloured according to magnitude, see legend) around production well MOL-GT-02 (blue line in NE direction) plot on a satellite image of the area. Text boxes indicate maximum magnitudes of seismic events for successive periods in time. Seismic station close to the well site is also indicated (yellow square). Left figures: Cumulative number of seismic events between 5 December 2018 and 4 December 2019 (1 year, each figure shows additional seismic events for a 3 month period). Right figures: Weekly occurrence of seismic events in June 2019 that led to the maximum M_L 2.1 on 23 June 2019, following an accidental power cut on the local electricity grid. Source: VITO (2020)[45].

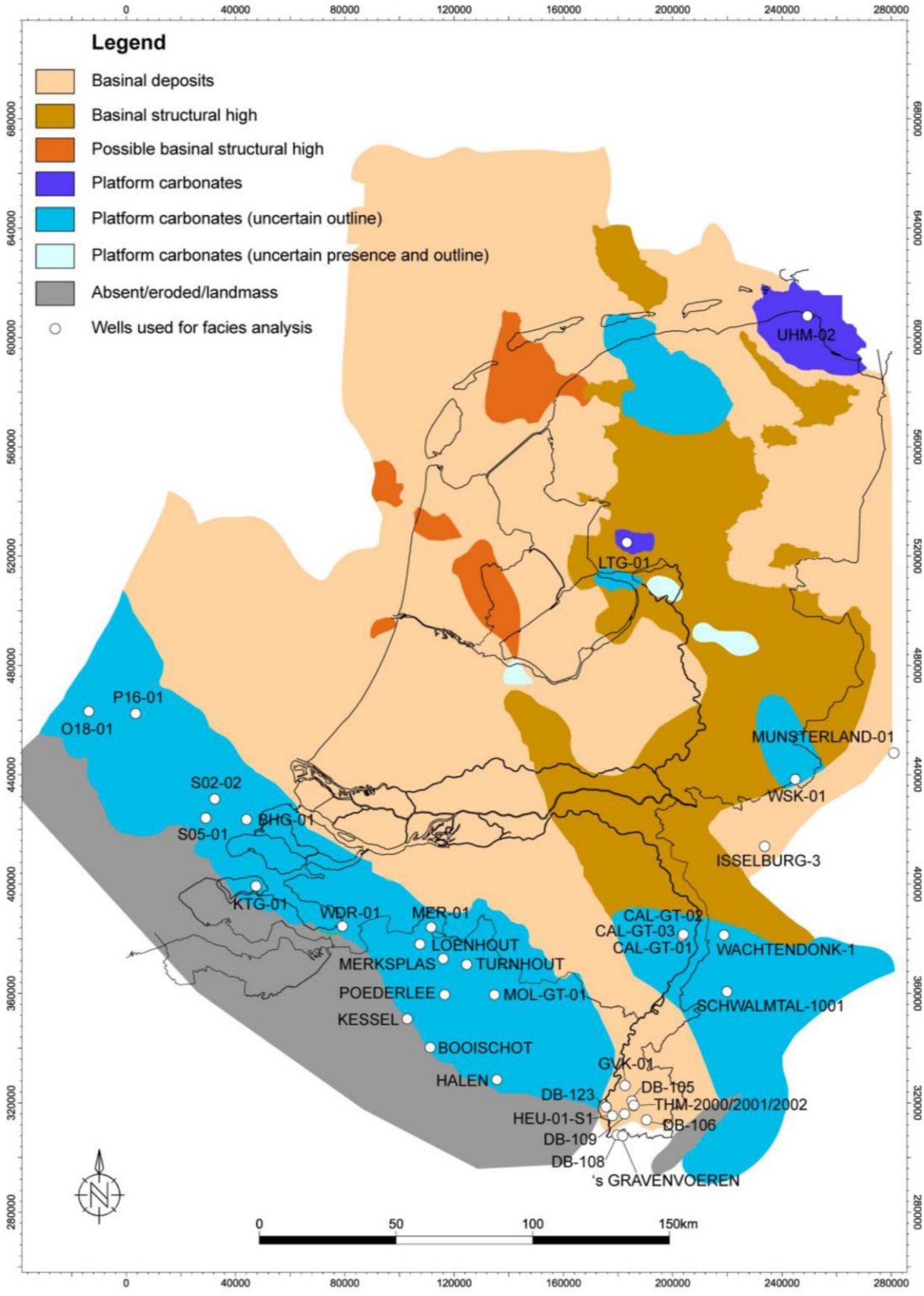
Legend
Basinal deposits
Basinal structural high
Possible basinal structural high
Platform carbonates
Platform carbonates (uncertain outline)
Platform carbonates (uncertain presence and outline)
Absent/eroded/landmass
Wells used for facies analysis
UHM-02
LTG-01
P16-01
O18-01
S02-02
S05-01
BHG-01
KTG-01
WDR-01
MER-01
LOENHOUT
MERKSPLAS
TURNHOUT
POEDERLEE
MOL-GT-01
KESSEL
BOOISCHOT
HALEN
GVK-01
DB-123
DB-105
THM-2000/2001/2002
HEU-01-S1
DB-106
DB-109
DB-108
's GRAVENVOEREN
MUNSTERLAND-01
WSK-01
ISSELBURG-3
CAL-GT-02
CAL-GT-03
CAL-GT-01
WACHTENDONK-1
SCHWALMTAL-1001
0
40000
80000
120000
160000
200000
240000
280000
320000
360000
400000
440000
480000
520000
560000
600000
640000
680000
0
50
100
150km

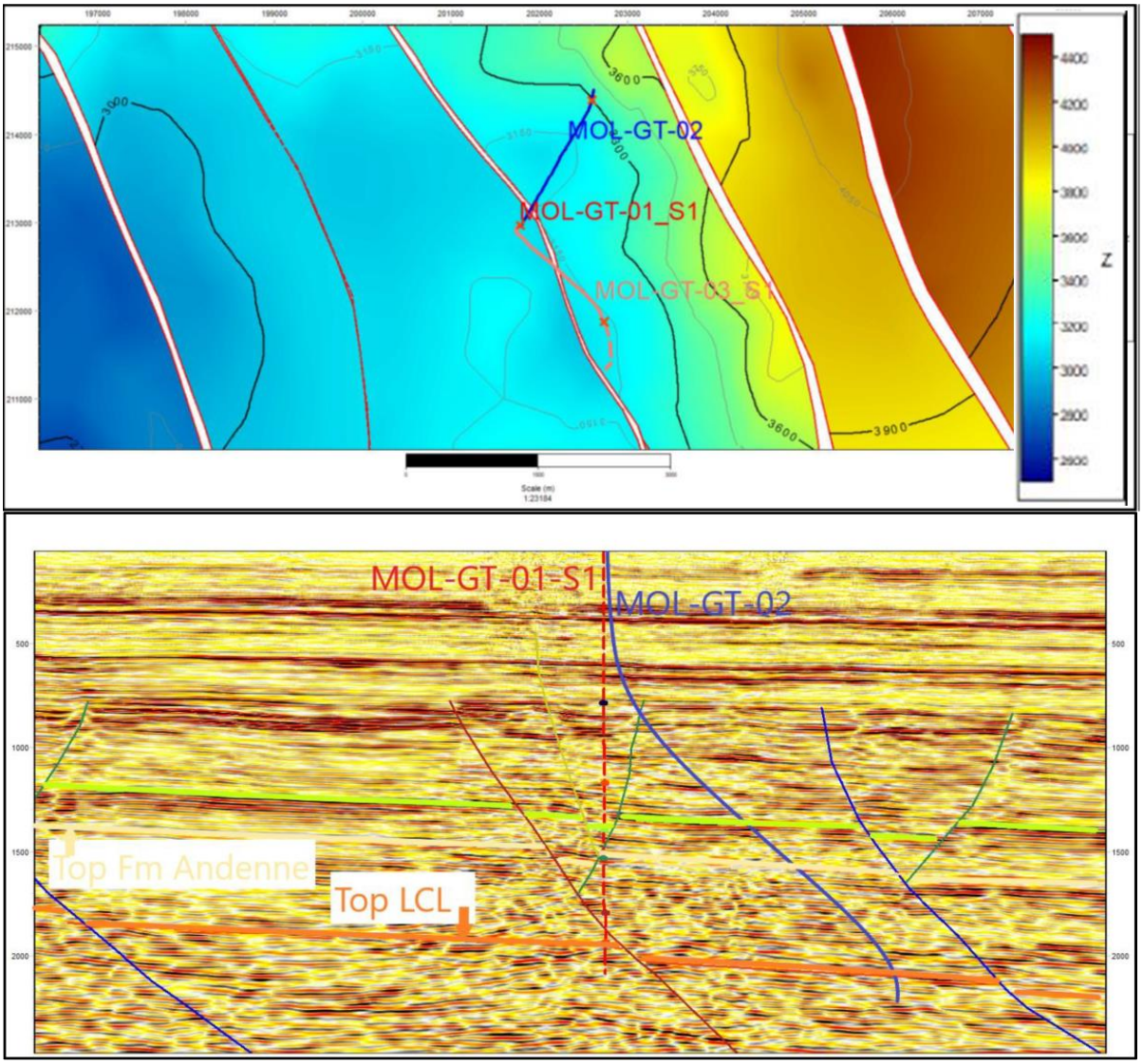

Figure 7-6 Top figure (previous page): Reconstructed facies map showing the conservative distribution of carbonate platforms during Molinacian to Livian interval, and Warnantian (Asbian to Brigantian) with locations of wells that access Lower Carboniferous (Dinantian) carbonates (Mozafari et al., 2019). Middle figure: Depth map of the top of the Carboniferous 'Kolenkalk' Group (depth scale blue to brown for depths of 2600-4400 m). Well trajectories (blue and orange line) and entry-points into the top of the Lower 'Kolenkalk' Group (red crosses) are shown. Bottom figure: Seismic section (line MH 10-04) showing wells MOL-GT-01-S1 and MOL-GT-02, top of the Lower Carboniferous 'Kolenkalk' Group (LCL, orange line), and top of Andenne Formation (transparent yellow line). The length of the cross-section from left (Southwest) to right (Northeast) is approximately 6 km. Vertical scale is approximately 2.500 ms TWT. From: Broothaerts et al. (2019).

7.3 Projects in the Molasse Basin near Munich in Germany

Around 50 geothermal concessions are currently granted in the Molasse Basin in southern Germany, and more than 50 geothermal wells have been drilled in 22 projects (**status May 2019**, Erdwerk[47]). Currently, 16 projects produce heat in the greater Munich area, mainly for district heating (Seithel et al., 2019). In two of the 16 projects, induced seismicity with M_L > 2 has occurred (Table 7-4), which may be considered as 'felt' seismicity (Buijze et al., 2019a). In 6 other projects, induced seismicity with lower magnitudes have been reported (Seithel et al., 2019). The description given here is a summary of the earlier review by Buijze et al. (2019a)[38], extended with some recent studies that investigate the occurrence and mechanisms of the seismicity in the area (Erdwerk, 2019; Savvatis et al., 2019; Seithel et al., 2019).

Geological setting of the Molasse Basin

The Molasse Basin (North Alpine Foreland Basin) is a typical foreland basin found directly north of the Alps, ranging from Geneva in the west to Bavaria in the east (Figure 7-7). Flexure of the lithosphere due to the Alpine mountain building caused the formation of a deep foreland basin in the Eocene, which was filled by Tertiary Molasse sediments (e.g. Bachmann et al., 1987; Reinecker et al., 2010). The deepest, oldest formation below the basin is the Variscan Basement, which consists of gneisses and granites. During the Variscan orogeny in the Carboniferous NW-SE troughs developed locally, which were filled with Permo-Carboniferous sediments (Bachmann et al., 1987). The basement outside of the troughs was subject to erosion. During the Triassic lithospheric cooling and subsidence caused the formation of a basin (part of the Thetys Ocean) which extended eastwards (Mazurek et al., 2006). Triassic sediments were deposited unconformably on top of the basement, or locally the Permo-Carboniferous troughs. The Triassic sediments are thickest in the west and were deposited increasingly to the east with time; the Early Triassic Bundsandstein is found only up to the westernmost tip of the current-day Molasse Basin, the Middle Triassic was deposited up to halfway between Zurich and Munich, and the Upper Triassic Keuper and Lower Jurassic sediments were deposited almost up to Munich (Bachmann et al., 1987). The Middle Jurassic pelitic and oolitic limestones of the Dogger are present below almost the entire Molasse Basin, ranging in thickness from 0 m in the SE to 200 m the NE. The Upper Jurassic Malm limestones are also ubiquitous below the basin, and vary in thickness from 600 m in the south to 400 m in the north. Subsequent uplift caused karstification of the Jurassic sediments, and eroded parts of the Jurassic sediments and the Cretaceous sediments, before the Alpine orogeny caused the formation of the Molasse Basin and infill with Tertiary and Cenozoic sediments. During subsidence of the Molasse Basin E-W striking normal faults developed (Figure 7-7), but these are currently inactive. Stress measurements and focal mechanisms indicate the present day stress regime to be transpressional (strike-slip to thrust faulting). The maximum horizontal stress is oriented N-S in the eastern parts of the basin, and gradually rotates to NNW-SSE in the west (Reinecker et al., 2010).

The main geothermal target in the Molasse Basin is the karstified Malm limestone formation which has a high permeability. The reservoir sediments consist of thin-bedded marl and thick-bedded limestone or dolomitic units as well as porous reef structures (Seithel et al., 2019). It is located between 1.5 and 5.5 km with temperatures up to 160°C in the Molasse Basin. Projects in the greater Munich area target the limestone reservoirs between 2.0 and 4. km with temperatures up to 123°C (Table 7-4).

[47] https://www.erdwerk.com/en. Picture source: Link or link.

The greater Munich area is located in a region of relatively few occurrences of natural seismicity (Figure 7-8, Megies and Wassermann, 2014). No natural seismicity is recorded within a radius of 40 km around the Unterhaching well site prior to the start of operations. Overall, only 17 earthquakes with intensities of IV or above are documented in the Molasse Basin, of which only 8 are less than 150 km from the well. There is no record of any damaging earthquake in the entire Molasse Basin seismogeographic unit. Some historic mining-induced seismicity is located ~50 km SW of the area.

Relation between operations and seismicity for the Munich projects

Geothermal systems near Munich are based on fluid circulation using one or more production and injection wells. Due to the high permeability of the targeted limestones that allow flow rates of 80-140 l/s (Table 7-4), reservoir stimulation by fluid injection is not required. Operational data of individual projects is not publicly available, but seismicity at Unterhaching (6 events of $M_L > 2$) occurred soon after the onset of circulation, while seismicity at Poing (2 events of M_L 2.1) occurred 5 years after circulation started in 2016 (Seithel et al., 2019). In both Unterhaching and Poing projects the seismicity is located near the injection well (Figure 7-9). Earthquake hypocentre data of the Unterhaching project are located in basement rock underlying the geothermal target horizon, and can be associated to existing fault zones (Megies and Wassermann, 2014).

The relation between stress state at faults, seismicity and geothermal operations is further investigated by modelling fault reactivation potential or slip tendency (cf. ***BOX 4.3*** and ***BOX 4.6***; Savvatis et al., 2019; Seithel et al., 2019). Analysis of the reactivation potential suggest that fault structures in the area generally exhibit low seismic reactivation potential, as long as they trend ENE-WSW (Seithel et al., 2019). At Unterhaching, critically stressed fault segments require small changes in reservoir stress conditions to increase the reactivation potential of faults and associated induced seismicity. Seithel et al. (2019) suggest that fault segments are not critically stressed at Poing, but thermoelastic effects leading to stress rotation and reduction of fault cohesion and friction by carbonate dissolution leading to fault weakening can cause fault segments to become critically stressed over time. The studies indicate that geothermal operations in reservoirs with good permeability and associated high flow rates at low injection pressures are able to generate seismicity, even in low seismic hazard settings.

Seismic monitoring and mitigation measures for the Munich projects

Prior to 2001, regional networks had a magnitude of completeness higher than M_L 2.0, but occurrence of M_L 2.5-3.0 events with similar hypocentre depths as the seismicity at Unterhaching is likely (Megies and Wassermann, 2014). As of 2001, the regional seismic monitoring network has a detection threshold of M_L 2.0. Additional regional seismic monitoring stations became operational in February 2008, and continued improvements allows M_L down to -0.36 to be currently detected at sites Pullach, Oberhaching, Unterhaching, Taufkirchen, Kirchstockach and Dürrnhaar (Seithel et al., 2019). In the inner and northern part of Munich, the magnitude of completeness is M_L 1.0–1.5. Regulations require the installation of at least one seismometer at each geothermal site and a minimum of four additional seismic monitoring stations in case of local seismic events with M_L 1.5 or PGV ≥ 0.1 mm/s. Traffic light systems are not required in the area, but there is an obligation to report induced seismicity with $M_L > 2.0$, intensity[8] above IV, or PGV ≥ 1.0 mm/s to the regulatory authorities.

Country & place (lat, lon):	Germany, Munich					
Activity:	Geothermal production					
Start date – End date:	Unterhaching (UH, ~9 km SSE of Munich city centre) Poing (PO, ~18 km WNW of Munich city centre) Dürrnhaar (DH, ~21 km SE of Munich city centre) Sauerlach (SA, ~20 km SSE of Munich city centre) Kirchstockach (KS, ~15 km SE of Munich city centre) Oberhaching (OH, ~13 km S of Munich city centre) Taufkirchen (TK, ~11 km SSE of Munich city centre) Pullach (PU, ~10 km SSW of Munich city centre)					
Fluid + Fluid balance:	Water				Balanced, circulation	
Maximum activity depth:	**2.0-4.5 km**: 3580 mTVD (UH); 3049 mTVD (PO): 3720 mTVD (DH); 4480 mTVD (SA); 3730 mMD (KS); 3755 mMD (OH); ~3800 mTVD (TK); 3930 mMD (PU)					
Activity formations & rock types:	Upper Jurrassic (Malm) limestones					
In-situ temperature	**80-123°C**: 123°C (UH); 85°C (PO); 127°C (OH); 133°C (TK); 111°C (PU)					
Pressure:	Reservoir: ~380 bar; wellhead: ~10 bar (PO)					
Maximum flow rate:	**Tot. 1600 l/s (16 projects), wells: 80-140 l/s**: 140 l/s (UH); ~100 l/s (PO); 132 kg/s (OH); 120 l/s (TK); 80 l/s (PU)					
Max. geothermal power:	**Tot. 235.6 MW_{th}, 31 MW_{el}**: 38 MW_{th} (UH); 4.3 MW_{el} (TK)					
Monitoring system:	Regulations: Min. 1 seismometer, min. 4 additional stations if $M_L \geq 1.5$ or PGV $\geq$ 0.1 mm/s) of minimum four additional stations Magnitude of completeness: 1.0–1.5 inner & northern part of Munich					
Monitoring resolution:	Minimum magnitude detected: M_L -0.8 (UH)					
Seismicity (approx.. 2008-2017):	Date M_{max}	# events	Max. M_L	# > M 1.0	# > M 2.0	Loc.
Unterhaching	10.02.2008	> 657	2.4	27	6	Inj.
Poing	19.11.2016	21	2.1	-	2	Inj.
Dürrnhaar	31.07.2016	10	1.3	1	-	Inacc.
Sauerlach	19.06.2014	2	1.2	1	-	Inacc.
Kirchstockach	23.08.2012	33	0.8	-	-	Inj.
Oberhaching	01.02.2016	3	0.5	-	-	Inj.
Taufkirchen	19.07.2012	11	0.3	-	-	Inj.
Pullach	21.02.2015	1	-0.4	-	-	Inj.

Table 7-4 Characteristics of the geothermal projects in the Molasse Basin near Munich in Germany. Sources: Megies and Wassermann (2014); Buijze et al. (2019a); Seithel et al. (2019); www.tiefegeothermie.de[48]. Note that this table only indicates the projects where induced seismicity has been recorded (8 out of 16 projects). For the other projects, induced seismicity was absent, below the magnitude of completeness of seismic monitoring networks, or not reported in publicly available literature.

[48] https://www.tiefegeothermie.de/

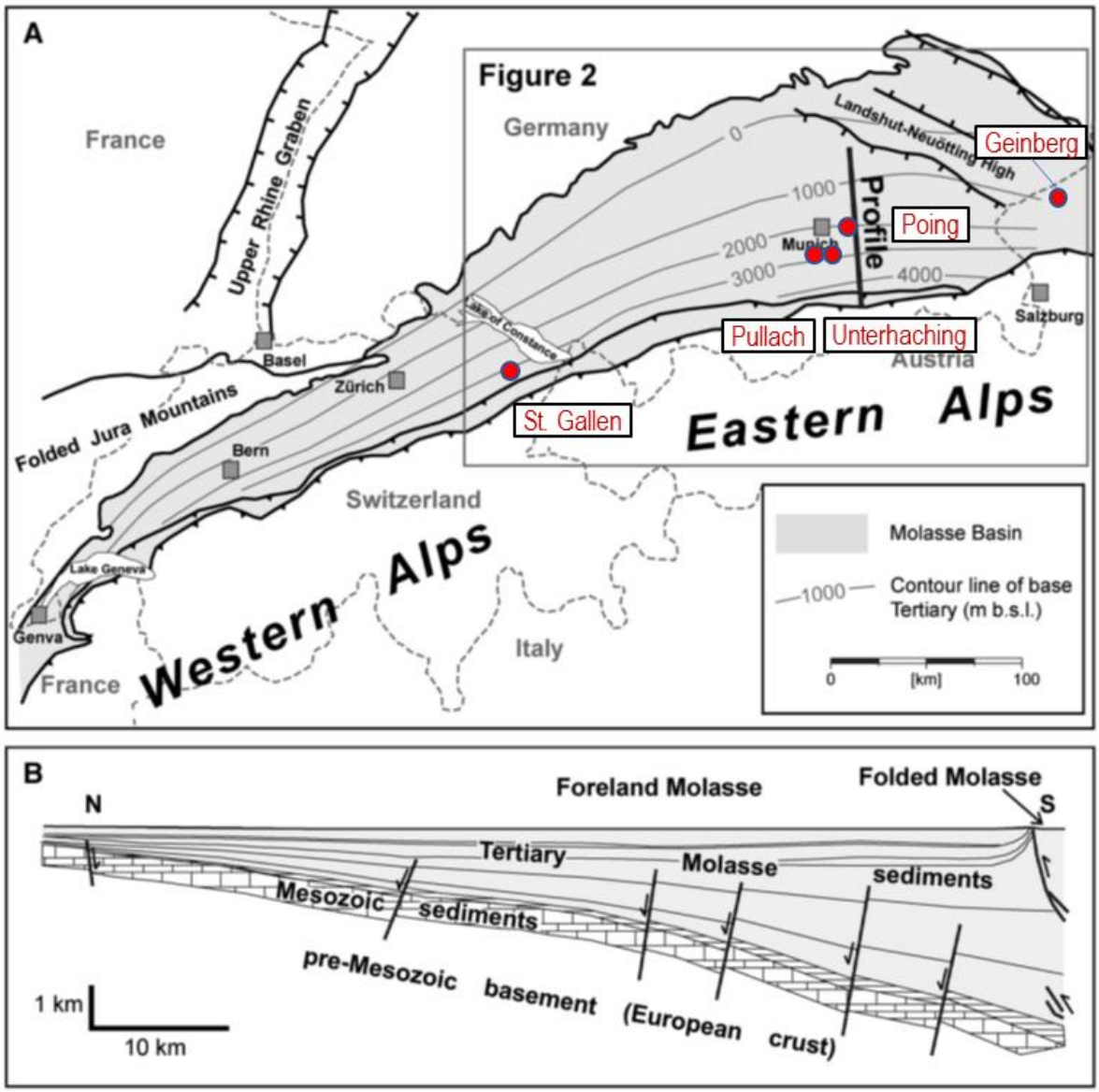

Figure 7-7 Overview of the Molasse Basin. (A) Extent of the Molasse Basin in Switzerland and Germany and thickness of the Tertiary sediments (contour lines). The locations of some typical geothermal sites are indicated (red dots). b) Cross-section through the Molasse Basin along profile line in A, east of Munich. From: Reinecker et al. (2010), modified by Buijze et al. (2019a). Copyright Elsevier, reproduced with permission.

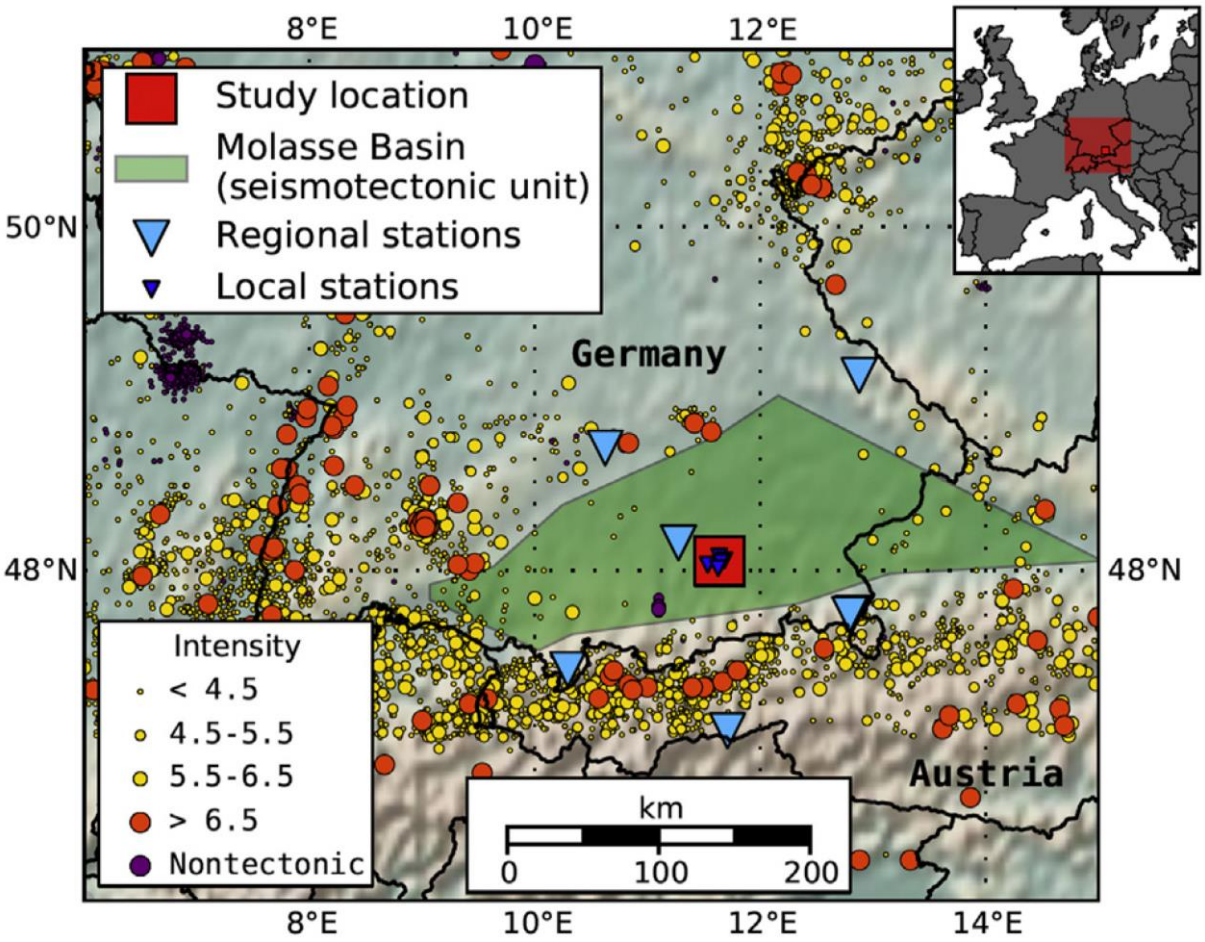

Figure 7-8 Overview map showing the area around Munich (red square) located in the Molasse Basin seismogeographic region (shaded in green), east of the Lake of Constance in southern Germany. Regional seismometer stations used in hypocentre relocation of the larger earthquakes are shown (light blue triangles). Earthquakes documented in the German catalogue are shown as circles (yellow/orange for tectonic and purple for non-tectonic events). Three earthquakes at the study location were removed from the original figure. From: Megies and Wassermann (2014).

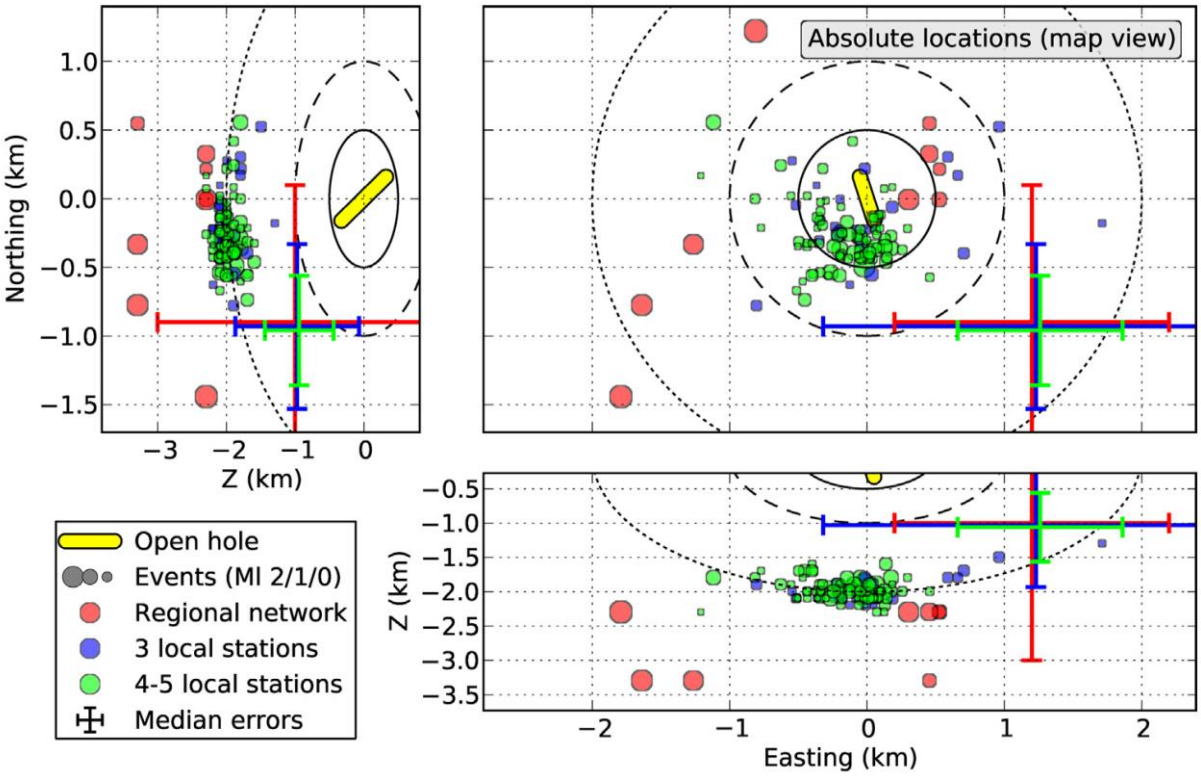

Figure 7-9 Absolute locations for all events in the vicinity of the Unterhaching injection well. Older events (2008/2009) with less accurate absolute locations (red circles), events detected with local stations and located using a 3D velocity model (green and blue circles), the open hole section of the Unterhaching re-injection well (in yellow), distance contours (500 m, 1 km and 2 km distance from midpoint of open hole section, solid, dashed and dotted circles, respectively), and error bars for the median error (coloured bars correspond to colours events) are indicated. From: Megies and Wassermann (2014).

7.4 Lessons learned from the case studies

Although the occurrence of seismicity near most of the projects described above is subject of ongoing research, current information suggests some findings that are of interest to the Dinantian carbonate geothermal play:

1. *Felt seismicity (M > 2) is rare in the case studies reviewed. If induced seismicity occurs, it is generally observed in the vicinity of injection wells.* In 8 out of 16 projects in the Molasse Basin near Munich, seismic events with $M_L < 2.5$ induced seismicity was recorded. In 6 out of 16 projects, seismic magnitudes ($M_L < 1.5$) were below the threshold for felt seismicity (cf. Table 7-4). Most of the seismic events are located in the vicinity of the injection well (cf. Figure 7-9 for the Unterhaching project). Observations at the Balmatt project (~266 events, $M_L < 2.1$ with one event $M_L > 2.0$; cf. Table 7-3) suggest a relation between seismicity and injection of cold fluids (cf. Figure 7-5). For the Californië projects (17 events, $M_L < 1.7$; cf. Table 7-1), a relation between seismicity and injection is also suggested (Burghout et al., 2019).

2. *Demonstration of spatial relations is critically hampered by lack of resolution of hypocentre locations*. For the Balmatt project, a spatial relation between seismicity and injection of cold fluids is apparent, although vertical separation between seismic events and the injection well is not given (cf. Figure 7-5). For the Unterhaching project in the Molasse Basin considerable errors for hypocentre locations apply even for local seismic monitoring networks (cf. Figure 7-9). As a result, horizontal and vertical separation between the injection well and seismicity are subject to uncertainty. Figure 7-9 suggest that vertical separation can be up to km's, which may be difficult to explain for geothermal operations that rely on fluid circulation only (i.e. given small stress changes away from the injection well). For the Californië projects, lack of resolution of hypocentre locations is a critical factor in disentangling effects of operations in the two geothermal projects that were active at the same time (for a limited period in time, cf. Figure 7-2), and effects of natural seismicity at critically stressed faults (cf. Figure 2-2).

3. *Temporal relations between seismicity and operations may be complex.* The projects indicate that time between onset of operations and the occurrence of induced seismicity may vary, i.e. seismicity is observed during injection tests at Balmatt while delays of years are reported for the projects at Californië and Poing (cf. Figure 7-2; section 7.2; Seithel et al., 2019). Placement and/or extension of seismic monitoring networks is a factor as high resolution monitoring networks are often only installed after (problematic) seismicity has been observed. The Californië and Balmatt suggest a relation between the occurrence of seismicity and operational changes such as (accidental) well shut-in. In particular, maximum seismic magnitudes are recorded after shut-in, but the time between shut-in and seismic events may vary (cf. Figure 7-2; Figure 7-5).

4. *Small stress changes caused by fluid circulation may lead to induced seismicity.* Modelling of coulomb stress changes (cf. ***BOX 4.1***) for the Californië projects seem to indicate that seismicity can occur for relatively small changes caused by fluid circulation in the vicinity of critically stressed faults (Burghout et al., 2019; see also Candela et al., 2018a). All case studies described above show induced seismicity for geothermal projects based on fluid circulation without stimulation of reservoir

permeability by fluid injection. For demonstration of causal relation between seismicity and operations, there is a relation with uncertainty of hypocentre locations as stress changes generally rapidly diminish away from operations. If seismic events are located far (typically km's) away from geothermal operations, the contribution of geothermal operations to coulomb stress changes at the hypocentre location may be very small and difficult to distinguish from other causes such as tectonic stress build-up.

5. *There is debate about the applicability of the Kaiser effect to geothermal operations.* The Kaiser effect describes the absence of seismic events below the stress initially required to induce seismicity, suggesting that seismicity may only occur if this initial stress is exceeded (Kaiser, 1950; Kurita and Fuji, 1979, Tang et al., 1997). For the Californië projects, it is suggested that the Kaiser effect indicates that future seismic events are not expected if pore pressures remain below previous values during fluid circulation, provided other sources for stress changes are absent. SodM (2019) states that the Kaiser effect does not apply to these operations because the physical state of the geothermal system changes during operations, i.e. (1) temperature changes occur due to injection, (2) different fault segments may become active that have not been subject to stress changes and seismic slip during past operations, (3) fault slip changes the fault block geometry ("juxtaposition") and thereby the physical state of the fault zone.

8. Conclusions

The research conducted in this project "*Induced seismicity potential for geothermal projects targeting Dinantian carbonates in the Netherlands*" is the result of an analysis of factors, models and case studies that are relevant for induced seismicity potentially associated with geothermal projects targeting the Dinantian carbonates in the Netherlands. It is a follow-up of an earlier study by Buijze et al. (2019a) "*Review of worldwide geothermal projects: mechanisms and occurrence of induced seismicity*" that focussed on reviewing international practice, knowledge and case studies relevant for understanding induced seismicity and assessing the seismogenic potential of geothermal operations. This earlier study was carried out in the period September 2018 to January 2019.

The analysis, results and conclusions mentioned here are based on both studies.

The main research activities of the current study focussed on:

- Analysis of key factors affecting induced seismicity (Chapter 2)
- Assessment of the seismogenic potential for different regions (Chapter 3)
- Review of modelling approaches (Chapter 4)
- Discussion of seismic hazard and risk analysis (Chapter 5)
- Recommendations for seismic monitoring (Chapter 6)
- Review of case studies targeting fractured carbonates (Chapter 7)

The research allows the following conclusions to be made:

1) **The induced seismicity (seismogenic) potential for projects targeting Dinantian carbonates is low to medium for most regions and operations. Lower seismogenic potential may be expected:**
   - **if projects are not within a critical distance of:**
     - **natural seismicity around the Roer Valley Graben,**
     - **gas depletion induced seismicity,**
     - **larger fault zones.**
   - **if projects are based on fluid circulation without stimulation of reservoir permeability by fluid injection.**
   - **if projects have low-moderate injection pressures and low temperature differences between the reservoir and re-injected fluid.**

   Within the current classification, the low to medium seismogenic potential is based on the analysis of effects of geological and operational factors on induced seismicity. It means that felt seismicity cannot be excluded but, if present, is most likely limited to some projects where the specific combination of site-specific factors lead to the occurrence of seismicity. The number and magnitude of earthquakes is dependent on these factors, and on implemented measures that mitigate the occurrence of felt seismicity. The medium seismogenic potential in some areas is based on the occurrence of seismicity in the Californië (max. M_L 1.7) and Balmatt (max. M_L 2.1) projects that target the Dinantian carbonates as well as the predicted effects of geological and operational factors on induced seismicity. A high seismogenic potential may only occur if fluid is injected at relatively high pressure or with high flow rates in larger fault zones. Such operations may cause significant stress changes in the faults due to pressure changes or cooling, and can potentially lead to seismic events with frequency and magnitude that are considerably

higher than local baselines. The key factors would indicate a high seismogenic potential in that case. A *hypothetical* example of such a case with high seismogenic potential would be fluid injection in one of the tectonically active faults of the Roer Valley Graben. Within the current classification a high seismogenic potential is otherwise associated with Enhanced Geothermal Systems (EGS) or Hydrothermal Systems (HS) that do not occur in the Netherlands and that do not apply to Dinantian carbonates. To further specify the local or regional seismogenic potential of the Dinantian carbonates, more data on local geology, reservoir properties, and local stress state is needed. Further specification between low and medium seismogenic potential also requires more region- or location-specific research, in particular on (modelling) the effects of short term cooling at injection wells and on long term cooling of the entire reservoir and associated stress changes at faults.

2) **For geothermal systems targeting Dinantian carbonates that are based on fluid circulation without stimulation of reservoir permeability by fluid injection, <u>key factors</u> that affect the induced seismicity potential are:**
    - **Occurrence of natural seismicity, indicative of critically stressed seismogenic faults in the vicinity of geothermal operations;**
    - **Distance of operations to large (critically stressed) faults and associated stress changes at the faults;**
    - **Interacting stress field, fracture populations and flow regime that determine the spatial distribution of stress changes (i.e. matrix- or fracture-dominated flow and associated flow isotropic or anisotropic flow patterns);**
    - **Reservoir depth and temperature, in particular related to temperature changes and associated thermoelastic stress changes;**
    - **Composition and competency of reservoir rock that determine how stresses are transferred within the reservoir and if rocks behave seismically or aseismically;**
    - **Hydraulic and mechanical decoupling with over- and underburden that determine how pressure and stress changes in the reservoir are transferred to (potentially seismogenic) over- and underlying formations;**
    - **Interacting operational factors (e.g., injection pressure and injection temperature) that combined determine the magnitude and spatial distribution of stress changes;**
    - **Interaction with other subsurface activities such as gas depletion, gas storage or salt mining that may lead to a cumulative effect on local stresses that is larger than the effect of geothermal operations alone.**

The location and timing of seismic events are determined by the interplay of direct pressure, poroelastic and thermoelastic effects. Stress transfer due to seismicity or chemical effects on fault strength may also play a role. Direct pressure and poroelastic effects occur on relatively short timescales, while thermoelastic effects caused by progressive cooling may occur on relatively long timescales. Seismicity can occur both inside and outside the reservoir, by pressure diffusion along faults, fractures or karsts, by (a)seismic stress transfer, or by poroelastic and thermoelastic effects.

The interaction between mechanisms is complex, i.e. effects cannot be simply added but need to be assessed in a non-linear manner. The relative contribution of different mechanisms depends on site-specific geological and operational factors. Operational factors (injection pressure, temperature and volume)) can be adjusted to minimize induced seismicity. Geological factors such as the presence, geometry and stress state of faults,

interaction between geological and operational factors, and interference between different subsurface operations are critical. Site-specific analysis is required to fully assess these factors for every single project. Natural seismicity indicates the presence of critically stressed faults that can generate seismic slip. Faults that are favorably oriented for reactivation and seismic slip need to be present for induced seismicity to occur. Small stress changes caused by geothermal operations may already be sufficient to induce seismicity at critically stressed faults.

The interaction of stress field, fractures and fluid flow determines the spatial distribution of stress changes for specific operational factors of a geothermal project. Reservoir temperature is increasing with depth, and so will thermoelastic effects due to larger temperature changes during operations. Composition of reservoir rock affects flow properties as well as mechanical properties of the reservoir, and thereby influences the transfer of stress changes to faults. Hydraulic and mechanical coupling with other formations control the pressure communication and stress transfer between the reservoir and overlying or underlying formations. It is particularly important if the reservoir exhibits pressure communication or mechanically coupling with underlying (basement-type) seismogenic formations which may be more prone to the presence of critically stressed faults. Interaction of geothermal operations with other subsurface activities, in particular gas depletion, will lead to complex interplay of stress changes and potentially enhanced induced seismicity potential.

3) **The <u>review of modelling approaches</u> indicates that problem-specific modelling can:**
   - **increase the understanding of mechanisms underpinning induced seismicity,**
   - **provide forecasts of characteristics of single seismic events or seismicity catalogues,**
   - **constrain and focus seismic hazard and risk assessment.**

The choice of modelling approach should be determined based on the specific problem under investigation, i.e.:

- Fast semi-analytical models allow assessment of uncertainties and can be used in probabilistic seismic hazard and risk assessment,
- Slower 2D or 3D numerical models can simulate single seismic events or seismicity catalogues and can be used to increase our understanding of underlying mechanisms by exploring scenarios of varying geological or operational factors.

Another distinction is between:

- Fully stochastic modelling approaches that are robust and efficient, and be used in near real-time to forecast seismic hazard and in adaptive traffic light systems,
- Physics-based models that better account for physical processes underpinning induced seismicity,
- Hybrid models that combine components of stochastic and physics-based models.

Full field 3D models or models with full coupling between flow, mechanics and temperature aid in mechanistic understanding of induced seismicity, but require many, often poorly constrained, input parameters and are generally computationally intensive.

The reactivation and seismicity potential of a new geothermal site can be screened using a (simplified) geological and reservoir model combined with a 1D or 'fast' 3D fault stability model. For induced seismicity potential of projects targeting the Dinantian carbonates, a staged approach may be valuable that first assesses the key processes controlling fault reactivation and seismic response of faults using more complex 2D and 3D models combined with observations from case studies. Subsequently, fast models can be developed that capture the key processes but are fast enough to account for (geological) uncertainties and can be used in Adaptive Traffic Light Systems and seismic hazard and risk analysis.

4) **<u>Comparison of approaches for seismic hazard and risk analysis</u> show that methods with different complexity are used in the Netherlands, depending on the level of detail required. The methods range from a qualitative screening of key geological and operational factors to a complete model chain consisting of seismic source models, ground motion models and damage models. The comparison suggest that it is currently not really feasible to apply a full model chain to geothermal projects targeting the Dinantian carbonates, but components from the model chain are very useful to perform simpler analysis of seismic hazards (in particular seismic source models can be applied).**

   The comparison includes the following approaches:
   - A probabilistic seismic hazard and risk analysis developed for gas depletion in Groningen (the Groningen Model Chain),
   - A qualitative screening of seismogenic potential based on the analysis of key geological and operational factors,
   - A method that distinguishes three hazard levels and associated risk mitigation protocols.

   Important considerations are that seismic hazard and risk assessment need to be site- and project-specific and that the combination of geological and operational factors controls seismic hazard and risks. Some modelling approaches and components in the Groningen Model Chain consisting of seismic source models, ground motion models and damage models can be used for geothermal projects, despite that mechanisms of induced seismicity are different for gas depletion production and geothermal operations and that the scenario of frequent occurrence of felt ($M > 2$) seismic events over years of operations does not really apply to geothermal projects.

5) **<u>Recommendations for seismic monitoring</u> include three main strategies for improved seismic monitoring of geothermal reservoirs at different depths such as the Dinantian carbonates:**
   - **A *project-based* deployment of a mobile arrays,**
   - **An *area-based* temporary placement of dense array of both surface and borehole stations,**
   - **A *national* permanent expansion of the national seismic monitoring network.**

   A project-based deployment of a mobile array can be followed by local permanent arrays to characterize noise conditions and monitor background seismicity, leading to better monitoring sensitivity and accuracy and thereby better detection of induced seismicity

during operations. An area-based temporary placement of dense array of both surface and borehole stations can be performed in areas where multiple doublets are foreseen to obtain a high signal-to-noise ratio, detection of small seismic events (e.g. down to M 0.0), and better resolution of hypocentre locations. A national permanent expansion of the current seismic monitoring network can be used to permanently reach lower magnitude completeness level in all parts of the Netherlands. Additional improvements of seismic monitoring can be achieved if different local networks are integrated, and if network development is aligned with development of different subsurface projects (e.g., deep, intermediate and shallow geothermal, gas storage and production, and energy (hydrogen) storage.

6) **Findings of the <u>review of case studies targeting fractured carbonates</u> (Californië, Balmatt, Molasse Basin projects) are that:**
    - **Felt seismicity (M > 2) is rare in the case studies reviewed. If induced seismicity occurs, it is generally observed in the vicinity of injection wells,**
    - **Demonstration of spatial relations is critically hampered by lack of resolution of hypocentre locations.** In all cases, uncertainties in local velocity models are such that vertical separation between operations and seismicity could be within 100 meter or up to km's. Disentangling effects of between different operations or with effects of natural seismicity at critically stressed faults is hampered by this lack of resolution,
    - **Temporal relations between seismicity and operations may be complex with different delays between onset or shut-in of operations and occurrence of seismicity.** In the Californië and Balmatt project, maximum seismic magnitudes are recorded after (accidental) shut-in, but the time between shut-in and seismic events may vary,
    - **Small stress changes caused by fluid circulation may lead to induced seismicity.** The contribution of geothermal operations to coulomb stress changes at faults is expected to decrease rapidly with distance between operations and faults. Progressive cooling of reservoir (sections) and complex (anisotropic) flow around faults or due to fracture networks may complicate analysis.
    - **There is debate about the applicability of the Kaiser effect to geothermal operations.** The Kaiser effect describes the absence of seismic events below the stress initially required to induce seismicity, suggesting that seismicity may only occur if this initial stress is exceeded. Its applicability to geothermal operations is questionable because of changes in the physical state of the geothermal system (i.e. temperature changes occur, different fault segments may become reactivated, the physical state of fault zones may change).

9. Recommendations for future studies and data acquisition

Throughout the report, key knowledge gaps have been identified that are of particular interest to geothermal projects targeting the Dinantian carbonates. These knowledge gaps are mainly associated with technical aspects contributing to understanding, modelling, forecasting and mitigating induced seismicity. The knowledge gaps can be clustered in some general recommendations for improving (1) *generic understanding* of controls on seismogenic potential, (2) *project-specific* causal relations between operations and seismicity, (3) *project-based, regional or national* monitoring of seismicity, (4) *project-based* mitigation measures, and (5) *the scientific knowledge base* for establishing the level of acceptable risks associated with (ultradeep) geothermal projects. The recommendations are given in combination with research or data acquisition efforts that can help solving them.

The main recommendations are to improve:

1) **The understanding of controls on the seismogenic potential, specifically for the Dinantian carbonates.** General concepts for the effect of geothermal operations are known, but specific knowledge on how different mechanisms lead to induced seismicity in Dinantian carbonates is lacking. Experimental and modelling studies should particularly focus on:
    - Assessing the contribution of different mechanisms (direct pressure, poroelasticity, thermoelasticity, stress transfer on faults) leading to induced seismicity and the relation with operations
    - Comparing the distribution and evolution of pressure, temperature and stress changes for matrix- and fracture-dominated geothermal reservoirs
    - Dynamic fault properties and brittle, velocity-weakening behaviour of fault zones in carbonate (compared to sandstone) rocks which makes them prone to seismic slip and induced seismicity

    Specific knowledge gaps and & research efforts include:

    - Knowledge gap: Dominant *mechanisms* ("*drivers"*) controlling the *spatial distribution of pressure, temperature and stress changes*, and driving *seismicity* in the Dinantian carbonates, and the relation between their contribution and geological and operational factors.
      Data acquisition & modelling: An integrated approach could be followed consisting of:
        - Physics-based numerical models of coupled thermo-hydro-mechanical processes to simulate the spatial distribution of pressure, temperature and stress changes and seismicity as well as effects on seismicity rates and magnitudes. Focus on (i) differences in the seismic response of carbonates with fracture- or matrix dominated flow, (ii) short term (fast) cooling at the injector and long term (gradual) cooling of the entire reservoir, and (iii) shut-in of wells and delayed seismicity with relatively large magnitude and seismicity rate.
        - Laboratory experiments on relevant reservoir rock samples to provide (i) input for models, and (ii) validation of model results (i.e. possibility to obtain systematic series of test data to investigate individual

processes). Priority are experiments on (rocks analogous to) Dinantian carbonates, and on parameters that are poorly constrained in available literature.
- Evaluation of model results using (extended) seismic monitoring and operational data from case studies (e.g., Californië, Balmatt). Integrate with additional data acquisition as suggested below (points 2, 3).
- Use modelling results to outline improvements for reservoir management of geothermal projects ("how to operate the engine").

- Knowledge gap: *Seismic versus aseismic response of faults* in the Dinantian carbonates to stress changes (post failure rupture), in particular controls on the frequency and magnitude of seismic events.
  Research/data acquisition efforts: Integration of experimental and modelling studies of the effects of mineralogy and chemical processes on seismicity in carbonate rocks:
  - Laboratory experiments on relevant reservoir rock sample to investigate the behaviour of fault gouges (velocity-strengthening or weakening, rate-and-state parameters, cf. Niemeijer and Spiers, 2006).
  - Physics-based models to forecast the contribution of seismic slip during fault reactivation for different pressure, temperature and stress conditions (cf. Van den Ende et al., 2018).

2) **Demonstration of causal relations between geothermal operations and induced seismicity.** In most cases *spatial and temporal relations between seismicity and operations* are used to demonstrate (lack of) causal relations. The review of case studies of Dinantian carbonate geothermal projects (cf. section 7) indicated that it is challenging to establish spatial and temporal relations between seismicity and operations. In particular, for Dinantian carbonates felt (M > 2) seismicity is rare so demonstration of causal relations mainly relies on data from local seismic monitoring networks which allow detection of lower magnitude seismic events. Also, many potential project locations are outside traditional areas of hydrocarbon exploration with more limited coverage of seismic surveys of regional seismic monitoring networks. *Project-, region- or play-based data acquisition* can be used to close specific knowledge gaps related to causal relations, and should particularly focus on:
   - Better linking seismic events to mapped faults
   - More accurately model stress changes (direct pressure, poroelastic and thermoelastic stress changes) at faults and hypocentre locations to evaluate critical distance between operations and faults
   - Better forecast induced seismicity potential of existing projects and improve mitigation measures for seismic risk
   - Disentangling seismicity between specific projects, wells or operations
   - Deploying a demonstration case to test spatial and temporal relations between seismicity and (varying) operations in the Dinantian carbonates, especially in an area with natural seismicity ("test field lab")
   - Better planning of future projects at safe distance from mapped faults

Specific knowledge gaps and data acquisition & modelling efforts include:

- Knowledge gap: Large (km's) errors in hypocentre locations due to uncertainties in *local velocity models* at project locations.
  Data acquisition & modelling: More accurate local seismic wave velocity models can be obtained by acquiring/performing:
  - Dipole sonic well log data to obtain compressional and shear wave velocities (shear wave velocities are mostly lacking)
  - Vertical seismic profiles to directly obtain velocity models at well locations
  - Data inversion using available information to obtain best velocity model and quantify uncertainties

- Knowledge gap: Uncertainties in the *location, size and geometry of faults* due to limited resolution of seismic surveys.
  Data acquisition & analysis: More accurate fault interpretations can be obtained by acquiring/performing:
  - Additional 2D and 3D seismic surveys to improve characterization of the subsurface at project locations
  - Improved (re-)processing of seismic data to obtain better fault interpretations

- Knowledge gap: Uncertainties in *hydraulic and mechanical interactions* within the geothermal reservoir and surrounding formations.
  Data acquisition & modelling: A better understanding of hydraulic and mechanical interactions can be obtained by performing:
  - Well interference tests to determine reservoir behaviour and associated extent of pressure and temperature perturbations
  - Combine well interference tests, high resolution seismic monitoring and coupled modelling of mechanical, thermal and flow processes to determine locations of critical faults and the spatial extent of stress changes

- Knowledge gap: Understanding observed *delays between operational changes and seismicity*.
  Data acquisition & analysis: Improved understanding of timing of seismicity in relation to operational changes can be obtained by performing:
  - Review of the occurrence of delays in (international) projects under different geological and operational conditions
  - Systematic analysis of the delays in combination with geomechanical modelling to explain delays in terms of direct pressure, poroelastic and thermoelastic effects

3) **Seismic monitoring by integration of data, linking of (local, regional and international) monitoring networks and deploying temporary networks.** *More seismicity data is of great value in improving insight into processes occurring during geothermal operations and their effects on local stresses*. Currently, some projects have deployed local networks (e.g., the Californië projects), some regions have more extensive networks in place (e.g., the area around the Groningen gas field), and coverage of national networks extends beyond national borders. Integration of these

different networks and data as well as (real time) open access to monitoring data can be improved. Additional *project-, play- or area-based networks* and integration with *national permanent networks* can improve seismic monitoring by (cf. section 6):

- Obtaining more (lower magnitude) seismicity data to more closely monitor effects of operations in the subsurface
- Using higher resolution seismic monitoring to identify precursors to seismic events with larger (problematic) magnitude
- Better linking monitoring data to modelling forecasts to improve understanding of relations between operations and seismicity
- Better planning of future projects by identifying regions with (expected) low induced seismicity potential

o Knowledge gap: Limits in the *resolution of seismic monitoring networks* (magnitude of completeness as well as hypocentre locations).
Data acquisition: Improved resolution of seismicity data can be obtained by performing:

- Installing (temporary) dense surface networks of seismometers or even downhole seismometers, preferably at reservoir level (cf. Bohnhoff et al., 2018)
- Integrating data from different local, regional and national networks, in particular integration with data from national seismic monitoring networks in Belgium and Germany

4) Mitigation measures for seismic risks by extending traffic light systems. The most commonly implemented mitigation measure for seismic risks is a traffic light system (TLS) which defines specific actions and operational changes if critical thresholds in characteristics of seismicity are exceeded. Current TLS implemented in the Dinantian carbonate geothermal projects in Californië and Balmatt use thresholds that are based on peak ground velocities, and on magnitude, frequency, spatial distribution of events and peak ground velocities, respectively (cf. section 7.1 and 7.2). TLS can be extended by using additional monitoring data and by optimizing actions based on the latest findings in case studies (cf. section 7), for example:

- Using monitoring data to identify precursors of larger magnitude events that may be problematic (e.g., alignment of seismic events along known or unknown fault planes or low magnitude precursor events to larger events based on Gutenberg-Richter type relations between frequency and magnitude of events)
- Using characteristics of natural (baseline) seismicity in areas with natural seismicity and identify practically measurable parameters that indicate deviations from the baseline (e.g., changes in slope or offsets in Gutenberg-Richter relations)
- Define actions for TLS based on integrating (i) modelling of pressure, temperature and stress, (ii) forecasts of practically measurable parameters (e.g., event rate), and (iii) continuous evaluation of model forecasts against observations (analogous to ATLS, cf. Bommer et al., 2006; Majer et al., 2012)
- Accounting for delays between abrupt well shut-in and seismicity (e.g., ensuring power backup to prevent abrupt shut-in due to power cuts and implementing more gradual well shut-in if TLS thresholds are exceeded, cf. Barth et al., 2013; Hofmann et al., 2018).

- Knowledge gap: Reliable *indicators in seismic monitoring data* that can be used as precursors to problematic seismic events or point to deviations from natural baselines.
  Data acquisition: The identification of indicators in seismic monitoring data requires routine acquisition of high resolution seismicity data as indicated above (point 3) for improving the resolution of seismic monitoring networks.

- Knowledge gap: Understanding the effects and feasibility of TLS actions that include modelling for seismicity forecasts or effects of (gradual) well shut-in.
  Data acquisition & modelling: Development of fast models and validating approaches against data from (international) projects as indicated above (point 2) for improving the understanding of observed delays between operational changes and seismicity.

5) **Establishing a scientific knowledge base to support the debate on acceptable seismic risks for development of geothermal projects, including (ultradeep) Dinantian carbonates.** The level of seismic risk that is considered acceptable for geothermal projects is central to the discussion on (i) the *requirements* for understanding the seismicity in the vicinity of geothermal projects as well as (ii) for seismic monitoring and (iii) measures to mitigate seismic risk. Determining this level is challenging as it will be site-specific and dependent on different *technical, economic and social factors*. For example, the Roer Valley Graben is known for relatively frequent occurrence of natural seismicity with earthquake magnitudes that can reach damaging levels (cf. section 2.1; Dost and Haak, 2007). A key question is if and to what extent induced seismicity may be allowed to exceed natural baseline levels in such areas. In most other areas in the Netherlands, natural seismicity is incidental or absent, and acceptable seismic risks need to evaluated against other types of risks. It has been suggested to base critical levels on *public perceptibility* (PGV typically above 0.1-0.3 mm/s) or *infrastructure vulnerability* (i.e. PGV > 3 mm/s for damage to vulnerable infrastructure or PGV > 5 mm/s for standard infrastructure)[49]. More conservative thresholds have been adopted in the Californië and Balmatt projects. Note that acceptable PGV levels may be site-specific and can be underpinned by site-specific attenuation of seismic waves *relating seismic events to surface motions* (cf. section 5.3; see also SodM, 2019). Focus should be on:
   - Constraints on the level of acceptable risk for geothermal projects targeting the Dinantian carbonates, in particular addressing site-specific technical, economic and social factors
   - Assessment of location-specific differences that affect the acceptable level of induced seismicity
   - Evaluation of procedures that help assessing if seismicity will remain below acceptable levels and establishing relations between measurable parameters and (acceptable) risks
   - Evaluation of seismic risks against other types of risks (e.g., natural seismicity or other natural hazards, other industries)

[49] See also Buijze et al. (2019a), p. 68 (section 5.1.1, Figure 5-2).

Specific knowledge gaps and & research efforts include:

- Knowledge gap: Acceptable seismic risks for development of geothermal projects including (ultradeep) Dinantian carbonates.
  Data acquisition & modelling: The approach should be to link technical, economic and social aspects:
    - Technical feasibility of assessing seismic risks (i.e. monitoring resolution, likelihood of seismic events, potential impacts of seismic events)
    - Assessment of economic feasibility of risk mitigation measures, i.e. the evaluation of mitigation measures against the economics of a geothermal project (also the dependence on level or phase of development in certain regions)
    - Inventory of criteria required to maintain a social license to operate for geothermal projects

10. References

Amantini, E., Ricaud, Y., and Grégoire, N. (2009). Development of the performance of the Loenhout UGS (Antwerp - Belgium) Drilling through a highly karstified and fissured limestone reservoir under gas storage operation. In 24th World Gas Conference (p. 9).

Bachmann, C.E., Wiemer, S., Woessner, J., Hainzl, S., 2011. Statistical analysis of the induced Basel 2006 earthquake sequence: introducing a probability-based approach for Enhanced geothermal system. Geophys. J. Int. 186, 793-807.

Baisch, S., Voros, R., Rother, E., Stang, H., Jung, R., Schellschmidt, R., 2010. A numerical model for fluid injection induced seismicity at Soultz-sous-Forêts. Int. J., Rock Mech. Min. Sc. 47 (3), 405-413.

Baisch, S., Koch, C., Stang, H., Pittens, B., Drijver, B., & Buik, N. (2016). Defining the framework for seismic hazard assessment in geothermal projects V0.1. Technical Report , Report No. 161005, Bad Bergzabern, Germany: prepared for KennisAgenda Aardwarmte.

Baisch, S., Koch, C., Muntendam-Bos, A., 2019. Traffic Light Systems: To What Extent Can Induced Seismicity Be Controlled? Seismological Research Letters 90 (3): 1145–1154. doi: https://doi.org/10.1785/0220180337.

Barth, A., Wenzel, F. & Langenbruch, C. J Seismol (2013) 17: 5. https://doi.org/10.1007/s10950-011-9260-9.

Bierman, S., Kraaijeveld, F., Bourne, S. (2015). Regularised direct inversion to compaction in the Groningen reservoir using measurements from optical leveling campaigns. The Netherlands (Technical Report). Assen, the Netherlands: Nederlandse Aardolie Maatschappij. (http://feitenencijfers.namplatform.nl/download/rapport/cc5ea278-c093-457b-b930-1869a3c26c21?open=true).

Bohnhoff, M., Malin, P., Ter Heege, J.H., Deflandre, J., & Sicking, C. (2018). Suggested best practice for seismic monitoring and characterization of non-conventional reservoirs First Break, 36 (2), 59.

Bommer, J. J., Oates, S., Cepeda, J. M., Lindholm, C., Bird, J., Torres, R., Marroquin, G., & Rivas, J. (2006). Control of hazard due to seismicity induced by a hot fractured rock geothermal project. Engineering Geology, 83 , 287.

Bommer, J. J., Edwards, B., Kruiver, P.P., Rodriquez-Marek, A., Stafford, P.J., Dost, B., Ntinalexis, M., Ruigrok, E. Spetzler, J. (2018). V5 Ground-Motion Model for the Groningen Field. Assen, the Netherlands: Nederlandse Aardolie Maatschappij. (https://nam-onderzoeksrapporten.data-app.nl/reports/download/groningen/en/52a1edec-6824-4ab3-8d92-3294c9cbec3a)

Bohnhoff, M., Malin, P., Heege, J. t., Deflandre, J., & Sicking, C. (2018). Suggested best practice for seismic monitoring and characterization of non-conventional reservoirs First Break, 36 (2), 59.

Bonnet, E., O. Bour, N.E. Odling, P. Davy, I. Main, P. Cowie, and B. Berkowitz. 2001. Scaling of fracture systems in geological media. *Rev. Geophys.* 39**:** 347-383.

Bos, S., and Laenen, B. (2017). Development of the first deep geothermal doublet in the Campine Basin of Belgium. European Geologist 43, 16-20.

Bourne, S. J., Oates, S. J. (2017). Extreme threshold failures within a heterogeneous elastic thin sheet and the spatial-temporal development of induced seismicity within the Groningen gas field. Journal of Geophysical Research: Solid Earth, 122, 10,299–10,320.

Bourne, S. J., Oates, S. J., Van Elk, J. (2018). The exponential rise of induced seismicity with increasing stress levels in the groningen gas field and its implications for controlling seismic risk. Geophysical Journal International 213, 1693–1700

Bouroullec, R., Nelskamp, S., Kloppenburg, A., Abdul Fattah, R., Foeken, J., Ten Veen, J., Geel, K., Debacker, T., and Smit, J. (2019). Burial and Structural Analysis of the Dinantian Carbonates in the Dutch Subsurface (SCAN). https://www.nlog.nl/scan.

Broothaers, M., Bos, S., Lagrou,D., Harcouët-Menou, V., and Laenen, B. (2019). Lower Carboniferous limestone reservoir in northern Belgium: structural insights from the Balmatt project in Mol. European Geothermal Congress 2019, Den Haag, The Netherlands, 11-14 June 2019.

Bruinen, P. (2019). Estimating geothermal power of ultra-deep Dinantian carbonates in the Dutch subsurface (SCAN). https://www.nlog.nl/scan.

Buijze, L., van Bijsterveldt, L., Cremer, H., Paap, B., Veldkamp, H., Wassing, B., and Ter Heege, J. (2019a) Review of worldwide geothermal projects: mechanisms and occurrence of induced seismicity. TNO-report 2019 R100043. https://www.nlog.nl/scan.

Buijze, L., van den Bogert, P.A.J., Wassing, B.B.T., Orlic, B., 2019b. Nucleation and Arrest of Dynamic Rupture Induced by Reservoir Depletion. Journal of Geophysical Research: Solid Earth, 124, 3620-3645. https://doi.org/10.1029/2018JB016941.

Burghout, L., Vorage, R., and Broothaers, M. (2019). Koepelnotitie Aardwarmtewinning en Seismiciteit Californie Lipzig Gielen Geothermie BV. https://www.californie.nu/nieuws/negatieve-reactie-sodm-op-verzoek-clg-geothermie-bv-om-weer-te-mogen-opstarten/109
Report:
https://www.californie.nu/download/738/downloads/seismische_analyse/190412_OverkoepelendeNota_CLG_april2019.pdf

Candela, T., Wassing, B., ter Heege, J., & Buijze, L. (2018a). How earthquakes are induced. Science, 360 (6389), 598-600.

Candela, T., van der Veer, E. F., & Fokker, P. A. (2018b). On the Importance of Thermo-elastic Stressing in Injection-Induced Earthquakes. Rock Mechanics and Rock Engineering, 51(12), 3925-3936.

Candela, T., Peters, E., Van Wees JD, Fokker, P. A., Wassing, B., Ampuero, J-P (2019a). Effect of fault roughness on injection-induced seismicity. In 53rd US Rock Mechanics/Geomechanics Symposium – ARMA.

Candela, T., Osinga, S., Ampuero, J.-P., Wassing, B., Pluymaekers, M., Fokker, P.A., et al. (2019b). Depletion-induced seismicity at the Groningen gas field: Coulomb rate-and-state models including differential compaction effect. Journal of Geophysical research: Solid Earth 124, 7081-7104.

Carpenter, B.M., Scuderi, M.M., Colletini, C., Marone, C., 2014. Frictional heterogeneities on carbonate-bearing normal faults: insights from the Monte Maggio fault, Italy. J.Geophys. Res. 119, 9062-9076 (2014).

Catalli, F., Rinaldi, A.P., Gischig, V., Nespoli, M., Wiemer, S. (2016). The importance of earthquake interactions for injection-induced seismicity: Retrospective modeling of the Basel Enhanced Geothermal System. Geophysical Research Letters, 43(10), DOI: 10.1002/2016gl068932.

Colette, C., Carmona-Fernandez, P., Janssens, S., Artoos, K., Guinchard, M., Hauviller, C. (2011). Review of sensors for low frequency seismic vibration measurement. CERN ATS/Note/2011/001 (TECH), 1-21.

Crowley, H., Pinho, R. (2017). Report on the v5 Fragility and Consequence Models for the Groningen Field. Assen, the Netherlands: Nederlandse Aardolie Maatschappij. (https://nam-onderzoeksrapporten.data-app.nl/reports/download/groningen/en/aaa228dc-71a3-4919-a560-571a4b262a9a).

Deckers J., De Koninck R., Bos S., Broothaers M., Dirix K., Hambsch L., Lagrou, D., Lanckacker T., Matthijs, J., Rombaut B., Van Baelen K. & Van Haren T. (2019). Geologisch (G3Dv3) en hydrogeologisch (H3D) 3D-lagenmodel van Vlaanderen – versie 3. Studie uitgevoerd in opdracht van: Vlaams Planbureau voor Omgeving (Departement Omgeving) en Vlaamse Milieumaatschappij 2018/RMA/R/1569, 286p. + bijlagen

Dieterich, J. (1994). A constitutive law for rate of earthquake production and its application to earthquake clustering. J. of Geophys. Research 99 B2, 2601-2618.

Dost, B., and Haak, H.W. (2007). Natural and induced seismicity. *Geology of the Netherlands*, Edited by Th.E. Wong, D.A.J. Batjes & J. de Jager, Royal Netherlands Academy of Arts and Sciences, 2007: 223–239**.**

Dost, B., Ruigrok, E., & Spetzler, J. (2017). Development of seismicity and probabilistic hazard assessment for the Groningen gas field. Netherlands Journal of Geosciences, 96(5), S235-S245. doi:10.1017/njg.2017.20

Ellsworth, W. L. (2013). Injection-Induced Earthquakes. Science, 341 (6142).

Erdwerk (2019). Deep Geothermal energy in Munich (and Bavaria) – progress to date.

Eyre, T.S., Eaton, D., Garagash, D.I., Zecevic, M., Venieri, M., Weir, R., Lawton, D.C., (2019). The role of aseismic slip in hydraulic fracturing-induced seismicity. Science Advances 5.

Evans, K. F., Zappone, A., Kraft, T., Deichmann, N., & Moia, F. (2012). A survey of the induced seismic responses to fluid injection in geothermal and CO2 reservoirs in Europe. *Geothermics, 41* (0), 30-54.

Faulkner, D.R., C.A.L. Jackson, R.J. Lunn, R.W. Schlische, Z.K. Shipton, C.A.J. Wibberley, M.O. Withjack (2010) A review of recent developments concerning the structure, mechanics and fluid flow properties of fault zones, Journal of Structural Geology, Volume 32, Issue 11, 1557-1575.

Fjaer, E., Holt, R.M., Horsrud, A.M.R.P. (2008). Petroleum Related Rock Mechanics, Volume 53, 2nd Edition.

Fokker, P.A., Wassing, B.B.T. (2019). A fast model for THM processes in geothermal applications. European Geothermal Congress 2019, Den Haag, The Netherlands, 11-14 June 2019.

Gan, Q., Elsworth, 2014. Thermal drawdown and late-stage seismic-slip fault reactivation in enhanced geothermal reservoirs. J. Geophys. Res. Solid Earth, 119, 8936-8949

Gaucher, E., Schoenball, M., Heidbach, O., Zang, A., Fokker, P.A., Van Wees, J-D., Kohl, T., 2015. Induced seismicity in geothermal reservoirs: A review of forecasting approaches. Renewable and Sustainable Energy Reviews 52 (2015) 1473-1490.

Geluk, M.C., Dusar, M. and De Vos, W.: Pre-Selisian. In: Wong, Th.E., Batjes, D.A.J. and De Jager, J. (2007). Geology of the Netherlands.

Giardini, D., Grünthal, G., Shedlock, K. M., and Zhang, P. (1999). The GSHAP Global Seismic Hazard Map. Annals of Geophysics, 42 (6).

Gischig, V.S. and Wiemer, S. (2013) A stochastic model for induced seismicity based on non-linear pressure diffusion and irreversible permeability enhancement. Geophysical Journal International 194, 1229-1249, https://doi.org/10.1093/gji/ggt164.

Heege Ter, J., Osinga, S., Wassing, B.B.T., Candela, C., Orlic, B., Buijze, L., Chitu, A., 2018. Mitigating induced seismicity around depleted gas fields based on geomechanical modeling. The Leading Edge, May 2018.

Herrmann, J., Rybacki, E., Sone, H. et al. (2019) Rock. Mech. Rock Eng. https://doi.org/10.1007/s00603-019-01941-2.

Hettema, M. H. H., Wolf, K.-H. A. A. De Pater, C. J. (1998). The influence of steam pressure on thermal spalling of sedimentary rock: Theory and experiments. Int. J. Rock Mech. Min. Sci. 35, 3-15.

Hirschberg, S., Wiemer, S., & Burgherr, P. (2015). Energy from the earth: Deep geothermal as a resource for the future?. Zürich: TA-SWISS Study TA/CD 62/2015, vdf Hochschulverlag AG. doi: https://doi.org/10.3929/ethz-a-01027769.

Hofmann, H., Zimmermann, G., Zang, A. *et al.* Cyclic soft stimulation (CSS): a new fluid injection protocol and traffic light system to mitigate seismic risks of hydraulic stimulation treatments. *Geotherm Energy* **6,** 27 (2018) doi:10.1186/s40517-018-0114-3

Homuth, S., Götz, A., Sass, I., 2015. Physical Properties of the Geothermal Carbonate Reservoirs of the Molasse Basin, Germany – Outcrop Analogue vs. Reservoir Data. Proceedings World Geothermal Congress 2015. Melbourne, Australia, 19-25 April 2015.

Houtgast, R. F., & Van Balen, R. T. (2000). Neotectonics of the Roer Valley Rift System, the Netherlands. *Global and Planetary Change, 27*, 131-146.

Izadi, G. and Elsworth, D. (2014) Reservoir stimulation and induced seismicity: Roles of fluid pressure and thermal transients on reactivated fracture networks. Geothermics 51, 368-379.

Jaeger, J.C., Cook, N.G.W., Zimmerman, R. *Fundamentals of Rock Mechanics, 4th Edition*, 488 p.

Jin and Zoback, 2018. Fully Dynamic Spontaneous Rupture Due to Quasi-Static Pore Pressure and Poroelastic effects: An Implicit Nonlinear Computational Model of Fluid-Induced Seismic Events. Journal of Geophys. Res. – Solid Earth, Vol. 123, Issue 11, 9430-9468.

Kaiser J 1950 A study of acoustic phenomena in tensile test PhD Thesis Technical University, Munich

Kang, J.-Q., Zhu, J.-B., Zhao, J., 2019. A review of mechanisms of induced earthquakes: from a view of rock mechanics. Geomech. Geophys. Geo-energ. Geo-resour. 34, 3.

Karvournis, D.C. and Wiemer, S. (2015). Decision Making Software for Forecasting Induced Seismicity and Thermal Energy Revenues in Enhanced Geothermal Systems. Proceedings World Geothermal Congress 2015, Melbourne, Australia, 19-25 April 2015.

Kiraly, E., Zechar, J.D., Gischig, V., Wiemer, S., Karvournis, D., Doetsch, J. (2016). Validating induced seismicity forecast models – Induced Seismicity Test Bench. J. Geophys. Res. Solid earth, 121, 6009-6029.

Kohl, T., Megel, T. (2007). Predictive modeling of reservoir response to hydraulic stimulations at the European EGS site Soultz-sous-Forêts. International Journal of Rock Mechanics & Mining Sciences 44, 1118-1131.

Kombrink, H. (2008). *The Carboniferous of the Netherlands and surrounding areas; a basin analysis.* (PhD, Utrecht University). *Geologica Ultraiectina, 294*, 184 pp.

Kurita K and Fuji N 1979 Stress memory of crystalline rocks in acoustic emission Geophys. Res. Lett. 6 9–12.

Langenaeker, V. (2000). *The Campine basin : stratigraphy, structural geology, coalification and hydrocarbon potential for the devonian to Jurassic*, Aardkundige Mededelingen 10, Leuven University Press, 142 pp.

Lapperre, R.E., Kasse, C., Bense, V.F., Woolderink, H.A.G., and Van Balen, R.T. (2019). An overview of fault zone permeabilities and groundwater level steps in the Roer Valley Rift System. Netherlands Journal of Geosciences, Volume 98, e5. https://doi.org/10.1017/njg.2019.4.

Leonard, M., 2010. Earthquake Fault Scaling: Self-Consistent Relating of Rupture Length, Width, Average Displacement, and Moment Release. Bulletin of the Seismological Society of America 100, 1971-1988.

Leonard, M., 2012. Erratum to Earthquake Fault Scaling: Self-Consistent Relating of Rupture Length, Width, Average Displacement, and Moment Release. Bull. Seis. Soc. Am. 102, 2797.

Lu, J., Ghassemi, A., 2019. Coupled Thermo-Hydro-Mechanical-Seismic Modeling of Fractured reservoir Stimulation with Application to EGS Collab. Proceedings, 44th Workshop on Geothermal Reservoir Engineering, Stanford University, February 11-13, 2019.

Madiaraga, R. (1979). On the Relation Between Seismic Moment and Stress Drop in the Presence of Stress and Strength Heterogeneity. Journal of Geophysical Research, Vol.84, No.B5.

Majer, E., Nelson, J., Robertson-tait, A., Savy, J., & Wong, I. (2012). Protocol for addressing induced seismicity associated with enhanced geothermal systems. Report No. DOE/EE-0662, U.S. Department of energy.

Mardia, K.V.,Jupp. P.E., 1999. Direction Statistics. John Wiley & Sons.

Mazurek, M., Hurford, A. J., & Leu, W. (2006). Unravelling the multi-stage burial history of the Swiss Molasse Basin: integration of apatite fission track, vitrinite reflectance and biomarker isomerisation analysis. *Basin Research, 18* (1), 27-50.

McGarr, A. (2002). Case histories of induced and triggered seismicity. In W. H. K. Lee, H. Kanamori, P. C. Jennings & C. Kisslinger (Eds.), *International Handbook of Earthquake and Engineering Seismology* 81A, pp. 647.

Megies, T., and Wassermann, J. (2014). Microseismicity observed at a non-pressure-stimulated geothermal power plant. Geothermics 52, 36–49.

Mozafari, M., Gutteridge, P., Riva, A., Geel, C. R., Garland, J., and Dewit, J. (2019). Facies analysis and diagenetic evolution of the Dinantian carbonates in the Dutch subsurface (SCAN). https://www.nlog.nl/scan.

NAM (Nederlandse Aardolie Maatschappij), (2016). Report on Mmax workshop. 8-10 March 2016. World Trade Centre, Schiphol Airport, The Netherlands. https://nam-onderzoeksrapporten.data-app.nl/reports/download/groningen/en/cef44262-323a-4a34-afa8-24a5afa521d5.

NAM (Nederlandse Aardolie Maatschappij). (2017). Groningen Meet- En regelprotocol. https://www.sodm.nl/documenten/publicaties/2017/07/03/meet--en-regelprotocol-final.

National Research Council. 1996. Rock Fractures and Fluid Flow: Contemporary Understanding and Applications. Washington, DC: The National Academies Press. https://doi.org/10.17226/2309.

Niemeijer, A.R. and Spiers, C.J. (2006). Velocity dependence of strength and healing behaviour in simulated phyllosilicate-bearing fault gouge, Tectonophysics 427, 231-253.

Ogata, Y. (1998). Space-time point-proces models for earthquake occurrences. Annals of the Institute of Statistical Mathematics, 50 (2), 379-402.

Osinga, S. and Buik, N. (2019). Stress field characterization in the Dinantian carbonates in the Dutch subsurface (SCAN). https://www.nlog.nl/scan.

Okrent, D. (1980). Comment on Societal Risk. Science 208, 372-375.

Paz, M. , K, Y.H. (2019) Structural Dynamics: Theory and Computation. Springer International Publishing. Sixth Edition (2019) doi.org/10.1007/978-3-319-94743-3

Pluymaekers, M.P.D., Doornenbal, J.C., Middelburg, H., 2017, Velmod-3.1. TNO-report TNO2017R11014, Utrecht.

Reinecker, J., Tingay, M., Müller, B., & Heidbach, O. (2010). Present-day stress orientation in the Molasse Basin. *Tectonophysics, 482* (1), 129-138.

Reith, D., Godderij, R., Jaarsma, B., Bertotti, G., Heijnen, L. (2019). Dynamic simulation of a geothermal reservoir. Case study of the Dinantian carbonates encountered in the Californië geothermal wells, Limburg, NL. European Geothermal Congress 2019 Den Haag, The Netherlands, 11-14 June 2019.

Reijmer, J. J. G., ten Veen, J. H., Jaarsma, B., & Boots, R. (2017). Seismic stratigraphy of Dinantian carbonates in the southern Netherlands and northern Belgium. *Netherlands Journal of Geosciences, 96* (4), 353-379.

Rinaldi, A.P., Nepoli, M., 2017. TOUGH2-seed: A coupled fluid flow and mechanical-stochastic approach to model injection-induced seismicity. Computers & Geosciences 108 (2017), 86-97.

SodM (2019). Aardwarmteproject nabij Venlo nu niet hervat. https://www.sodm.nl/actueel/nieuws/2019/07/11/aardwarmteproject-nabij-venlo-nu-niet-hervat.

Savvatis, A, Steiner, U., Krzikalla, F., Meinecke, M., Dirner, S. (2019). 4D-Geomechanical Simulations (Visage™) to Evaluate Potential Stress Relocation in a Geothermal Targeted Fault System in Munich (South Germany). European Geothermal Congress 2019, Den Haag, The Netherlands, 11-14 June 2019.

Scholz, C.H. (1998). Earthquakes and friction laws. Nature 391, 37-42.

Segall, P., Lu, S. (2015). Injection-induced seismicity: Poroelastic and earthquake nucleation effects. J. Geophys. Res. Solid Earth 120, 5082-5103.

Seithel, R., Gaucher, E., Mueller, B., Steiner, U., Kohl, T. (2019). Probability of fault reactivation in the Bavarian Molasse Basin. Geothermics 82, 81-90.

Smith, K. (2013). Environmental hazards: assessing risk and reducing disaster. Routledge, Oxon, United Kingdom, 478 p.

Spetzler, J., Ruigrok, J., Dost, B., Evers, L. (2018). Hypocenter Estimation of Detected Event near Venlo on September 3rd. KNMI Technical report ; 369. http://publicaties.minienm.nl/documenten/hypocenter-estimation-of-detected-event-near-venlo-on-september-3rd-2018

Tang C A, Chen Z H, Xu X H and Li C 1997 A theoretical model for the Kaiser effect in rock Pure Appl. Geophys. 150 203–15

Tchalenko, J.S. 1970. Similarities between Shear Zones of Different Magnitudes. Geological Society of America Bulletin 81**:** 1625-1640.

Ten Veen, J., De Haan, H., De Bruin, G., Holleman, N., and Schöler, W. (2019). Seismic Interpretation and Depth Conversion of the Dinantian carbonates in the Dutch subsurface (SCAN). https://www.nlog.nl/scan.

Ter Heege, J.H. (2016). Distribution and properties of faults and fractures in shales: Permeability model and implications for optimum flow stimulation by hydraulic fracturing. 50th US Rock Mechanics / Geomechanics Symposium held in Houston, Texas, USA, 26-29 June 2016.

Ter Heege, J.H., Osinga, S., Wassing, B.B.T., Candela, T., Orlic, B., Buijze, L. Chitu, A. (2018a) Mitigating induced seismicity around depleted gas fields based on geomechanical modeling. The Leading Edge 2018 37:5, 334-342.

TerHeege, J.H., Osinga, S. and Carpentier, S. (2018b) The geomechanical response of naturally fractured carbonate reservoirs to operation of a geothermal doublet. 52nd US Rock Mechanics / Geomechanics Symposium held in Seattle, Washington, USA, 17–20 June 2018.

TNO (2014). Report 2014 R11396. DoubletCalc 1.4 manual, English version for DoubletCalc 1.4.3.

Torabi, A., and S.S. Berg. 2011. Scaling of fault attributes: A review. *Marine and Petroleum Geology* 28**:** 1444-1460.

Urai, J.L., Spiers, C.J., Zwart, H.J., and Lister, G.S., 1986. Weakening of rock salt by water during long-term creep. Nature 324, 554– 557.

Van Adrichem Boogaert, H.A., Kouwe, W.F.P., 1993–1997. Carboniferous limestone Group. In: Stratigraphic Nomenclature of the Netherlands.

Van Baelen H. & Sintubin M., 2006. Evaluation of the tectonic activity in the Roer Valley Graben (NE Belgium). NIROND TR-2006-01, 207 pp.

Van Leverink, D., Geel, K. (2019). Fracture characterization of the Dinantian carbonates in the Dutch subsurface (SCAN). https://www.nlog.nl/scan.

Van den Ende, M.P.A., Chen, J., Ampuero, J.-P., Niemeijer, A.R. 2018. A comparison between rate-and-state friction and microphysical models, based on numerical simulations of fault slip. Tectonophysics 733, 273-295.

Van der Voet, E., Muchez, P., Laenen, B., Weltje, G.J., Lagrou, D., Swennen, R. (2020). Characterizing carbonate reservoir fracturing from borehole data – A case study of the Viséan in northern Belgium, Marine and Petroleum Geology 111, 375-389.

Van Leverink, D.J. and Geel, C.R. (2019). Fracture Characterization of the Dinantian Carbonates in the Dutch Subsurface (SCAN). Downloadable from: www.nlog.nl/scan

Van Thienen-Visser, K., & Breunese, J. (2015). Induced seismicity of the Groningen gas field: History and recent developments. *The Leading Edge*, *34* (6), 664-671.

Van Wees, J. D., Buijze, L., Van Thienen-Visser, K., Nepveu, M., Wassing, B. B. T., Orlic, B., & Fokker, P. A. (2014). Geomechanics response and induced seismicity during gas field depletion in the Netherlands. Geothermics, 52, 206-219.

Van Wees, J-D., Pluymaekers, M., Osinga, S., Fokker, P., Van Thienen-Visser, K., Orlic, B., Wassing, B., Hegen, D., Candela, T. (2019). 3-D mechanical analysis of complex reservoir: a novel mesh-free approach. Geophys. J. Int. 219, 1118-1130.

Van Wees, J-D, Kahrobaei, S., Osinga, S., Wassing, B., Buijze, L., Candela, T., Fokker, P., Heege Ter, J., Vrijlandt, M. (2020). 3D models for stress changes and seismic hazard assessment in geothermal doublet systems in the Netherlands. World Geothermal Congress 2020, Reykjavik, Iceland, April 26-May 2, 2020; submitted.

Vanneste K., Camelbeeck Th., De Vos W., Degrande G., Dusar M., Haegeman W., Schevenels M., Vancampenhout P., Van Dyck J., Verbeeck K., 2009. Compilatiestudie betreffende de seismiciteit in Vlaanderen – Samenvatting. Studie voor LNE – ALBON VLA07-4.2, 30p.

Veldkamp, H. (2020) Temperature modelling for Dinantian carbonates (SCAN). https://www.nlog.nl/scan.

VITO (2020). https://vito.be/nl/vito-seismometernetwerk-onderzoekt-aardbevingen.

Walsch F.R. and Zoback, M.D., 2016. Probabilistic assessment of potential fault slip related to injection-induced earthquakes: Application to north-central Oklahoma, USA. Geology (2016) 44 (12): 991-994.

Zhai, G., Shirzaei, M., Manga, M., Chen, X. (2019). Pore-pressure diffusion, enhanced by poroelastic stresses,controlsinduced seismicity in Oklahoma. PNAS, 2019. www.pnas.org/cgi/doi/10.1073/pnas.1819225116.

Zoback, M. D. (2010). Reservoir geomechanics. Cambridge University Press.

Zoback, M.D., and Gorelick, S.M. Earthquake triggering and carbon sequestration. Proceedings of the National Academy of Sciences 109 (26), 10164-10168; DOI: 10.1073/pnas.1202473109.

11. Appendices

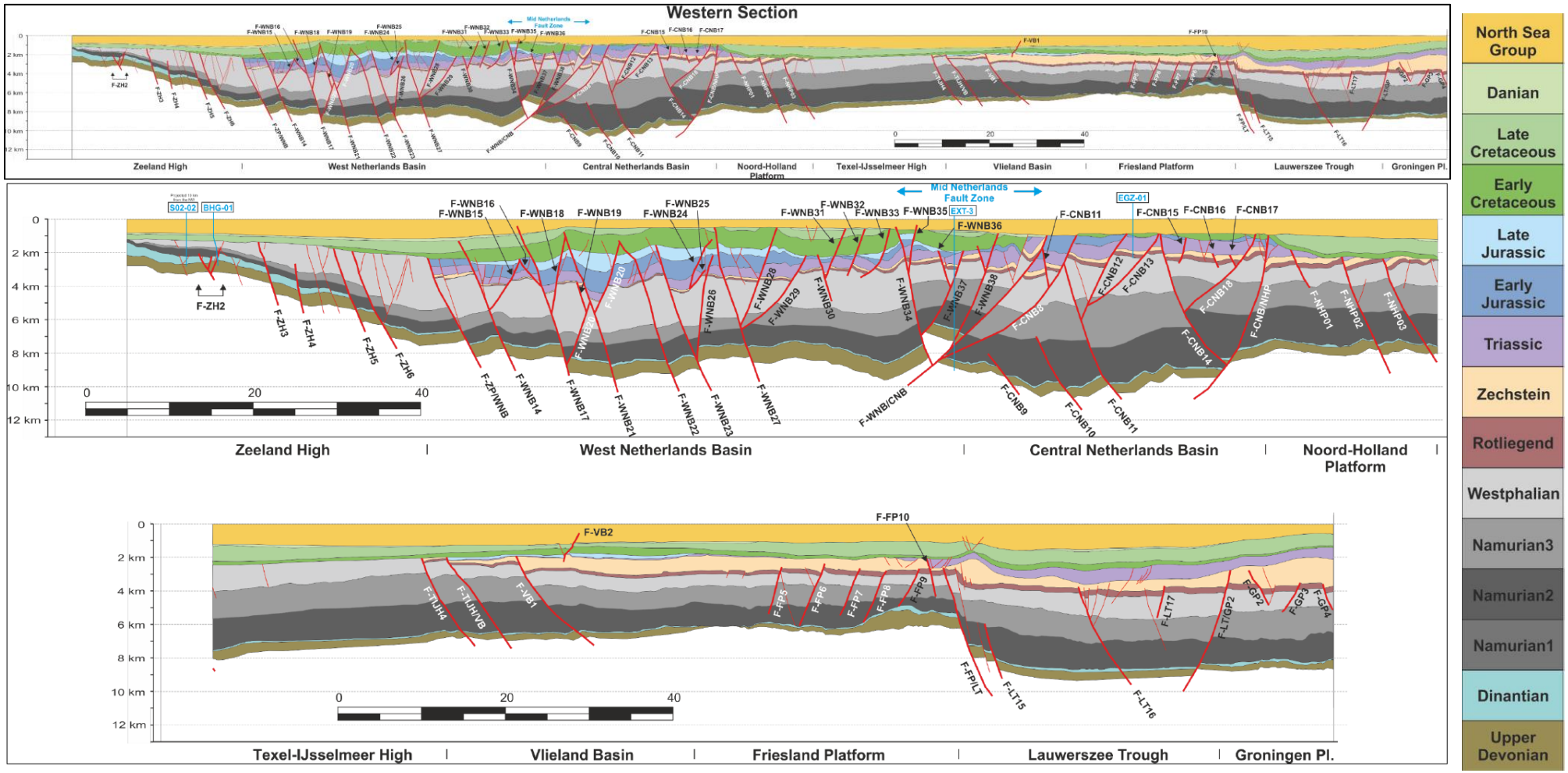

Figure 11-1 Fault interpretation along the Western cross-section constructed in the SCAN burial and reconstruction study. Top figure: Full section. Bottom two figures: Section split at Noord-Holland Platform-Texel-IJsselmeer High boundary. Location of cross-sections can be found in Figure 2-6. Dinantian deposits shown in aqua blue (legend at right margin, see also Figure 11-3). From: Bouroullec et al. (2019).

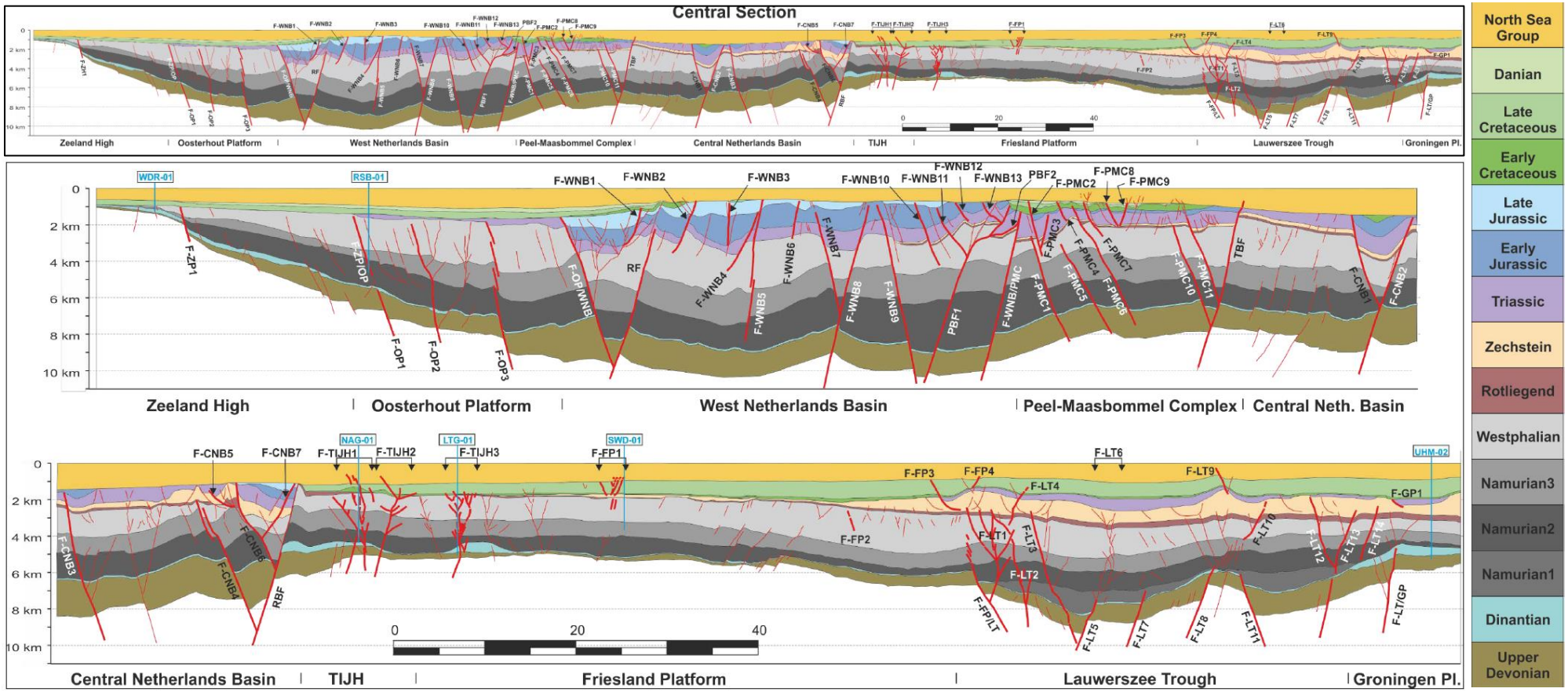

Figure 11-2 Fault interpretation along the Central cross-section, constructed in the SCAN burial and reconstruction study. Top figure: Full section. Bottom two figures: Section split at the Northern & Southern boundary of the Central Netherlands Basin. Location of cross-sections can be found in Figure 2-6. Dinantian deposits shown in aqua blue (legend at right margin, see also Figure 11-3). From: Bouroullec et al. (2019).

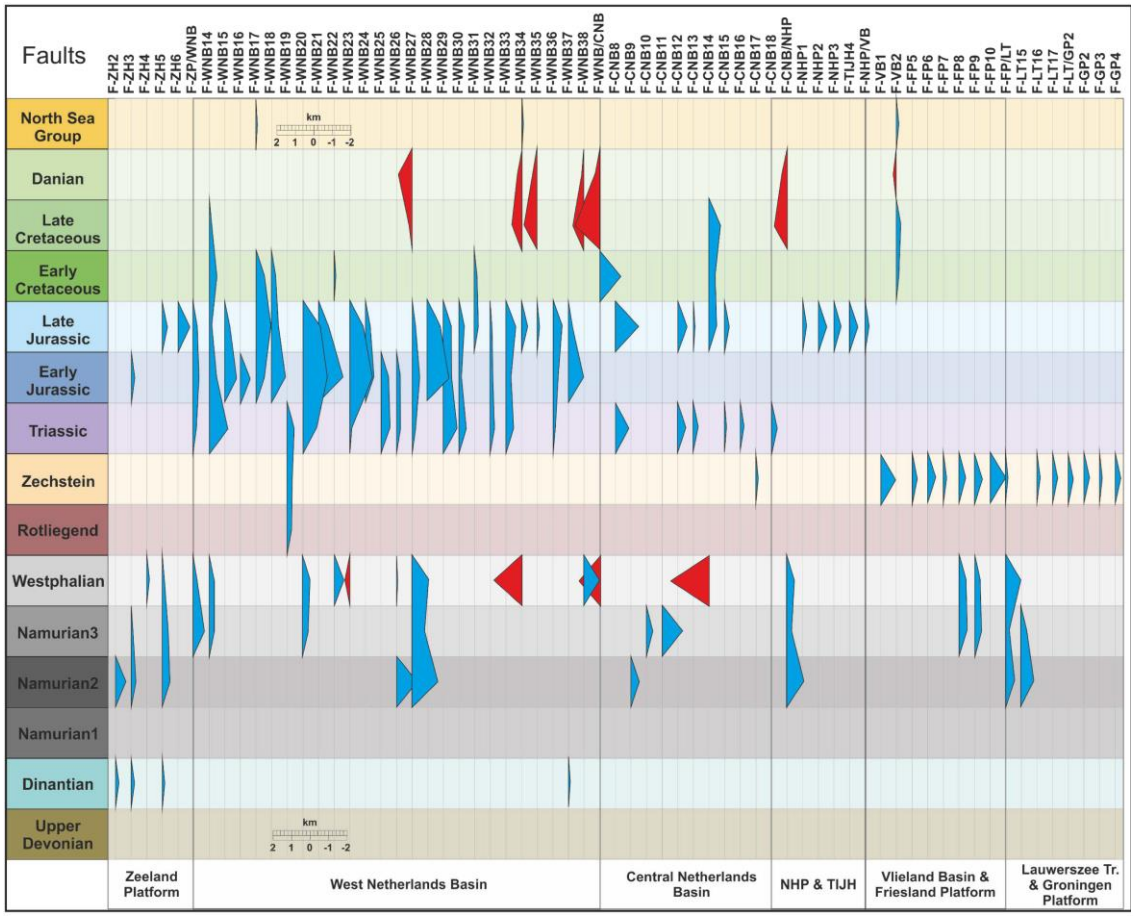
Faults
F-ZH2
F-ZH3
F-ZH4
F-ZH5
F-ZH6
F-ZP/WNB
F-WNB14
F-WNB15
F-WNB16
F-WNB17
F-WNB18
F-WNB19
F-WNB20
F-WNB21
F-WNB22
F-WNB23
F-WNB24
F-WNB25
F-WNB26
F-WNB27
F-WNB28
F-WNB29
F-WNB30
F-WNB31
F-WNB32
F-WNB33
F-WNB34
F-WNB35
F-WNB36
F-WNB37
F-WNB38
F-WNB/CNB
F-CNB8
F-CNB9
F-CNB10
F-CNB11
F-CNB12
F-CNB13
F-CNB14
F-CNB15
F-CNB16
F-CNB17
F-CNB18
F-CNB/NHP
F-NHP1
F-NHP2
F-NHP3
F-TIJH4
F-NHP/VB
F-VB1
F-VB2
F-FP5
F-FP6
F-FP7
F-FP8
F-FP9
F-FP10
F-FP/LT
F-LT15
F-LT16
F-LT17
F-LT/GP2
F-GP2
F-GP3
F-GP4
North Sea Group
Danian
Late Cretaceous
Early Cretaceous
Late Jurassic
Early Jurassic
Triassic
Zechstein
Rotliegend
Westphalian
Namurian3
Namurian2
Namurian1
Dinantian
Upper Devonian
km
2 1 0 -1 -2
Zeeland Platform
West Netherlands Basin
Central Netherlands Basin
NHP & TIJH
Vlieland Basin & Friesland Platform
Lauwerszee Tr. & Groningen Platform

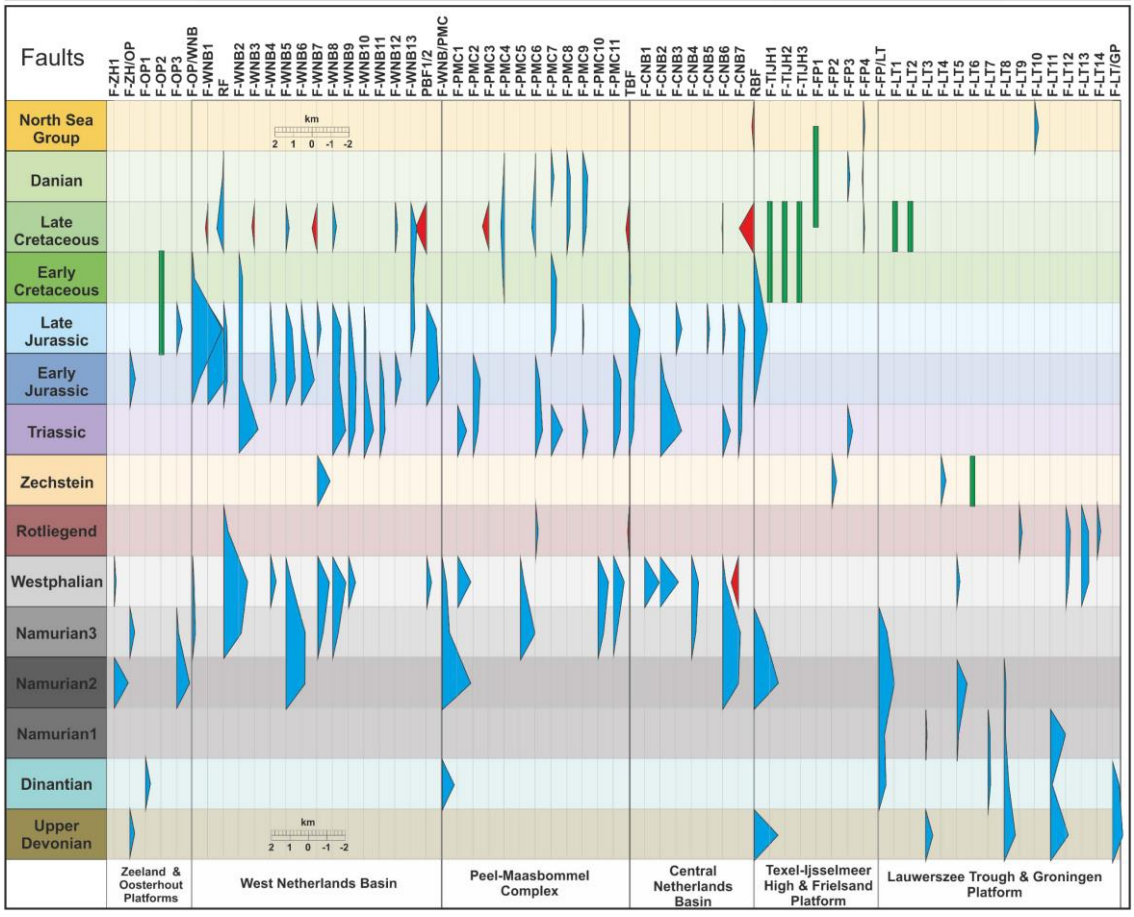
Faults
F-ZH1
F-ZH/OP
F-OP1
F-OP2
F-OP3
F-OP/WNB
F-WNB1
RF
F-WNB2
F-WNB3
F-WNB4
F-WNB5
F-WNB6
F-WNB7
F-WNB8
F-WNB9
F-WNB10
F-WNB11
F-WNB12
F-WNB13
PBF1/2
F-WNB/PMC
F-PMC1
F-PMC2
F-PMC3
F-PMC4
F-PMC5
F-PMC6
F-PMC7
F-PMC8
F-PMC9
F-PMC10
F-PMC11
TBF
F-CNB1
F-CNB2
F-CNB3
F-CNB4
F-CNB5
F-CNB6
F-CNB7
RBF
F-TIJH1
F-TIJH2
F-TIJH3
F-FP1
F-FP2
F-FP3
F-FP4
F-FP/LT
F-LT1
F-LT2
F-LT3
F-LT4
F-LT5
F-LT6
F-LT7
F-LT8
F-LT9
F-LT10
F-LT11
F-LT12
F-LT13
F-LT14
F-LT/GP
North Sea Group
Danian
Late Cretaceous
Early Cretaceous
Late Jurassic
Early Jurassic
Triassic
Zechstein
Rotliegend
Westphalian
Namurian3
Namurian2
Namurian1
Dinantian
Upper Devonian
km
2 1 0 -1 -2
Zeeland & Oosterhout Platforms
West Netherlands Basin
Peel-Maasbommel Complex
Central Netherlands Basin
Texel-Ijsselmeer High & Frielsand Platform
Lauwerszee Trough & Groningen Platform

Figure 11-3 ***(previous page)***: Fault kinematic summary chart showing the growth history for all main faults present on the Western (top figure) and Central (bottom figure) sections. Red polygons show reverse fault throws and blue polygons show normal fault throw. The amplitude of the polygon at each time step are proportional to the throw measured for each structural restoration steps. The vertical scale in km is show in the charts. From: Bouroullec et al. (2019).